

May 2021

**Approach Toward the Total Synthesis of Some Sarpagine Related Indole Alkaloids: Histrixnine, Gelsempervine A, Gelsempervine B, O-Methylmacusine B & 19,20-Dihydro-O-Methylmacusine B, Design, Synthesis & Biological Study of Some Novel Gamma-Aminobutyric Acid Type (GABAA) Receptor Ligands**

Md Zubair Ahmed Khan  
*University of Wisconsin-Milwaukee*

Follow this and additional works at: <https://dc.uwm.edu/etd>

 Part of the [Analytical Chemistry Commons](#), and the [Organic Chemistry Commons](#)

---

**Recommended Citation**

Ahmed Khan, Md Zubair, "Approach Toward the Total Synthesis of Some Sarpagine Related Indole Alkaloids: Histrixnine, Gelsempervine A, Gelsempervine B, O-Methylmacusine B & 19,20-Dihydro-O-Methylmacusine B, Design, Synthesis & Biological Study of Some Novel Gamma-Aminobutyric Acid Type (GABAA) Receptor Ligands" (2021). *Theses and Dissertations*. 2635.  
<https://dc.uwm.edu/etd/2635>

This Dissertation is brought to you for free and open access by UWM Digital Commons. It has been accepted for inclusion in Theses and Dissertations by an authorized administrator of UWM Digital Commons. For more information, please contact [scholarlycommunicationteam-group@uwm.edu](mailto:scholarlycommunicationteam-group@uwm.edu).

**PART 1: APPROACH TOWARD THE TOTAL SYNTHESIS OF SOME SARPAGINE RELATED INDOLE  
ALKALOIDS: HISTRIXNINE, GELSEMPERVINE A, GELSEMPERVINE B, O-METHYLMACUSINE B &  
19,20-DIHYDRO-O-METHYLMACUSINE B**

**PART 2: DESIGN, SYNTHESIS & BIOLOGICAL STUDY OF SOME NOVEL GAMMA-AMINOBUTYRIC  
ACID TYPE (GABA<sub>A</sub>) RECEPTOR LIGANDS**

by

Md Zubair Ahmed Khan

A Dissertation Submitted in  
Partial Fulfillment of the  
Requirements for the Degree of

Doctor of Philosophy  
in Chemistry

at

The University of Wisconsin-Milwaukee

May 2021

## ABSTRACT

PART 1: APPROACH TOWARD THE TOTAL SYNTHESIS OF SOME SARPAGINE RELATED INDOLE ALKALOIDS: HISTRIXNINE, GELSEMPERVINE A, GELSEMPERVINE B, O-METHYLMACUSINE B & 19,20-DIHYDRO-O-METHYLMACUSINE B

PART 2: DESIGN, SYNTHESIS & BIOLOGICAL STUDY OF SOME NOVEL GAMMA-AMINOBUTYRIC ACID TYPE (GABA<sub>A</sub>) RECEPTOR LIGANDS

by

Md Zubair Ahmed Khan

The University of Wisconsin-Milwaukee, 2021  
Under the Supervision of Professor James Cook

Indole alkaloids are chemically, biologically and commercially significant, as well as diversely distributed important group of natural products. These are of prominence because of their resemblance with various biologically essential molecules including tryptophan, tryptamine, and serotonin. The sarpagine type indole alkaloids comprise one of the most diverse series of indole alkaloid natural products. These indole alkaloids are primarily isolated from three plant families: *Apocynaceae*, *Rubiaceae*, and *Loganiaceae* which have been used in traditional and folk medicines in many countries around the world. Biological screening of these alkaloids is not always possible, presumably, due to the paucity of the isolated natural products. However, some of the bases from this group of structurally related alkaloids have been shown to possess important biological activity. Considering the useful bioactivity and complex structural features, the total synthesis of these alkaloids is of importance. Some key transformations in our strategy include the diastereospecific asymmetric Pictet-Spengler cyclization, diastereospecific

Dieckmann condensation, and an enolate driven palladium catalyzed cross-coupling process. The total synthesis of hystrixnine, gelsempervines A and B were approached with the key challenge of solving the C(3)-N(4) bond breaking of pentacyclic core. But attempts to get into this oxo series were not successful despite many attempts. However, the synthesis of two other target indole alkaloids, O-methylmacusine B and 19,20- dihydro - O - methylmacusine B have also been approached using the enantiospecific Pictet-Spengler reaction as the key chiral step.

In the second part, I will show my research on some novel GABA<sub>A</sub> receptor ligands. Benzodiazepine related compounds are the class of psychoactive drugs which act as a positive allosteric modulator of gamma-aminobutyric acid type A (GABA<sub>A</sub>) receptor ion channels. Due to their potent activity, low toxicity, minimal drug-drug interactions in the liver, rapid penetration across the blood-brain barrier (BBB), rapid absorption from the gastrointestinal tract, and ready distribution in the brain, BZDs have been used in the clinic as anxiolytics, sedative-hypnotics, myorelaxants and anticonvulsants for over four decades. The pharmacological action exerted by the BZD depends upon different subunits of the GABA<sub>A</sub> receptor complex. Throughout the years several GABA<sub>A</sub>  $\alpha$ 2/ $\alpha$ 3 receptor subtype-selective ligand has been developed in Milwaukee for the treatment of epilepsy and chronic pain. Among them KRM-II-81, the bioisostere of lead  $\alpha$ 2/ $\alpha$ 3 subtype-selective ligand HZ-166, demonstrated significant anticonvulsant, antinociceptive, antiepileptic and antidepressant efficacy in different rodent models without causing amnesia, sedation, ataxia, or the propensity for addiction/dependence. As a part of the continued search for improved drug with less side effects, some novel bioisosteres of HZ-166 has been synthesized and characterized along with some biological studies due to their strong resemblance with the successful lead candidate KRM-II-81.

## TABLE OF CONTENTS

TABLE OF CONTENTS.....	iv
LIST OF FIGURES.....	xiii
LIST OF TABLES.....	xvi
LIST OF SCHEMES.....	xviii
ACKNOWLEDGEMENTS.....	xxi
Chapter 1.....	1
Approach towards the total synthesis of some sarpagine related indole alkaloids: histrixnine, gelsempervine A, gelsempervine B, O-methylmacusine B and 19,20- dihydro - O - methylmacusine B.....	1
1.1 Introduction.....	1
1.2 Access to the tetracyclic core of sarpagine/macroline alkaloids.....	22
1.3 Current examples of total synthesis of indole and oxindole alkaloids.....	25
1.3.1 The total synthesis of dispegatrine by Edwankar et al.....	25
1.3.2 The total synthesis of ervincidine, by Rallapalli et al. ....	27

1.3.3 The total synthesis of alstonisine- and chitosenine-type oxindole alkaloids by Fonseca <i>et al.</i> .....	28
1.3.4 General synthetic strategy for the total synthesis of C-19 methyl- substituted sarpagine/macroline/ajmaline alkaloids by Edwankar <i>et al.</i> .....	30
1.3.5 Total synthesis of C-19 methyl substituted macroline-type indole alkaloids by Rahman <i>et al.</i> <sup>72</sup> .....	32
1.3.6 Access to the common bicyclo [3,3,1] tetracyclic system in reduced steps by Rahman <i>et al.</i> .....	35
1.3.7 100 percent Stereoselectivity in the asymmetric Pictet-Spengler reaction by Rahman <i>et al.</i> .....	36
1.3.8 Objectives .....	38
1.4 Synthetic approach .....	42
1.4.1 Retrosynthetic analysis.....	42
1.5 Results and discussion .....	45
1.5.1 Synthesis of pentacyclic ketone 29 .....	45
1.5.2 Study of model reactions to break the C(3)-N(4) bond of the sarpagine core .....	49
1.5.3 Formation of the quaternary amine 92 and use of the material in the bond breaking approach.....	50

1.5.4 Formation of the quaternary amine 93 and the use of 93 in the bond breaking approach	55
1.5.5 Approach towards the formation of the amide 95 and subsequent use of 95 in the C(3) - N(4) bond breaking attempts .....	59
1.5.6 Attempts to reduce the enol ether bond of 94 .....	63
1.5.7 Selective methylation of alcohol 85 to the ether 95 .....	65
1.5.8 Selective dimethylation of alcohol 85 .....	67
1.5.9 Synthetic approach towards 19,20-dihydro-O-methylmacusine B.....	71
1.6 Experimental .....	74
1.6.1 General experimental considerations .....	74
1.6.2 D-(-)-Tryptophan methyl ester 13 .....	76
1.6.3 D-(+)-Nb-Benzyltryptophan methyl ester 13a.....	77
1.6.4 Preparation of methyl 4,4-dimethoxybutyrate 14 .....	78
1.6.5 Diastereospecific preparation of the <i>trans</i> -(1 <i>S</i> ,3 <i>R</i> )-(-)-2-benzyl-3-methoxycarbonyl- 1-methoxycarbonylethyl-1,2,3,4-tetrahydro-9 <i>H</i> -pyrido-[3,4- <i>b</i> ]indole (15) via the newly modified Pictet-Spengler reaction. ....	80

1.6.6	Dieckmann cyclization of the N <sub>a</sub> -H diester 15 to provide (6S,10S)-(-)-methyl - 9 - oxo-12-benzyl-6, 7, 8, 9, 10, 11-hexahydro - 6, 10-imino - 5H cyclooct [b]indole-8-carboxylate 15a	81
1.6.7	Preparation of (6S,10S)-(-)-9-oxo-12-benzyl-6,7,8,9,10,11-hexahydro-6,10-imino-5H-cyclo-oct[b]indole 49 via acid mediated hydrolysis of the N <sub>a</sub> -H, β-ketoester 16 .....	83
1.6.8	Catalytic debenylation of 16 to provide (6S,10S)-(-)-9-oxo-12-H-6,7,8,9,10,11-hexahydro-6,10-imino-5H-cyclooct[b]indole 37 over Pd/C/H <sub>2</sub> .....	84
1.6.9	Synthesis of (Z)-1-bromo-2-iodobut-2-ene 91.....	86
1.6.10	Alkylation of (6S,10S)-(-)-9-oxo-12-H-6,7,8,9,10,11-hexahydro-6,10-imino-5H-cyclooct [b] indole (37) to provide (6S,10S)-(-)-9-oxo-12-(Z-2' -iodo-2' -butenyl)-6,7,8,9,10,11-hexahydro-6,10-imino-5H-cyclooct[b] indole 87.....	87
1.6.11	Palladium catalyzed cyclization of (6S, 10S)-(-)-9-oxo-12-(Z-2'-iodo-2'butenyl)-6,7,8,9,10,11-hexahydro-6,10-imino-5H-cyclooct [b] indole (87) to provide pentacyclic ketone 29	89
1.6.12	Conversion of the pentacyclic ketone (29) into (+)-3-ethylidene-1,3,4,7,12,12b-hexahydro-2H, 6H- 2,6-methano-indole[2,3,-α]-quinolizine-13-carboxaldehyde[(+)-vellosimine, 81] via the Wittig reaction followed by acid mediated hydrolysis. ....	90
1.6.13	Sodium borohydride mediated reduction of (+)-3-ethylidene-1,3,4,7,12,12b-hexahydro-2H,6H-2,6-methano-indole[2,3-α]-quinolizine-13-carboxaldehyde[(+)- vellosimine, 81] to	

provide the (+)-3-ethylidene-1,3,4,7,12,12b-hexahydro-13-hydroxymethyl-2H,6H-2,6-methano-indole [2,3- $\alpha$ ]-quinolizine [(+)-normacusine B, 85].	92
1.6.14 Synthesis of quarternary amine 93	93
1.6.15 Formation of N <sub>b</sub> -benzyl product 94b	94
1.6.16 General procedure for the synthetic approach of 92b, 93a and 94c (see Tables 5-7 and 9)	95
1.6.17 General procedure for the reaction Scheme 20 (approach towards the reduction of enol ether 94) (see table 10 for results)	96
Chapter 2	97
Synthesis, characterization, and biological study of some novel gamma-aminobutyric acid type A (GABA <sub>A</sub> ) receptor ligands.	97
2.1 Introduction	97
2.1.1 GABA receptors	97
2.1.2 GABA <sub>A</sub> receptor structure and functions.	98
2.1.3 Benzodiazepines (BZD)	101
2.1.4 Different GABA <sub>A</sub> R subtypes and their distinct functions	103

2.2 Designing of novel $\alpha 2/3$ -GABA <sub>A</sub> R subtype-selective ligands. ....	107
2.2.1 Exploring the benzodiazepine binding modes. ....	108
2.2.1.1 Structures of a $\alpha 1\beta 3\gamma 2L$ GABA <sub>A</sub> receptor in desensitized states induced by GABA and alprazolam or GABA and diazepam <sup>126</sup> .....	108
2.2.1.2 Conformational differences between closed/resting and desensitized states in a GABA <sub>A</sub> receptor. <sup>126</sup> .....	111
2.3 Project background .....	113
2.4 Results and Discussion .....	115
2.5 Biological Studies on KRM-II-81 (107).....	123
2.5.1 Pharmacology of KRM-II-81.....	123
2.5.2 Pharmacokinetics .....	124
2.5.3 Antiepileptic activity .....	124
2.5.3.1 Acute seizure models.....	125
2.5.3.2 Seizure sensitization models.....	126
2.5.3.3 Pharmaco-resistant models .....	128
2.5.3.4 Post-traumatic epilepsy .....	129
2.5.3.5 Antinociceptive activity.....	129

2.5.3.6 Anxiolytic activity .....	131
2.5.3.7 Antidepressant activity.....	131
2.5.3.8 Study of side effects.....	132
2.5.4 Chemistry and Results .....	134
2.5.4.1 Synthesis of $\alpha$ 2/ $\alpha$ 3 Subtype Selective Ligands.....	134
2.5.4.2 Some Biological studies.....	140
2.5.4.2.1 Rotarod Motor Impairment Study with Nick Zahn and Coworkers .....	140
2.5.4.2.1 clogP data .....	142
2.5.4.2.2 PDSP Compound-induced Radioligand Displacement Assays for 31 Receptors with Dr. Bryan Roth.....	143
2.6 Conclusion.....	144
2.7 Experimental .....	145
2.7.1 (S)-8-Bromo-N-(1-hydroxypropan-2-yl) -6- (pyridin-2-yl) - 4H-benzo [f]imidazo [1,5- a][1,4]diazepine-3-carboxamide (118a).....	145
2.7.2 (S)-8-Bromo-N-(1-chloropropan-2-yl)-6-(pyridin-2-yl)-4H                      benzo[f]imidazo[1,5- a][1,4]diazepine-3-carboxamide (119a).....	146

2.7.3 (S)-2-(8-Bromo-6-(pyridin-2-yl)-4H-benzo[f]imidazo[1,5-a][1,4]diazepin-3-yl)-4-methyl-4,5-dihydrooxazole (108).....	148
2.7.4 (S)-2-(8-Ethynyl-6-(pyridin-2-yl)-4H-benzo[f]imidazo[1,5-a][1,4]diazepin-3-yl)-4-methyl-4,5-dihydrooxazole (111).....	149
2.7.5 (R)-8-Bromo-N-(1-hydroxypropan-2-yl)-6-(pyridin-2-yl)-4H-benzo[f]imidazo[1,5-a][1,4]diazepine-3-carboxamide (118b).....	151
2.7.6 (R)-8-Bromo-N-(1-chloropropan-2-yl)-6-(pyridin-2-yl)-4H-benzo[f]imidazo[1,5-a][1,4]diazepine-3-carboxamide (119b).....	153
2.7.7 (R)-2-(8-Bromo-6-(pyridin-2-yl)-4H-benzo[f]imidazo[1,5-a][1,4]diazepin-3-yl)-4-methyl-4,5-dihydrooxazole (109).....	154
2.7.8 (R)-2-(8-Ethynyl-6-(pyridin-2-yl)-4H-benzo[f]imidazo[1,5-a][1,4]diazepin-3-yl)-4-methyl-4,5-dihydrooxazole (112).....	156
2.7.9 (R)-8-bromo-N-(1-oxopropan-2-yl)-6-(pyridin-2-yl)-4H-benzo[f]imidazo[1,5-a][1,4]diazepine-3-carboxamide (120).....	158
2.7.10 ..... 2-(8-bromo-6-(pyridin-2-yl)-4H-benzo[f]imidazo[1,5-a][1,4]diazepin-3-yl)-4-methyloxazole (110).....	159
2.7.11 ..... 2-(8-Ethynyl-6-(pyridin-2-yl)-4H-benzo[f]imidazo[1,5-a][1,4]diazepin-3-yl)-4-methyloxazole (113).....	161
2.8 Rotarod assay.....	162

3 Reference .....	164
Appendix Part 1.....	190
Appendix Part 2.....	205
Curriculum Vitae.....	216

## LIST OF FIGURES

### Chapter 1

Figure 1. Bisindoles from <i>Alstonia</i> species.....	3
Figure 2. Dimeric Indole Alkaloid -(+)dispegatine .....	8
Figure 3. Macroline and sarpagine .....	8
Figure 4. Biosynthetic relationship between macroline and sarpagine. <sup>23</sup> .....	9
Figure 5.1 Sarpagine indole alkaloids <sup>23, 32</sup> .....	10
Figure 5.2 Sarpagine indole alkaloids <sup>23, 32</sup> .....	11
Figure 5.3 Sarpagine indole alkaloids <sup>23, 32-35</sup> .....	12
Figure 5.4 Sarpagine indole alkaloids <sup>23, 32</sup> .....	13
Figure 5.5 Sarpagine indole alkaloids <sup>23, 32, 36-39</sup> .....	14
Figure 5.6 Sarpagine indole alkaloids <sup>23, 32</sup> .....	15
Figure 5.7 Sarpagine indole alkaloids <sup>23, 32</sup> .....	16
Figure 5.8 Sarpagine indole alkaloids <sup>23, 32</sup> .....	17
Figure 5.9 Sarpagine indole alkaloids <sup>23, 40-44</sup> .....	18
Figure 5.10 Sarpagine indole alkaloids <sup>45</sup> .....	19
Figure 5.11 Sarpagine indole alkaloids <sup>45, 46</sup> .....	20

Figure 5.12 Sarpagine indole alkaloids <sup>37, 45, 47-50</sup> .....	21
Figure 6. Indole alkaloids extracted from the <i>T. hystrix</i> by Monnerat et al. <sup>41</sup> .....	39
Figure 7. (A) Flowers and leaves from <i>Gelsemium elegans</i> . (B) Roots of <i>Gelsemium elegans</i> . (C) Flowers of <i>Gelsemium sempervirens</i> .....	40
Figure 8. Target alkaloids hystrixnine ( <b>70</b> ), gelsempervine A ( <b>76</b> ), gelsempervine B ( <b>77</b> ) O- methylnacusine B ( <b>84</b> ) and 19,20-dihydro-O-methylnacusine B ( <b>83</b> ) .....	42

## Chapter 2

Figure 12. (Modified from Samuele Maramaia et.al.) <sup>114</sup> 3D-reconstruction of the $\alpha 1\beta 3\gamma 2$ - GABAAR <sup>114, 115</sup> . annel pore itself, for example the picrotoxin (or convulsant) binding site. 99	
Figure 13. The structures of most common BZDs: diazepam, chlordiazepoxide, imidazodiazepine (IMDZ) midazolam and flumazenil. Diazepam, chlordiazepoxide, and midazolam can bind only to the DS sites, whereas flumazenil can bind to both the DS and DI (diazepam insensitive)sites. <sup>123</sup> Librium is metabolized to valium in vivo.....	102
Figure 14. (Modified from Masiulis <i>et al.</i> <sup>126</sup> ) a. Structures of diazepam and alprazolam. Diazepine ring atoms are numbered with labelled Imidazole (I) and benzene (A) rings. b, c.. .....	110
Figure 15. (Modified from Masiulis <i>et al.</i> <sup>126</sup> ) a. Superposition of extra cellular domains (ECD) from PTX (grey) and ALP/GABA (red/blue/yellow) structures based on the global TMD alignment.	

GABA- and ALP-induced ECD rotation angles around the rotational ECD axes, and the direction of motion are shown. b. Global TMD alignment for the PTX-bound (grey) and ALP/GABA-bound (coloured) structures. 9' Leu side chains are shown as sticks. c. Schematic illustration of conformational changes initiated by GABA binding at the ECD level..... 112

Figure 16. Structures of Hz-166 (**105**), MP-III-080 (**106**), and KRM-II-81 (**107**)..... 114

Figure 17. Structures of ZK-III-51(**108**), ZK-III-56 (**109**) and ZK-III-58(**110**)..... 116

Figure 18. Enlarged cryoEM structure of the human full-length  $\alpha 1\beta 3\gamma 2L$  GABA<sub>A</sub> receptor ion complex with alprazolam using AutoDock Vina. .... 117

Figure 19. Structures of ZK-IV-04 (**111**), ZK-IV-5 (**112**) and ZK-IV-7 (**113**). .... 118

Figure 20. Enlarged cryoEM structure of the human full-length  $\alpha 1\beta 3\gamma 2L$  GABA<sub>A</sub> receptor ion complex with Diazepam using AutoDock Vina. .... 119

Figure 21. CryoEM structure of the human full-length  $\alpha 1\beta 3\gamma 2L$  GABA<sub>A</sub> receptor ion complex with ligands **108** and **109** using AutoDock Vina..... 120

Figure 22. CryoEM structure of the human full-length  $\alpha 1\beta 3\gamma 2L$  GABA<sub>A</sub> receptor ion complex with ligands **110** and **107** using AutoDock Vina..... 121

Figure 23. CryoEM structure of the human full-length  $\alpha 1\beta 3\gamma 2L$  GABA<sub>A</sub> receptor ion complex with ligand HZ-166 (**105**) using AutoDock Vina ..... 122

Figure 24. Effect of ligands ZK-III-51, ZK-III-56 and ZK-III-58 on sensorimotor coordination.... 141

## LIST OF TABLES

### Chapter 1

Table 1. Antiamoebic and Antimalarial Activity of Selected Alstonia Alkaloids <sup>6</sup> .....	4
Table 2. IC <sub>50</sub> Values of Alkaloids Tested Against Plasmodia falciparum (K1 and T9-96 strains) <sup>12</sup> .....	5
Table 3. IC <sub>50</sub> Values of Alkaloids Tested Against Plasmodia falciparum (K1 strain) <sup>12</sup> .....	7
Table 4. Reaction conditions for the approaches toward the synthesis of <b>92a</b> . (Note: SM= Starting material) .....	52
Table 5. Reaction conditions for the approaches toward the synthesis of <b>92b</b> . (Note: SM= Starting material) .....	54
Table 6. Reaction conditions for the approaches toward the synthesis of <b>93a</b> . (Note: SM= Starting material) .....	58
Table 7. Reaction conditions for the approaches toward the synthesis of <b>93a</b> . (Note: SM= Starting material) .....	59
Table 8. Reaction conditions for the approaches toward the synthesis of <b>94a</b> . (Note: SM= Starting material) .....	61
Table 9. Reaction conditions for the approaches toward the synthesis of <b>94c</b> . (Note: SM= Starting material) .....	62
Table 10. Reaction conditions for the approaches toward the synthesis of <b>96</b> . (Note: SM= Starting material) .....	64

Table 11. Reaction conditions for the approaches toward the synthesis of <b>101</b> using methyl iodide.....	69
--	----

## Chapter 2

Table 12. The CNS effects at GABAA $\alpha$ 1-6 $\beta$ 2/3 $\gamma$ 2 receptor subtypes. <sup>111, 123, 137-148</sup> Presented at the Mona Symposium (2014), University of the West Indies. <sup>149,59</sup> Earlier reported, in part, by Mckernan et al. (ACNP). Later, reported at the Pharm R and D meeting, Los Angeles, 2019 and 2021 (virtual) by Cook et al. ....	104
Table 13. Docking score (computed binding affinity) of bioisosteric ligands. ....	116
Table 14. cLogP values of the selected ligands <sup>a</sup> .....	143

## LIST OF SCHEMES

### Chapter 1

scheme 1. A schematic flow chart of the P-S/Dieckmann protocol (picture modified from Rahman et al. <sup>66</sup> ).....	23
Scheme 2. Synthesis of tetracyclic core developed in Milwaukee (picture modified from Rahman et al. <sup>66</sup> ).....	24
Scheme 3. Total synthesis of dispegatrine by Edwankar et al. (picture modified from Rahman et al. <sup>66</sup> ).....	25
Scheme 3a. Total synthesis of ervincidine by Ralapalli et al. (picture modified from Rahman et al. <sup>66</sup> ).....	27
Scheme 4. Strategy towards the total synthesis of some alstonisine related indole alkaloids by Fonseca et al. (picture modified from Rahman et al. <sup>66</sup> ) .....	29
Scheme 6. General strategy towards the synthesis of C-19 methyl- substituted sarpagine /Macroline /ajmaline alkaloids by Edwankar et al. (picture modified from Rahman et al. <sup>66</sup> ) .....	31
Scheme 7. Total synthesis of some C-19 substituted macroline-type indole alkaloids by Rahman et al. <sup>66, 72</sup> .....	33
Scheme 8. Access to the common bicyclo [3,3,1] tetracyclic system in reduced steps by Rahman et al. <sup>72</sup> .....	36
Scheme 9. Stereoselectivity in the asymmetric Pictet-Spengler reaction by Rahman et al.....	37

Scheme 10. Retrosynthetic analysis .....	43
Scheme 11. Synthesis of pentacyclic ketone <b>29</b> .....	45
Scheme 12. Synthesis of methyl 4,4-dimethoxy-butylate <b>14</b> .....	47
Scheme 13. Synthesis of (Z)-1-bromo-2-iodo-2-butene <b>91</b> .....	48
Scheme 14. Mechanistic approach towards the breaking of the C-(3) and N <sub>b</sub> -(4) bond of <b>29</b> ....	50
Scheme 15. Synthesis of methiodide salt <b>92</b> and approach towards the breaking of the C(3)- N(4) bond of <b>92</b> using the reaction conditions of Table 4 to provide <b>92a</b> .....	51
Scheme 16 Synthesis of <b>92</b> and approach towards the breaking of C(3)- N(4) bond of <b>92</b> using the reaction conditions outlined in Table 5 to get <b>92b</b> .....	53
Figure 8. Mass spectroscopy data on formation of <b>92b</b> from <b>92</b> .....	55
Scheme 17. Synthesis of <b>93</b> and approach towards the breaking of the C(3)- N(4) bond of <b>93</b> using the reaction condition of Tables 6 and 7 to provide <b>93a</b> .....	56
Scheme 18. Synthesis of <b>94</b> via the Wittig reaction condition and approach towards the protection of the N(4) group of <b>94</b> with the carbamate Cbz-Cl using the reaction conditions of Table 8. ....	60
Scheme 19. Synthetic attempts to produce <b>94c</b> using the reaction conditions from Table 9. ....	62
Scheme 20. Approach towards the reduction of enol ether bond of <b>94</b> .....	64
Scheme 20. Approach towards the selective methylation of <b>85</b> to <b>95</b> using trimethylsilyl-diazomethane. ....	66

Scheme 21. Proposed mechanism for the formation of diazomethane illustrated in Scheme 20 .....	67
Scheme 22. Approach towards the selective methylation of <b>85</b> to <b>101</b> using methyl iodide and base.....	68
Scheme 22. Synthesis of <b>99</b> from <b>94</b> .....	71
Scheme 23. Synthesis of <b>103</b> from <b>29</b> .....	73
Scheme 24. Synthesis of <b>104</b> from <b>99</b> .....	73

## Chapter 2

Scheme 25. Synthesis of imidazodiazepine <b>117</b> .....	134
Scheme 26. Synthesis of 8-Bromo imidazodiazepines <b>108</b> and <b>109</b> .....	136
Scheme 27. Synthesis of 8-ethinyl imidazodiazepines (ZK-IV-4) <b>111</b> and (ZK-IV-5) <b>112</b> .....	137
Scheme 28. Synthesis of the oxazole (ZK-III-58) <b>110</b> .....	138
Scheme 29. Mechanism of the formation of oxazole <b>110</b> .....	139
Scheme 30. Synthesis of oxazole (ZK-IV-07) <b>113</b> .....	140

## ACKNOWLEDGEMENTS

First and foremost, I would like to express my gratitude to my advisor Dr. James Cook, for giving me the opportunity to work in the lab. I am grateful to him for mentoring me professionally as a researcher. I greatly appreciate the way he inspired me to incorporate various technique in my research. He has always been patient to train me as a scientist. It is my pleasure to be a part of Cook lab.

I am grateful to my committee members Dr. Alan Schwabacher, Dr. Mahmum Hussain, Dr. Peng & Dr. Andy Pacheco for their feedback and encouragement in my research and dissertation. I would also like to thank Dr. Anna Benko Dr. Frank Holger Foersterling for their enormous support through the last few years to train me in MS and NMR. I appreciate the help of our collaborators.

I am thankful to my lab members and friends for their consistent support during my research.

I want to Thank my wife especially, Lamia Tabassum Badhon, for her unconditional support and loveduring all these years. His endless consolation and encouragement helped me towards my graduation. My little angel Zaira Ahmed Khan also deserves a big thanks for staying calm during my graduation.

Last but not the least, I am grateful to my parents Jesmin Akter & Md Abul Hashem Khan, for understanding me and being patient during my stressful days.

## Chapter 1

Approach towards the total synthesis of some sarpagine related indole alkaloids: histrixnine, gelsempervine A, gelsempervine B, O-methylmacusine B and 19,20-dihydro-O-methylmacusine B.

### 1.1 Introduction

Indole alkaloids (tryptophan derived) are structurally complex and chemically, biologically, commercially significant, and diversely distributed important group of natural products. These alkaloids have been used as a form of medicine for hundreds of years in many places of the world and some of these have greater significance as a drug still today.<sup>1,2</sup> They could be found in higher plants and microorganisms and are the largest class of alkaloids isolated mainly from three families of plants : *Apocynaceae*, *Rubiaceae* and *Loganiaceae*. Many of these indole alkaloids have shown significant biological activity and, of these, some are extremely useful therapeutic agents. Consequently, scientists are still studying these indole alkaloids to find out the important biological activities, which are still unexplored. In most cases the reason behind this is due to the paucity of material available for testing purposes.<sup>1-3</sup> In early 1958,<sup>4</sup> and later in 1967<sup>5</sup> the bisindole macralstonine **1a** (Figure 1), which had been isolated from *Alstonia macrophylla* Wall and *Alstonia muelleriana* Domin, was found to exhibit potent hypotensive activity. This result

along with the antimalarial activity created tremendous amount of interest in the alkaloids of the family *Apocynaceae* with respect to the genera *Alstonia*.

Wright et al.<sup>6</sup> tested nine alkaloids from *Alstonia angustifolia* for antiprotozoal activity against *Entamoeba histolytica* and *Plasmodium falciparum* in vitro (Table 1). Three dimeric alkaloids, macralstonine O-acetate **1b**,<sup>7</sup> (-)-macrocarpamine **2a**,<sup>8</sup> and (+)-villalstonine **3a**,<sup>9,10</sup> (Figure 1) were found to possess significant activity against both protozoa. Macrocarpamine **2a** was found to be the most active antiamebic compound with an antiamebic activity one fourth that of the standard drug emetine. The alkaloid villalstonine **3a** was found to be the most potent alkaloid against *P. falciparum* and was about fifteen times less active than the clinical antimalarial drug chloroquine.

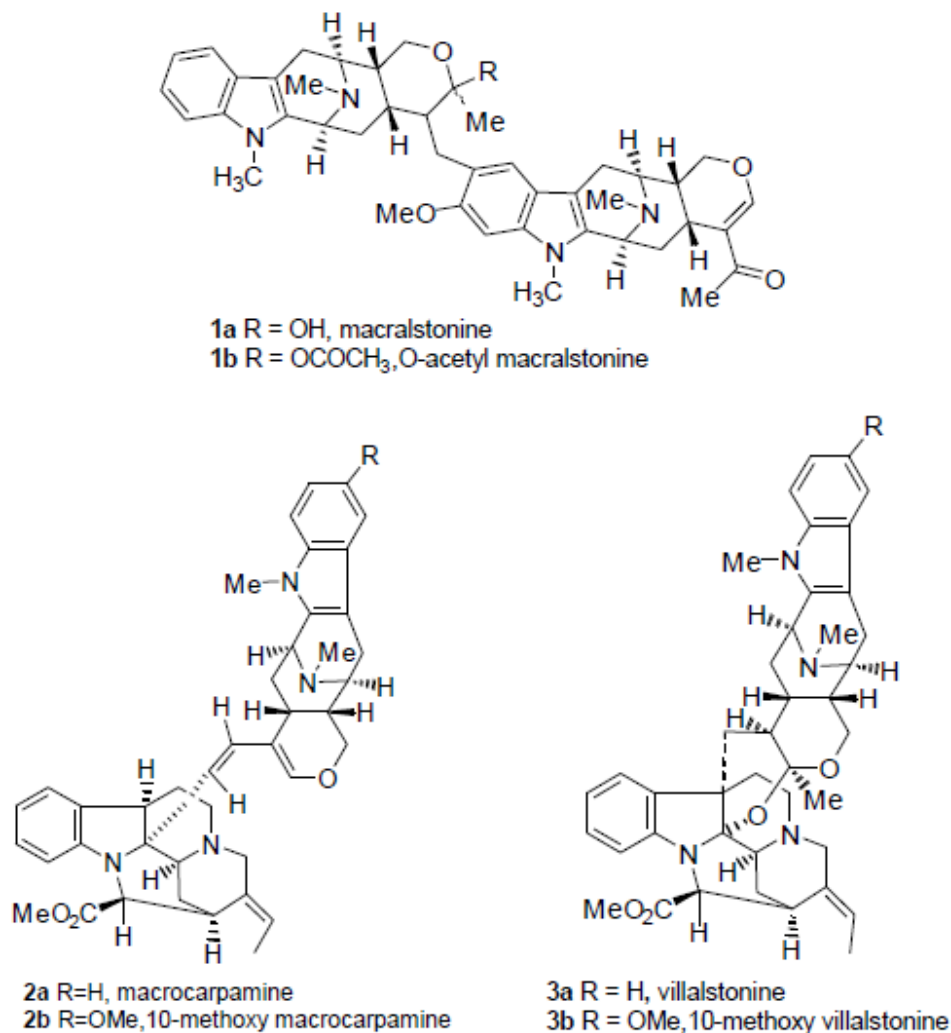


**Figure 1.** Bisindoles from *Alstonia* species

The alkaloid **1b**, which is the acetate of macralstonine, showed much more activity against both protozoa when compared with the parent macralstonine **1a**. From the studies carried out by Houghton et al. (Tables 2 and 3),<sup>11, 12</sup> it can be seen that, the bisindole alkaloids were found to be considerably more active than the monomeric indoles. These in vitro studies provide some basis for the traditional use of the plant extract from *Alstonia angustifolia* for the treatment of amoebic dysentery and malaria by the people of the Malay peninsula.<sup>13, 14</sup>

**Table 1.** Antiamoebic and Antimalarial Activity of Selected *Alstonia* Alkaloids<sup>6</sup>

Alkaloids	<i>E. histolytica</i> ED <sub>50</sub> (95% C. I.) μM	<i>P. falciparum</i> ED <sub>50</sub> (95% C. I.) μM
alstonerine	75.3(65.0-85.6)	46.3(27.7-77.3)
alstophylline	67.7(57.2-78.2)	82.3(65.9-102)
macralstonine	inactive at 70	inactive at 178
O-acetyl macralstonine	15.51(14.78-16.24)	3.43(1.86-6.34)
villalstonine	11.8(11.7-12.0)	2.92(1.11-3.14)
pleiocarpamine	47.4(46.8-52.90)	20.5(12.6-33.17)
macrocarpamine	8.21(7.76-8.48)	9.36(7.20-12.1)
11-methoxyakuammicine	70.5(65.3-75.6)	41.3(26.5-64.3)
norfurocurarine	84.1(82.9-89.6)	129(70.2-239)
vincamajine	inactive at 70	138(79.3-238)

ED<sub>50</sub>: Effective dose at 50% inhibition.

In 1986, using radioligand binding experiments and bioassays, Feng et al.<sup>15, 16</sup> compared the effects of spegatrine **4a** and dispegatrine **4b** (Figure 2) on  $\alpha$ -adrenoreceptors. Their results gave them a good indication that the effect of the dimer **4b** on both  $\alpha_1$  and  $\alpha_2$  adrenoreceptors was more potent than that of the monomer. Dimeric alkaloids are often more potent in vivo than their monomeric progenitors. Much of the early isolation and structural work on the *Alstonia*

alkaloids was performed in the laboratories of Elderfield<sup>17</sup> and Schmid,<sup>18, 19</sup> and was followed by the biomimetic interconversions of LeQuesne et al.<sup>7, 9, 10, 20-23</sup>

**Table 2.** IC<sub>50</sub> Values of Alkaloids Tested Against Plasmodia falciparum (K1 and T9-96 strains)<sup>12</sup>

Alkaloids	K1 (μM, n = 3)	T9-96 (μM, n = 3)	K1/T9-96 ratio
O-acetyl macralstonine	0.53 ± 0.09	12.4 ± 1.6	0.04
villalstonine	0.27 ± 0.06	0.94 ± 0.07	0.29
alstomacroline	1.12 ± 0.35	10.2 ± 0.4	0.11
macrocarpamine	0.36 ± 0.06	>39*	<0.009
chloroquine diphosphate	0.20 ± 0.07	0.019 ± 0.002	10.53

K1: the multidrug-resistant strain, which is highly resistant to chloroquine; T9-96: the chloroquine sensitive strain; n: number of independent experiments; \*: % inhibition at 39 μM (7.5 μg/mL), the highest concentration tested was 32.6 ± 4.1 μM. The experiment was done with infected human red blood cells.

When working on the structural elucidation of bisindole alkaloid villastonine, Schmid et al.<sup>18, 19</sup> found macroline **6** (Figure 3) as a degradation product from villalstonine **3a**. It is believed that macroline **6** is a biomimetic precursor to many *Alstonia* alkaloids.<sup>7, 8, 10, 21, 22</sup> as it has not been isolated as a natural product, to date.

From individual studies on selective sarpagine/ajmaline indole alkaloids, it was found that normacusine B exhibited sedative and ganglion blocking activity,<sup>24</sup> lochnerine elicited hypoglycemic activity,<sup>25</sup> pericyclivine has been shown to exhibit weak cytotoxic activity against P-388 leukemia,<sup>26</sup> while gardnutine, gardnerine, and hydroxygardnutine have been shown to elicit ganglion blocking effects.<sup>12, 27, 28</sup> The mixture of constituents (normacusine B, affinisine, N<sub>a</sub>-methylpericyclivine, and voachalotine) present in *Peschiera van Heurck* from the tropical rain forest in Bolivia is known for its alleged leishmanicidal and bactericidal activity.<sup>23, 29</sup> Like many quaternary alkaloids, the major quaternary sarpagine alkaloid from *Strychnos angolensis*, 11-methylmacusine A, demonstrated muscle relaxant activity.<sup>23, 30</sup>

**Table 3.** IC<sub>50</sub> Values of Alkaloids Tested Against Plasmodia falciparum (K1 strain)<sup>12</sup>

ALKALOID	n	IC <sub>50</sub> (µg/mL)
talcarpine	3	40.3 ± 2.9
pleiocarpamine	2	6.44 ± 0.98
alstoumerine	2	13.1 ± 2.7
20- <i>epi</i> -antirhine	3	7.51 ± 1.17
alstonerine	2	9.67 ± 3.57
alstophylline	2	12.7 ± 1.7
macralstonine	3	8.92 ± 2.95
<b>O-methylmacralstonine</b>	<b>2</b>	<b>0.85 ± 0.20</b>
<b>O-acetylmacralstonine</b>	<b>3</b>	<b>0.53 ± 0.09</b>
alstomacrophylline	2	1.10 ± 0.30
<b>villalstonine</b>	<b>3</b>	<b>0.27 ± 0.06</b>
villalstonine <i>N</i> <sub>6</sub> -oxide	2	10.7 ± 1.9
alstomacroline	3	1.12 ± 0.35
<b>macrocarpamine</b>	<b>3</b>	<b>0.36 ± 0.06</b>
chloroquine diphosphate	3	0.20 ± 0.07

K1 strain: multidrug resistant strain; n: number of independent experiments. The test was done with infected human red blood cells.

In Chinese folk medicine, the crude mixture of nine alkaloids present in *Ervatamia yunnanensis* is being used for the treatment of hypertension.<sup>26</sup> These important findings led scientists to evaluate these alkaloids for the activity against malaria,<sup>12</sup> cancer<sup>28</sup> and HIV.<sup>27, 29</sup> However, the scarcity of isolable material from these plants has retarded in depth evaluation.

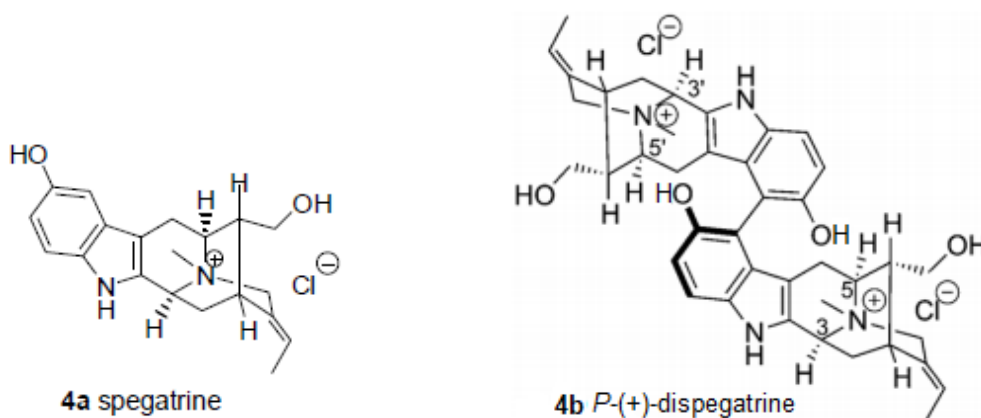


**Figure 2.** Dimeric Indole Alkaloid *-(+)*dispegatrine

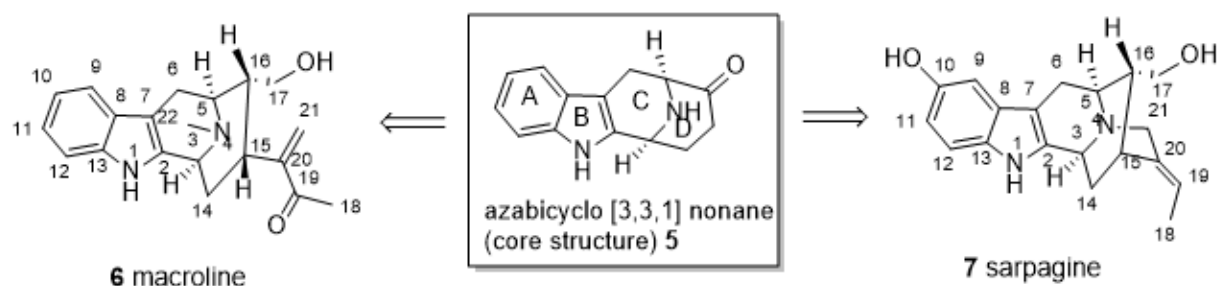


**Figure 3.** Macroline and Sarpagine

The serpagine group of indole alkaloids (represented by **7**, Figure 3) is the largest class of natural products related to the macroline bases. Both the sarpagine and macroline series of indoles have common biogenetic, azabicyclo [3,3,1] nonane core **5**. The biogenetic numbering of LeMen and Taylor<sup>31</sup> is used throughout this Chapter. It can be noted that, in macroline there are four stereocenters at C-3, C-5, C-15 and C-16. The  $\beta$ -hydrogen atom at C-15 of this group, as well as the chiral centers at C-3, C-5 and C-16 are the same for the sarpagine series. In a synthetic sense, both classes can be related by a Michael addition of the nitrogen atom of N-4 of macroline **6** to the  $\alpha$ ,  $\beta$ -unsaturated carbonyl system at C-21, or by direct 1, 2 addition of N-4 to the ketone at C-19 (Figure 4). In the same way, sarpagine can be converted into macroline **6** by a retro-Michael reaction or Hoffmann elimination of the N<sub>b</sub>-methyl intermediate (LeQuésne *et al.*)<sup>21</sup>

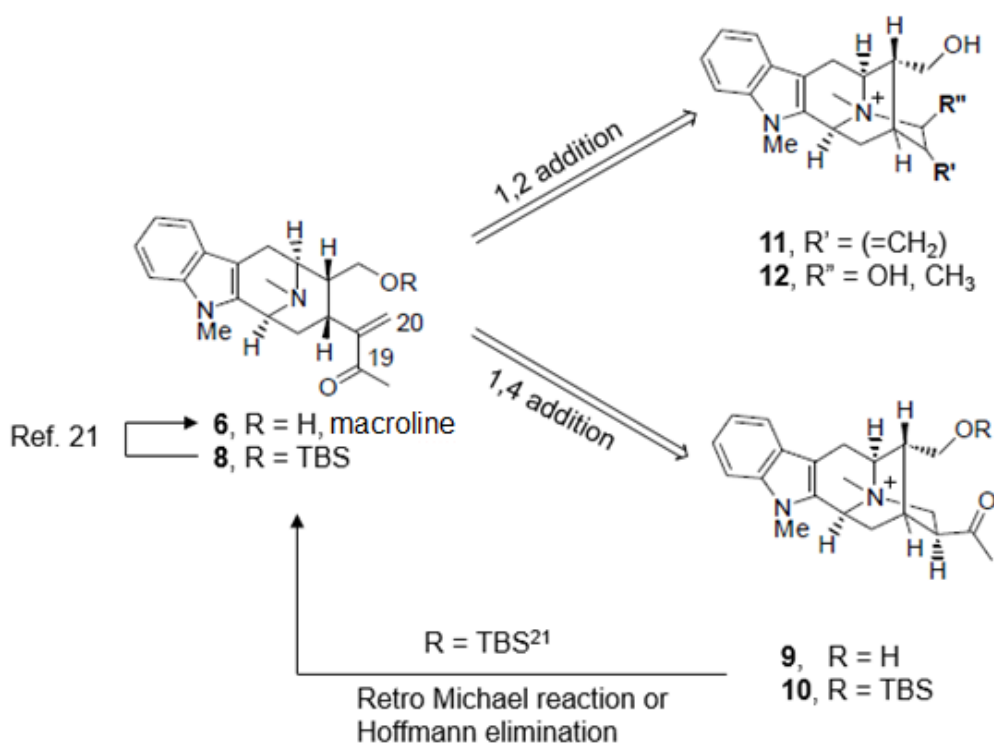
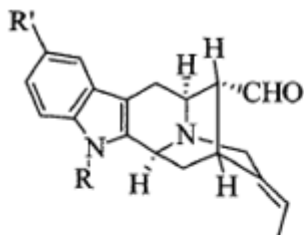
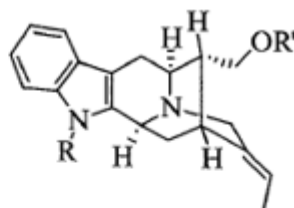


**Figure 4.** Biosynthetic Relationship Between Macroline and Sarpagine.<sup>23</sup>

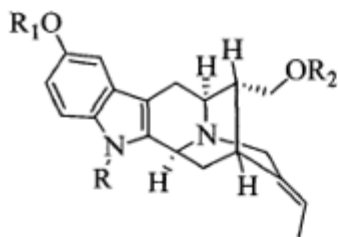
In Figure 5.1-5.12 the different sarpagine related indole alkaloids are presented.



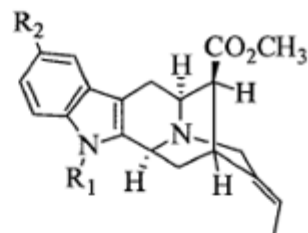
R = H, R' = H, vellosimine  
 R = Me, R' = H, *N*<sub>a</sub>-methylvellosimine  
 R = H, R' = OMe, 10-methoxyvellosimine  
 R = Me, R' = OMe, majvinine



R = H, R' = H, normacusine B  
 R = H, R' = Ac, O-acetylnormacusine B  
 R = H, R' = C(=O)Ph, O-benzoyl normacusine B  
 R = H, R' = Me, O-methylnormacusine B  
 R = Me, R' = H, affinisine

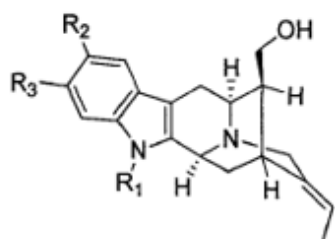


R = R<sub>1</sub> = R<sub>2</sub> = H, sarpagine  
 R = H, R<sub>1</sub> = Me, R<sub>2</sub> = H, lochnerine  
 R = R<sub>1</sub> = H, R<sub>2</sub> = Ac, O-acetylsarpagine  
 R = Me, R<sub>1</sub> = R<sub>2</sub> = H, *N*<sub>a</sub>-methylsarpagine



R<sub>1</sub> = R<sub>2</sub> = H, pericyclivine  
 R<sub>1</sub> = CH<sub>3</sub>, R<sub>2</sub> = H, *N*<sub>a</sub>-methylpericyclivine  
 R<sub>1</sub> = H, R<sub>2</sub> = OH, 10-hydroxy pericyclivine  
 R<sub>1</sub> = H, R<sub>2</sub> = OMe, 10-methoxy pericyclivine  
 R<sub>1</sub> = Me, R<sub>2</sub> = OH, 10-hydroxy-*N*<sub>a</sub>-methylpericyclivine  
 R<sub>1</sub> = Me, R<sub>2</sub> = OMe, 10-methoxy-*N*<sub>a</sub>-methylpericyclivine

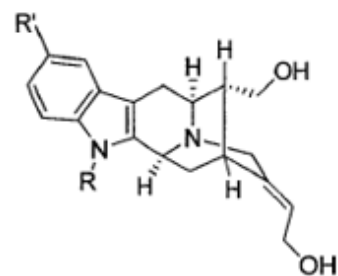
Figure 5.1 Sarpagine indole alkaloids<sup>23, 32</sup>



$R_1=R_3=H$ ,  $R_2=OH$ , 16-episarpagine

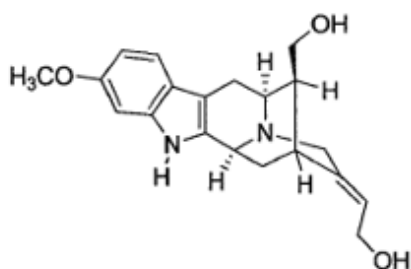
$R_1=R_3=H$ ,  $R_2=OMe$ , lochvinerine

$R_1=R_2=H$ ,  $R_3=OCH_3$ , gardnerine

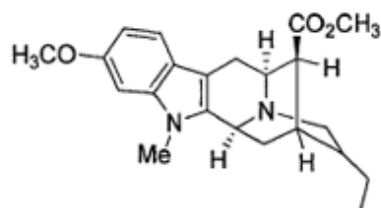


$R'=OMe$ ,  $R=H$ , 18-hydroxy lochnerine

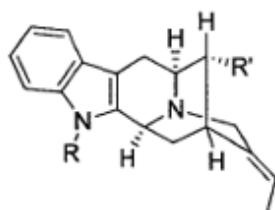
$R'=H$ ,  $R=Me$ , 18-hydroxy affinisine



18-hydroxygardnerine



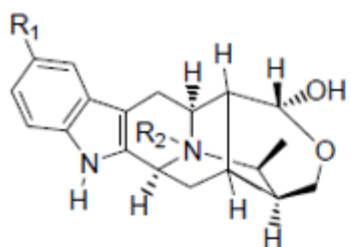
11-methoxy- $N_a$ -methyl-dihydro-pericyclivine



$R=H$ ,  $R'=CH=CHCOCH_3$ , difforine

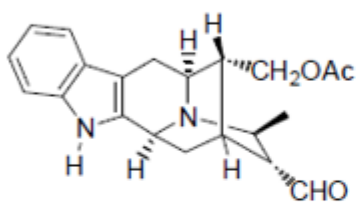
$R=CH_3$ ,  $R'=CO_2CH_3$   
 $N_a$ -methyl-16-epipericyclivine

Figure 5.2 Sarpagine indole alkaloids<sup>23, 32</sup>

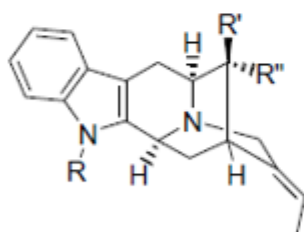


$R_1=OH$ ,  $R_2=CH_3$   
verticillatine (Cl salt)

$R_1=H$ , peraksine  
(vomifoline)



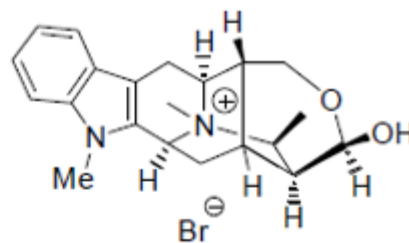
O-acetylpreperakine



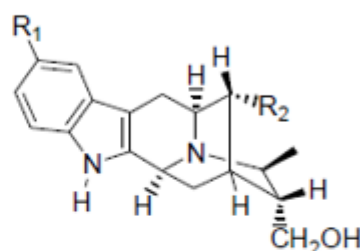
$R=R''=H$ ,  $R'=CH_2OH$ ,  
16-epinormacusine B

$R=Me$ ,  $R'=CH_2OH$ ,  $R''=H$ ,  
16-epiaffinisine

$R=Me$ ,  $R'=CH_2OAc$ ,  $R''=H$ ,  
O-acetyl-16-epiaffinisine



macrosalhin bromide

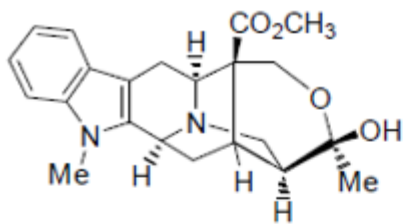


$R_1=H$ ,  $R_2=CH_2OH$ ,  
19(S),20(R)-dihydroperaksine

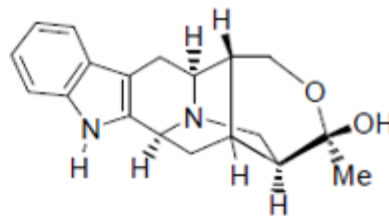
$R_1=OH$ ,  $R_2=CH_2OH$ ,  
10-hydroxy-19(S),20(R)-  
dihydroperaksine

$R_1=H$ ,  $R_2=CHO$ ,  
19(S),20(R)-dihydroperaksine-17-  
al

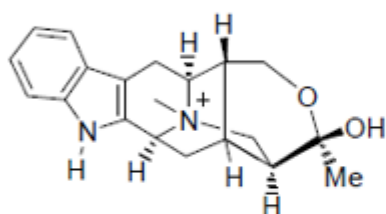
Figure 5.3 Sarpagine indole alkaloids<sup>23, 32-35</sup>



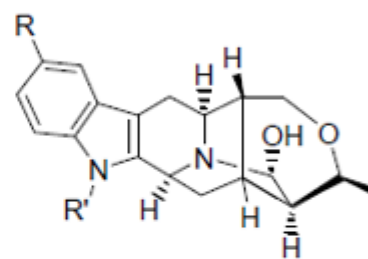
voacoline



trinervine

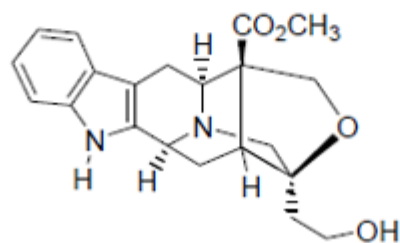


venecurine



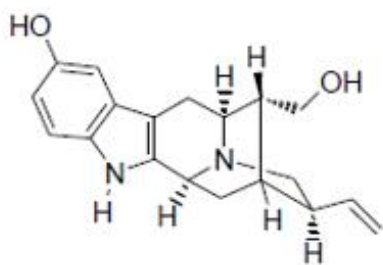
R=H, R'=Me, talpinine

R=OMe, R'=H, 21-hydroxy  
cyclolochnerine

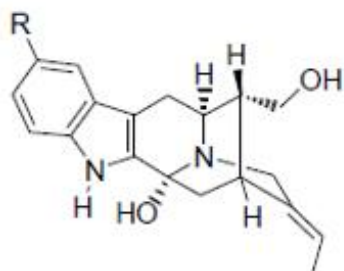


eburnaphylline

Figure 5.4 Sarpagine indole alkaloids<sup>23, 32</sup>

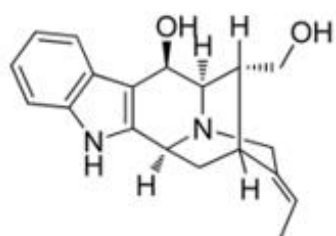


neo-sarpagine

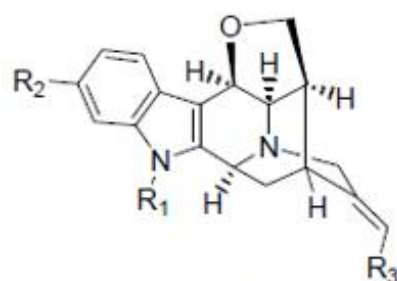


R=H,  
*N<sub>a</sub>*-demethylaccedine  
(amerovolfine)

R=OH, 3-hydroxysarpagine



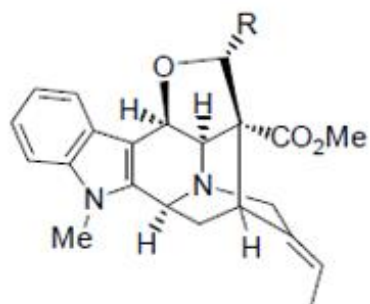
ervincidine



R<sub>1</sub>=CH<sub>3</sub>, R<sub>2</sub>=H, R<sub>3</sub>=CH<sub>3</sub>,  
dehydro-16-epiaffinisine

R<sub>1</sub>=H, R<sub>2</sub>=OCH<sub>3</sub>, R<sub>3</sub>=CH<sub>3</sub>,  
gardnutine

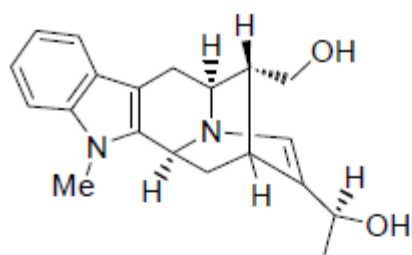
R<sub>1</sub>=H, R<sub>2</sub>=OCH<sub>3</sub>, R<sub>3</sub>=CH<sub>2</sub>OH,  
18-hydroxygardnutine



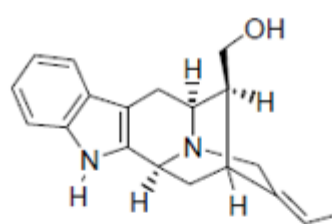
R=H, dehydrovoachalotine

R=OH, 17-hydroxy-  
dehydrovoachalotine

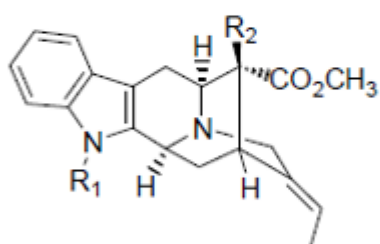
Figure 5.5 Sarpagine indole alkaloids<sup>23, 32, 36-39</sup>



alstoumerine



koumidine

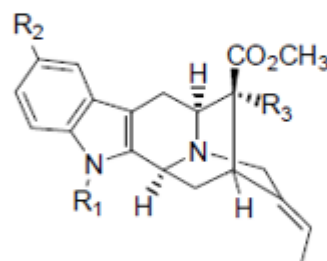


$R_1=H$ ,  $R_2=CHO$ ,  
polyneuridine aldehyde

$R_1=H$ ,  $R_2=CH_2OH$ , polyneuridine

$R_1=CH_3$ ,  $R_2=CHO$ , voachalotinal

$R_1=CH_3$ ,  $R_2=CH_2OH$ , voachalotine

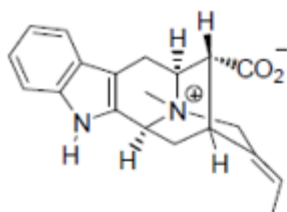


$R_1=R_2=H$ ,  $R_3=CH_2OH$ ,  
E-akuammidine

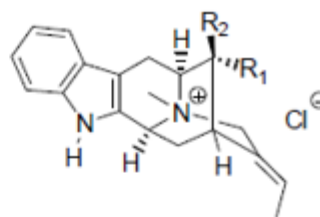
$R_1=R_2=H$ ,  $R_3=CH_2OAc$ ,  
acetylakuammidine

$R_1=CH_3$ ,  $R_2=OCH_3$ ,  $R_3=CH_2OH$ ,  
10-methoxy- $N_\alpha$ -methylakuammidine

Figure 5.6 Sarpagine indole alkaloids<sup>23, 32</sup>



panarine



$R_1=CH_2OH$ ,  $R_2=H$ , macusine B

$R_1=CH_2OCH_3$ ,  $R_2=H$ ,  
O-methylmacusine B

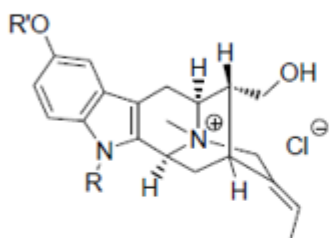
$R_1=CO_2CH_3$ ,  $R_2=H$ , alkaloid Q3

$R_1=H$ ,  $R_2=CH_2OCH_3$ ,  
O-methyl-16-epimacusine B

$R_1=H$ ,  $R_2=CO_2^-$ , 16-epipanarine

$R_1=CO_2CH_3$ ,  $R_2=CH_2OH$   
macusine A

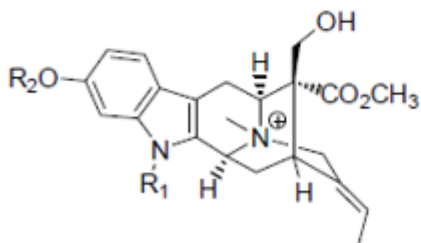
$R_1=CH_2OH$ ,  $R_2=CO_2CH_3$ ,  
 $N_b$ -methylakuammidine



$R=H$ ,  $R'=H$ , spegatrine

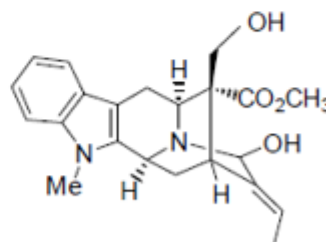
$R=H$ ,  $R'=Me$ , lochneram

$R=Me$ ,  $R'=H$ ,  
 $N_a$ -methylsarpagine metho salt



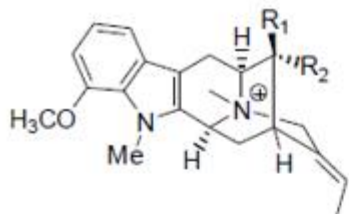
$R_1=CH_3$ ,  $R_2=H$ ,  
 $N_a$ -methyl-11-hydroxymacusine A

$R_1=H$ ,  $R_2=CH_3$ ,  
11-methoxymacusine A



21-hydroxyvoachalotine

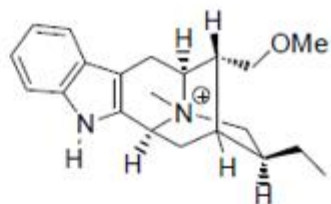
Figure 5.7 Sarpagine indole alkaloids<sup>23, 32</sup>



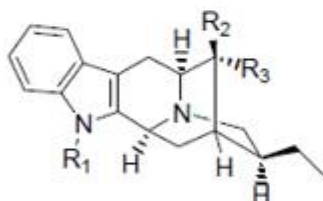
$R_1=H$ ,  $R_2=CO_2Et$ , fuchsiaefoline

$R_1=CH_2OH$ ,  $R_2=CO_2Me$ ,  
12-methoxy-*N*<sub>b</sub>-methylvoachalotine

$R_1=CH_2OH$ ,  $R_2=CO_2Et$   
12-methoxy-*N*<sub>b</sub>-methylvoachalotine  
ethyl ester



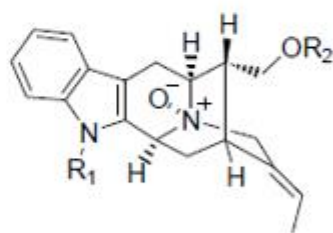
19,20-dihydro-O-methylmacusine B



$R_1=H$ ,  $R_2=CO_2CH_3$ ,  $R_3=CH_2OH$ ,  
19,20-dihydroakuummidine

$R_1=H$ ,  $R_2=CH_2OH$ ,  $R_3=CO_2CH_3$ ,  
19,20-dihdropolyneuridine

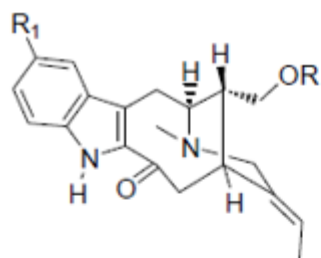
$R_1=CH_3$ ,  $R_2=CH_2OAc$ ,  $R_3=CO_2CH_3$ ,  
17-O-acetyl-19,20-dihydrovoachalotine



$R_1=CH_3$ ,  $R_2=H$ , affinisine *N*<sub>b</sub>-oxide

$R_1=H$ ,  $R_2=CH_3$ ,  
O-methylnormæusine B *N*<sub>b</sub>-oxide

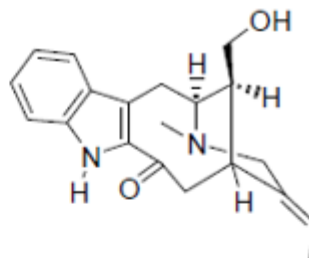
Figure 5.8 Sarpagine indole alkaloids<sup>23, 32</sup>



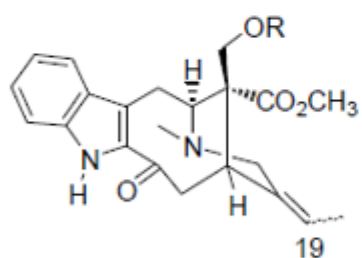
R = R<sub>1</sub> = H, 16-epiaffinine

R = Me, R<sub>1</sub> = H, hystrixnine

R = H, R<sub>1</sub> = OMe, pelirine



affinine

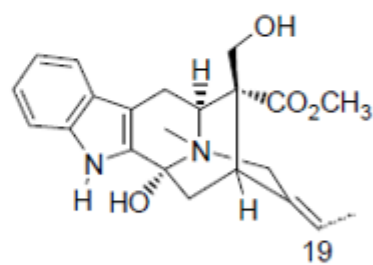


R = H, 19E, gelsempervine-A

R = Ac, 19E, gelsempervine-B

R = H, 19Z, gelsempervine-C

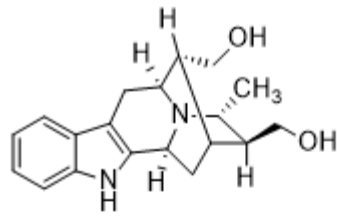
R = Ac, 19Z, gelsempervine-D



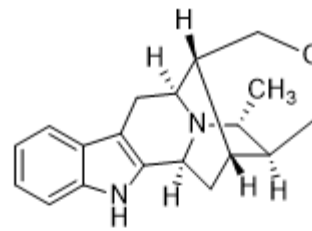
19Z, 19Z-16-epivoacarpine

19ZE, 19E-16-epivoacarpine

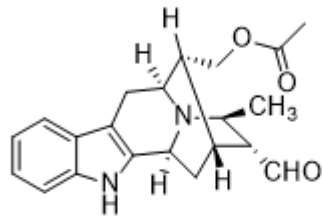
Figure 5.9 Sarpagine indole alkaloids<sup>23, 40-44</sup>



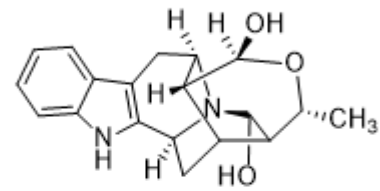
dihydroperaksine



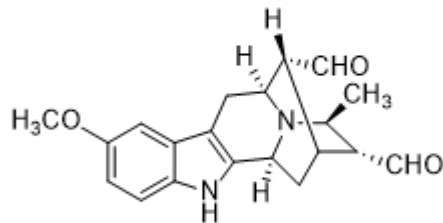
deoxyperaksine



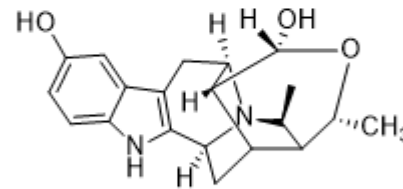
O-acetylperaksine



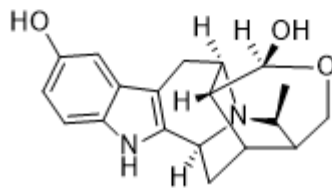
rauvovertine A



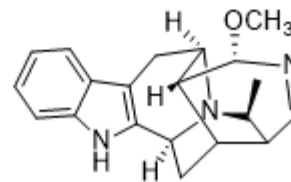
vinmajine F



rauvovertine B

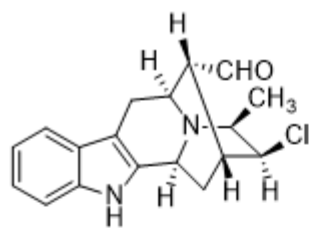


17-epi-rauvovertine B

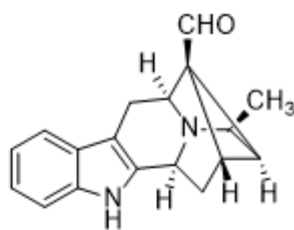


rauvovertine C

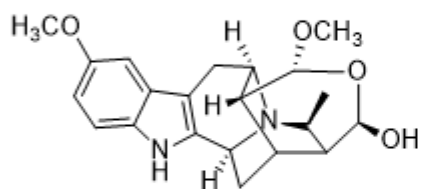
Figure 5.10 Sarpagine indole alkaloids<sup>45</sup>



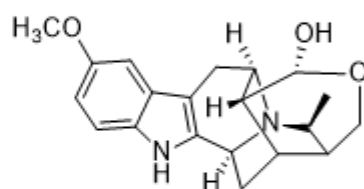
rauvomine A



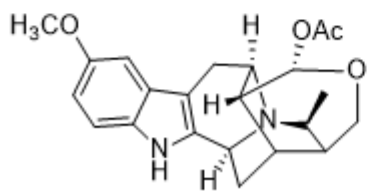
rauvomine B



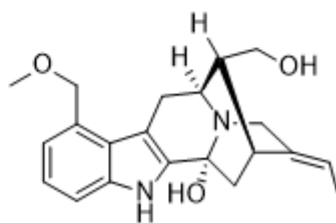
vinmajorine C



vinmajorine D



vinmajorine E



rauvomitorine A

Figure 5.11 Sarpagine indole alkaloids<sup>45, 46</sup>

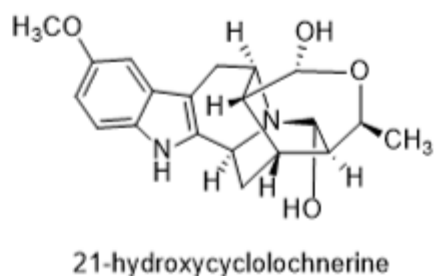
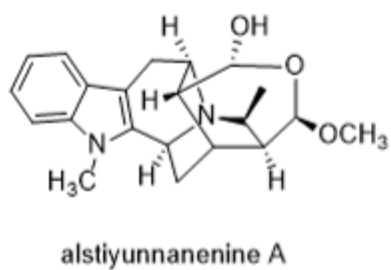
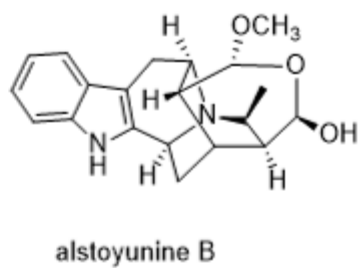
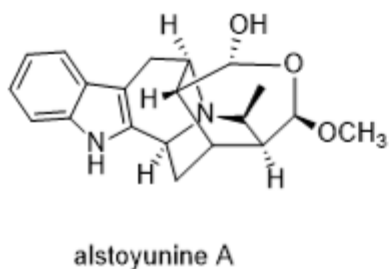
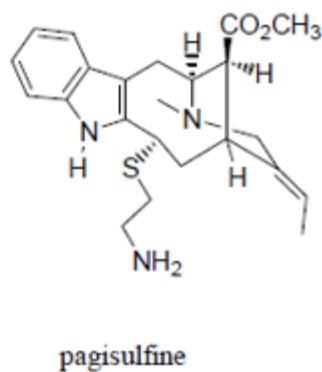
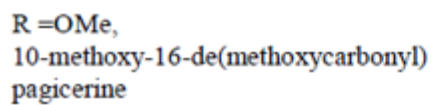
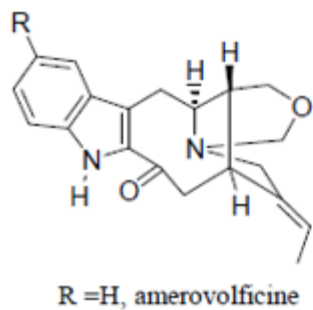
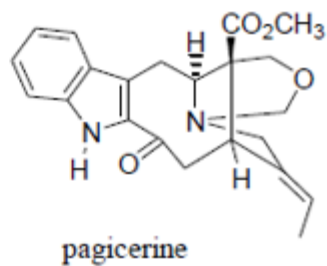
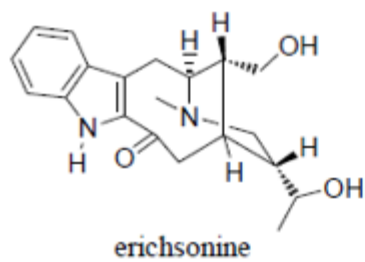
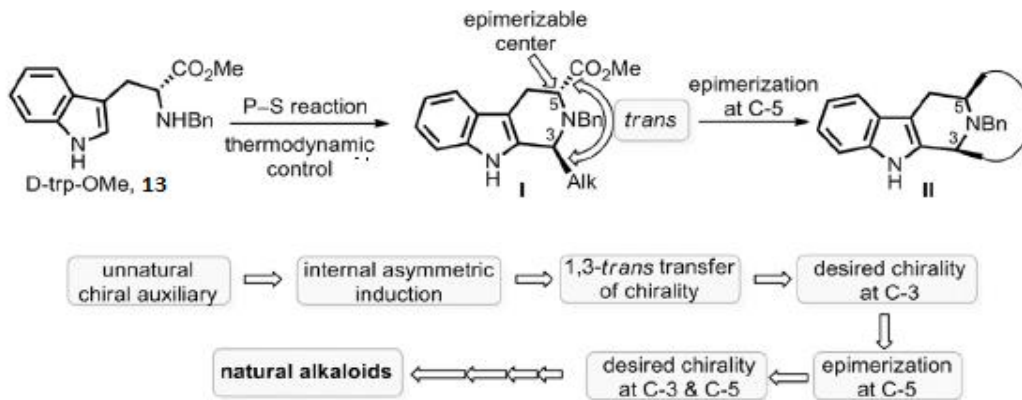


Figure 5.12 Sarpagine indole alkaloids<sup>37, 45, 47-50</sup>

## 1.2 Access to the tetracyclic core of sarpagine/macroline alkaloids

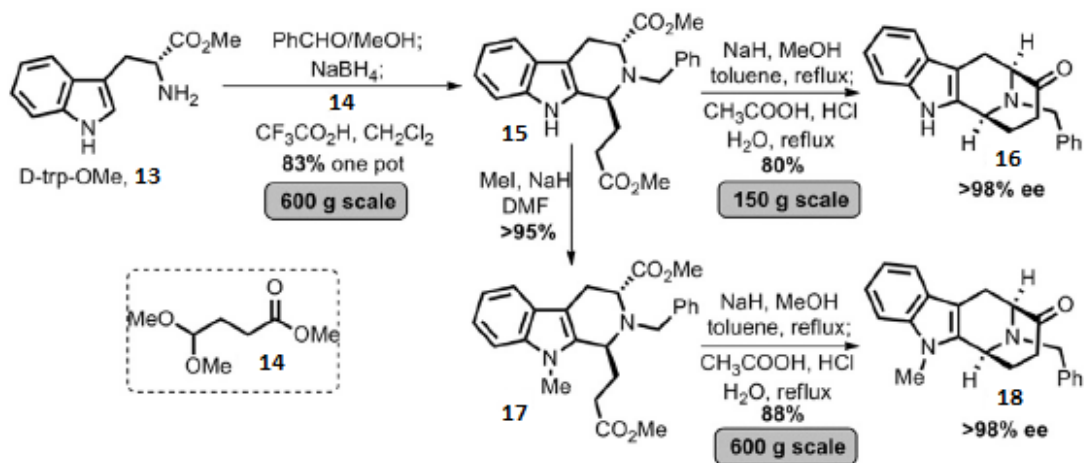
As mentioned before, the tetracyclic ketone **5** is the common intermediate towards the synthesis of the majority of the alkaloids of the sarpagine and macroline family of alkaloids, it has been used extensively for the total synthesis of indole alkaloids as well as oxindoles.<sup>51-55</sup> Hence the synthesis of this tetracyclic core enantiospecifically on large scale and maintenance of the correct stereochemistry at C-3 and C-5 position is of great importance. Some important contributions from Hobson<sup>56</sup>, Yoneda<sup>57</sup>, Kluge<sup>58</sup>, Mashimo<sup>59</sup>, Soerens<sup>60</sup>, Sakai<sup>61</sup>, Zhang,<sup>62</sup> Bailey<sup>63</sup>, Sandrin<sup>64</sup>, and Ungemach<sup>65</sup> have paved the way for the large-scale synthesis in multihundred gram scale with greater than 98% *ee* to this key [3.3.1] system.

Commercially available D-tryptophan methyl ester **13**, serves as the chiral auxiliary in the asymmetric Pictet-Spengler reaction which exerts an internal asymmetric induction which sets the natural stereochemistry at the biogenetic C-3<sup>31</sup> position of alkaloids via the 1,3-trans transfer of chirality.<sup>66</sup> This process produced the 1,3-trans-diester (**I**) with 100% diastereoselectivity under thermodynamically controlled conditions; the C-3 carbon atom can undergo epimerization to give pure trans. Then a large scale (300g) Dieckmann condensation occurs by base catalyzed epimerization at C-5 and ring closure. The subsequent Dieckmann conditions were important for, the C-5 stereocenter first epimerizes to the desired cis configuration at C-5, and the cis-diester then cyclized intramolecularly to give the desired [3,3,1] bicyclic system (**II**) with the correct stereochemistry at C-3 (S) and C-5 (S) positions. (Scheme 1).



**scheme 1.** A schematic flow chart of the P-S/Dieckmann protocol (picture modified from Rahman *et al.*<sup>66</sup>)

The current practice of synthesizing this tetracyclic core, developed in Milwaukee<sup>67</sup> employs a two-pot procedure for accessing the N<sub>a</sub>-H or N<sub>a</sub>-Me, N<sub>b</sub>-benzyl tetracyclic ketones on a multihundred gram-scale in high yield and enantiomeric excess (> 98% *ee*).<sup>66</sup>

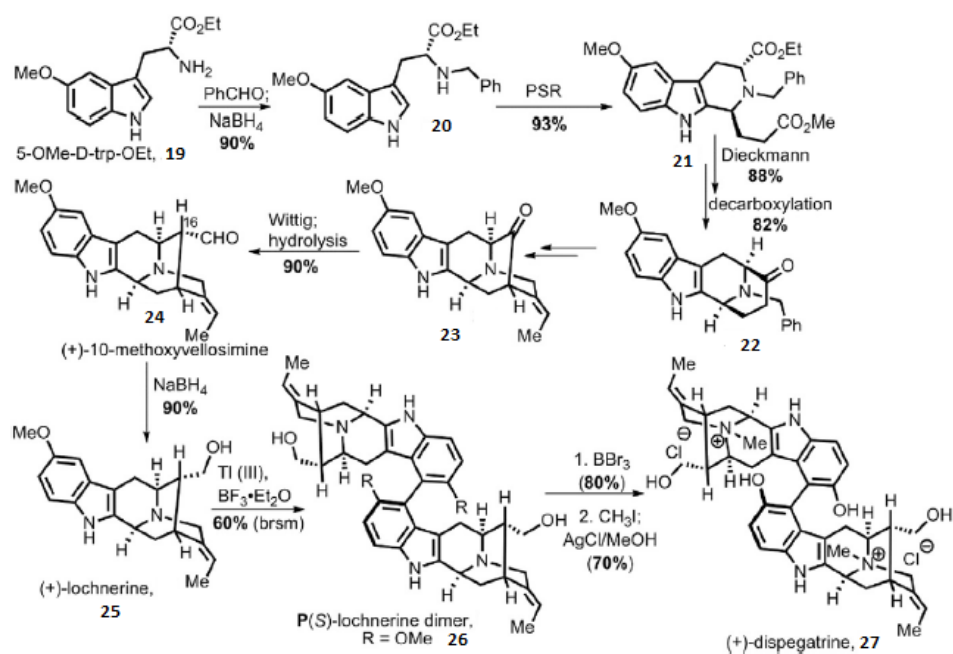


**Scheme 2.** Synthesis of tetracyclic core developed in Milwaukee (picture modified from Rahman *et al.*<sup>66</sup>)

The iminium species **15** could be formed when N<sub>b</sub>-benzylation of D-tryptophan methyl ester **13** was condensed with benzaldehyde in methanol at room temperature followed by NaBH<sub>4</sub> - mediated reduction at -10°C. The crude mixture is then reacted thermodynamically with methyl 4,4-dimethoxybutyrate **14** in presence of TFA to furnish the 1,3-trans diester **15** without any chromatographic separation. After that, the **15** (or N<sub>a</sub> – Me diester **17**) can be converted into the tetracyclic ketone **16** and **18**, respectively through Dieckmann cyclization by heating it in toluene with an excess of NaOMe, generated in situ with NaH and dry MeOH in toluene followed by acid hydrolysis. (Scheme 2).

## 1.3 Current examples of total synthesis of indole and oxindole alkaloids

### 1.3.1 The total synthesis of dispegatrine by Edwankar et al.



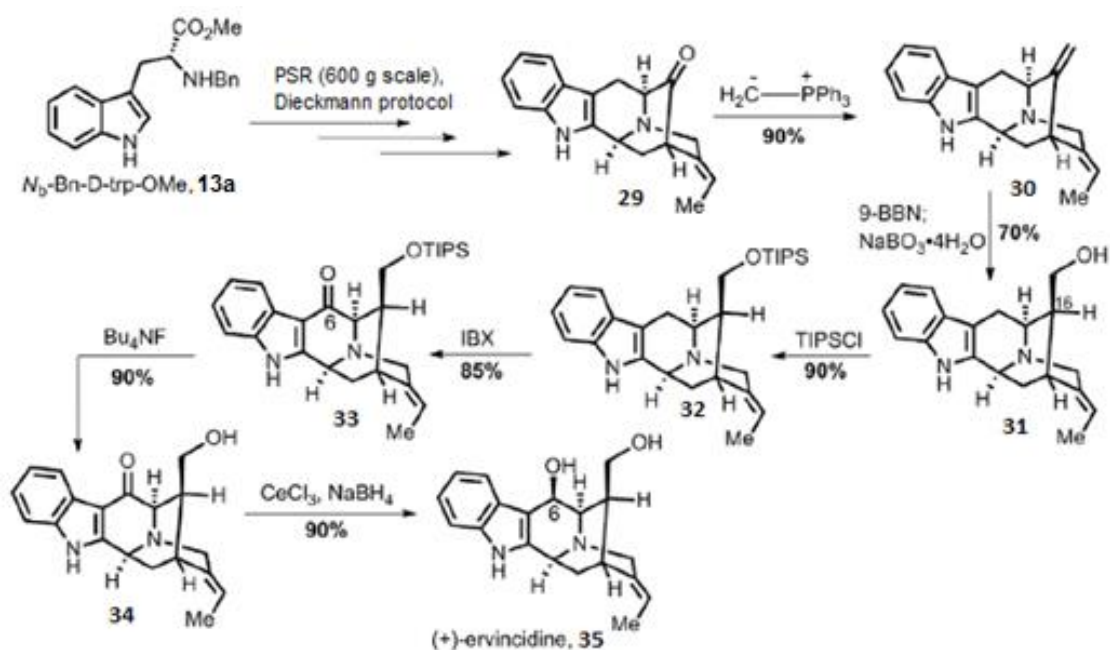
**Scheme 3.** Total synthesis of dispegatrine by Edwankar et al. (picture modified from Rahman et al.<sup>66</sup>)

The quaternary dimeric sarpagine alkaloid dispegatrine **27**, isolated from *Rauwolfia verticillata* (Lour.) var. *hainanensis* Tsiang, exhibited potent antihypertensive activity<sup>15</sup> and was found to be more active in blocking  $\alpha$ -adrenergic receptors<sup>16</sup> than its corresponding monomeric unit spegatrine (not shown). For the total synthesis of dispegatrine, Edwanker *et al.* employed the

previously mentioned reaction protocol of the P-S/Dieckmann process to access the 10-methoxy N<sub>a</sub>-H, N<sub>b</sub>-benzyl tetracyclic ketone **22**, which began from 5-methoxy D-tryptophan ethyl ester **19** on large scale and in >98% ee. This tetracyclic ketone was then converted into the pentacyclic ketone **23** via a palladium-catalyzed intramolecular  $\alpha$ -vinylation of the ketone (not shown here). The synthesis of 10-methoxyvellosimine **24** with the C-16 aldehyde in the more stable and desired  $\alpha$ -orientation was then achieved through a one-carbon homologation of the ketone **23** via a Wittig olefination, followed by acidic hydrolysis. The reduction of the aldehyde **24** with NaBH<sub>4</sub> provided the alkaloid lochnerine **25** in excellent yield. The P(S) atropodiastereomer of the lochnerine dimer **26** was then synthesized selectively via a thallium (III) acetate mediated oxidative coupling of **25**. Then the first total synthesis of dispegatine **27** as the chloride salt was achieved by the subsequent demethylation of the aryl methyl ether with BBr<sub>3</sub> and quaternization of the N<sub>b</sub>-nitrogen function with iodomethane in the presence of AgCl. (Scheme 3.) The stereochemistry of the C(9)-C(9') bond was P(S) as demonstrated by low temperature X-ray analysis of the lochnerine dimer.

### 1.3.2 The total synthesis of ervincidine, by Rallapalli et al.

The first total synthesis of ervincidine<sup>68</sup> **35**, a sarpagine alkaloid isolated from *Vinca erecta* Rgl. et Schmalh, contains a hydroxyl functional group at the C-6 position and a hydroxymethyl group at the C-16 position was reported by Ralapalli *et al.*<sup>69</sup> in 2014. Starting from N<sub>b</sub>-benzyl-D-tryptophane methyl ester **13a** and following the process mentioned before, which was developed in Milwaukee, the pentacyclic ketone **29** was synthesized on large scale.

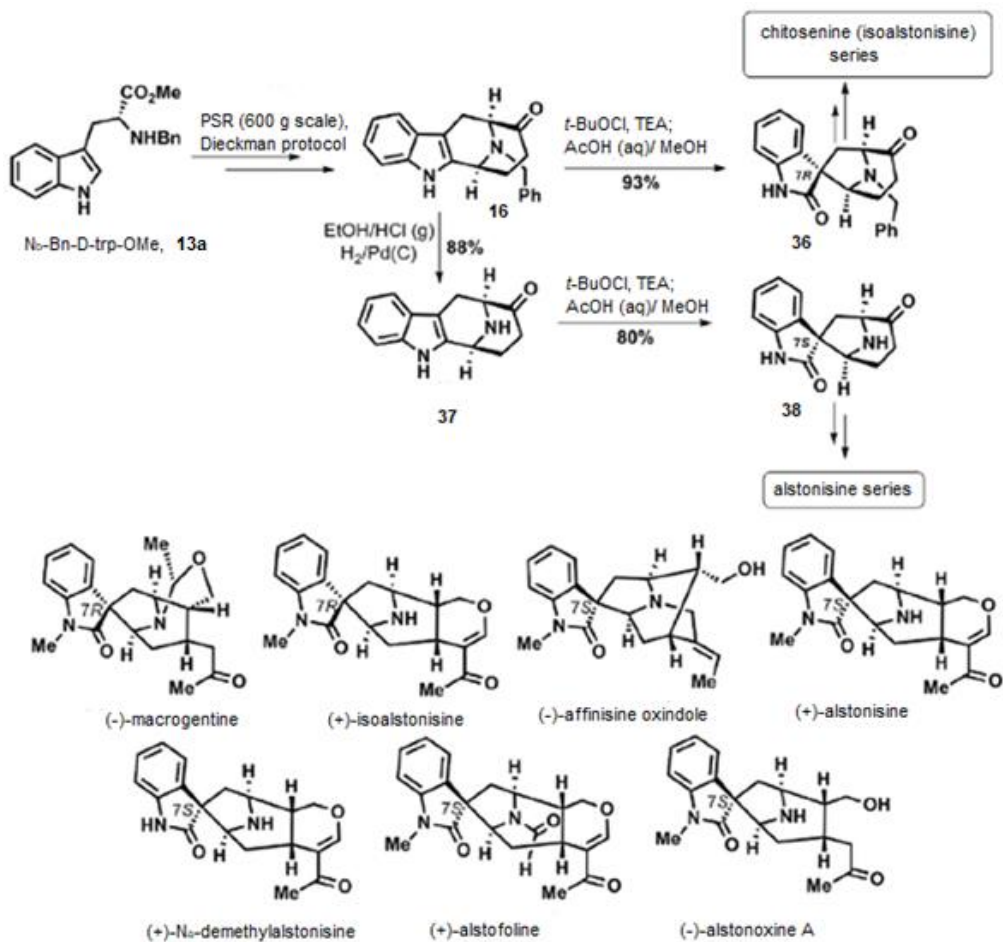


**Scheme 3a.** Total synthesis of ervincidine by Ralapalli et al. (picture modified from Rahman et al.<sup>66</sup>)

The ketone **29** was then converted to **30** via a Wittig olefination reaction. The olefin **30** was then converted to the hydroxymethyl function **31** with the desired  $\beta$ - orientation at C-16 position via a hydroboration-Kabalka oxidation reaction. The hydroxyl group of **31** was then protected with a TIPS group to get **32**, followed by an IBX-mediated radical oxidation process to introduce the ketone function (**33**) at the benzylic C-6 position in high yield. It was then reduced under Luche reduction conditions after deprotecting the silyl group to furnish ervincidine **35**. The spectral and optical properties of this diastereomer were in excellent agreement with the natural ervincidine<sup>20, 68</sup>(Scheme 3a).

### 1.3.3 The total synthesis of alstonisine- and chitosenine-type oxindole alkaloids by Fonseca et al.

The total synthesis of a number of oxindole alkaloids were reported by Fonseca *et al.*<sup>70, 71</sup> through the same tetracyclic intermediate **16**. A series of oxindole alkaloids from both the chitosenine (7*R*) and alstonisine (7*S*) class has been synthesized using the N<sub>b</sub>-benzyl tetracyclic ketone **16** as the



**Scheme 4.** Strategy towards the total synthesis of some alstonine related indole alkaloids by Fonseca et al. (picture modified from Rahman et al.<sup>66</sup>)

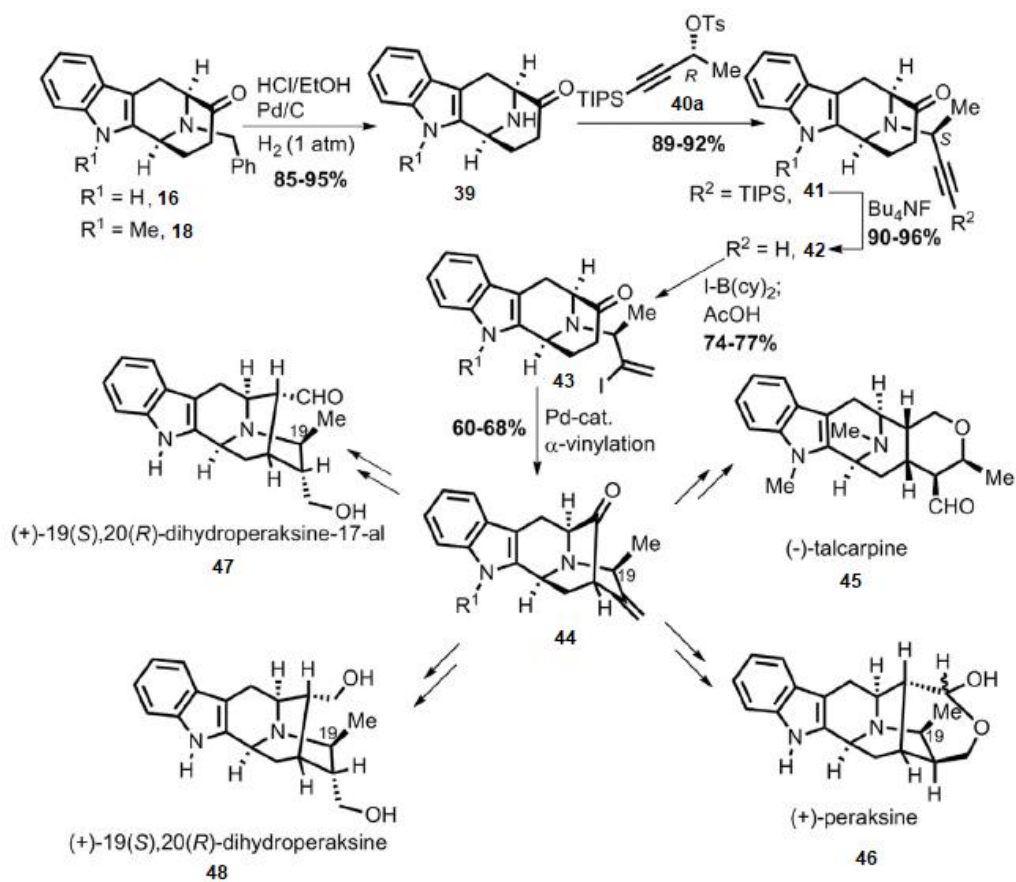
key intermediate<sup>71</sup>. The diastereospecific access to *spiro*-oxindole **36** with the C-7(*R*) configuration was achieved via tert-butyl hypochlorite mediated oxidative rearrangement of the N<sub>b</sub>-benzyl tetracyclic ketone **16**. On the other hand, the oxidative rearrangement on the debenzylated amine **37**, mediated by the tert-butyl hypochlorite provided the *spiro*-oxindole **38** with the

opposite C-7(S) configuration. The intermediates **37** and **38** were then used to synthesize the alstonisine related oxindole alkaloids including affinisine oxindole, alstonisine, N<sub>a</sub>-demethylalstonisine, alstofoline, and alstonoxine A (Scheme 4; synthesis not discussed here).

### 1.3.4 General synthetic strategy for the total synthesis of C-19 methyl-substituted sarpagine/macroline/ajmaline alkaloids by Edwankar *et al.*

The first total synthesis of several C-19 methyl substituted sarpagine/macroline indole alkaloids have been reported by Edwankar *et al.* using the previously mentioned strategy (scheme 5). Starting from D-tryptophan methyl ester, the general strategy towards the synthesis of the C-19 methyl substituted alkaloids followed the P-S/Dieckmann protocol to access the tetracyclic ketone **16** (R<sup>1</sup> = H) or **17** (R<sup>1</sup> = Me) on large scale. This was followed by the debenzoylation of **16** or **17** respectively. Then the optically pure (R)-tosylate unit **40a** was reacted with the N<sub>b</sub>-nitrogen atom of amine **39** by an S<sub>N</sub>2 alkylation to furnish **41**, which contain the C-19(S) methyl equivalent function. The terminal alkyne **42** was achieved by the deprotection of the TIPS group in excellent yield. A novel haloboration reaction using dicyclohexyliodoborane followed by protodeboronation and provided the vinyl iodide **43**. Then the pentacyclic ketone was synthesized through a palladium-catalyzed intramolecular  $\alpha$ -vinylation of the ketone **43** which was then used as a common intermediate for several members of C-19 methyl-substituted alkaloid subfamily (scheme 6). This strategy was then employed by Edwankar *et al.* to furnish the

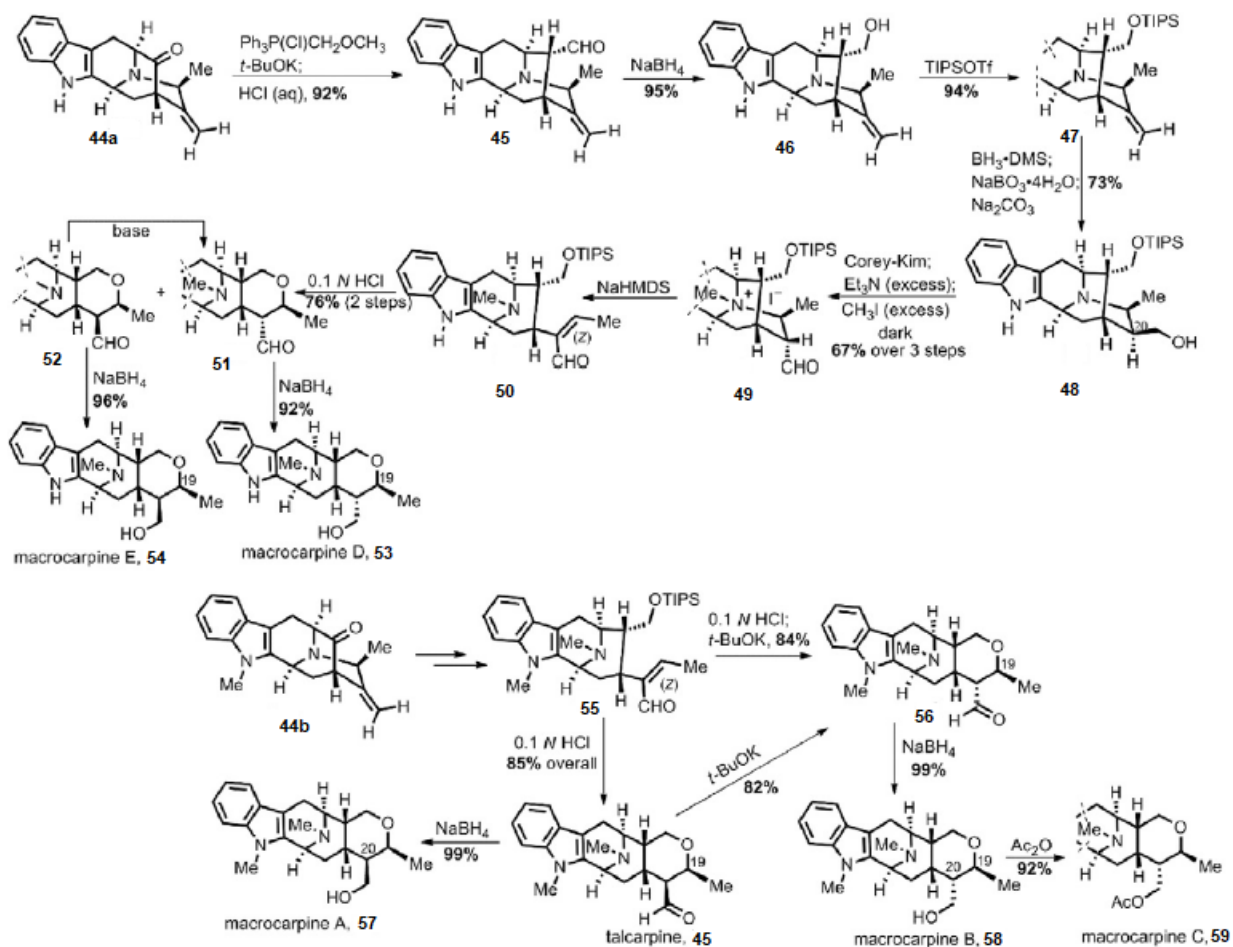
first total synthesis of 19(*S*), 20(*R*)-dihydroperaksine-17-al **47** and 19(*S*), 20(*R*)-dihydroperaksine **48**. Later a similar strategy was employed by Rahman *et al.* to sththesyze (-)-talcarpine **45**<sup>72</sup>.



**Scheme 6.** General strategy towards the synthesis of C-19 methyl- substituted sarpagine /Macroline /ajmaline alkaloids by Edwankar *et al.* (picture modified from Rahman *et al.*<sup>66</sup>)

### 1.3.5 Total synthesis of C-19 methyl substituted macroline-type indole alkaloids by Rahman *et al.*<sup>72</sup>

The first total synthesis of some C-19 substituted macroline-type indole alkaloids was reported by Rahman *et al.*<sup>72</sup> where the core synthetic strategy was to use the pentacyclic ketone **44a** as a common precursor. This was followed by a one carbon homologation via a Wittig reaction and hydrolysis. The ketone **44a** which formed, was converted into the aldehyde **45** in the desired  $\alpha$ -orientation at C-16 in excellent yield. The silyl ether **47** was synthesized by the sodium borohydride mediated reduction and this was followed by protection of the primary alcohol **46** by the TIPS group.



**Scheme 7.** Total synthesis of some C-19 substituted macroline-type indole alkaloids by Rahman *et al.*<sup>66, 72</sup>

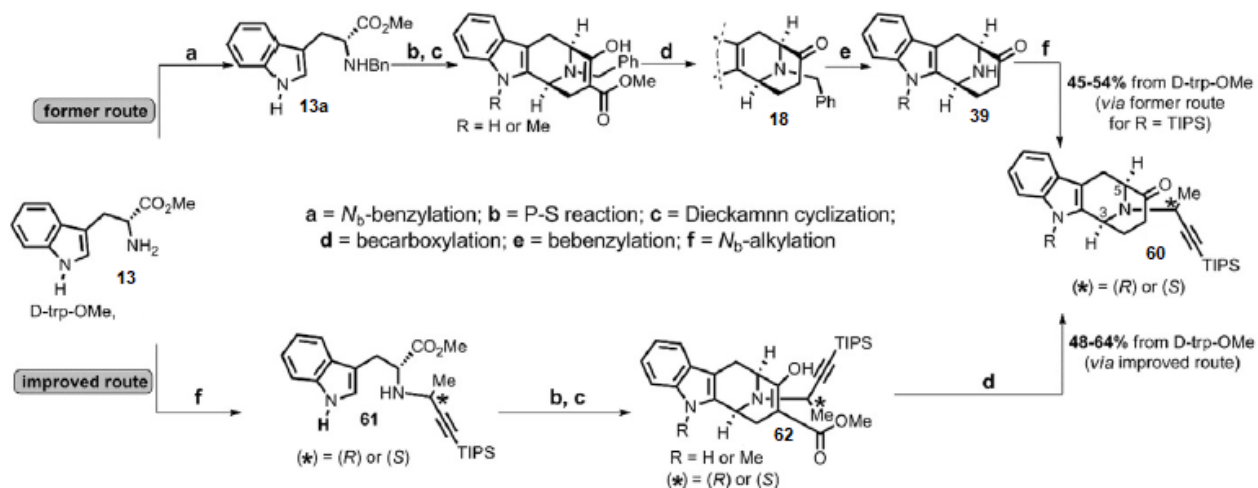
The olefin **47** was subjected to a hydroboration-Kabalka oxidation sequence to furnish the primary alcohol **48** in good yield. Then by following the Corey-Kim oxidation protocol this gave the  $\alpha$ -epimer of the aldehyde at C-20, which was then allowed to react with excess methyl iodide to provide the methiodide salt **49** in 67% yield over three steps. The enal **50** was then synthesized

via a retro-Michael ring opening of the  $\beta$ -quaternary ammonium carbonyl compound **49**, with the desired (*Z*)-geometry across the olefinic double bond. After deprotecting the TIPS group, the so formed alcohol underwent an intramolecular Michael reaction with the  $\alpha,\beta$ -unsaturated carbonyl function to provide a mixture of  $\alpha$ - and  $\beta$ -epimers of aldehyde (**51** and **52**, respectively) in good, combined yield. The  $\alpha$ -epimer **51** could be synthesized from  $\beta$ -epimer **52** on the treatment with base. The synthesis of macrocarpine D **53** and macrocarpine E **54** was then achieved, in excellent yield, by reducing the aldehyde function of **51** and **52** respectively with sodium borohydride (Scheme 7).

The pentacyclic ketone **50b** was used as a common precursor for some other C-19 methyl substituted macrolin-type indoles. Using a similar general strategy, the **50b** was converted into the enal **55**<sup>73</sup>, the (*Z*) stereochemistry of which was confirmed by NOE, NMR and HR mass spectroscopy. Following the same synthetic strategy analogous to the above section, the synthesis of  $\alpha$ -C-20 aldehyde, N<sub>4,21</sub>-secotalpinine **56** and  $\beta$ -C-20 aldehyde, talcarpine **45** was achieved. The reduction of aldehyde **45** provided the macrocarpine A **57** whereas the reduction of aldehyde **56** provided the macrocarpine B **58** in excellent yield. Interestingly the aldehyde **45** can be converted to aldehyde **56** with the treatment of base in good yield. The macrocarpine C was synthesized through the simple acylation of **58**, in good yield.

### 1.3.6 Access to the common bicyclo [3,3,1] tetracyclic system in reduced steps by Rahman *et al.*

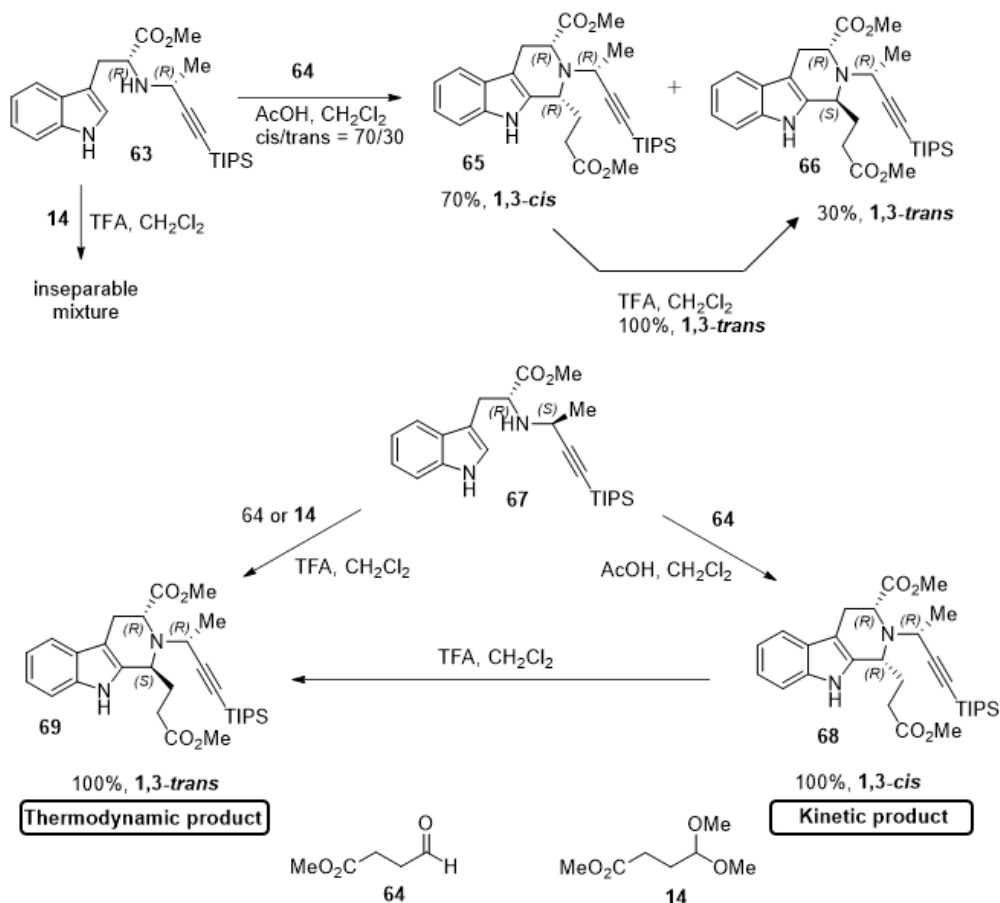
The previously established protocol<sup>67</sup> for the synthesis of the N<sub>b</sub>-H bicyclo [3,3,1] tetracyclic core **37** involved the benzylation and debenylation of the N<sub>b</sub>-4 nitrogen atom of the tetracyclic core in the sequence. To introduce the C-19(*S*) methyl function into the tetracyclic system **39**, a S<sub>N</sub>2 reaction was carried out on an optically pure (*R*)-tosylate (e.g., **40a**) by Edwankar *et al.* (Scheme 6) after debenylation of **18**. In order to reduce these two steps to incorporate either the C-19(*S*) or C-19(*R*) methyl functions into the natural products (since both *S*- and *R*-methyl groups at C-19 could be found in alkaloids), Rahman *et al.* developed a method to alkylate the N<sub>b</sub>-nitrogen function of D-tryptophan methyl ester **13a** earlier by reacting it with either the (*R*)- or (*S*)-tosylates (**40a** and **40b**, individually) to synthesize the N<sub>b</sub>-ethynyl derivatives **61** (scheme 8). The β-keto esters, represented by the tertiary amines **62** were synthesized in high yield through the asymmetric Pictete-Spengler reaction, followed by the Dieckman reaction. Which were then subjected to the acidic condition with heating to provide the N<sub>b</sub>-ethynyletethered tetracyclic ketones **60** (with *R*- and *S*-methyl functions) individually in 48 to 64% overall yield by loss of CO<sub>2</sub>. This was two steps shorter than the previously developed method<sup>73</sup>. (Scheme 8)



**Scheme 8.** Access to the common bicyclo [3,3,1] tetracyclic system in reduced steps by Rahman *et al.*<sup>72</sup>

### 1.3.7 100 percent Stereoselectivity in the asymmetric Pictet-Spengler reaction by Rahman *et al.*

From the recent studies carried out by Rahman *et al.*<sup>73</sup> various experimental results with unprecedented stereoselectivity were achieved with controlling the reaction conditions of the Pictet-Spengler reaction, both thermodynamically and kinetically. For example, the D-tryptophan derivative with an (R)-methyl substituted ethynyl group tethered to the  $N_b$ -nitrogen atom **63** resulted in a complex, inseparable reaction mixture under the common thermodynamic conditions



**Scheme 9.** Stereoselectivity in the asymmetric Pictet-Spengler reaction by Rahman et al.

of the Pictete-Spengler reaction using the acetal **14**, whereas the 1,3-*trans* diester **69** could be synthesized from the (*S*)-methyl derivative **67** as the sole product in excellent yield under the same condition developed previously (Scheme 9). It was also found that under mild acidic condition the 1,3-*cis* diester could be synthesized as a kinetic product using **64**, whereas the use of TFA and either **14** or **64** facilitated the thermodynamically more stable 1,3-*trans* diester **69**. Interestingly, the 1,3-*cis* diester **68** could be converted to the 1,3-*trans* **69** diester on treatment

with TFA in excellent yield (Scheme 9). This achievement of gave unprecedented stereoselectivity was used to synthesize different stereoisomers.<sup>45, 52, 66, 72, 73</sup> It is termed the ambidextrous Pictet-Spengler reaction.<sup>72, 73</sup>

### 1.3.8 Objectives

Indole alkaloids found in the plants of the *Apocynaceae*, *Rubiaceae*, and *Loganiaceae* families exhibit numerous biological activities (such as anti-tumor, anti-microbial, anti-HIV, anti-hypertensive and central nervous system stimulant).<sup>74</sup> Among the *Apocynaceae*, the genus *Tabernaemontana* is especially rich in indole alkaloids. Among the *Apocynaceae*, the genus *Tabernaemontana* is especially rich in indole alkaloids. In 2005, Monnerat *et al.* studied *Tabernaemontana hystrix*, a native species of the Atlantic forest in Southeastern Brazil and reported the phytochemical analysis of the crude methanolic extract of *T. hystrix*, which allowed them to characterize the presence of five indole alkaloids ibogamine (**71**), olivacine (**72**), affinine (**73**), affinisine(**74**), N<sub>b</sub>-methyllaffinisine (**75**) along with the new sarpagine related indole alkaloid named hystrixnine (**70**).<sup>74</sup> The structures of this novel sarpagine related alkaloids was elucidated via analysis of 1D and 2D NMR spectroscopy.<sup>41</sup>

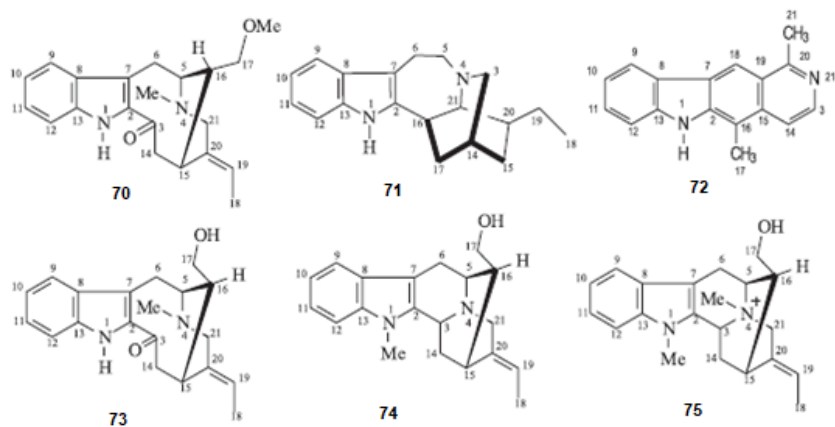


**Figure 6.** Indole alkaloids extracted from the *T. hystrix* by Monnerat *et al.*<sup>41</sup>

In 2008, Vieira *et al*<sup>75</sup>. investigated this hystrixnine along with some other indole alkaloids extracted from *T. hystrix.*, *T. laeta.*, and *T. australis* and found that the hystrixnine exhibit acetylcholinesterase (AChE) inhibitory activity. We know that symptomatic pharmacological treatment of Alzheimer’s disease (AD) is mainly based on the use of acetylcholinesterase inhibitors (AChEI) (e.g., donepezil, rivastigmine, and galanthamine). These inhibitors have beneficial effects on cognitive, functional, and behavioral symptoms of the disease as well as some undesired side effects.<sup>76</sup> The need for novel treatments of AD with reduced side effects is an unmet therapeutic need. Moreover the role of cholinesterase inhibitors in AD are still not completely understood; therefore the investigation of the natural AChE inhibitors such as hystrixnine could lead to clinically or at least scientifically important results for AD.

*Gelsemium* is a genus of flowering plants in the *Gelsemiaceae* family (previously classified in the *Loganiaceae* family; Struwe et al., 1994)<sup>77</sup>. This genus contains three species: the Asian *Gelsemium elegans* (Gardn. & Champ.) Benth. and two North American species, *Gelsemium sempervirens* (L.) and *Gelsemium rankinii* Small (Ornduff, 1970<sup>78</sup>; Robert and Broyles, 1993<sup>79</sup>). All three of the species are well-known for their toxicity.



**Figure 7.** (A) Flowers and leaves from *Gelsemium elegans*. (B) Roots of *Gelsemium elegans*. (C) Flowers of *Gelsemium sempervirens*

Among them *Gelsemium elegans* species is distributed in the Fujian, Yunnan, Guizhou, Guangdong and Guangxi provinces in southern China and over southeastern Asia (Wu et al., 1996).<sup>80</sup> It has been used in traditional Chinese medicine to treat certain types of skin ulcers, headaches and cancer pain (Editorial Committee of Zhonghua Bencao National Traditional Chinese Herb Administration, 1999)<sup>81</sup>. *Gelsemium sempervirens*, commonly known as yellow jasmine in North America, and is native to the southern regions of the United States<sup>82</sup>. *Gelsemium*

*sempervirens* is being used in traditional homeopathic medicine, as a well-known remedy for the treatment of neuralgia, migraines, uterine pain, rheumatism, influenza, nausea and whooping cough (Dewey, 1921; Grieve, 1971; Gutman, 1972; King, 1900; Bousta et al., 2001; Bellavite, 2011a; Paris et al., 2012). It is also frequently used as a mild sedative for a variety of anxiety-like psychological and behavioral condition (Bellavite et al., 2009; Dutt et al., 2010). Magnani et al. (2010) reported that series of centesimal dilutions of *Gelsemium sempervirens*, prepared according to the homeopathic pharmacopeia, has anxiolytic-like effects in mice. From *In vitro* experiments it was found that *Gelsemium sempervirens* effectively changes the emotional responses of mice to novel environments, which increases exploratory behavior and decreases thigmotaxis or neophobia (Magnani et al., 2010; Bellavite et al., 2011b).

Consequently, considering the biological and medicinal activity of the compounds isolated from these plant families it is desirable to synthesize these compounds along with some other closely related sarpagine related indole alkaloids like O-methyl macusine B and 16,17-dihydro-O-methyl macusine B, in amount large enough for further biological investigation or provide a route by which this result could be achieved.

## 1.4 Synthetic approach

### 1.4.1 Retrosynthetic analysis

The selected target indole alkaloids hystrixnine (**70**), gelsempervine A (**76**), gelsempervine B (**77**) O-methylmacusine B (**84**) and 19,20-dihydro-O-methylmacusine B (**83**) belongs to the sarpagine family of indole alkaloids, which contain a common pentacyclic core of sarpagine alkaloid **7**. The three alkaloids **70**, **76** and **77** also share a common C=O group at the C-3 position.

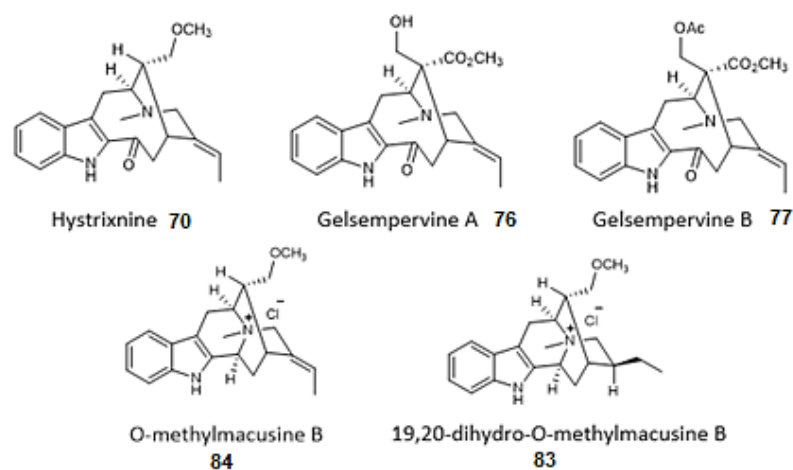
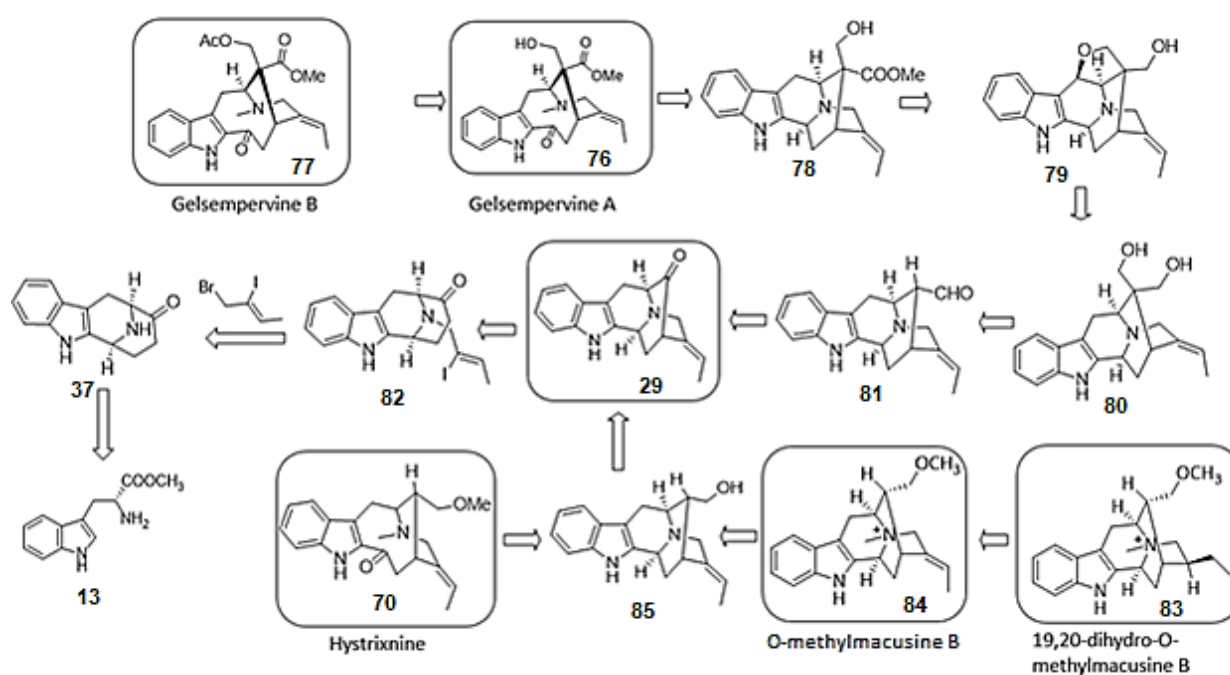


**Figure 8.** Target alkaloids hystrixnine (**70**), gelsempervine A (**76**), gelsempervine B (**77**) O-methylmacusine B (**84**) and 19,20-dihydro-O-methylmacusine B (**83**)

In a retrosynthetic sense, the alkaloid **77** could be synthesized from (**76**) via acetylation of the axial alcohol at the C-17 position. The compound **76** could be synthesized from selective bond breaking of the C-3 and N<sub>6</sub>-4 bond of **78**, which is the key to the synthesis of three of the target alkaloids. All three can be derived from the beta-hydroxy ester **78**. The beta hydroxy ester **78** could be synthesized from the reductive cleavage of the cyclic  $\alpha$ -methyl ester **79**. The cyclic ester **79** could be synthesized by radical oxidation of the diol **80**, which in turn could be derived from the aldehyde **81** through Tollens-like (cross Cannizzaro) reaction.



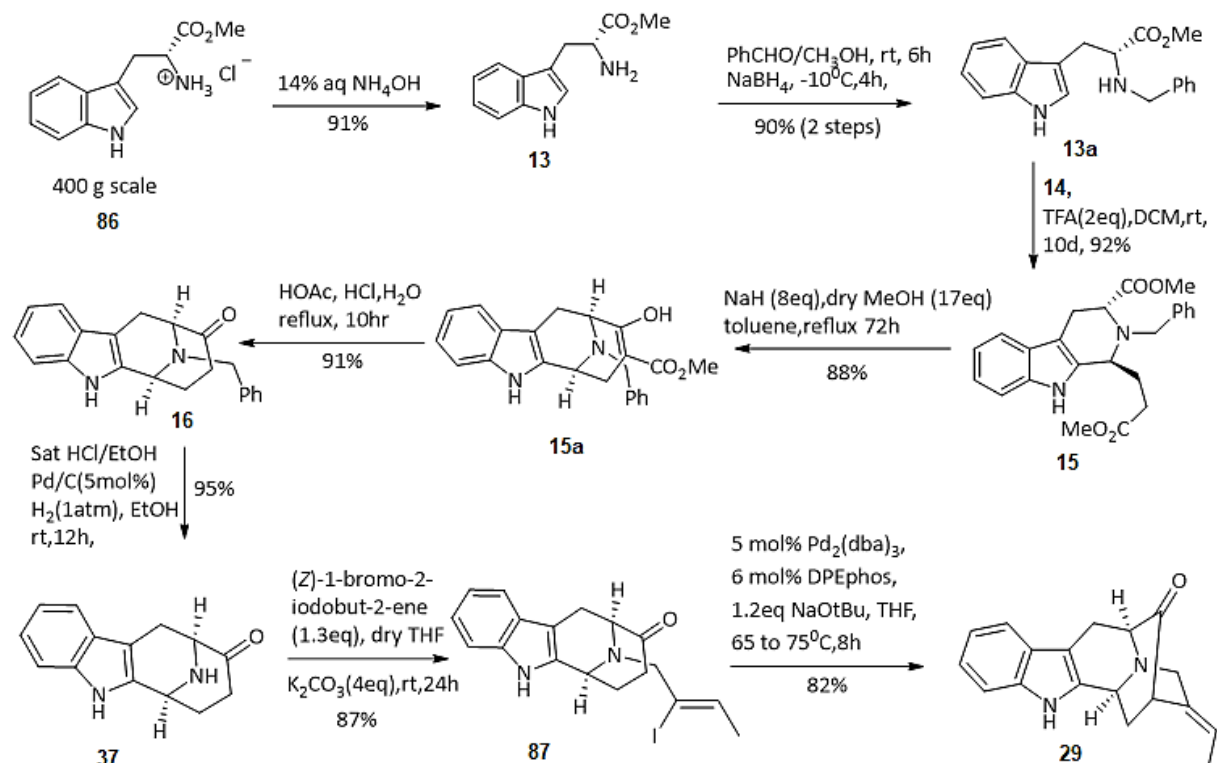
*Scheme 10. Retrosynthetic analysis*

The aldehyde **81** can be synthesized from the pentacyclic ketone **29** via a Wittig reaction, followed by reduction. This pentacyclic ketone core intermediate **29** is the key to the synthesis of all the target alkaloids mentioned before in this section and could be synthesized from the D-tryptophan methyl ester **13** via subsequent steps, which includes the formation of key intermediates **37** and **82**. The other target alkaloids hystrixnine (**70**), O-methylmacusine B (**84**) and 19,20-dihydro-O-methylmacusine B (**83**) could be derived from the common intermediate **85**, which in turn could be synthesized from the pentacyclic ketone **29**.

## 1.5 Results and discussion

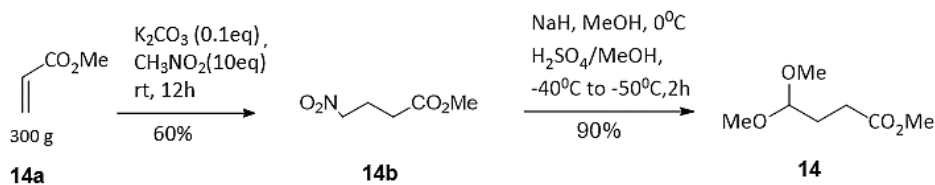
### 1.5.1 Synthesis of pentacyclic ketone **29**

The first goal was to synthesis of the pentacyclic ketone **29**, which was achieved by employing the protocols developed previously in Milwaukee by J. Li.<sup>67</sup> (Scheme 11)



**Scheme 11.** Synthesis of pentacyclic ketone **29**

As illustrated in Scheme 11, the D-tryptophan methyl ester **13** was synthesized by treating the commercially available D-tryptophane methyl ester hydrochloride salt **86** with 14% aq NH<sub>4</sub>OH on 400g scale. This was then converted into N<sub>b</sub>-benzyltryptophan methyl ester **13a** on stirring with benzaldehyde at room temperature (6 hours), followed by reduction of the imine, which resulted, *in situ* with sodium borohydride [-10 °C to -8 °C (2-5 hours, according to the scale)]. The optical purity of the N<sub>b</sub>-benzyltryptophan methyl ester **13a** prepared in this manner was found to be greater than 98% ee as determined by comparison to data from authentic samples.<sup>83</sup> To introduce the desired stereocenter at C-3 the asymmetric Pictet-Spengler reaction<sup>84-89</sup> was employed with methyl 4,4-dimethoxy-butyrate **14**, which can be prepared on a kilogram scale; and N<sub>b</sub>-benzyl tryptophan **13a** to provide the trans diester **15** as a single diastereomer in 92% yield. The purification of **15** was achieved by recrystallization from ethanol. The synthesis of **14** was achieved by a two step synthesis process; the first step of which was the synthesis of  $\gamma$ -nitro butyrate **14b** from the reaction of methyl acrylate with excess nitrobenzene in the presence of K<sub>2</sub>CO<sub>3</sub>. The yield of this reaction was about 60%, which is much better than the previously reported yield in Milwaukee (30%), where the reaction process involved the use of 0.6 N aqueous NaOH and it took 3 days to finish. Whereas, the much improved process reported here, produced almost twice the yield then before with only 12 hours needed to finish the reaction and a much easier workup to obtain the isolated nitro ester from the reaction mixture. (Scheme 12)

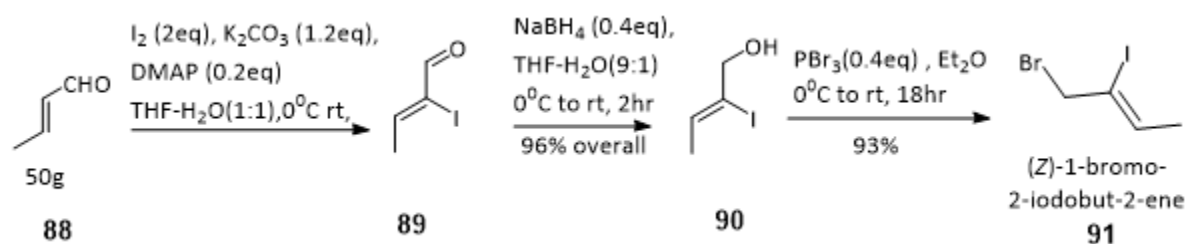


**Scheme 12.** Synthesis of methyl 4,4-dimethoxybutyrate **14**

In the next sequence, diester **15** was heated in toluene with an excess of NaOMe, generated *in situ* with NaH and dry MeOH in toluene, which was heated to reflux to achieve the Dieckmann cyclization. This was followed by quenching the reaction mixture with glacial acetic acid at 0 °C. After the removal of the solvent, glacial acetic acid, concentrated aqueous HCl, and water were added to the mixture at 0°C and this was followed by heating the reaction mixture at reflux temperature to effect hydrolysis and decarboxylation of the ester function to furnish the N<sub>b</sub>-benzyl tetracyclic ketone **16** in 91% yield and 98% ee. The ketone **16** was subjected to debenzylation in the presence of Pd/C and H<sub>2</sub> to furnish the synthesis of key tetracyclic ketone **37** in 97% yield and the optical purity was confirmed by optical rotation.

In the next sequence, the N<sub>b</sub>-alkylation of the secondary amine **37** was carried out with (*Z*)-1-bromo-2-iodo-2-butene **91** under the conditions developed in Milwaukee (THF-H<sub>2</sub>O/K<sub>2</sub>CO<sub>3</sub> rt)<sup>90-92</sup> in 87% yield (Scheme 11). The product **37** was purified by chromatography. The vinyl iodide **91** required for this route was synthesized via α-iodination of an α,β-unsaturated aldehyde **88** under the conditions of Kraft,<sup>50,93</sup> which exclusively formed only the *Z*-isomer **89**. This material without further purification underwent the subsequent reduction<sup>94</sup> to provide the desired

alcohol **90** in 96% overall yield. This alcohol **90** was then treated with PBr<sub>3</sub> in dry ether at 0 °C for 12 hours to provide the desired bromide **91** in 93% yield. (Scheme 13)



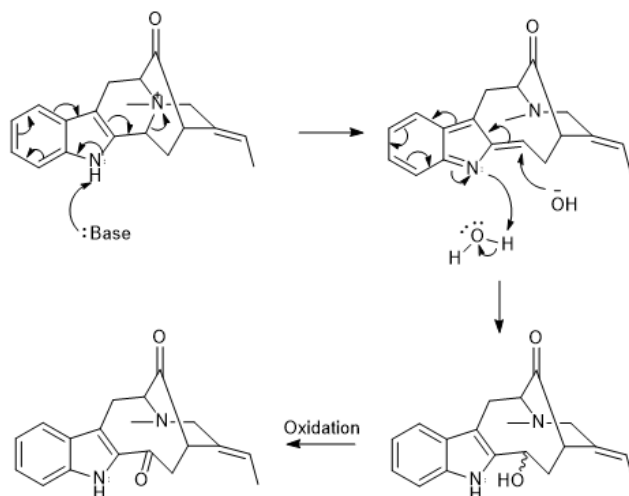
**Scheme 13.** Synthesis of (Z)-1-bromo-2-iodobut-2-ene **91**

The synthesis of the pentacyclic ketone **29** was achieved via an enolate mediated intramolecular palladium cross-coupling reaction using 5.0 mol% Pd<sub>2</sub>(dba)<sub>3</sub>, 7.0 mol% DPEphos as a ligand and 1.5 equivalents of NaOtBu as a base in THF at 80 °C for 5 hours in 82% yield. The structure of **29** was confirmed by NMR, HR mass spectroscopy and the optical purity of the **29** was confirmed by comparison of the optical rotation with the known material<sup>23</sup>.

## 1.5.2 Study of model reactions to break the C(3)-N(4) bond of the sarpagine core

After obtaining the pentacyclic ketone **29**, it was utilized to do model reactions to determine if the C<sub>3</sub>-N<sub>4</sub> bond was breakable, which was vital to the synthesis of three of the target indole alkaloids. The similar reaction conditions were employed using the N<sub>b</sub>-benzyl tetracyclic ketone **16** as the reactant for the same reason.

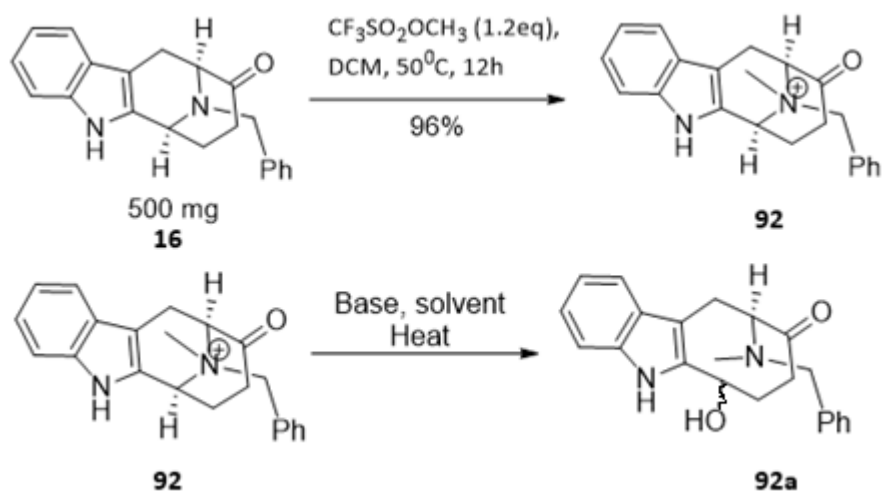
The synthetic strategy with the model reactions was to prepare the salts of the tetracyclic and pentacyclic ketones by methylating the N<sub>b</sub>-4 position since the final target indoles have a methyl group at that position or by protecting the N<sub>b</sub>-4 with a carbamate such as Cbz-Cl which would then be subjected to the basic conditions; strong enough to break the bond at elevated temperature, as well as introducing the -OH group at C-3 position, which could be converted into a ketone to achieve the desired functionality of the final targets. The mechanistic explanation for these synthetic approaches is shown in Scheme 14. The same mechanistic approach was implemented to carry out some reactions with various reaction conditions using the N<sub>b</sub>-benzyl tetracyclic ketone **16**. It should be mentioned here that similar types of reactions have been done on different indole alkaloid by Schill *et al.*<sup>95</sup> and Bonjoch *et al.*<sup>96</sup> in moderate to good yields. The reaction conditions employed to obtain the desired bond breaking at C(3)-N(4) in the reaction scheme are being described in the next sections.



**Scheme 14.** Mechanistic approach towards the breaking of the C(3) and N<sub>b</sub>(4) bond of **29**.

### 1.5.3 Formation of the quaternary amine **92** and use of the material in the bond breaking approach

Originally, the synthesis of the quaternary amine **92** was carried out several times using the N<sub>b</sub>-benzyl tetracyclic ketone and methyl triflate in dichloromethane at 50 °C for 12 hours in 96% yield. Then a series of bases were used to break the C(3)-N(4) bond of the quaternary amine **92**, as well as introduce the -OH functionality at C(3) position of **92**. At this point achieving the *S* or *R* stereo isomer was not the point of interest since the alcohol will be converted to the ketone functionality later on to synthesize the final targets (**70**, **76** and **77**). Unfortunately, none of the reaction conditions have worked with zero product formation.



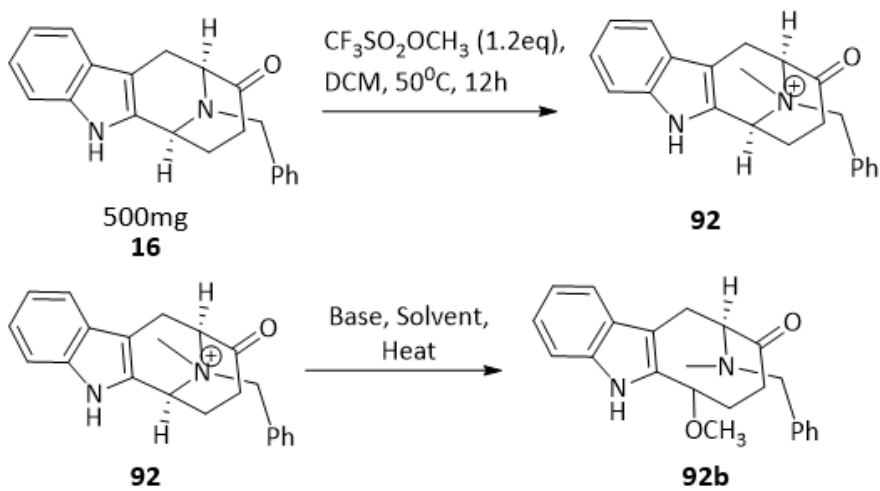
**Scheme 15.** Synthesis of methiodide salt **92** and approach towards the breaking of the C(3)- N(4) bond of **92** using the reaction conditions of Table 4 to provide **92a**

**Table 4.** Reaction conditions for the approaches toward the synthesis of **92a**. (Note: SM= Starting material)

<b>92</b>	Base	Solvent	Temperature	Time	Result
10 mg	Na <sub>2</sub> CO <sub>3</sub> , 3eq	THF, H <sub>2</sub> O	Reflux	24h	SM
10 mg	Na <sub>2</sub> CO <sub>3</sub> , 5eq	THF, H <sub>2</sub> O	Closed tube, 80 <sup>o</sup> C	24h	SM
10 mg	Na <sub>2</sub> CO <sub>3</sub> , 9eq	THF, H <sub>2</sub> O	Reflux	24h-36h	SM
10 mg	Cs <sub>2</sub> CO <sub>3</sub> , 5eq	THF, H <sub>2</sub> O	Closed tube, 80 <sup>o</sup> C	24h	SM
10 mg	Cs <sub>2</sub> CO <sub>3</sub> , 5eq	DMF, H <sub>2</sub> O	Reflux, 150 <sup>o</sup> C	12h, 24h	SM
10 mg	<u>NaOH</u> , 5eq	THF, H <sub>2</sub> O	Reflux	24h	SM
10 mg	<u>NaOH</u> , 5eq	DMF, H <sub>2</sub> O	Reflux/Closed tube	24h, 36h	SM

Similarly, for the same purpose of breaking the C(3)-N(4) bond of the quaternary amine **92**, as well as to introduce the -OCH<sub>3</sub> functionality at C(3) position of **92**, the base NaOCH<sub>3</sub> (both commercially available and freshly prepared *in situ*) was used (Scheme 16) at various reaction conditions (Table 5). From the examination of the primary mass spectrometric data on the crude material (Figure 8) it was found that the ether **92b** was formed under a reaction condition when 18 equivalents of NaH was used as a base and methanol: toluene (1: 2) was used as solvents in closed tube at 110<sup>o</sup>C for 36 hours (Table 5). But the product could not be confirmed by NMR spectroscopy since it was not stable during the attempts to take an NMR spectrum on the crude mixture and was found to be converted back into the starting material **92**. Similar attempts were

taken later to regenerate the same reaction result under the same condition, but the attempts proved to be unsuccessful.



**Scheme 16** Synthesis of **92** and approach towards the breaking of C(3)-N(4) bond of **92** using the reaction conditions outlined in Table 5 to get **92b**

**Table 5.** Reaction conditions for the approaches toward the synthesis of **92b**. (Note: SM= Starting material)

<b>92</b>	<b>Base</b>	<b>Solvent</b>	<b>Temperature</b>	<b>Time</b>	<b>Result</b>
20 mg	NaOCH <sub>3h</sub> (3eq)	MeOH	Reflux	24h	SM
20 mg	NaOCH <sub>3</sub> (3eq)	MeOH	Closed tube, 80 <sup>0</sup> C	24h	SM
20 mg	NaH (3eq)	MeOH	Reflux	24h-36h	SM
20 mg	NaH (3eq)	MeOH	Closed tube, 80 <sup>0</sup> C	24h	SM
20 mg	NaH (5eq)	MeOH	Closed tube, 80 <sup>0</sup> C	24h	SM
20 mg	NaH (9eq)	MeOH	Closed tube, 80 <sup>0</sup> C	36h	SM
20mg	NaH (18eq)	MeOH: Toluene (1: 2)	Closed tube, 110 <sup>0</sup> C	36h	Product

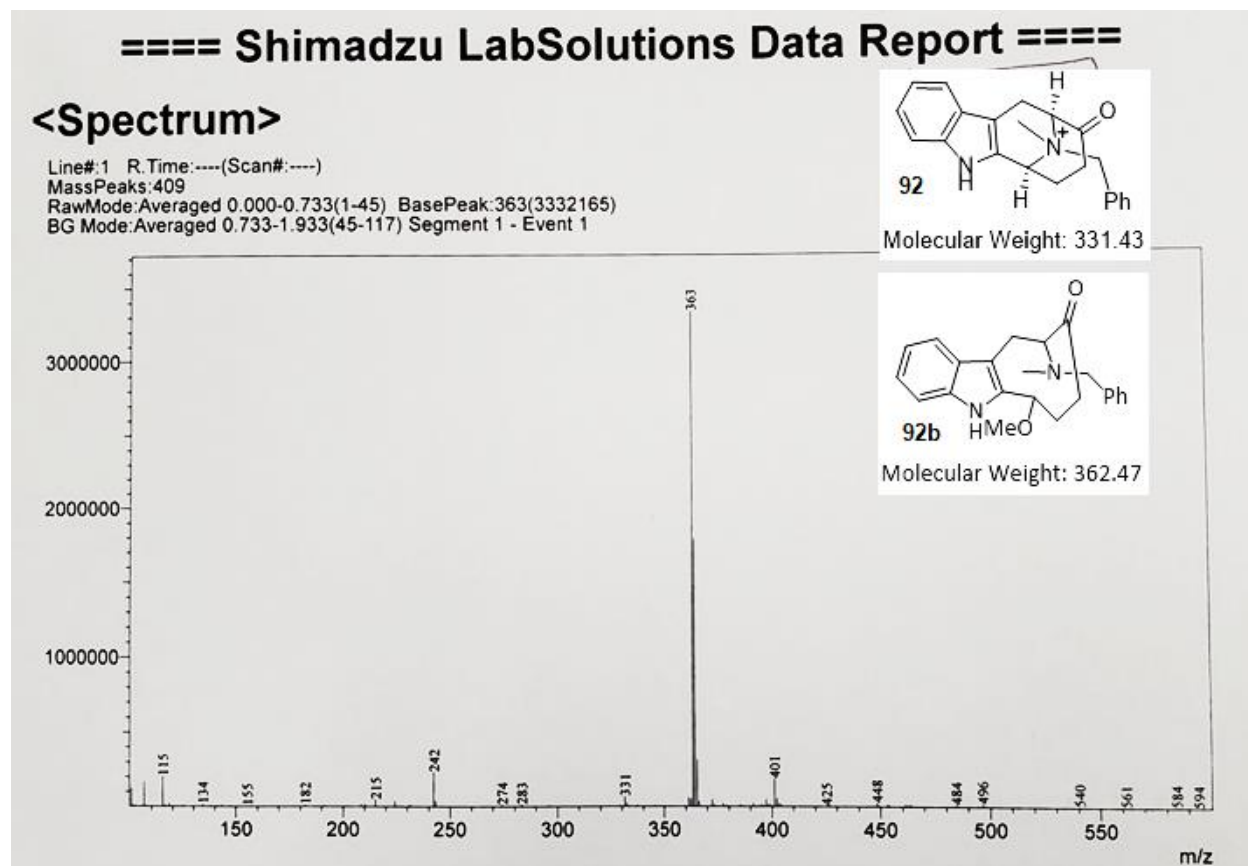
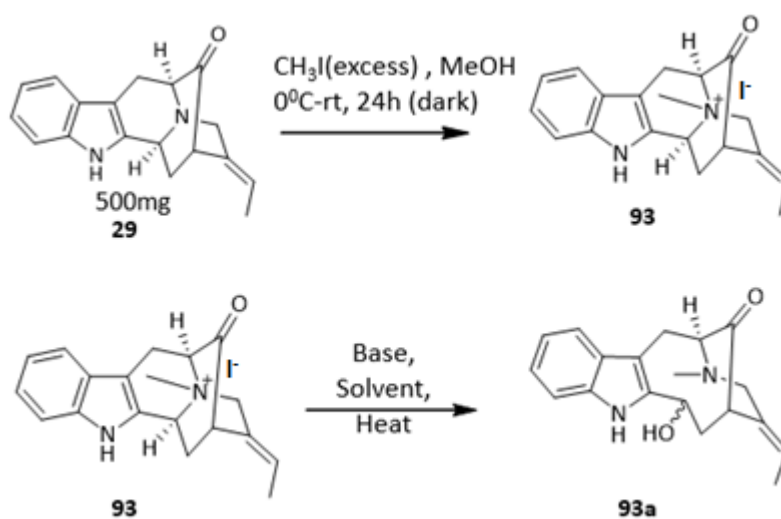


Figure 8. Mass spectroscopy data on formation of **92b** from **92**

### 1.5.4 Formation of the quaternary amine **93** and the use of **93** in the bond breaking approach

Similar to the previously mentioned reaction conditions in Section 1.5.3, the same approach was taken to determine if the C(3)-N(4) bond would break. In this case, to methylate the N(4) nitrogen atom of the pentacyclic ketone **29**, excess  $\text{CH}_3\text{I}$  in dry MeOH was used and the reaction was carried out in dark at  $0^\circ\text{C}$  to room temperature for 24 hours to obtain the quaternary amine **93** (Scheme 17). Again, all the approaches (Table 6 and 7) to introduce the  $-\text{OH}$  functionality at the

C(3) position of **93** was unsuccessful. But in order to introduce the -OCH<sub>3</sub> functionality at the C(3) position the quaternary salt **93** was used in the synthetic approaches employing the reaction conditions of Table 8. In this study the partial conversion of **93** was observed to the product **93a** under the reaction condition, where 10 equivalents of commercially available NaOCH<sub>3</sub> was used as a base; MeOH:Toluene (1:1) mixture was used as solvent and the reaction mixture was heated at 110° in a closed tube for 24 hours.



**Scheme 17.** Synthesis of **93** and approach towards the breaking of the C(3)-N(4) bond of **93** using the reaction condition of Tables 6 and 7 to provide **93a**

The primary mass spectral data on the crude mixture showed the product **93b** had formed but the conversion of reactants to products was not significant. (Figure 9)

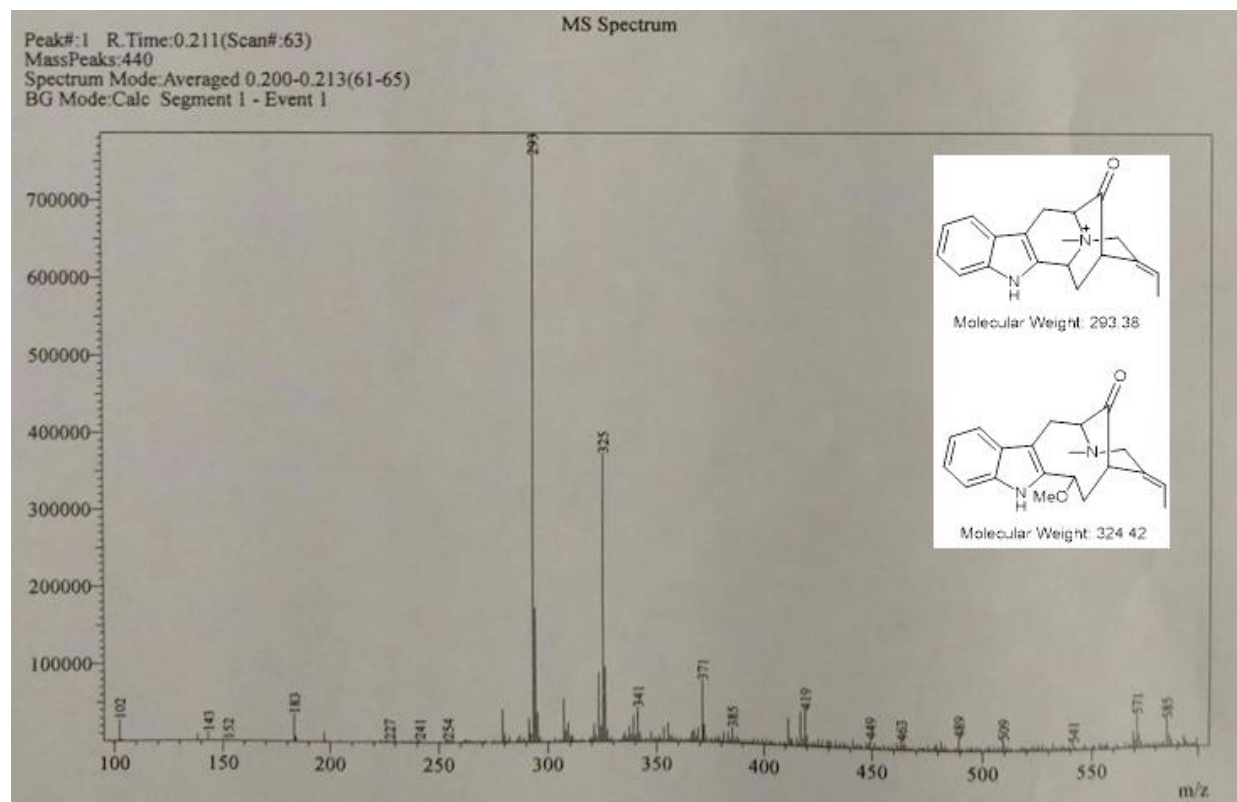


**Figure 9.** Mass spectroscopy data of the partial formation of **93b** from **93** in the crude reaction mixture

Again, these reaction conditions could not be improved, as the product seemed to be highly unstable and the conversion of reactant to product was significantly low. Instead of conceding at this point, other reactions were carried out later by using different amine protecting groups instead of methylation of N(4). The Wittig reaction to the enol ether of **29** was attempted to

determine if the C(3)- N(4) bond would break and stabilize the product long enough to carry out the next reaction necessary to obtain the final target.

**Table 6.** Reaction conditions for the approaches toward the synthesis of **93a**. (Note: SM= Starting material)

<b>93</b>	<b>Base</b>	<b>Solvent</b>	<b>Temp. (°C)</b>	<b>Time</b>	<b>Result</b>
15mg	Na <sub>2</sub> CO <sub>3</sub> (2eq)	DMF, H <sub>2</sub> O	120	24h	SM
15mg	Na <sub>2</sub> CO <sub>3</sub> (3eq)	DMF, H <sub>2</sub> O	120	24h	SM
15mg	K <sub>2</sub> CO <sub>3</sub> (2eq)	DMF, H <sub>2</sub> O	120	24h	SM
15mg	Cs <sub>2</sub> CO <sub>3</sub> (2eq)	DMF, H <sub>2</sub> O	120	24h	SM
15mg	Cs <sub>2</sub> CO <sub>3</sub> (3eq)	DMF, H <sub>2</sub> O	120	24h	SM

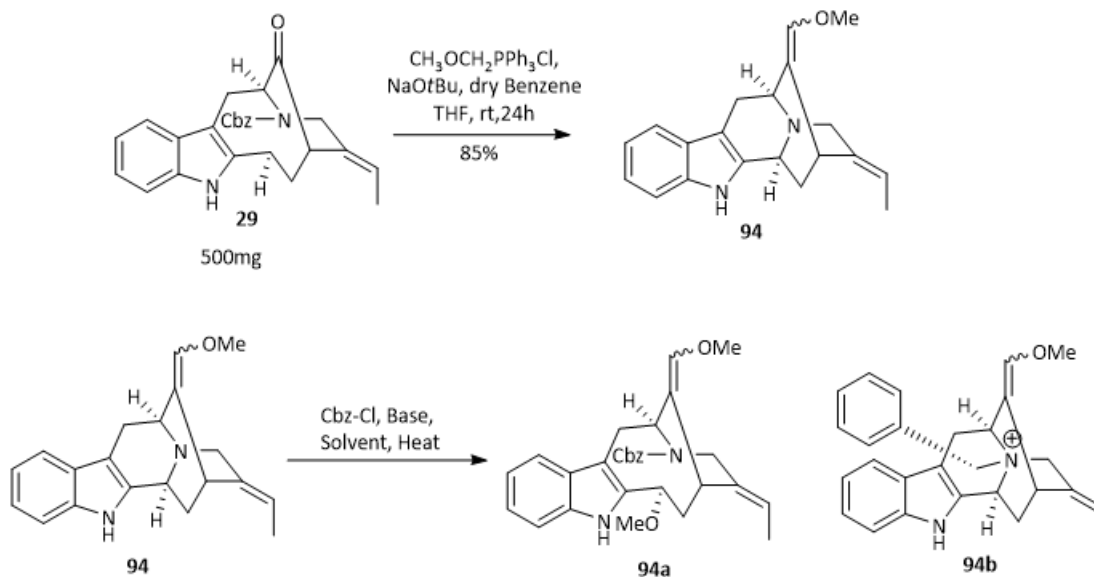
**Table 7.** Reaction conditions for the approaches toward the synthesis of **93a**. (Note: SM= Starting material)

Scale of SM	Base	Solvent	Temperature (°C)	Time	Result
10 mg	Na <sub>2</sub> CO <sub>3</sub> , 5eq	THF, H <sub>2</sub> O	Reflux	24h	SM
10 mg	Na <sub>2</sub> CO <sub>3</sub> , 5eq	DMF, H <sub>2</sub> O	Reflux	Up to 24h	SM
10 mg	NaOH, 5eq	THF, H <sub>2</sub> O	Reflux	24h	SM
10 mg	NaOH, 5eq	DMF, H <sub>2</sub> O	Reflux/Closed Tube	24h, 36h	-SM
10mg	NaOH, 10eq	THF, H <sub>2</sub> O	Reflux	24h	SM
10mg	KOH, 5eq	THF, H <sub>2</sub> O	Reflux	24h	SM
10mg	Cs <sub>2</sub> CO <sub>3</sub> , 5eq	DMF, H <sub>2</sub> O	Rt to reflux	36h	SM

### 1.5.5 Approach towards the formation of the amide **95** and subsequent use of **95** in the C(3) -N(4) bond breaking attempts

After being unsuccessful in using the previous reaction conditions using the N<sub>b</sub>-benzyl tetracyclic ketone **16** and the pentacyclic ketone **29**, it was decided to synthesize the compound **94** through the Wittig reaction conditions using methoxymethyltriphenylphosphoniumchloride and NaOtBu in anhydrous benzene at room temperature (24 hours). The product was purified by column chromatography after workup and the yield of the reaction was more than 85%. Although two

diastereomeric products were observed in TLC only one of the diastereomers **94** is major one which was separated by column chromatography (stereochemistry unknown) from the other and was used in further reactions to protect the N-4 nitrogen atom of **94** with Cbz-Cl. (Scheme 18)

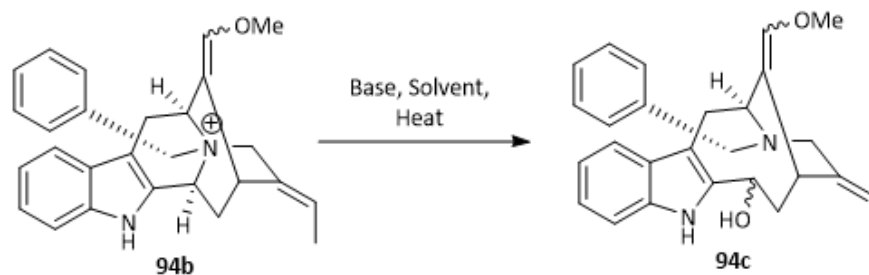


**Scheme 18.** Synthesis of **94** via the Wittig reaction condition and approach towards the protection of the N(4) group of **94** with the carbamate Cbz-Cl using the reaction conditions of Table 8.

**Table 8.** Reaction conditions for the approaches toward the synthesis of **94a**. (Note: SM= Starting material)

SM	CbzCl	Base	Solvent	Temp. (°C)	Time	Result
15mg	5eq	Na <sub>2</sub> CO <sub>3</sub> (3eq)	DMF, H <sub>2</sub> O	90	24h	SM
15mg	5eq	Na <sub>2</sub> CO <sub>3</sub> (5eq)	DMF, H <sub>2</sub> O	90	24h	SM
15mg	5eq	K <sub>2</sub> CO <sub>3</sub> (3eq)	DMF, H <sub>2</sub> O	90	24h	SM
15mg	5eq	K <sub>2</sub> CO <sub>3</sub> (5eq)	DMF, H <sub>2</sub> O	90	24h	SM
15mg	5eq	Cs <sub>2</sub> CO <sub>3</sub> (3eq)	DMF, H <sub>2</sub> O	90	24h	SM
15mg	10eq	Cs <sub>2</sub> CO <sub>3</sub> (5eq)	DMF, H <sub>2</sub> O	120	24h	SM+ <b>94b</b>
15mg	10eq	NaOH (3eq)	DMF, H <sub>2</sub> O	120	24h	SM
15mg	10eq	TEA (3eq)	DMF, H <sub>2</sub> O	120	24h	SM
15mg	5eq	K <sub>2</sub> CO <sub>3</sub> (3eq)	THF, H <sub>2</sub> O	Rt to reflux	24h	<b>94b</b>

From the experimental results (Table 8) it was found that the benzyle carbamate protection could not be achieved at the N(4) position and when 5 equivalents of Cbz-Cl was used with K<sub>2</sub>CO<sub>3</sub> as base in THF/H<sub>2</sub>O. The mixture was allowed to stir at room temperature to reflux for 24 hours and the N(4) benzyl protected **94b** was formed with no starting material left. The structure of **94b** was confirmed by the NMR and mass spectroscopy. The amine **94b** was then used to study the previously discussed C(3)-N(4) bond breaking process to furnish the alcohol **94c** and experimentally these attempts also did not produce useful results. (Scheme 19)



*Scheme 19. Synthetic attempts to produce 94c using the reaction conditions from Table 9.*

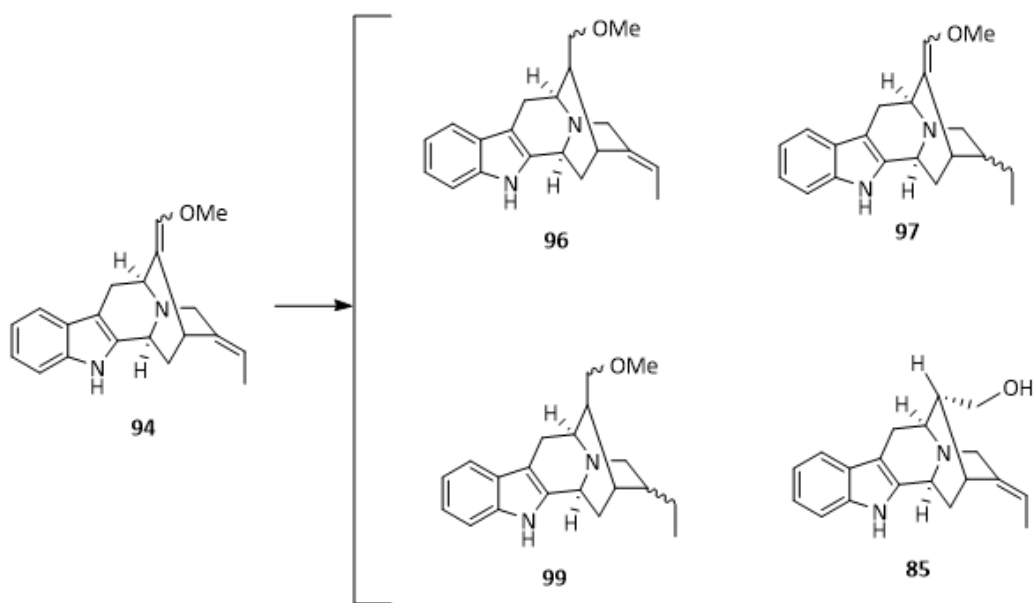
**Table 9.** Reaction conditions for the approaches toward the synthesis of **94c**. (Note: SM= Starting material)

SM	Base	Solvent	Temp (°C)	Time	Result
20mg	Na <sub>2</sub> CO <sub>3</sub> (3eq)	THF, H <sub>2</sub> O	65	16h	SM
20mg	Cs <sub>2</sub> CO <sub>3</sub> (3eq)	THF, H <sub>2</sub> O	65	16h	SM
15mg	NaH (3eq)	DMF, H <sub>2</sub> O	90	16h	SM

From the synthetic studies carried out in sections 1.5.3 to 1.5.5 it was observed that the breaking of C(3)-N(4) bond was too difficult to successfully execute in this work. It was cleavable at certain reaction conditions but could not be repeated. It can be said that the bond cleavage at C(3) –N(4) position was not stable unless the resultant product can be stabilized chemically by some other means. If one could have incorporated a hydroxyl group at C(3) position the opportunity to carry out further oxidation of the C(3) –OH group, could potentially have led to the synthesis of the initial 3-oxo target alkaloids.

### 1.5.6 Attempts to reduce the enol ether bond of **94**

Another study was carried out to reduce the reaction steps in going from the enal reactant **94** to the product **95**, which was usually be carried out by acidic hydrolysis of **94** to aldehyde **81**. Then the aldehyde **81** would be epimerized completely to the  $\alpha$  aldehyde and then into the alcohol **85** by sodium borohydride reduction at 0°C in ethanol for 8 hours in good yield. By selective methylation of this alcohol, this could then lead us to the expected ether **96**. If the selective reduction of **94** could be achieved, then the previously mentioned steps could be reduced, as well as the overall number of steps in the total synthesis of hystrixnine **70**. For the reduction of the enol ether the following reaction conditions have been explored (see Table 10) and the experimental results have shown in Scheme 20.



*Scheme 20. Approach towards the reduction of enol ether bond of 94*

**Table 10.** Reaction conditions for the approaches toward the synthesis of **96**. (Note: SM= Starting material)

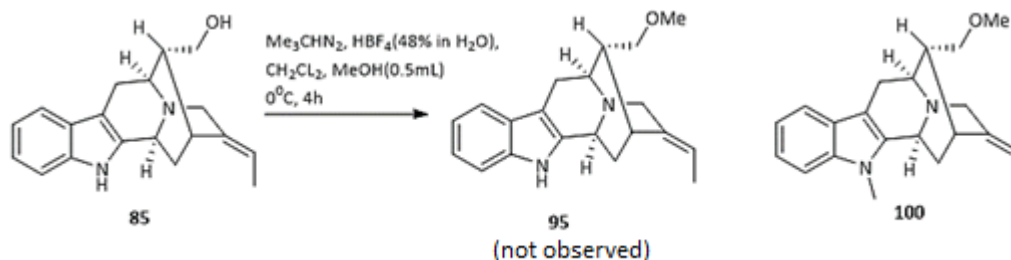
SM	Reagents	Solvent	Temp (°C)	Time	Result
20mg	Et <sub>3</sub> SiH, BF <sub>3</sub> ·Et <sub>2</sub> O	MeOH	rt to 50	8h	SM
20mg	Et <sub>3</sub> SiH, TFA	CH <sub>2</sub> Cl <sub>2</sub>	0 –rt to reflux	8h	<b>85</b>
20mg	Pd(OH) <sub>2</sub>	MeOH, H <sub>2</sub>	rt	16h	<b>97</b> and <b>99</b> (major)
20mg	Pt(IV)Oxide	Ethanol, H <sub>2</sub>	rt	16h	<b>97</b> and <b>99</b> (major)
20mg	Pd(OAc) <sub>2</sub>	Ethanol, H <sub>2</sub>	rt	12h	<b>99</b>

No formation of ether was observed for the reaction condition ( $\text{Et}_3\text{SiH}$ ,  $\text{BF}_3 \cdot \text{Et}_2\text{O}/\text{MeOH}$ , rt to  $50^\circ\text{C}$  for 8 hours). Whereas the use of the triethylethylsilylether and TFA lead to the product **85**, which could be due to the presence of moisture in TFA during the reaction. Under this condition the enol ether may have hydrolyzed to aldehyde and later was reduced to the alcohol **85**. On the other hand, use of both  $\text{Pd}(\text{OH})_2 / \text{MeOH}$ ,  $\text{H}_2$  and  $\text{Pt}(\text{IV})\text{oxide} / \text{EtOH}$ ,  $\text{H}_2$  reaction condition resulted in formation of the two different types of products **97** and **99** (major). The enal **97** was the result of the reduction of the C(19)-C(20) ethylidene bond and the **99** was the result of the reduction of both the C(19)-C(20) ethylidene bond and the enol ether bond at C(16)-C(17). These results were confirmed by analysis of the crude NMR of the reaction products and compared it with the known NMR of the reactant **94**. Interestingly, when  $\text{Pd}(\text{OAc})_2/\text{EtOH}$ ,  $\text{H}_2$  was used at room temperature only the product **99** was formed with two chiral diastereomers (the major *S* diastereomer at C-19 was isolated through and confirmed by NOESY and NOE). This **99** was later utilized to synthesize the 19,20-dihydro-O-methylmacusine B. However, the bottom line was the desired product **96** could not be synthesized using any of the reaction conditions discussed above.

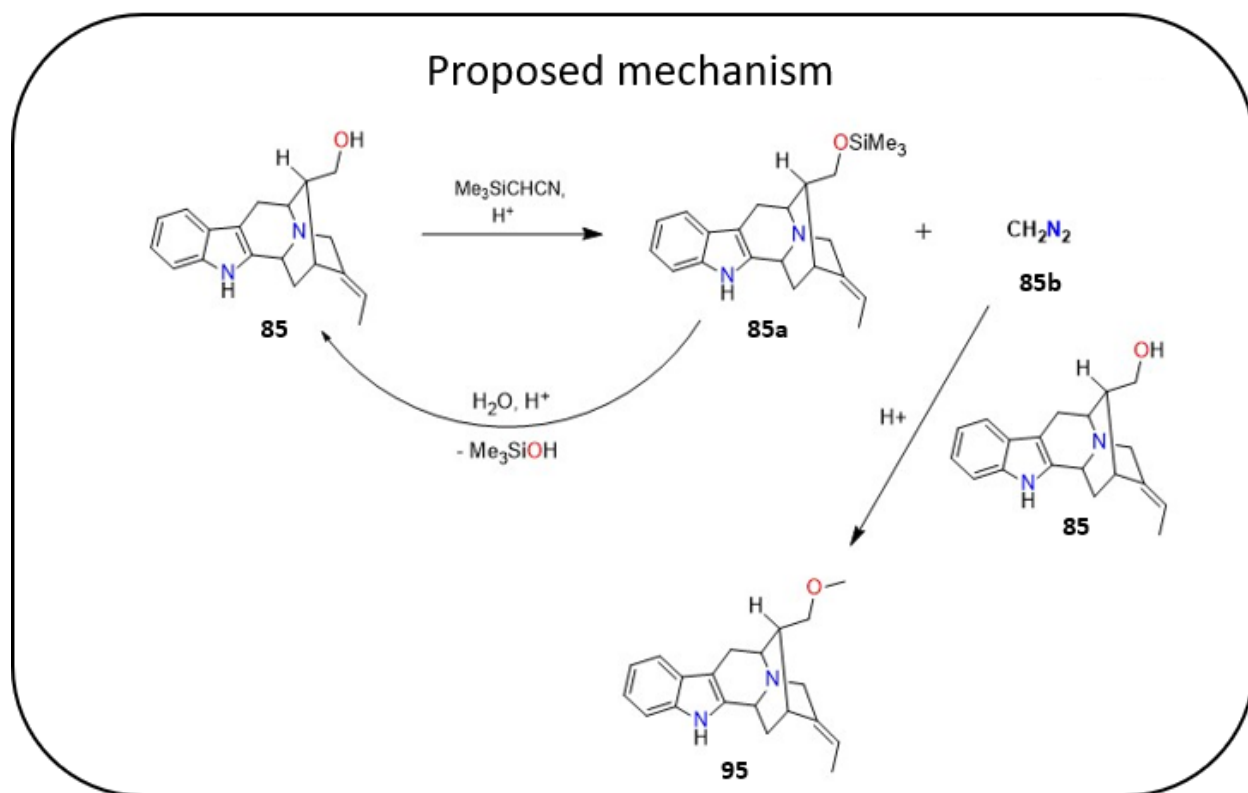
### 1.5.7 Selective methylation of alcohol **85** to the ether **95**

Since the selective reduction of enol ether **94** to the ether **96** was not successful, the selective methylation of alcohol **85** to ether **95** was attempted by using the methylating agent trimethylsilyldiazomethane/  $\text{HBF}_4$  (48% in  $\text{H}_2\text{O}$ ) depicted in (Scheme 20). This reaction was attempted by following the reaction condition developed by Toyohiko Aoyama *et al.*<sup>97</sup> At first the alcohol **85** should react with trimethylsilyldiazomethane under acidic condition to provide the

trimethylsilyldiazonium salt **85a** and free diazomethane **85b**, which will then react with another molecule of alcohol **85** to produce the methyl ether **95**. Under acidic condition the byproduct **85a** should convert back to the starting alcohol **85**. To maintain this reaction cycle 0.5 equivalent of trimethylsilyldiazomethane was introduced into the reaction mixture after every half an hour at 0°C. The reaction was monitored by TLC (silica gel, 10% methanol and 90% dichloromethane) up to 4 hours (Scheme 21). It was observed that the reaction was never complete and resulted in a mixture of the starting alcohol **85** and unexpected demethylated product **100** (product confirmed by NMR spectroscopy of the crude and mass spectroscopy). The complex reaction conditions with continuous addition of trimethylsilyldiazomethane led to the undesired product formation of **100**. It should be noted that the same reaction conditions were used by Toyohiko Aoyama *et al.* to methylate simple alcohols, which was less complex as compared to the alcohol **85**, and even for the selective methylation of the Aoyama alcohols, the percent yield was not impressive all the time.



**Scheme 20.** Approach towards the selective methylation of **85** to **95** using trimethylsilyldiazomethane.

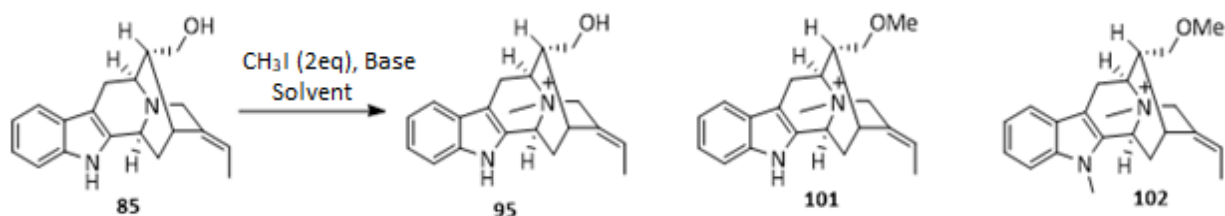


**Scheme 21.** Proposed mechanism for the formation of diazomethane illustrated in Scheme 20

### 1.5.8 Selective dimethylation of alcohol **85**

Since three of the target alkaloids **70**, **83** and **84** share the common structural resemblance of having a methyl group at the N(4) position and an ether group at the C(16) position, the selective dimethylation of **85** using **85**/bases and methyl iodide in different solvents could result in the expected product **101**, the precursor of the target alkaloids **70**, **83** and **84**. Consequently, the different reaction processes depicted in Table 11 were carried out and it was observed from the

results of those reactions that due to the similar acidity of the indole N-H and the alcohol at C-17, using more than 1 equivalent of base resulted in the unwanted product **102**. This is from the methylation of the N<sub>b</sub>-4 nitrogen atom and alcohol at C-17 as well as the indole N-H. When the K<sub>2</sub>CO<sub>3</sub> was used in less than 1 equivalent, this unwanted trimethylated **102** was not formed. The products **95** and **101** could not be separated through column chromatography since both stayed at the baseline when it was attempted to separate them using TLC (silica gel, 10% methanol and 90% dichloromethane). Consequently, further improvement to this reaction could be achieved by introducing 1.1 equivalent of K<sub>2</sub>CO<sub>3</sub> slowly into the reaction mixture at low temperature and monitoring the reaction carefully using TLC and mass spectroscopy by collection of a sample from the reaction mixture after every half an hour. This condition was not attempted due to lack of starting material **85**, but is a useful experiment to try in the future.



**Scheme 22.** Approach towards the selective methylation of **85** to **101** using methyl iodide and base.

**Table 11.** Reaction conditions for the approaches toward the synthesis of **101** using methyl iodide.

Scale of SM	Base	Solvent	Temperature	Time	Result
10 mg	K <sub>2</sub> CO <sub>3</sub> (2eq)	MeOH	rt	10h	101 and 102
10 mg	DIPEA (2eq)	MeOH	rt	10h	102
10 mg	K <sub>2</sub> CO <sub>3</sub> (2eq)	MeOH	-15 <sup>0</sup> C to rt	12h	101 and a02
10 mg	K <sub>2</sub> CO <sub>3</sub> (0.9 eq)	THF	0 <sup>0</sup> C to rt	12 h	B, C

Mass Spectrum  
ZK-04-01\_ZK-04-01-Omethylproduct\_002.lcd  
Line#:1 R.Time:----(Scan#:----)  
MassPeaks:464  
RawMode:Averaged 0.060-0.260(19-79) BasePeak:309.20(1450673)  
BG Mode:Averaged 0.260-1.987(79-597) Segment 1 - Event 1

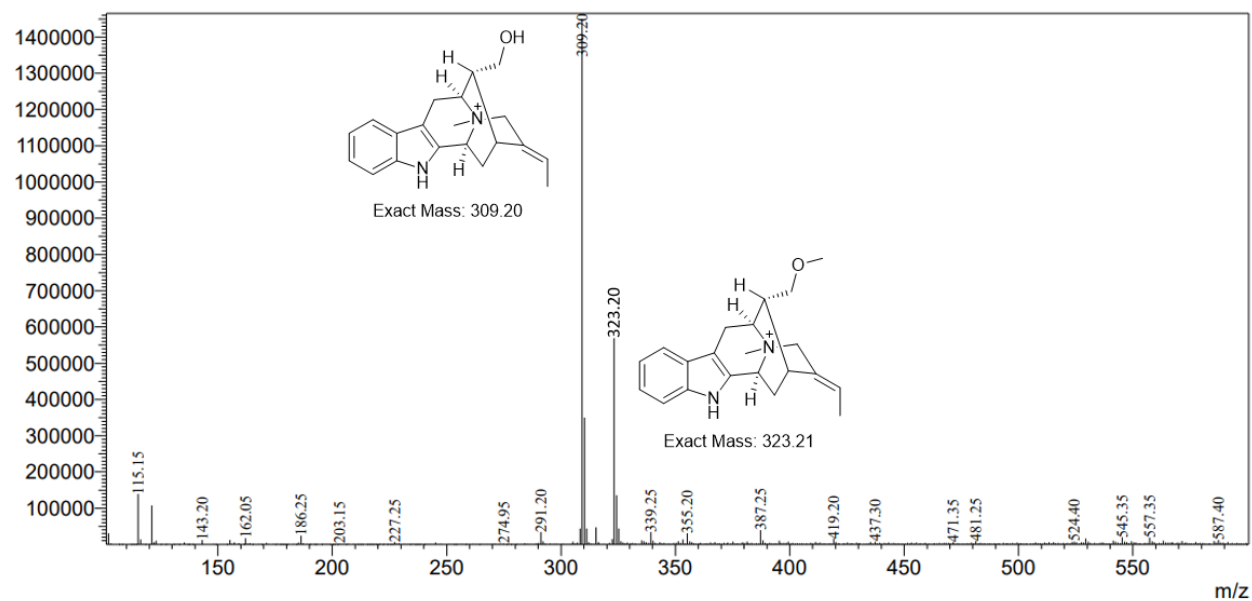
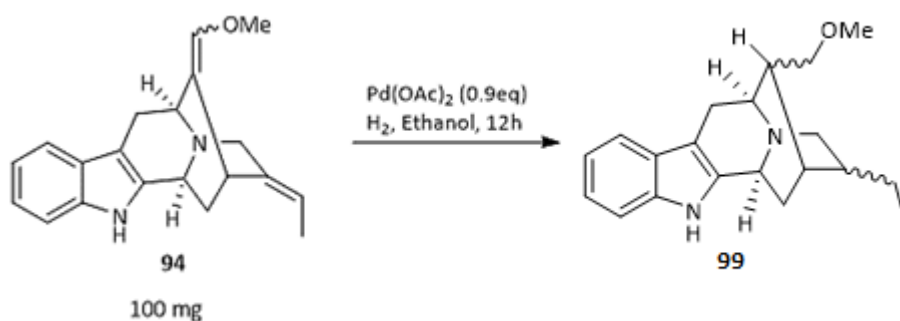


**Figure 10.** Mass spectroscopic data of the reaction Scheme 22 using 0.9 eq  $K_2CO_3$  / THF (as a base and solvent) , respectively

### 1.5.9 Synthetic approach towards 19,20-dihydro-O-methylmacusine B

From the results found previously from the reduction of enol ether **94**, this led to the use of  $\text{Pd}(\text{OAc})_2$  reduction of **94** to provide product **99** (Scheme 23) which was the precursor to the target alkaloid 19,20-dihydro-O-methylmacusine B (**83**). When this reaction was repeated a couple of times at 100 mg scale it was observed from TLC (silica gel, 10% methanol and 90% dichloromethane) that two major materials could be detected with significantly close  $R_f$  values. These two spots (one spot was major and the other was minor) were separated using the column chromatography (5% to 7% methanol and  $\text{CH}_2\text{Cl}_2$ ). Examination of the spectroscopy of the crude material indicated each component, contains two different sets of protons (one major sets of protons) but the mass spectroscopy shows indicated only one peak for both spots. This implies that there were in total four possible diastereomers **99a-99d** from this reaction with the same molecular weight (Figure 11).



**Scheme 22.** Synthesis of **99** from **94**

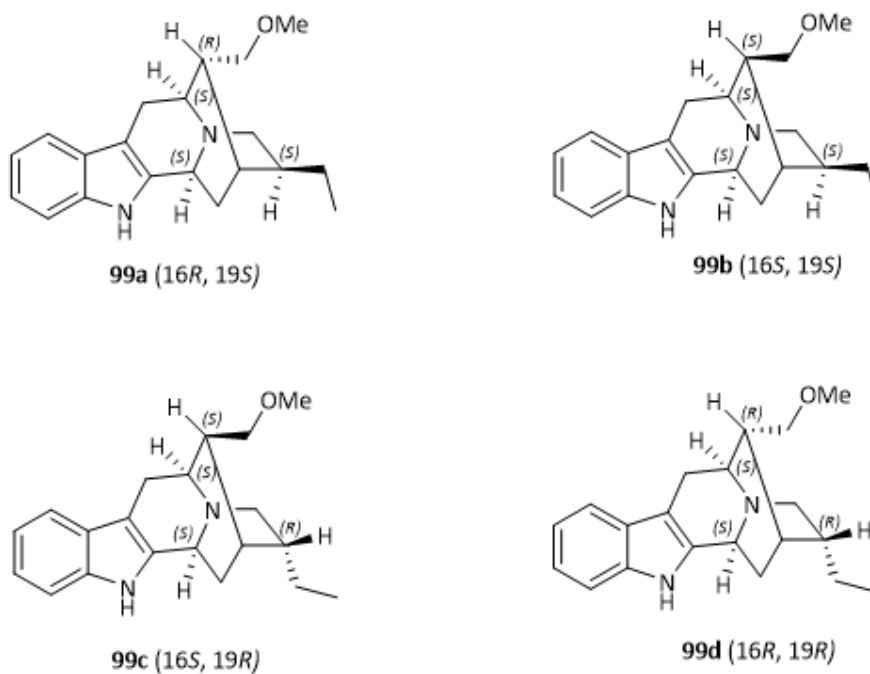
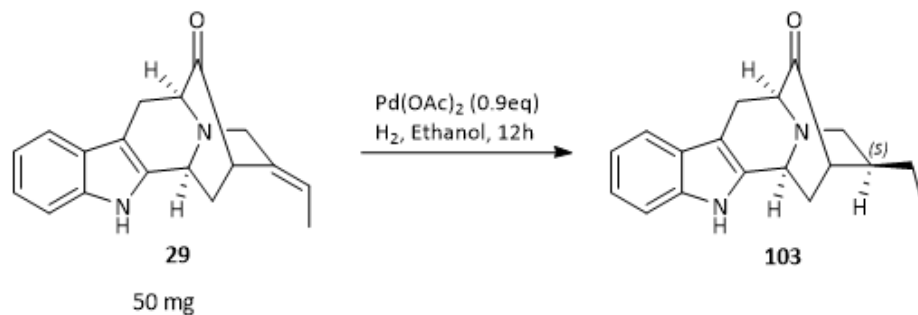


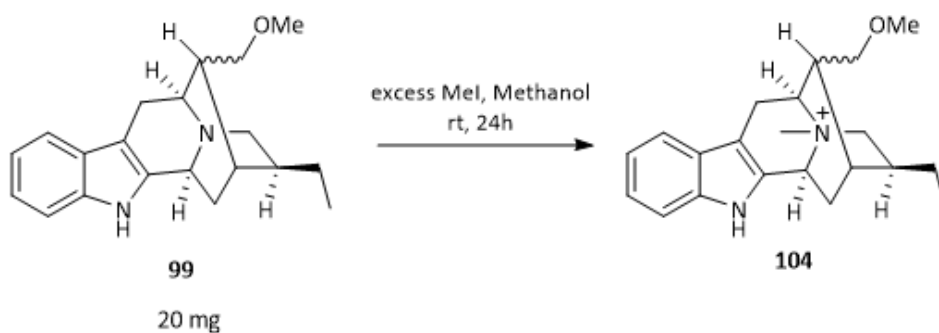
**Figure 11.** Four diastereomeric products formed from the reaction Scheme 22

The stereochemistry of the compound **99** at C-19 was confirmed from the study of the reaction Scheme 23 where the major product was isolated from the reaction of pentacyclic ketone **29** with palladium acetate under H<sub>2</sub> furnished the C-19*S* stereochemistry, which was confirmed by NOESY and NOE experiments. It was still necessary to carry out the chiral HPLC to find out the purity of the dihydro compound **103** as well as the ratio of the diastereomers formed in these reactions.



**Scheme 23.** Synthesis of **103** from **29**

The isolated product with the unknown stereochemistry at C-16 position was allowed to react with excess  $\text{CH}_3\text{I}$  in dry MeOH to get the product **104** (Scheme 24). It was difficult to integrate the crude NMR of the product since it was a mixture of two diastereomers. To get the selective stereochemistry of 19,20-dihydro-O-methyl macusine B at C-16 some chiral ligand should be used with palladium acetate and  $\text{H}_2$ .



**Scheme 24.** Synthesis of **104** from **99**

Overall, from the results shown above from different experiments, done at various reaction conditions provides some significant insights into the synthesis of the targeted natural products. The underlying reason for the unsuccessful C(3)-N(4) bond breaking approach could be due to the unstable ten membered ring which would be formed after the breaking of the C(3)- N(4) bond. Although the attempts were unsuccessful most of the time it provides useful information about the synthetic pathway towards the targets. Different synthetic strategies could be attempted to synthesize these products by avoiding the unsuccessful reaction pathways explored so far during these studies.

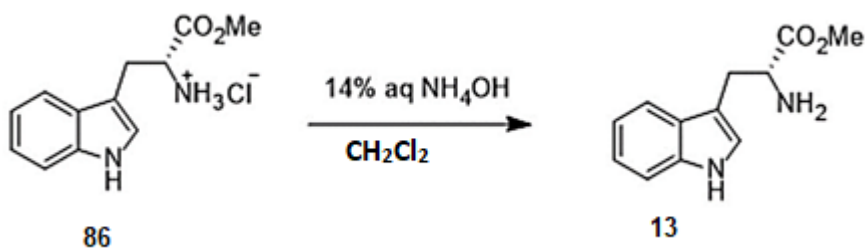
## 1.6 Experimental

### 1.6.1 General Experimental Considerations

All reactions were carried out under an argon atmosphere with dry solvents using anhydrous conditions unless mentioned otherwise. Some cases, the solvents (THF, DMF, toluene, DCM, MeCN, and MeOH) were dried using an Innovative Technology solvent purification system, Pure Solv™. Occasionally, tetrahydrofuran was freshly distilled from Na/ benzophenone ketyl prior to use. Dichloromethane was distilled from calcium hydride prior to use. Methanol was distilled over magnesium sulfate. Benzene was distilled over CaH<sub>2</sub>. Reagents were purchased of the highest commercial quality and used without further purification unless otherwise stated. Thin layer chromatography (TLC) was performed on UV active silica gel plates, 200 μm, aluminum

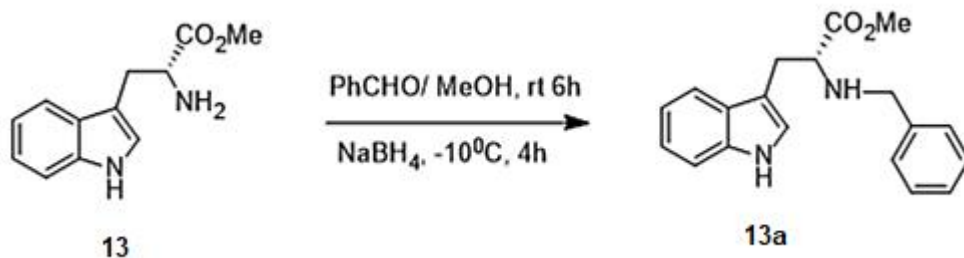
backed and UV active alumina N plates, 200  $\mu\text{m}$ , F-254 aluminum backed plates. Flash and gravity chromatography were performed using silica gel P60A, 40-63  $\mu\text{m}$ , basic alumina (Act I, 50-200  $\mu\text{m}$ ) and neutral alumina (Brockman I,  $\sim$ 150 mesh). TLC plates were visualized by exposure to short wavelength UV light (254 nm). Indoles were visualized with a saturated solution of ceric 166 ammonium nitrate (CAN) in 50% phosphoric acid. Melting points were taken on a Stuart melting point apparatus SMP3 manufactured by Barloworld Scientific US Ltd. Proton ( $^1\text{H}$  NMR) and carbon high resolution nuclear magnetic resonance spectra ( $^{13}\text{C}$  NMR) were obtained on a Bruker 300-MHz or a Bruker 500-MHz NMR spectrometer. The  $^1\text{H}$  NMR data are reported as follows: chemical shift, multiplicity (br s = broad singlet, s = singlet, d = doublet, t = triplet, q = quartet, quin = quintet, dd = doublet of doublets, dt = doublet of triplets, ddd = doublet of doublet of doublets, td = triplet of doublets, qd = quartet of doublets, m = multiplet), integration, and coupling constants (Hz). The  $^{13}\text{C}$  NMR data are reported in parts per million (ppm) on the  $\delta$  scale. The low-resolution mass spectra (LRMS) were obtained as electron impact (EI, 70eV) mass spectrometer and as chemical ionization (CI) using a magnetic sector (EBE) analyzer. HRMS were recorded by electrospray ionization (ESI) using a TOF analyzer, electron impact (EI) using a trisector analyzer and Atmospheric Pressure Chemical Ionization (APCI) using a TOF analyzer. Optical rotations were measured on a JASCO Model DIP-370 polarimeter.

### 1.6.2 D-(-)-Tryptophan methyl ester **13**



The free base **13** was prepared by the treatment of commercially available D-(-)-tryptophan methyl ester.HCl salt **86** (500g, 1.96 mol) with cold aq  $\text{NH}_4\text{OH}$  (10%), followed by extraction with  $\text{CH}_2\text{Cl}_2$  in methanol (4:1, 3 x 1000 mL). The solvent was evaporated under reduced pressure, after which the solid was re-dissolved in  $\text{CH}_2\text{Cl}_2$  and dried ( $\text{K}_2\text{CO}_3$ ). The  $\text{CH}_2\text{Cl}_2$  layer was removed under reduced pressure to provide D-(-)-tryptophan methyl ester **13** (392 g, 91%); mp 92-93 °C ;  $[\alpha]_D^{27} = -37.2$  (c 1.0 in MeOH); IR (KBr) 1730  $\text{cm}^{-1}$ ;  $^1\text{H NMR}$  (250 MHz,  $\text{CDCl}_3$ )  $\delta_{\text{H}}$  1.62 (2H, s), 3.05 (1H, dd,  $J = 14.5, 7.5$  Hz), 3.29 (1H, dd,  $J = 14.6, 5.8$  Hz), 3.74 (3H, s), 3.86 (1H, dd,  $J = 7.5, 4.8$  Hz), 7.04-7.23 (3H, m), 7.35 (1H, d,  $J = 7.5$  Hz), 7.61 (1H, d,  $J = 7.5$  Hz), 8.24 (1 H, s);  $^{13}\text{C NMR}$  (62.8 MHz,  $\text{CDCl}_3$ )  $\delta_{\text{C}}$  30.83, 51.86, 55.06, 111.19, 118.73, 119.49, 122.11, 122.87, 127.57, 136.37, 175.71. **EIMS** (m/e, relative intensity) 218 ( $\text{M}^+$ , 78), 159 (57), 130 (100), 117 (33). Anal. Calcd. for  $\text{C}_{12}\text{H}_{14}\text{O}_2\text{N}_2$  : C, 66.06; H, 6.42, N, 12.84. Found: C, 66.14; H, 6.33; N, 12.77. This material was identical to that employed in previous experiments.<sup>73</sup>

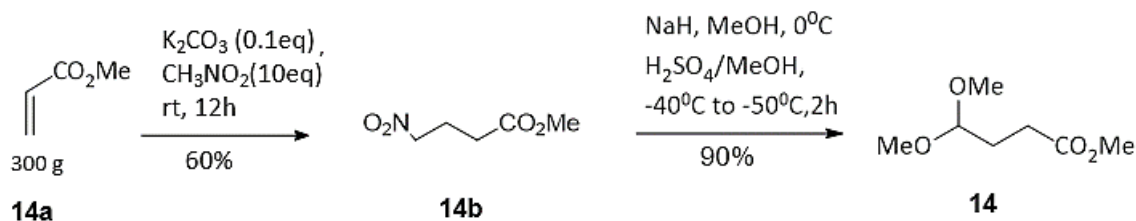
### 1.6.3 D-(+)-Nb-Benzyltryptophan methyl ester **13a**



To a round bottom flask (3000 mL) which contained a solution of D-(-)-tryptophan methyl ester **13** (408 g, 1.87 mol) in dry CH<sub>3</sub>OH (1500 mL), benzaldehyde (260.0 g, 2.3 mol) was added. The solution which resulted was stirred with an overhead stir for 6 h at 22 °C, until examination by TLC (silica gel) indicated the disappearance of **13**. The mixture was then cooled in an ice-salt bath to -5 °C [It was much easier to maintain the inside temperature between -10°C to -5°C by the employment of a dry ice bath (without solvent)]. If the temperature falls below -15°C, a large amount of solid will appear and it is too difficult to stir the reaction mixture. Sodium borohydride (42 g, 1.1 mol) was then added portion wise at -5 °C over a period of 2.5 h [The slow addition and lower temperature of this process are critical to avoid racemization of the chiral center]. The solution was stirred for 3 h and then followed by the addition of ice water (50 mL). The solvent was removed under reduced pressure. The residue was dissolved in CHCl<sub>3</sub> (2000 mL) and washed with brine (2 x 500 mL). The organic layer was dried (K<sub>2</sub>CO<sub>3</sub>) and the solvent was removed under reduced pressure to give the free base **13a** (525 g, 90%) which could be further purified by crystallization from EtOH. mp 109-110 °C; [α]<sub>D</sub><sup>22</sup> = + 9.07° (c 1.0 in CH<sub>3</sub>OH), [lit.152 [α]<sub>D</sub><sup>22</sup> = +8.65°

(c 1.0 in CH<sub>3</sub>OH)]; IR (film) 1745 cm<sup>-1</sup>; <sup>1</sup>H NMR (250 MHz, CDCl<sub>3</sub>) δ<sub>H</sub> 2.10 (1H, s), 3,15 (2H, m), 3.65 (3H, s), 3.75 (3 H, s), 3.80 (3H, m), 6.90 (1H, s), 7.10 (1H, t, *J* = 8.2 Hz), 7.25 (5H, m), 7.55 (1H, d, *J* = 8.2 Hz); <sup>13</sup>C NMR (62.8 MHz, CDCl<sub>3</sub>) δ<sub>C</sub> 29.35, 51.68, 52.20, 61.38, 111.18, 111.38, 118.84, 119.45, 122.07, 122.88, 127.03, 127.62, 128.19, 128.32, 136.30, 139.79, 175.36; EIMS (m/e, relative intensity) 308 (M<sup>+</sup>, 28), 249 (22), 178 (57), 130 (100). Anal. Calcd. For C<sub>19</sub>H<sub>20</sub>O<sub>2</sub>N<sub>2</sub> : C, 74.03; H, 6.49; N, 9.08. Found: C, 73.99; H, 6.56; N, 8.99. This was used directly in the next step.

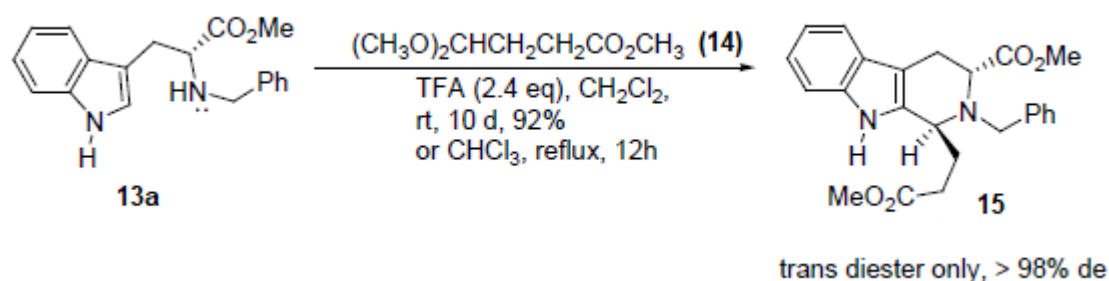
#### 1.6.4 Preparation of methyl 4,4-dimethoxybutyrate **14**



To a round bottom flask (5 L) equipped with an overhead stir which contained a solution of methyl acrylate **14a** (300 g, 3.5 mol) and nitromethane (1875 g, 35 mol), was added solid K<sub>2</sub>CO<sub>3</sub> (48.4 g, 0.35 mol) at 0 °C. The mixture which resulted was stirred at rt for 12 h. The organic layer was filtered using a Büchner funnel and washed with small amount of CHCl<sub>3</sub>. The solvent was then removed under reduced pressure and the residue was distilled under reduced pressure (95-100 °C/8 mm of Hg) to give the pure methyl γ-nitro butyrate **14b** (307.6 g, 60%). This was dissolved in methanolic sodium methoxide [3080 mL, 0.8 N, freshly prepared from 98.55 g of NaH

(60% dispersion in mineral oil)] and the solution which resulted was added dropwise with an overhead stirrer at a rate of 1 drop per second to a round bottom flask (10 L) which contained a solution of conc sulfuric acid (770 mL) in methanol (2310 mL) at -45 to -50 °C. After the addition was completed, the reaction mixture was poured into CH<sub>2</sub>Cl<sub>2</sub> (5 L). The organic layer was separated and washed with ice water (2 x 1000 mL), aq 4N NaOH (2 x 350 mL) and dried (K<sub>2</sub>CO<sub>3</sub>). The solvent was removed under reduced pressure and the residue was distilled (110-115 °C/8 mm of Hg) to provide methyl 4,4- dimethoxybutyrate **14** (305 g, 90%). <sup>1</sup>H NMR (250 MHz, CDCl<sub>3</sub>) δ<sub>H</sub> 1.92 (2H, q, *J* = 7.5 Hz), 2.37 (2H, t, *J* = 7.5 Hz), 3.31 (6H, s), 3.66 (3H, s), 4.38 (1H, t, *J* = 15.8 Hz); <sup>13</sup>C NMR (62.8 MHz, CDCl<sub>3</sub>) δ<sub>C</sub> 27.92, 29.07, 51.45, 53.14, 103.14. CIMS (*m/e*, relative intensity) 375 (M<sup>+</sup> + 1, 100). The spectral data for **14** were identical to the published values.<sup>73</sup>

1.6.5 Diastereospecific preparation of the *trans*-(1*S*,3*R*)-(-)-2-benzyl-3-methoxycarbonyl-1-methoxycarbonylethyl-1,2,3,4-tetrahydro-9*H*-pyrido-[3,4-*b*]indole (**15**) via the newly modified Pictet-Spengler reaction.

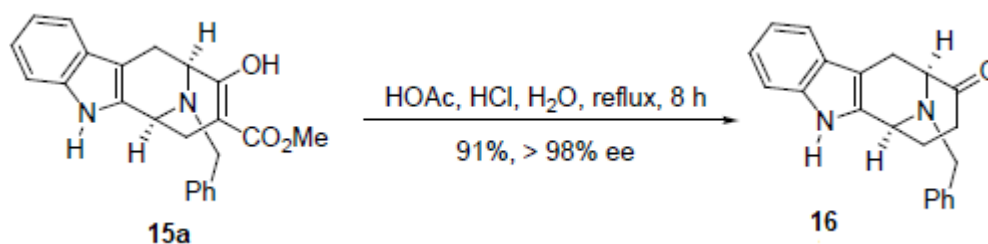


To a round bottom flask (5000 mL), which contained a solution of optically active *N*<sub>b</sub>-benzyl-*D*-tryptophan methyl ester **13a** (400 g, 1.3 mol) in  $\text{CH}_2\text{Cl}_2$  (2500 mL) was added methyl 4,4-dimethoxybutyrate acetal 95 (315 g, 1.9 mol) and TFA (238.75 g, 2.4 eq) at 0 °C with stirring. The reaction mixture which resulted was allowed to stir at rt for 10 d and then cooled in an ice bath and brought to pH = 8 with a cold aq solution of NaOH (3 N). The aq layer was separated and extracted with  $\text{CH}_2\text{Cl}_2$  (3 x 1500 mL). The combined organic layers were washed with brine (2 x 600 mL) and dried ( $\text{K}_2\text{CO}_3$ ). The volume of the solution was reduced to 300 mL under reduced pressure and EtOAc (100 mL) and hexanes (300 mL) were added to the above solution. The solution was cooled to -20 °C. The *trans* diester **15** (402 g, 76%) precipitated out as white crystals



To a round bottom flask (5000 mL), which contained a solution of Na-H, trans diester **15** (100 g, 0.25 mol) in toluene (3000 mL), which had been predried by azeotropic removal of H<sub>2</sub>O by a DST (refluxed 6 h), was added sodium hydride (88.7 g, 2.2 mol, 60% dispersion in mineral oil) at 0 °C. Anhydrous CH<sub>3</sub>OH (174 mL, 4.3 mol) was then added into the above mixture dropwise under Ar at 0 °C. The solution, which resulted, was held at reflux for 72 h (the flask was covered with aluminum foil on the top to keep the temperature at reflux without carbonizing any compound on the sides of the flask). The reaction was quenched with ice. The aq layer was extracted with CH<sub>2</sub>Cl<sub>2</sub> (3 x 1 L). The combined organic extracts were washed with brine and dried (K<sub>2</sub>CO<sub>3</sub>). The solvent was removed under reduced pressure and the mineral oil was separated by decantation. The residue which resulted was purified by flash chromatography (silica gel, EtOAc/hexane, 1/4) to provide the Na-H, β-ketoester **15a** (82 g, 88%). mp 149-150 °C; [α]<sub>D</sub><sup>27</sup> = -176.9° (c, 1.0 in CHCl<sub>3</sub>); IR (KBr) 1670, 1630 cm<sup>-1</sup>; <sup>1</sup>H NMR (250 MHz, CDCl<sub>3</sub>) δ<sub>H</sub> 2.30 (1H, d, J = 15.6 Hz), 2.82 (1H, dd, J = 15.5, 5.6 Hz), 2.90 (1H, d, J = 15.3 Hz), 3.18 (1H, dd, J = 15.9, 5.9 Hz), 3.66 (3H, s), 3.71 (1H, d, J = 13.4 Hz), 3.77 (1H, d, J = 5.3 Hz), 3.82 (1H, d, J = 13.4 Hz), 3.98 (1H, d, J = 5.4 Hz), 7.11 (1H, t, J = 7.1 Hz), 7.16 (1H, t, J = 7.0 Hz), 7.24-7.39 (6H, m), 7.50 (1H, d, J = 7.1 Hz), 7.63 (1H, s), 11.98 (1H, s); <sup>13</sup>C NMR (75 MHz, CDCl<sub>3</sub>) δ<sub>C</sub> 22.2, 28.6, 49.7, 51.3, 55.2, 55.9, 94.3, 106.2, 110.8, 118.1, 119.5, 121.6, 127.0, 127.2, 128.4, 128.7, 133.4, 135.7, 138.3, 171.6, 172.5; CIMS (CH<sub>4</sub>) (m/e, relative intensity) 389 (M<sup>+</sup> + 1, 100). Anal. Calcd. for C<sub>23</sub>H<sub>22</sub>N<sub>2</sub>O<sub>3</sub>: C, 73.78; H, 5.92; N, 7.48. Found: C, 74.19; H, 6.23; N, 7.35. This was used in a later step.

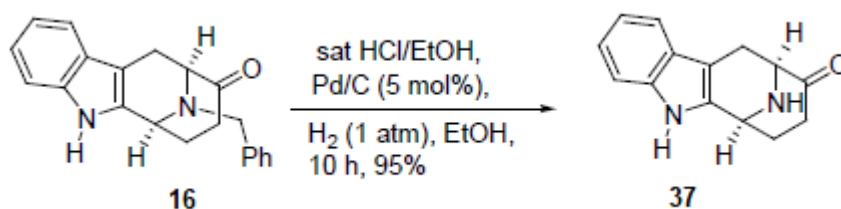
1.6.7 Preparation of (6*S*,10*S*)-(-)-9-oxo-12-benzyl-6,7,8,9,10,11-hexahydro-6,10-imino-5H-cyclo-oct[b]indole **49** via acid mediated hydrolysis of the N<sub>a</sub>-H, β-ketoester **16**



To a round bottom flask (500 mL) which contained the N<sub>a</sub>-H, β-ketoester **15a** (45.0 g, 0.12 mol) was added glacial acetic acid (167 mL), aq hydrochloric acid (245 mL, conc.) and water (65 mL) with stirring (magnetic stir). The solution, which resulted, was heated at reflux for 8 h. After removal of the solvent under reduced pressure, the residue was brought to pH = 9 with a cold aq solution of NaOH (3 N). The mixture which resulted was extracted with CH<sub>2</sub>Cl<sub>2</sub> (4 x 250 mL) and the combined organic extracts were washed with a saturated aq solution of NH<sub>4</sub>Cl (100 mL), brine (2 x 100 mL) and dried (K<sub>2</sub>CO<sub>3</sub>). Removal of the solvent under reduced pressure afforded an oil. After a short wash column on silica gel, the N<sub>a</sub>-H, N<sub>b</sub>-benzyltetracyclic ketone **16** (24.5 g, 64%) was crystallized from EtOAc/ hexane (1:4, 30 mL). The mother liquor was concentrated under reduced pressure and the residue was chromatographed on silica gel with EtOAc/hexane (1:4) to provide additional ketone **16** (10.5 g, 27%). The combined yield of **16** (35.0 g) was 91%.  $[\alpha]_D^{27} = -246.3^\circ$  (C = 1.07 in CHCl<sub>3</sub>); IR (KBr) 2933, 1715 cm<sup>-1</sup>; <sup>1</sup>H NMR (250 MHz, CDCl<sub>3</sub>) δ<sub>H</sub> 2.02(1H, m), 2.15 (1H, m), 2.49 (2H, m), 2.71 (1H, d, J = 16.9 Hz), 3.27 (1H, dd, J = 16.9, 6.8 Hz), 3.78 (2H, s),

3.80 (1H, s), 4.02 (1H, s), 7.17 (1H, dt, J = 7.3, 1.0 Hz), 7.23 (1H, dt, J = 7.6, 1.0 Hz), 7.30-7.38 (6H, m), 7.54 (1H, d, J = 7.6 Hz), 7.81 (1 H, s); <sup>13</sup>C NMR (62.8 MHz, CDCl<sub>3</sub>) δ<sub>c</sub> 20.40, 30.37, 34.51, 49.40, 56.13, 65.22, 106.73, 110.94, 118.21, 119.72, 122.01, 126.86, 127.42, 128.43, 128.60, 131.98, 135.85, 138.25, 210.40; CIMS (m/e, relative intensity) 317 (M<sup>+</sup> + 1). Anal. Calcd. for C<sub>21</sub>H<sub>20</sub>N<sub>2</sub>O: C, 79.72; H, 6.37; N, 8.85. Found: C, 79.51; H, 6.37; N, 8.85. This was used in the next step.

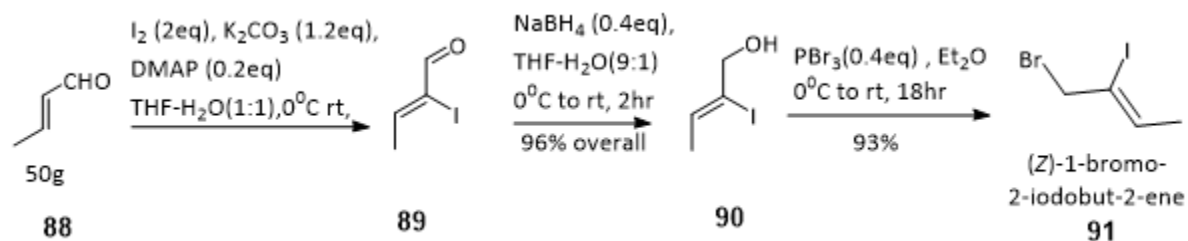
### 1.6.8 Catalytic debenzoylation of **16** to provide (6S,10S)-(-)-9-oxo-12-H-6,7,8,9,10,11-hexahydro-6,10-imino-5H-cyclooct[b]indole **37** over Pd/C/H<sub>2</sub>



Tetracyclic ketone **16** (40 g, 127 mmol) was dissolved in anhydrous ethanol (1300 mL). A saturated solution of EtOH/HCl (g) was then added dropwise into the above mixture until the solid completely dissolved. The solvent was then removed under reduced pressure to furnish an HCl salt. The residue was then dissolved in dry ethanol (1000 mL) and the solvent was removed under reduced pressure to remove the excess HCl. This process was repeated 3 times to make

sure there was no excess HCl. The HCl salt was degassed under reduced pressure at rt and back filled with argon (2 times). Dry Pd/C (10% by wt, 8.1 g, 60 mmol) was added to the above HCl salt followed by addition (slow addition, initially) of dry ethanol (1300 mL). The mixture was degassed under reduced pressure at rt and back filled with H<sub>2</sub> (3 times). The mixture which resulted was allowed to stir at rt under an atmosphere of H<sub>2</sub> for 10 h. Analysis by TLC (silica gel plate was exposed to NH<sub>3</sub> vapours) indicated the absence of starting material **16**. The catalyst was removed by filtration (Celite) and washed with ethanol (3 x 100 mL). The solvent was removed under reduced pressure. The residue was dissolved in a mixture of CH<sub>2</sub>Cl<sub>2</sub> and brought to pH = 8 with 10% aq NH<sub>4</sub>OH. The aq layer was extracted with CH<sub>2</sub>Cl<sub>2</sub> (3 x 400 mL). The combined organic layers were washed with brine (2 x 200 mL) and dried (K<sub>2</sub>CO<sub>3</sub>). The solvent was removed under reduced pressure to afford the crude amine which was chromatographed (flash) on silica gel (CHCl<sub>3</sub>/EtOH, 9/1) to provide pure N<sub>a</sub>-H, N<sub>b</sub>-H tetracyclic ketone **37** (27.2 g, 95%). FTIR (NaCl) 3393, 3382, 1705 cm<sup>-1</sup>, <sup>1</sup>H NMR (300 MHz, CDCl<sub>3</sub>) δ<sub>H</sub> 8.06 (1H, bs), 7.44 (1H, d, J = 7.62 Hz), 7.29 (1H, d, J = 7.9 Hz), 7.16 (1H, d, J = 7.4 Hz), 7.10 (1H, d, J = 7.4 Hz), 4.27 (1H, d, J = 3.9 Hz), 3.92 (1H, d, J = 6.7 Hz), 3.09 (1H, dd, J = 16.5, 6.8 Hz), 2.80 (1H, d, J = 16.4 Hz), 2.36-2.50 (3H, m), 2.08-2.15 (2H, m); <sup>13</sup>C NMR (75.5 MHz, CDCl<sub>3</sub>) δ<sub>C</sub> 211.0, 135.7, 134.0, 126.9, 122.1, 119.7, 118.1, 110.9, 107.5, 59.8, 46.1, 35.0, 32, 25.8; CIMS (m/e, relative intensity) 227 (M<sup>+</sup>+1, 100%). Anal. Calcd. For C<sub>14</sub>H<sub>14</sub>N<sub>2</sub>O: C, 74.31%; H, 6.24%; N, 12.38%. Found: C, 74.39%; H, 6.35%; N, 12.41%. This was used in next step.

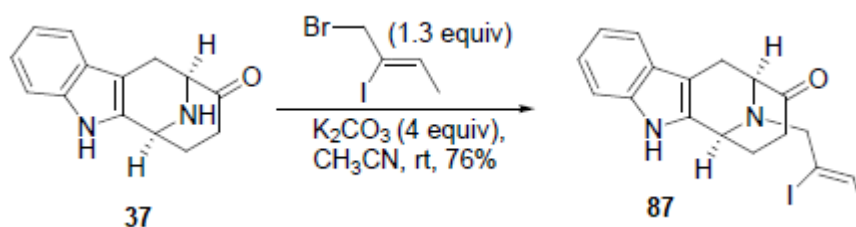
### 1.6.9 Synthesis of (Z)-1-bromo-2-iodobut-2-ene **91**



A solution of crotonaldehyde **88** (30mL, 0.363 mol) in THF-H<sub>2</sub>O (1:1, 150mL) was cooled to -15 to -20 °C (dry ice). To the cold solution was added K<sub>2</sub>CO<sub>3</sub> (60g, 0.445 mol, 1.2 equiv), I<sub>2</sub> (138.3g, 0.545 mol, 1.5 equiv) and DMAP (8.86g, 0.0726 mol, 0.2 equiv) successively (the temperature increase was controlled by the rate of addition of I<sub>2</sub>). The reaction was allowed to stir for 12 h until the disappearance of starting material (TLC, silica gel, I<sub>2</sub>) during which the temperature was allowed to increase to rt. Then solid Na<sub>2</sub>S<sub>2</sub>O<sub>3</sub> (60g) and a saturated solution of Na<sub>2</sub>S<sub>2</sub>O<sub>3</sub> (about 500 mL) was added until the reaction mixture became colorless. The mixture was extracted with EtOAc (3x 800 mL) and the organic layers were combined. The majority of the solvent was removed under reduced pressure. The residue **89** was dissolved in THF-H<sub>2</sub>O (9:1, 800 mL) and cooled to -5 to -10 °C (dry ice) after which NaBH<sub>4</sub> (7.0 g, 0.18 mol, 0.5 equiv) was added in portions and the temperature maintained at 0°C. The mixture was extracted with EtOAc (3x800 mL) and dried (MgSO<sub>4</sub>). The solvent was removed under reduced pressure to provide a brown oil. After a simple wash column to remove some baseline material, iodide **90** was obtained as light yellow oil (650g, 90%). <sup>1</sup>H NMR (300 MHz, CDCl<sub>3</sub>) δ<sub>H</sub> 6.02 (q, 1H, J=3.9Hz), 4.30 (s, 2H), 1.85 (t, 3H, J=6.3Hz). The spectral properties of this iodide were identical to the published values<sup>98</sup>. (Z)-2-iodo-2-buten-1-

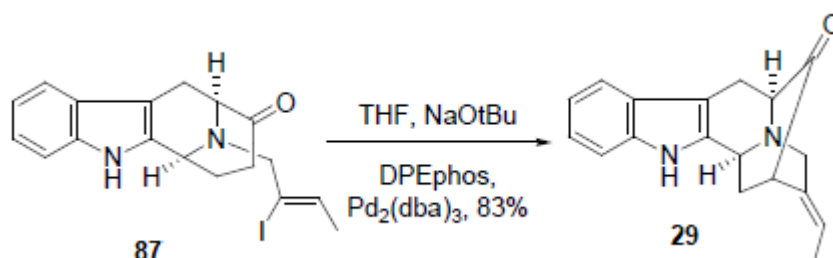
ol **90** (2 g, 10 mmol) was dissolved in anhydrous ethyl ether (20 mL). Phosphorus tribromide (0.380 mL, 4 mmol) was added dropwise to this solution at 0°C. This reaction mixture which resulted was stirred for 18 h at rt. The reaction was quenched with a cold aq solution of K<sub>2</sub>CO<sub>3</sub> and extracted with ethyl ether after which it was washed with brine. The organic layer was dried (Na<sub>2</sub>SO<sub>4</sub>) and concentrated in vacuo to give **91** (2.45 g, 93% yield) which was directly used in the next step. <sup>1</sup>H NMR: δ<sub>H</sub> 6.08 (q, J = 6.4 Hz, 1H); 4.36 (s, 2H); 1.81 (d, J = 6.4 Hz, 3H). The spectral properties of this bromide were identical to the published values<sup>99</sup>. This was directly used in the following alkylation.

1.6.10 Alkylation of (6S,10S)-(-)-9-oxo-12-H-6,7,8,9,10,11-hexahydro-6,10-imino-5H-cyclooct [b] indole (**37**) to provide (6S,10S)-(-)-9-oxo-12-(Z-2'-iodo-2'-butenyl)-6,7,8,9,10,11-hexahydro-6,10-imino-5H-cyclooct[b] indole **87**



A solution of the N<sub>a</sub>-H, N<sub>b</sub>-H tetracyclic ketone **37** (1.5g, 6.637mmol) was dissolved in dry CH<sub>3</sub>CN (20mL). To this mixture, K<sub>2</sub>CO<sub>3</sub> (3.66g, 26.54 mmol) and Z-1-bromo-2-iodo-2-butene **91** (2.6g, 9.95mmol) were added. This reaction mixture was stirred for 14h at rt. Analysis by TLC indicated the absence of tetracyclic ketone. The K<sub>2</sub>CO<sub>3</sub> was removed by passing the mixture through a bed of celite with EtOAc. After removal of the solvent under reduced pressure, the crude product was purified by flash chromatography (silica gel, hexane:EtOAc = 9:1) to provide N<sub>b</sub>-Z-2'-iodo-2'-butenyl tetracyclic ketone **87** (2.04g, 76%). FTIR (NaCl) 3393, 1705, 1450cm<sup>-1</sup>; <sup>1</sup>H NMR (300 MHz, CDCl<sub>3</sub>) δ<sub>H</sub> 1.73 (3H, d, J=6.27Hz), 2.19-2.05 (2H, m), 2.37-2.47 (2H,m), 2.65(1H, d, J=16.87Hz), 3.05 (1H, dd, J=16.94, 6.72 Hz), 3.19-3.37 (2H,m), 3.64 (1H, d, J=6.37Hz), 3.96 (1H, bs), 5.76 (1H, q, J=6.17Hz), 6.97-7.16 (2H, m), 7.25 (1H, d, J=7.72Hz), 7.40 (1H, d, J=7.52Hz), 8.05 (1H, bs); <sup>13</sup>C NMR (75.5 MHz, CDCl<sub>3</sub>) δ<sub>C</sub> 20.60, 21.71, 30.35, 34.49, 49.73, 63.36, 64.07, 106.69, 108.47, 110.94, 118.09, 119.62, 121.97, 125.72, 132.11, 132.76, 135.79, 210.40; CIMS (m/e, relative intensity) 407 (M<sup>+</sup> +1, 100%). Anal. Calcd. For C<sub>18</sub>H<sub>19</sub>N<sub>2</sub>O: C, 53.22%; H, 4.71%; N, 6.90%. Found: C, 53.15%; H, 4.80%; N, 6.64%. This material was used in the next step.

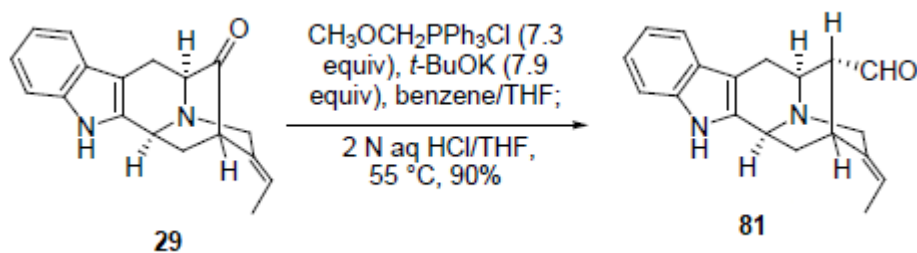
1.6.11 Palladium catalyzed cyclization of (6*S*, 10*S*)-(-)-9-oxo-12-(*Z*-2'-iodo-2'-butenyl)- 6,7,8,9,10,11-hexahydro-6,10-imino-5*H*-cyclooct indole (**87**) to provide pentacyclic ketone **29**



The N<sub>8</sub>-*Z*-2'-iodo-butenyl tetracyclic ketone **87** (1 g, 2.46 mmol) was dissolved in anhydrous THF (20mL). To this mixture NaOtBu (0.354 g, 3.69 mmol), DPEphos (0.0927 g, 7.0 mol %) and Pd<sub>2</sub>(dba)<sub>3</sub> (0.112g, 5.0 mol %) was added. This reaction mixture was degassed 3-4 times under vacuum and back filled with argon and placed in a preheated oil bath at 80 °C for 5hrs. The reaction was quenched with water and ethyl acetate. The organic layer was separated and dried (Na<sub>2</sub>SO<sub>4</sub>). The EtOAc was then removed under reduced pressure and the residue was flash chromatographed with CH<sub>2</sub>Cl<sub>2</sub> /MeOH (4.5:0.5) to provide the coupling product **29** (0.569g, 83% yield). <sup>1</sup>H NMR (300 MHz, CDCl<sub>3</sub>) δ<sub>H</sub> 1.63 (3H, J=6.86 Hz, d), 2.15-2.20 (1H, m), 2.38 (1H, t, J=9.9 Hz), 2.97 (1H, dd, J=15.58, 6.20 Hz), 3.27 (1H, d, J=14.43 Hz), 3.37 (1H, bs), 3.59 (1H, d, J=5.70 Hz), 3.78 (2H, bs), 4.26 (1H, d, J=59.11 Hz), 5.49 (1H, q, J=6.85 Hz), 7.05-7.15 (2H, m), 7.25 (1H, d, J=7.25Hz), 7.47 (1H, d, J=4.7Hz), 7.93 (s, 1H); <sup>13</sup>C NMR (75.5 MHz, CDCl<sub>3</sub>) δ<sub>C</sub> 12.68, 22.39, 36.40, 44.55, 50.83, 55.24, 64.17, 105.62, 110.89, 118.54, 119.69, 121.26, 122.00, 126.88, 131.88,

135.87, 136.34, 217.00; HRMS C<sub>18</sub>H<sub>18</sub>N<sub>2</sub>O: calcd. 278.1419; found 278.1437. This material was used in the next step.

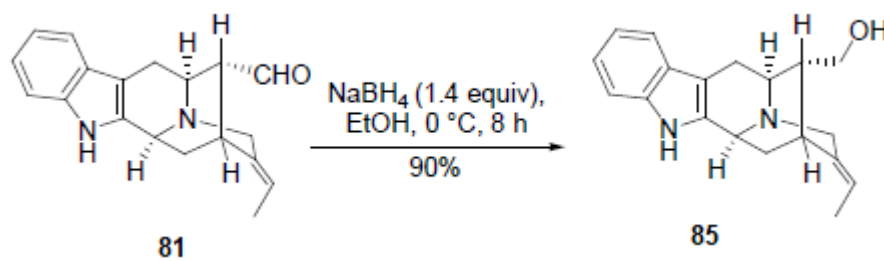
1.6.12 Conversion of the pentacyclic ketone (**29**) into (+)-3-ethylidene-1,3,4,7,12,12b-hexahydro-2H, 6H-2,6-methano-indole[2,3- $\alpha$ ]-quinolizine-13-carboxaldehyde[(+)-vellosimine, **81**] via the Wittig reaction followed by acid mediated hydrolysis.



A mixture of anhydrous potassium *t*-butoxide (12.8g, 0.114 mol) and methoxymethyl triphenylphosphonium chloride (36g, 0.105 mol) in dry benzene (500mL) was allowed to stir at rt for 1h. The pentacyclic ketone **29** (4g, 14.4mmol) in THF (160mL) was then added into the above orange colored solution dropwise at rt. The mixture, which resulted, was stirred at rt for 24h. The mixture was diluted with EtOAc (3x700mL), washed with H<sub>2</sub>O (3x50mL), brine (50mL) and dried (K<sub>2</sub>CO<sub>3</sub>). The solvent was removed under reduced pressure to afford an oil, **94**. (In some cases,

this **94** was isolated by chromatography, to do some experiments). The solvent was removed under reduced pressure and the residue was dissolved (without further purification) in a solution of aq HCl (2N) in H<sub>2</sub>O-THF (1:1, 400mL). The solution which resulted was refluxed 55 °C (oil bath temperature) under an atmosphere of argon for 6h. The reaction mixture was brought to rt and concentrated under reduced pressure. The reaction mixture was diluted with water and extracted with ether to remove the triphenyl phosphine oxide. The aq layer was brought to pH 8 with an ice cold aq solution of NaOH (1N). The aq layer was extracted with CH<sub>2</sub>Cl<sub>2</sub> and the combined organic layers were washed with H<sub>2</sub>O (3x100mL), brine (100mL) and dried (K<sub>2</sub>CO<sub>3</sub>). The solvent was removed under reduced pressure to afford an oil which was crystallized to provide the aldehyde **81** (3.78g, 90%). The spectral data for (+)-vellosimine, **81** were in good agreement with the published values<sup>100</sup>.

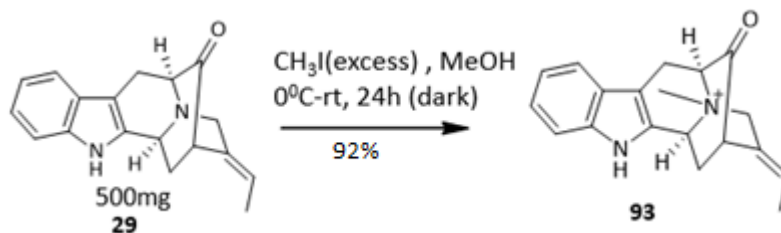
1.6.13 Sodium borohydride mediated reduction of (+)-3-ethylidene-1,3,4,7,12,12b-hexahydro-2H,6H-2,6-methano-indole[2,3- $\alpha$ ]-quinolizine-13-carboxaldehyde[(+)-vellosimine, **81**] to provide the (+)-3-ethylidene-1,3,4,7,12,12b-hexahydro-13-hydroxymethyl-2H,6H-2,6-methano-indole [2,3- $\alpha$ ]-quinolizine [(+)-normacusine B, **85**].



The (+)-vellosimine **81** (100mg, 0.34mmol) was dissolved in EtOH (5mL). The NaBH<sub>4</sub> (12mg, 0.33 mmol) was added to the above solution at 0 °C in one portion. The mixture was then stirred for 8 h. The reaction mixture was diluted with CH<sub>2</sub>Cl<sub>2</sub> (50mL) and poured into cold water (10mL). The aq layer was extracted with additional CH<sub>2</sub>Cl<sub>2</sub> (3x20mL) and the combined organic layers were washed with brine (10mL) and dried (K<sub>2</sub>CO<sub>3</sub>). The solvent was removed under reduced pressure to afford the crude product which was chromatographed to provide normacusine B **85** (90mg, 90%).  $[\alpha]_D^{28} = +40.5^\circ$  (c=0.75, C<sub>2</sub>H<sub>5</sub>OH); lit  $[\alpha]_D^{25} = +42^\circ$  (c=1.0, C<sub>2</sub>H<sub>5</sub>OH)<sup>174</sup>; FTIR (NaCl) 3198 cm<sup>-1</sup>; <sup>1</sup>H NMR (300 MHz, CDCl<sub>3</sub>)  $\delta_H$  1.57 (3H, d, J=6.76 Hz), 1.66 (1H, dt, J=12.54, 3.69 Hz), 1.78 (1H, q, J=7.49 Hz), 1.93 (1H, t, J=10.00Hz), 2.61(1H, d, J=15.37Hz), 2.72 (1H, s), 2.74 (1H, d, J=6.51 Hz),

3.03 (1H, dd, J=15.39, 5.10 Hz), 3.43-3.49 (4H, m), 4.07 (1H, d, J=10.29Hz), 5.26 (1H, q, J=6.68Hz), 7.03-7.14 (1H, m), 7.28 (1H, d, J=6.00Hz), 7.42 (1H, d, J=7.00Hz), 8.22 (1H, s); <sup>13</sup>C NMR (75.5 MHz, CDCl<sub>3</sub>) δ<sub>c</sub> 12.75, 26.95, 27.58, 33.37, 44.14, 050/48, 54.47, 55.85, 64.90, 0104.52, 110.99, 116.84, 118.07, 119.35, 121.44, 127.59, 135.33, 136.33, 137.80; HRMS C<sub>19</sub>H<sub>22</sub>N<sub>2</sub>O: calcd. 294.1732; found 294.1705.

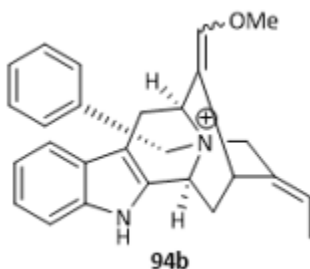
### 1.6.14 Synthesis of quarternary amine **93**



The pentacyclic ketone **29** (500 mg, 1.8 mmol) was taken in a 50 mL two neck round bottom flask and dissolved in 30 mL anhydrous MeOH. Excess MeI was added to the solution and the whole reaction flask was then covered by aluminium foil. The reaction was stirred in the dark and under argon for 24 hr. The excess MeI was removed under reduced pressure to get the crude quaternary amine **93**. The crude **93** was then dissolved in dichloromethane and evaporated three times to remove any remaining MeI to get the pure **93**, in 92% yield. <sup>1</sup>H NMR (500 MHz, CDCl<sub>3</sub>) δ<sub>H</sub> 9.97 (s, 1H), 7.39 (d, J = 8.7 Hz, 2H), 7.19 (s, 1H), 7.14 (dd, J = 11.4, 3.8 Hz, 1H), 7.06 (dd, J = 11.3, 4.4 Hz, 1H), 5.73 (q, J = 6.8 Hz, 1H), 5.00 (d, J = 15.1 Hz, 1H), 4.88 (d, J = 5.5 Hz, 1H), 4.79

(d,  $J = 15.2$  Hz, 1H), 3.60 (d,  $J = 3.9$  Hz, 1H), 3.57 (d,  $J = 17.1$  Hz, 1H), 3.47 (s, 3H), 3.17 (dd,  $J = 17.1$ , 5.8 Hz, 1H), 2.89 (dd,  $J = 12.3$ , 10.7 Hz, 1H), 2.32 (dd,  $J = 13.4$ , 4.5 Hz, 1H), 1.60 (d,  $J = 6.7$  Hz, 3H).  
 $^{13}\text{C}$  NMR (126 MHz,  $\text{CDCl}_3$ )  $\delta_{\text{C}}$  198.88 (s), 137.05 (s), 128.78 (s), 127.74 (s), 125.01 (s), 123.74 (s), 120.67 (d,  $J = 17.2$  Hz), 119.83 (s), 118.67 (s), 112.23 (s), 101.60 (s), 72.16 (s), 61.97 (s), 53.45 (s), 47.98 (s), 42.00 (s), 30.96 (s), 20.31 (s), 13.12 (s).

### 1.6.15 Formation of $\text{N}_b$ -benzyl product **94b**



The enol ether **94** (50mg, 0.16 mmol) was taken up in a 25 mL round bottom flask and dissolved in 10 mL dry THF. The Cbz-Cl (0.81 mmol) was then added into the reaction mixture and refluxed for 24hr. Once the reaction was done it was allowed to cool to rt, the quaternary salt **94b** was appeared as a powder-like material at the bottom of the flask. The amine **94b** was separated and washed with cold THF using a filter paper. Then it was dried under vacuum overnight to afford the pure **94b**.  $^1\text{H}$  NMR (300 MHz,  $\text{CDCl}_3$ )  $\delta_{\text{H}}$  11.79 (s, 1H), 7.54 (d,  $J = 5.8$  Hz, 3H), 7.46 (d,  $J = 7.5$  Hz, 1H), 7.37 (d,  $J = 6.9$  Hz, 3H), 7.20 – 7.07 (m, 2H), 5.85 (s, 1H), 5.56 (d,  $J = 9.5$  Hz, 1H), 5.15

(s, 2H), 4.70 (t, J = 13.7 Hz, 2H), 3.98 (dd, J = 26.1, 16.5 Hz, 2H), 3.55 (s, 3H), 3.47 (s, 1H), 3.07 (s, 1H), 2.47 (d, J = 15.1 Hz, 1H), 2.39 (d, J = 11.2 Hz, 1H), 2.08 (d, J = 10.6 Hz, 1H), 1.52 (d, J = 6.5 Hz, 3H). <sup>13</sup>C NMR (75 MHz, CDCl<sub>3</sub>) δ<sub>c</sub> 141.76, 137.15, 133.35, 131.61, 130.51, 129.43, 129.03, 126.71, 125.90, 122.44, 119.58, 118.03, 116.51, 112.65, 110.54, 110.02, 100.36, 67.96, 64.67, 61.19, 60.39, 58.00, 34.03, 29.47, 25.60, 21.89, 12.32.

### 1.6.16 General procedure for the synthetic approach of **92b**, **93a** and **94c** (see Tables 5-7 and 9)

For these reactions, at first, the quarternery salts (starting material) were taken into a appropriately sized reaction flask and dissolved in the corresponding solvent. After that, the base was added into the reaction mixture and heated in a sealed tube (or in some cases refluxed) for an appropriate amount of time. The reaction progress was monitored by TLC (10 % MeOH and 90% DCM). If any product was formed during these reactions, then the reaction mixture was brought back to room temperature and the solvent was evaporated under reduced pressure and the NMR of the crude material was taken after doing a wash column using DCM and methanol at different compositions, to see the nature of the product formation or to see the change in the starting material. Water work up was avoided in most of the cases because starting material used in these reactions were salts.

### 1.6.17 General procedure for the reaction Scheme 20 (approach towards the reduction of enol ether **94**) (see table 10 for results)

For this reaction scheme, different reaction conditions and different catalysts was used as mentioned in Table 10. Most of the time the enol ether **94** was taken up in a 20mL round bottom flask and dissolved in the solvent. For triethylsilyl hydride mediated reactions, the reagents were added at room temperature as well as low temperature to see the changes in the reactions; then the reactions were heated up to reflux conditions. For the palladium and platinum catalyzed reactions at first the enol ether **94** was dissolved in the dry solvent, followed by degassing of the solution three times. After that the catalyst was added in the degassed solution followed by degassing it for two more time under argon. Then the reaction flask was back filled with H<sub>2</sub> gas and the reaction was allowed to run at room temperature under a H<sub>2</sub> atmosphere for 12 to 16 hrs. The reaction progress was monitored by TLC (10 % MeOH and 90% DCM) and once the reaction finished the reaction mixture was filtered through the celite followed by removal of the solvent at reduced pressure. The NMR of the crude material was then taken to monitor the rection outcome.

## Chapter 2

Synthesis, characterization, and biological study of some novel gamma-aminobutyric acid type A (GABA<sub>A</sub>) receptor ligands.

### 2.1 Introduction

#### 2.1.1 GABA receptors

GABA is known as the most widely distributed and active central nervous system (CNS) receptors and functions as the primary inhibitory neurotransmitter. This type of neurotransmitters primarily falls into two distinct classes known as GABA<sub>A</sub> and GABA<sub>B</sub> receptors and are differentiated from each other by their pharmacological, biochemical and electrophysiological properties.<sup>101</sup>

The gamma-aminobutyric acid type A receptors (GABA<sub>A</sub>Rs) are the major inhibitory neurotransmitter receptors in the CNS and are classified as a Cys-loop superfamily of ligand-gated ion channels or ionotropic receptors with a very rich pharmacology.<sup>102</sup> In the central nervous system these type of receptors mediate both the phasic and tonic neuronal inhibition.<sup>103</sup> When activated, the GABA<sub>A</sub>Rs receptors generally permit the flow of chloride ions from the outer to inner part of the neuron, which results in a hyperpolarization of the membrane potential and as a result inhibit the neuron to further fire an action potential.

On the other hand, the metabotropic GABA<sub>B</sub>Rs are the members of G-protein coupled receptor family, which mediate the activity of potassium and calcium channels.<sup>104</sup>

### 2.1.2 GABA<sub>A</sub> receptor structure and functions

This type of GABA receptors are heteropentamers and consist of a total of 19 subunit ( $\alpha$ 1-6,  $\beta$ 1-3,  $\gamma$ 1-3,  $\delta$ ,  $\epsilon$ ,  $\theta$ ,  $\pi$  and  $\rho$ 1-3). Of which the most abundant form comprises of  $\alpha$ ,  $\beta$  and  $\gamma$  subunits in a 2:2:1 stoichiometry<sup>105, 106</sup> where the  $\gamma$  subunit can be replaced by  $\delta$ ,  $\epsilon$  or  $\pi$ . The pentameric chloride ion channel is composed of a large extracellular domain, which contains an orthosteric binding pocket, a transmembrane domain which contains the pore-lining M2 helices and a small intracellular domain which is found to be a site for modulation of the associated protein.<sup>107</sup> The neurotransmitter GABA binds at the interface between the  $\alpha$  and  $\beta$  subunits and allows the rapid influx of chloride ions by triggering the opening of the channel through allosteric modulation. There are typically two GABA binding sites per heteropentamer. In addition to that, GABAARs have different recognition sites for other allosteric modulators such as barbiturates, alcohols, benzodiazepines (BZDs) and neurosteroids.<sup>108-111</sup> From recent studies by Sighart, Knutson *et al.* it has been found that the GABA receptor also has a site (PQ) for  $\alpha$ 6 receptor subtype selective ligands.<sup>112, 113</sup>

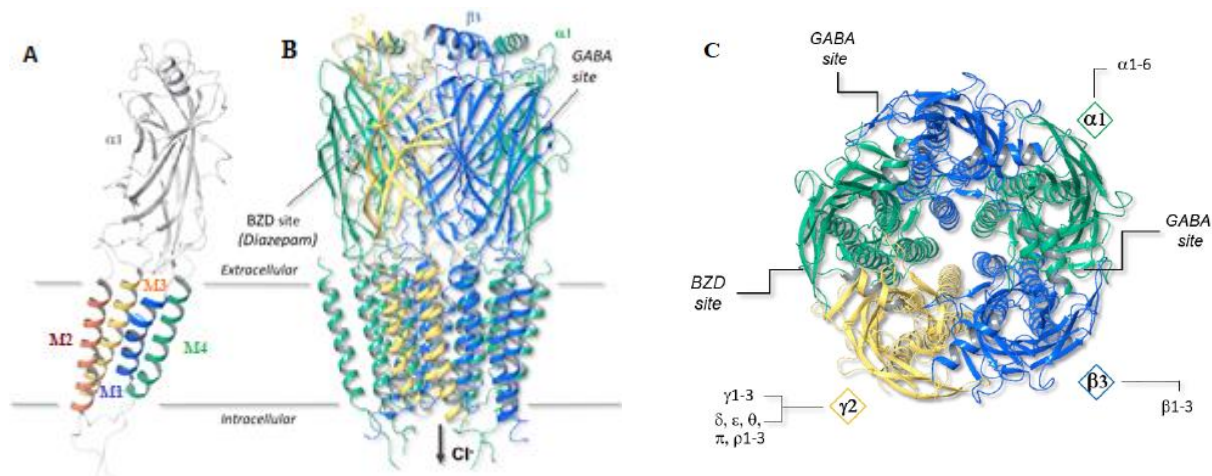


**Figure 12.** (Modified from Samuele Maramaia *et.al.*)<sup>114</sup> 3D-reconstruction of the  $\alpha 1\beta 3\gamma 2$ -GABAAR<sup>114, 115</sup>. Images were generated using Maestro Version 11.9.011, MMshare Version 4.5.011, Release 2019-1. The  $\alpha 1$  subunits are shown in grey (A) or green (B, C),  $\beta 3$  in blue and  $\gamma 2$  in yellow color. A) GABAARs belong to the Cys-loop family of ligand-gated ion channels with each subunit being characterized by a long extracellular N-terminus, which contains the defining Cys-loop, and four trans-membrane domains (M1-4), two short loops that link M1-M2 and M2-M3, a longer intracellular loop between M3 and M4 (modulated by phosphorylation), and a small extracellular C-terminus. B) Side view: the heteropentameric arrangement of subunits in the 2:2:1 stoichiometry of  $\alpha$ ,  $\beta$  and  $\gamma$  subunits that comprise the most abundant form of GABA<sub>A</sub>R, arranged around the central chloride-permeable channel pore, lined by the M2 regions of the different subunits. C) Top view: two GABA binding sites are found at the junctions between  $\alpha$  and  $\beta$  subunits while the BZD site is located at the interface of a  $\gamma 2$  and either an  $\alpha 1$ ,  $\alpha 2$ ,  $\alpha 3$  or  $\alpha 5$  (but not  $\alpha 4$  or  $\alpha 6$ ) subunit.<sup>10,11,12,17</sup> The  $\gamma$  subunit may be replaced by a variety of less abundant subunits (e.g.,  $\delta$ ,  $\epsilon$ ,  $\vartheta$  or  $\pi$ ), whereas the  $\rho 1-3$  subunit can form homopentameric assemblies that are also known as GABAC receptors.<sup>22</sup> Not illustrated here are the multiple additional binding sites on the

*GABA<sub>A</sub>R that occur, for example, within the transmembrane region, such as the anesthetic and neurosteroid binding sites, or within the ion channel pore itself, for example the picrotoxin (or convulsant) binding site.*

It should be mentioned here that, overdose of drugs such as barbiturates<sup>108, 116, 117</sup> and ethanol<sup>118, 119</sup> dangerous because they can bind to in the inner portion of the chloride ion channel and can enhance the response of GABA. This in turn, can open the chloride ion channel longer and results in some cases in death.<sup>108, 116, 120</sup> In the mammalian brain GABA<sub>A</sub>R subtypes could be found, in subcellular (i.e., synaptic or extrasynaptic), regions and have circuit specific distributions. This suggests that different subtypes are associated with distinct CNS functions<sup>114, 121</sup>. It has been found by various neuroscientists(Sieghart, Siegel, Olson, Mohler, Siegel, Seeburg) that  $\alpha$ 1,  $\beta$ 1-3 and  $\gamma$ 2 are highly expressed throughout the brain both synaptically and extrasynaptically<sup>122</sup>. In the rat brain the most abundant combination of GABA<sub>A</sub>R is  $\alpha$ 1 $\beta$ 2 $\gamma$ 2, which comprises approximately 50-60% of the total GABA<sub>A</sub>Rs.<sup>109, 117, 122, 123</sup> The  $\alpha$ 2 and  $\alpha$ 3 containing GABA<sub>A</sub>Rs constitute approximately 20-30% of GABA<sub>A</sub>R in rat brain.<sup>109, 117, 122</sup> The  $\alpha$ 5 containing GABA<sub>A</sub>Rs are found mostly in the cortex, and the hippocampus, and represent about 5 % of the total GABA<sub>A</sub>Rs, which is much lower in comparison to the other subtypes assembles rat brain.<sup>110, 117, 122, 124</sup> It is evident from the significant amount of data that GABA<sub>A</sub>Rs are not only found in the CNS, but also be found in other types of tissues including the lungs, stomach, intestines heart sinus node, etc.<sup>108</sup>

Recently, high-resolution cryo-electron microscopy (cryo-EM) structures of human  $\alpha 1\beta 2\gamma 2$  and  $\alpha 1\beta 3\gamma 2$  GABA<sub>A</sub>Rs have been reported<sup>114, 115, 125, 126</sup>. From the detailed analysis of the receptors in complexes with the orthosteric agonist GABA and the GABA agonist bicuculline as well as open channel blocker picrotoxin (picture emerged of this GABA<sub>A</sub> ion – channel). In addition, the allosteric BZD ligands such as diazepam (Figure 12), alprazolam and flumazenil which bind between  $\alpha$  and  $\gamma$  subunits provide a detailed observation of the overall arrangement and heteromeric interaction of GABA<sub>A</sub>Rs. It also explained the structural basis of receptor activation and allosteric modulation.<sup>114, 127</sup>

### 2.1.3 Benzodiazepines (BZD)

First discovered in 1955 by Dr. Leo Sternbach, the benzodiazepines (BZDs) are a class of psychoactive drugs. BZDs are the positive allosteric modulators of GABA<sub>A</sub>Rs. Initially, the most successful drugs introduced in the market in early 1960s,<sup>128</sup> were chlordiazepoxide and diazepam (marketed as Valium). Due to their potent anxiolytic activity, low toxicity,<sup>127</sup> minimal drug-drug interactions in the liver,<sup>129</sup> rapid penetration across the blood-brain barrier (BBB), rapid absorption from the gastrointestinal tract, and ready distribution in the brain,<sup>130</sup> BZDs have been used in the clinic as anxiolytics, sedative-hypnotics, myorelaxants and anticonvulsants<sup>128, 131, 132</sup> for over four decades. The core structure of these BZDs contain a benzene ring fused with a seven-membered diazepine ring, along with a pendant phenyl C ring (Figure 13). In typical BZDs, the pendent phenyl ring is located at C(5), in midazolam it is at C(6)

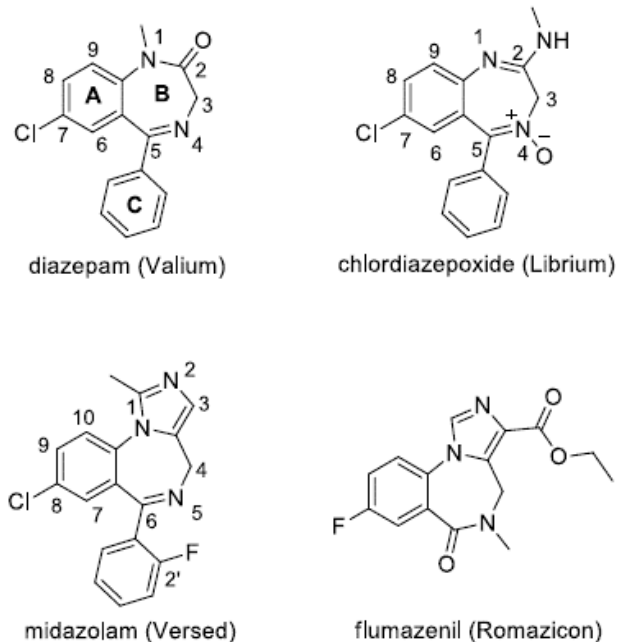


**Figure 13.** The structures of most common BZDs: diazepam, chlordiazepoxide, imidazodiazepine (IMDZ) midazolam and flumazenil. Diazepam, chlordiazepoxide, and midazolam can bind only to the DS sites, whereas flumazenil can bind to both the DS and DI (diazepam insensitive)sites. <sup>123</sup> Librium is metabolized to valium in vivo.

BZDs can only modulate GABA<sub>A</sub>R in presence of GABA. When BZDs binds to a GABA<sub>A</sub>R ion channel, the potency to GABA<sub>A</sub>R is enhanced. As a result, opening of chloride ion channel remains open longer and results in hyperpolarization of the membrane potential.<sup>133</sup>

This phenomena of GABA<sub>A</sub>R results in inhibition of neural firing and hence is responsible for exhibiting different pharmacological properties including anxiolytic, amnesic, ataxic, sedative and anticonvulsant effects, as mentioned earlier. Due to these properties of BZDs, scientists have developed these compounds for the treatment of various CNS disorders GAD, SAD, PTSD as well

as status epilepticus, and panic disorders. At this moment, the scientists are still in search of a better BDZs because most of these compounds demonstrate some adverse side effects due to their unwanted nonselective binding to many GABA<sub>A</sub>Rs.<sup>116</sup> Prior experiments have revealed the common side effects generated by BZDs include amnesia, ataxia, sedation, muscle relaxation, drug dependence or withdraw issues as well as tolerance to the antinociceptive and anticonvulsant effects.<sup>134-136</sup> There is a large number of side effects that must be erased and much improved  $\alpha$ 2/3-GABA<sub>A</sub>R subtype-selective BZD ligands can be developed for the treatment of various CNS disorders.

#### 2.1.4 Different GABA<sub>A</sub>R subtypes and their distinct functions

In order to develop new compounds, which retain efficacy but have a reduced side effect profile as compared to the current series of BZDs, it is important to understand the various pharmacological features of BZDs that can be attributed to specific subtypes. The pioneering work of Mohler, Sieghart, McKernan, Sigel, Seeburg, Squires, and Haefely through molecular genetic studies with  $\alpha$ -subunit knock-out and point-mutated knock in coupled with mice and medicinal chemistry have selectively target particular subtypes. This has led to the general concept that pharmacological effects of the GABA<sub>A</sub>Rs depend on modulation of specific receptor subtypes, principally due to the type of  $\alpha_x$  subunits.<sup>123</sup> The pharmacological effects of different subtypes are presented in (Table 12).

**Table 12.** The CNS effects at GABA<sub>A</sub>  $\alpha$ 1-6 $\beta$ 2/3 $\gamma$ 2 receptor subtypes.<sup>111, 123, 137-148</sup> Presented at the Mona Symposium (2014), University of the West Indies.<sup>149</sup> Earlier reported, in part, by Mckernan et al. (ACNP). Later, reported at the Pharm R and D meeting, Los Angeles, 2019 and 2021 (virtual) by Cook *et al.*

Subtype	Associated effect
$\alpha$ 1	Sedation, anterograde amnesia, ataxia, some anticonvulsant action, addiction, dependence, as well as involved in the development of tolerance, and muscle relaxation
$\alpha$ 2	Anxiolytic, anticonvulsant action, antihyperalgesic effects
$\alpha$ 3	Some anxiolytic action, some antinociceptive effects, anticonvulsant action at higher doses, some muscle relaxation
$\alpha$ 4	Diazepam-insensitive (DI) site, important in lung disorders in the periphery such as asthma
$\alpha$ 5	Cognition, learning, temporal and spatial memory (maybe memory component of anxiety); schizophrenia, depression and in the peripheral asthma
$\alpha$ 6	Diazepam-insensitive (DI) site, important in Tic disorders, Tourette's syndrome, migraine, trigeminal orofacial pain and perhaps schizophrenia

The  $\alpha 1$ -GABA<sub>A</sub>Rs mediate the sedative effects, anterograde amnesia, ataxia, some anticonvulsant action, anxiolysis, addiction, dependence, as well as involved in the development of tolerance, and muscle relaxation.<sup>137</sup> Whereas  $\alpha 2$ - and/or  $\alpha 3$ -GABA<sub>A</sub>Rs are associated with anxiolytic, antinociceptive and anticonvulsant effects<sup>150</sup>. In some cases,  $\alpha 2$ -GABA<sub>A</sub>Rs may play a role in expressing some hypnotic effects and some muscle relaxation at higher doses. But this has not been confirmed by lot of laboratories. However, much of the antihyperalgesic effects from the GABA<sub>A</sub>R occur in the region of spinal cord.<sup>139, 145</sup> The  $\alpha 3$ -containing GABA<sub>A</sub>Rs have some involvement in the anxiolytic-like effects, anticonvulsant action, antinociceptive effects and perhaps muscle relaxation at higher doses.<sup>141-143, 150</sup> and  $\alpha 5$ -GABA<sub>A</sub>Rs play a role in cognitive processes, spatial memory and learning.<sup>138, 144</sup> Due to the lack of a large binding pocket for the pendant C ring of BZDs the  $\alpha 4$ - and  $\alpha 6$ -containing GABA<sub>A</sub>R are Diazepam-insensitive (DI) sites and therefore no corresponding CNS effect is associated with these two subtypes or treatment with typical BZDs.<sup>151, 152</sup>

But recent studies have shown (Mizuta, K. et al. and Gallos, G. et al.) that  $\alpha 4$ -containing GABA<sub>A</sub>Rs and  $\alpha 5$  GABA<sub>A</sub>Rs are expressed in the peripheral nervous system (PNS), most importantly in lungs,<sup>146-148</sup> which provides a new way to treat asthma using these subtype selective ligands. New activity have been reported by Sieghart, Knutson et al. which shows the involvement of  $\alpha 6$  Bz/GABAergic subtypes, at the PQ site. The activity of ligands related to the  $\alpha 6$  subtype, to date is Tic disorders such as Tourette's syndrome, migraine, trigeminal orofacial pain and perhaps schizophrenia.<sup>112, 113, 153</sup>

In addition to the subtype selectivity, the pharmacological effects of GABA<sub>A</sub>Rs in the CNS depends on this chloride ion influx which regulates the allosteric modulation of GABA. BZDs bind to the

GABA<sub>A</sub>R BZD allosteric site and hence increase the orthosteric binding of GABA to the chloride ion channel. This binding increasing the length of opening of chloride ion channel and results in a decrease in the membrane potential as mentioned above. As a result of this hyperpolarization neurons further inhibit neuronal transmission and this results in decreased anxiety, sedation, amnesic, hypnotic and anticonvulsant effects in the CNS, as well as muscle relaxant effects.<sup>154-156</sup>

These BZD allosteric modulators work in three different way. The agonist BZDs which are also called positive allosteric modulators (PAM), bind to the BZD binding site and enhance the binding of the GABA neurotransmitter in the GABA binding site with increasing influx of chloride ions through the ion channel pore. The inverse agonist or the negative allosteric modulators (NAM) BZDs bind to the BZD binding site and trigger an opposite effect to PAMs, and reduce the chloride ion influx, and results in the depolarization of the membrane (negative modulation). There are some BZDs which may show variable efficiency of both PAM and NAM at different subtypes. These are known as partial agonists and partial inverse agonists, respectively. Other types of BZDs, known as antagonists,<sup>116</sup> do not have a direct effect on GABA functionality but displace PAMs from binding to BZR site, as well as NAMs. They do not show any pharmacological effect. But they occupy the BzR site and decrease the interaction of other PAMs and NAMs due to their more potent binding affinity over the BZD ligands, as mentioned (such as flumazenil and BCCT).<sup>111</sup>

Considering these agonists, inverse agonists and antagonists effect and the concept of the multiplicity of GABA<sub>A</sub>R subtypes, one can have a good understanding of the complex pharmacological nature of GABA<sub>A</sub>R subtypes and design of ligands for the treatment of various CNS disorders.

## 2.2 Designing of novel $\alpha 2/3$ -GABA<sub>A</sub> R subtype-selective ligands.

As pointed out, gamma-aminobutyric acid type A receptors (GABAARs) are the major inhibitory neurotransmitter receptors in the CNS and are responsible for the effect on brain functions depending on the allosteric modulation of ligands at different subunits of the protein complex.<sup>157</sup> BZDs are the classic proactive drug clinically prescribed for over four decades for various CNS disorders including anxiety, convulsions, as well as insomnia.<sup>137, 150, 158, 159</sup> However, some BZD drugs, for example, diazepam, shows moderate to less efficacy in a number of patients. On top of that, they can produce serious adverse effects, as mentioned above, including sedation, ataxia, amnesia, and addiction.<sup>137</sup> To improve treatment it is necessary to develop new ligands with considerably fewer side effects.

It is evident from the data collected, to date, of various experiments that,  $\alpha 2\beta 2/3\gamma 2$  and/or  $\alpha 3\beta 2/3\gamma 2$  GABAAR subtype selective ligands exhibit agonist efficacy and are responsible for the anxiolytic, antinociceptive, and much of the anticonvulsant actions of the BZD when there is little or no efficacy at  $\alpha 1$ -subtypes.<sup>123, 160-167</sup> These results provide an indication that, GABA<sub>A</sub>  $\alpha 2$  or  $\alpha 3$  agonists are good candidates for the treatment of anxiety, epilepsy, as well as neuropathic pain with reduced side effects.

A series of imidazodiazepine (IMDZ) agonists, selective for GABA<sub>A</sub>  $\alpha 2/\alpha 3$  subtypes were designed, synthesized and investigated, based on the previously developed BZD/GABA<sub>A</sub> pharmacophore model.<sup>111, 168</sup> In order to expand on this issue, Masiulis *et al.* studied five structures of the human synaptic  $\alpha 1\beta 3\gamma 2L$  GABA<sub>A</sub> receptors in complexes with PTX (Picrotoxin), PTX and GABA (PTX/GABA), BCC (Bicuculline), DZP (Diazepam) and GABA (DZP/GABA), as well as

ALP (Alprazolam) and GABA (ALP/GABA).<sup>126</sup> They established the binding modes and structural effect of these ligands in the ion channel and shed light on the molecular basis for their function. To obtain the structures in which GABA<sub>A</sub> receptors can be observed in physiologically relevant conformations, they used a full-length receptor variant from a thoroughly characterized cell line<sup>169</sup> and reconstituted it in a lipid bilayer.<sup>125, 126</sup> The series of IMDZ agonist developed in our group has close resembles to the hybrid structure of DZP+ Flumazenil, as well as ALP. Therefore, the understanding of the binding models of these BZDs in the  $\alpha 1\beta 3\gamma 2$  are of great interest here.

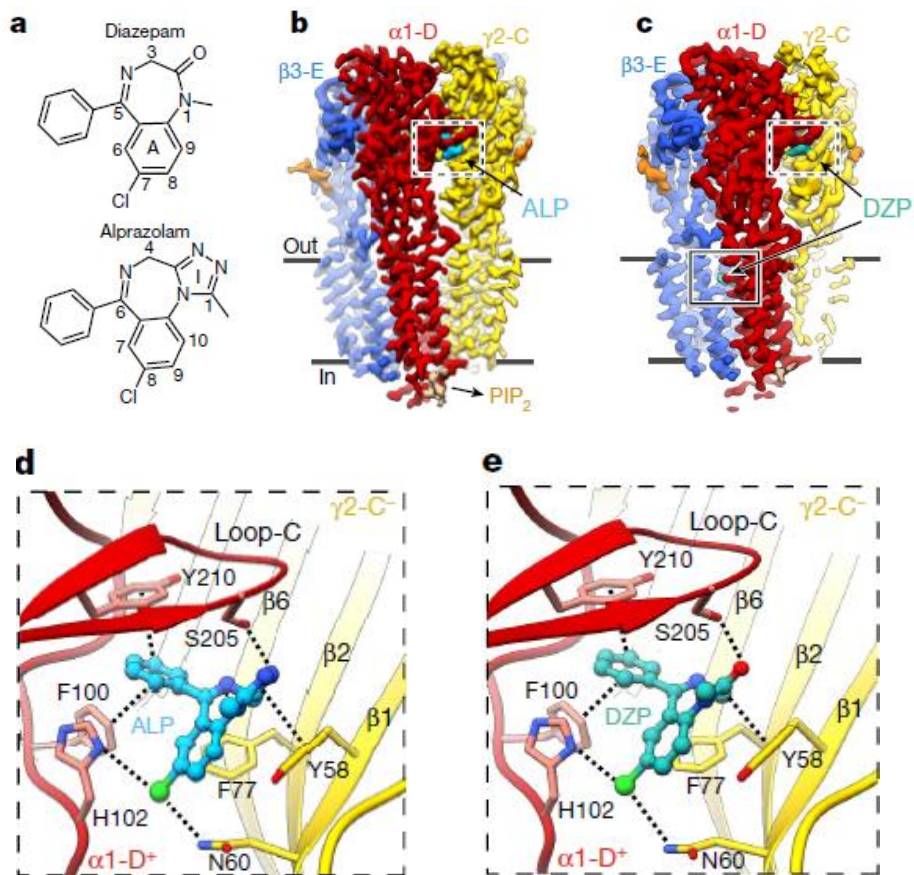
## 2.2.1 Exploring the benzodiazepine binding modes.

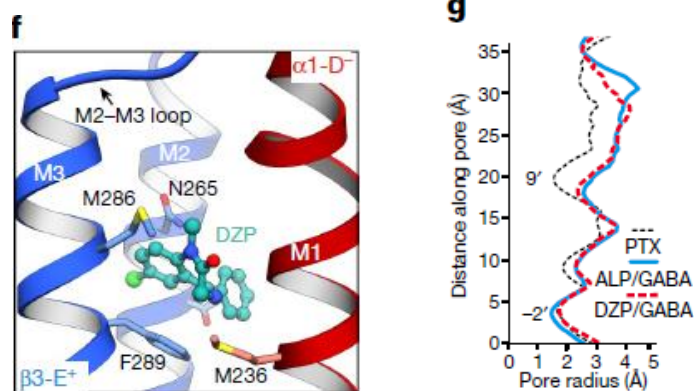
### 2.2.1.1 Structures of a $\alpha 1\beta 3\gamma 2$ L GABA<sub>A</sub> receptor in desensitized states induced by GABA and alprazolam or GABA and diazepam<sup>126</sup>

Masiulis *et al.* established the cryo-EM structures of the  $\alpha 1\beta 3\gamma 2$ L receptor in a complex with GABA and ALP, as well as with GABA and DZP, to nominal resolutions of 3.26 Å and 3.58 Å, respectively (Figure 14 a–c, Extended Data Figure 14 d–f). In both structures, GABA molecules are bound to the orthosteric agonist pockets and ALP or DZP occupy the canonical allosteric BZD-binding site at the  $\alpha 1+$ /  $\gamma 2-$  interface, where they form extensive interactions (Figure 14. d, e).

In the cryo-EM structures of the  $\alpha 1\beta 3\gamma 2$ L receptor in complex with GABA and ALP, and with GABA and DZP (Figure 14) it can be seen that GABA molecules are bound to the orthosteric agonist pockets and ALP or DZP occupy the canonical BZD-binding site at the  $\alpha 1+$ /  $\gamma 2-$  interface, where

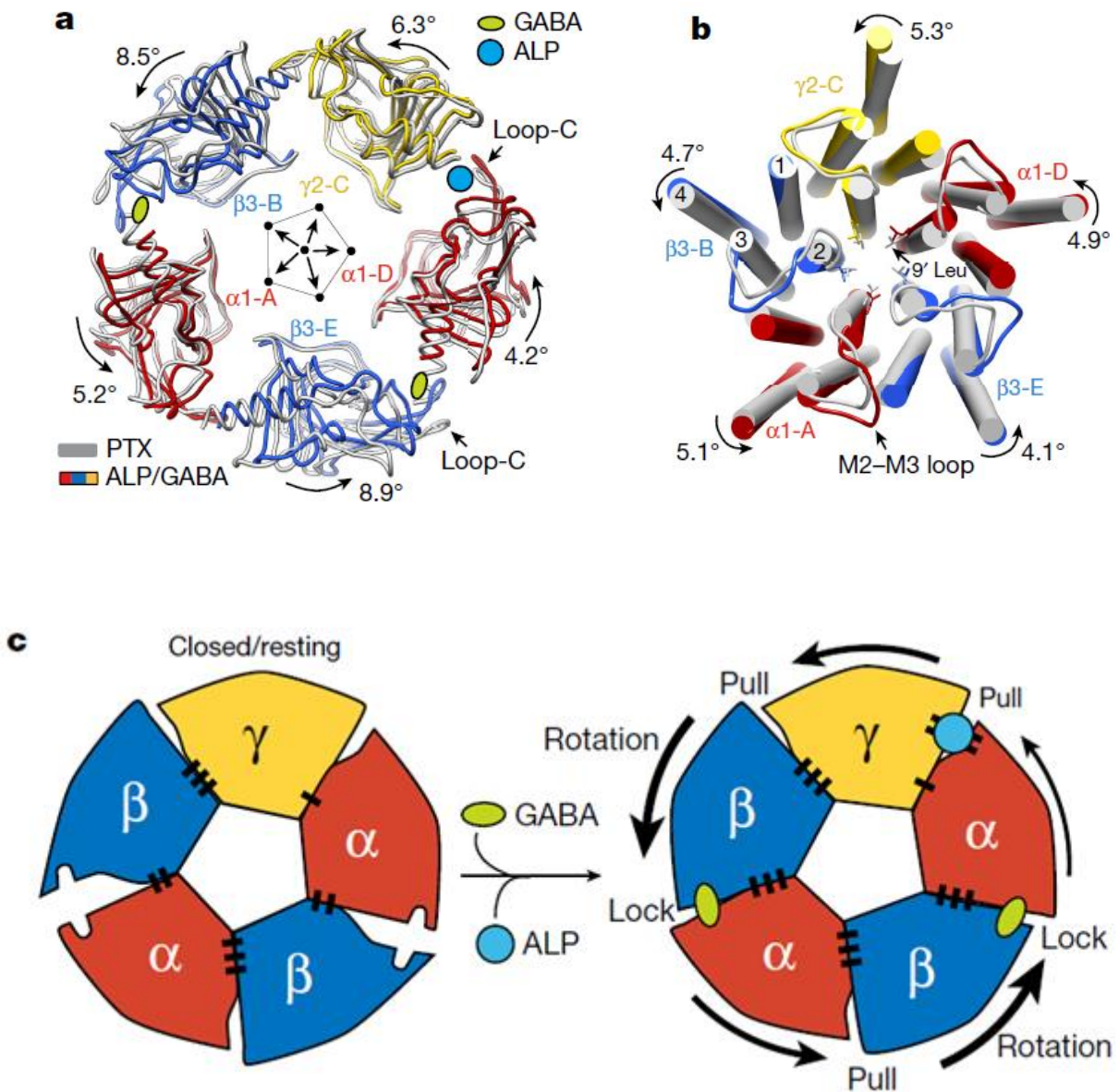
they form extensive interactions (Figure 14. d, e). It is shown in Figure 14g. that the densities of ALP and DZP are defined in such a way that the fused benzene-diazepine ring is easily distinguishable from the pendant phenyl rings. It can be noted that, the chlorine atoms at the C8 and C7 positions in ALP and DZP, respectively, interact with the  $\alpha$ 1His102 side chain in a halogen bond. In comparison in the  $\alpha$ 4 and  $\alpha$ 6 subunits the equivalent positions are occupied by arginine residues, the larger side chains of which exert a steric clash with ALP and DZP. This is why the classical BZDs do not show any activity towards GABA<sub>A</sub> receptor subtypes containing  $\alpha$ 4 or  $\alpha$ 6 subunits.<sup>170-172</sup>





**Figure 14.** (Modified from Masiulis et al.<sup>126</sup>) a. Structures of diazepam and alprazolam. Diazepine ring atoms are numbered with labelled Imidazole (I) and benzene (A) rings. b, c. the cryo-EM map of the  $\alpha 1\beta 3\gamma 2$  GABAA receptor in complex with ALP (cyan) (b) and DZP (teal) (c) viewed parallel to the membrane plane. d, e. Views of the benzodiazepine binding site at the  $\alpha 1+\gamma 2-$  interface showing ALP (d) and DZP (e) binding modes. Dashed lines indicate  $\pi-\pi$  interactions and hydrogen bonds. f. The low-affinity DZP-binding site in the  $\beta 3+/\alpha 1-$  interface of transmembrane domain (TMD) region. g. Plot of the pore radii for the receptor bound to PTX (black dashed line), ALP/GABA (blue line) and DZP/ GABA (red dashed line).

2.2.1.2 Conformational differences between closed/resting and desensitized states in a GABA<sub>A</sub> receptor.<sup>126</sup>



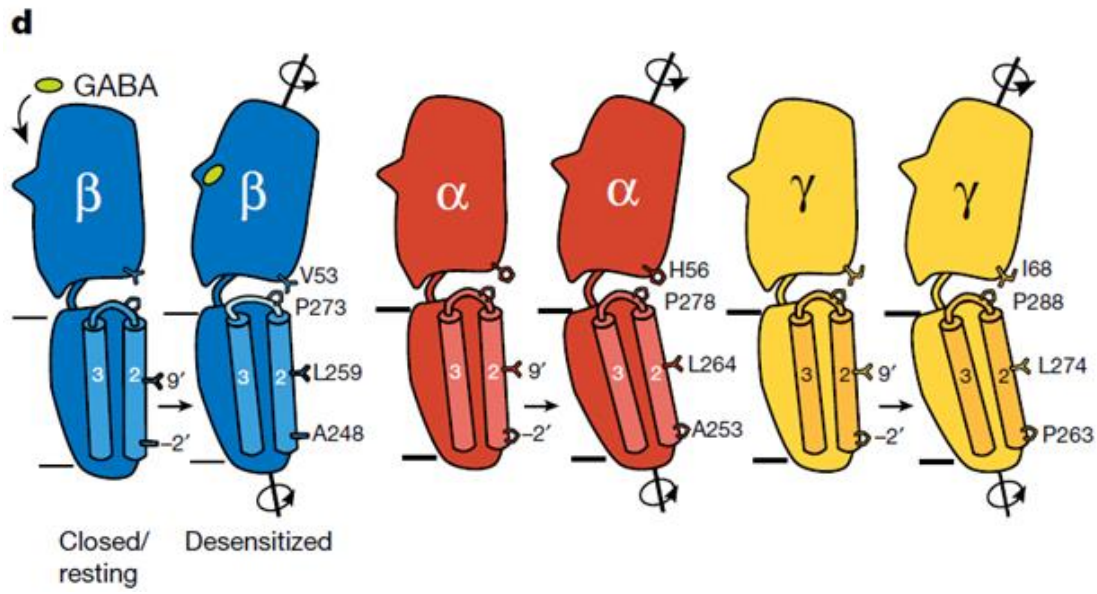


**Figure 15.** (Modified from Masiulis et al.<sup>126</sup>) a. Superposition of extra cellular domains (ECD) from PTX (grey) and ALP/GABA (red/blue/yellow) structures based on the global TMD alignment. GABA- and ALP-induced ECD rotation angles around the rotational ECD axes, and the direction of motion are shown. b. Global TMD alignment for the PTX-bound (grey) and ALP/GABA-bound (coloured) structures. 9' Leu side chains are shown as sticks. c. Schematic illustration of conformational changes initiated by GABA binding at the ECD level. GABA stabilizes closure of loop-C in each  $\beta$  subunit, causing ECDs to rotate and form stronger  $\beta 3+\alpha 1-$  interfaces. The black arrows indicate the direction of rotation, with increasing arrow thickness representing a greater magnitude of rotation. BZDs such as alprazolam bind at the  $\alpha 1+\gamma 2-$  interface and reinforce it, facilitating the concerted rotation of the ECDs. The representation of the black bars ('stitches') at the subunit interfaces indicates the binding strength of the interfaces. d. Differences in the relative orientations of ECD–TMD between the closed/resting and desensitized states illustrate how GABA

*binding and ECD rotation affect TMDs. It can be noted that, the M2–M3 loops in  $\beta$  subunits deform more than the  $\alpha$  and  $\gamma$  equivalents, resulting in lower degrees of M2 tilt and TMD rotation.*

## 2.3 Project background

Based on the BZD/GABA(A) pharmacophore model developed by Diaz, He, Zhang and Clayton *et al.*<sup>111</sup> a series of rigid GABA(A)  $\alpha$ 2/3 subtype selective imidazodiazepine (IMDZ) agonists have been synthesized and investigated. Among them, ligand HZ- 166 (**105**) (Figure 16) was one of the first lead compounds containing an acetylene (ethinyl) group at the C-8 position and it is the acetylene group which is thought to be responsible for the reduced  $\alpha$ 1-subtype efficacy and/or the binding affinity.<sup>111, 168</sup> This compound showed antiseizure activity in a subcutaneous metrazole seizure (scMET) test in an animal model (both mice and rats) at ASP (NINDS) with both oral and i.p. administration<sup>173</sup> as well as non-sedating anxiolytic effect at 1 mg/kg in rhesus monkeys in the Geller-Seitzer conflict assay.<sup>162</sup> As compared to the commonly used drug gabapentin (used for the treatment of neuropathic pain), this ligand (**105**) showed better activity in models of inflammatory and neuropathic pain and exerted a dose-dependent antihyperalgesic effect with less sedation, motor impairment or development of tolerance.<sup>123, 174</sup> But due to the enzymatic hydrolysis of the ester function to its carboxylic acid in the liver, it degraded quite rapidly in mouse liver microsomes (MLMs) regardless of showing good stability in human liver microsomes (HLMs).<sup>175</sup> As a result, the C(3) acid metabolite was not able to penetrate the blood-brain barrier and achieve the desired effects for a long period of time and hence limits the ability to do ADME toxicity studies in rodents.

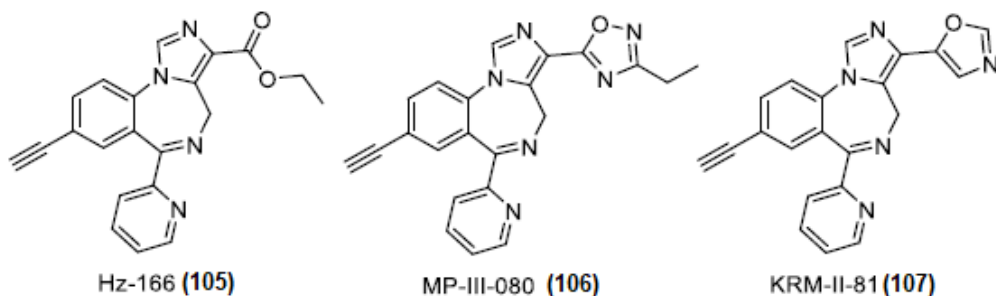


Figure 16. Structures of Hz-166 (**105**), MP-III-080 (**106**), and KRM-II-81 (**107**).

To improve the metabolic stability and pharmacological efficiency, new ester bioisosteres have been designed and studied in the current drug development.<sup>176-179</sup> By keeping the main characteristic of the lead compound (**105**) and to prevent the hydrolysis of its ester functionality, a number of bioisosteres have been designed, synthesized and evaluated by replacing the C(3) ester functional group.<sup>180-182</sup> Among these ligands the most potent analogs were MP-III-080 (**106**) and the 1,3-oxazole KRM-II-81 (**107**), both of which showed improved pharmacokinetic properties in human, mouse, rat and dog liver microsomes, as compared to the parent compound (**105**). Recent studies have shown that in a rat Vogel conflict assay at 10 mg/kg when given i.p., oxazole (**107**) exhibited anxiolytic effects. As a model of anxiety, a mouse marble burying assay<sup>163, 164, 167, 183</sup> was performed with ligand (**106**) and it has shown significantly reduced marble burying activity at 10 mg/kg, which is the indication of potent anxiolytic-like effects. It has been found that both ligand (**106**) and (**107**) show anxiolytic activity at 30mg/kg.<sup>163</sup> All three  $\alpha_2/3$  subtype selective PAMs and have shown little or no agonist efficacy at  $\alpha_1$ -containing GABA<sub>A</sub>Rs and no

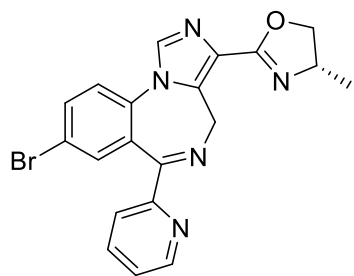
sedation and dependence.<sup>162, 164, 184</sup> In addition to that in the model of acetic acid- and lactic acid-induced pain in mice ligand (**107**) exhibited potent antinociceptive activity.<sup>184</sup> Together these results indicate one should synthesize and study additional bioisosters of ligand (**107**) in search of more potent drug candidates for the treatments of seizures, pain and anxiety without causing amnesia, sedation, ataxia, or the propensity for addiction/dependence.

## 2.4 Results and Discussion

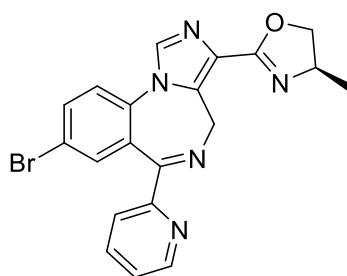
Newly designed bioisosteres of HZ-166 (**105**) or direct analogs of KRM-II-81 (**107**) have been synthesized based on the comparative study of molecular docking of HZ-166 (Figure 12), and KRM-II-81 (Figure 11) performed using AutoDock Vina 1.5.6.<sup>185</sup> The recently published CryoEM structure of the human full-length  $\alpha 1\beta 3\gamma 2L$  GABAA receptor ion complex with alprazolam (PDB bound: 6HUO) by Masiulis S. *et al.*<sup>126</sup> was used to perform the docking studies. The molecular docking scores (binding affinity) of the designed ligands (ZK-III-51, ZK-III-56, ZK-III-58) were determined (Table 13) and examination of these data shows that the binding poses of most of the ligands prepared herein are similar to HZ-166 (data not shown) and KRM-II-81. The binding affinities (based on docking scores) of all these ligands was found to be within +/- 1 kcal/mol difference from the lead compound HZ-166 (-9 kcal/mol) and KRM-II-81 (-9.4 kcal/mol). This suggested that all these new bioisosteres would bind with the receptor complex with a similar affinity compared to the lead compound ester HZ-166 and KRM-II-81.

**Table 13.** Docking score (computed binding affinity) of bioisosteric ligands.

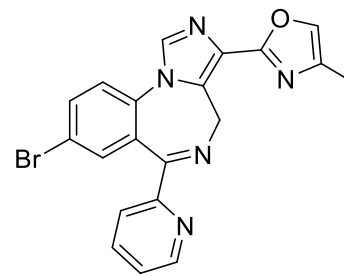
Compound	Binding affinity (kcal/mol) In the computed model
HG-166	-9
KRM-II-81	-9.4
ZK-III-51	-10
ZK-III-56	-9.8
ZK-III-58	-7.4



ZK-III-51 (108)



ZK-III-56 (109)



ZK-III-58 (110)

**Figure 17.** Structures of ZK-III-51(108), ZK-III-56 (109) and ZK-III-58(110).

The halogen substituted benzodiazepines e.g. diazepam and alprazolam undergo a halogen bond interaction with the carbonyl oxygen of the backbone of the  $\alpha$ 1His102 amino acid in the CryoEM structure (Figure 18. Alprazolam, Figure 20. Diazepam). Examination of the docking of 8-

bromosubstituted bioisosteres **108**, **109** (Figure 21) and **110** (Figure 22) shows a similar halogen bond interaction with the carbonyl oxygen of the backbone of the  $\alpha$ 1His102 amino acid, but most of the docking software (including AutoDock Vina)<sup>186</sup> does not include halogen bonding in their scoring functions and, are unable to successfully predict the correct docking score of such complexes.

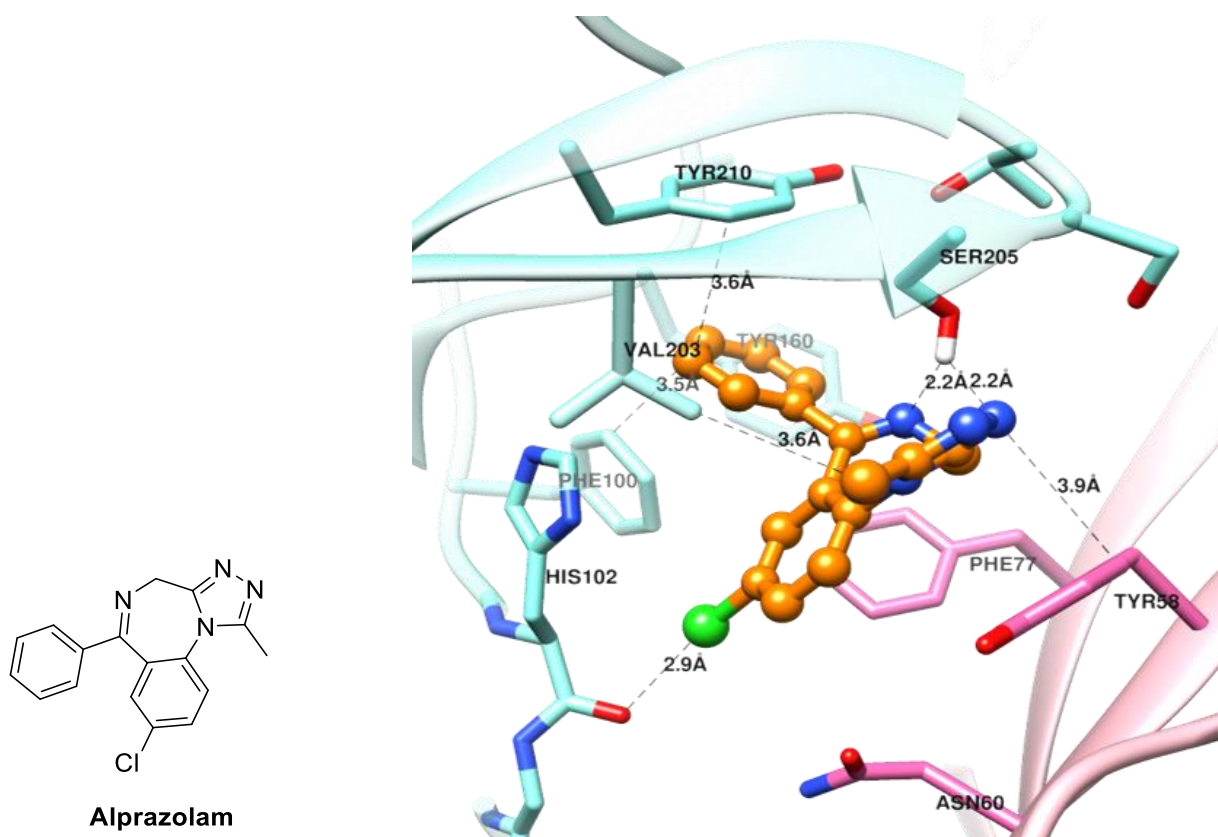


**Figure 18.** Enlarged cryoEM structure of the human full-length  $\alpha$ 1 $\beta$ 3 $\gamma$ 2L GABA<sub>A</sub> receptor ion complex with alprazolam using AutoDock Vina.

Therefore, based on the previously developed ligands, in collaboration with Dr. Lalit Golani it can be expected that, these ligands with bromine at position 8 would bind stronger to the  $\alpha 1\beta 3\gamma 2L$  GABA<sub>A</sub> receptor complex, as compared to the other ligands [ ZK-IV-04 (**111**), ZK-IV-05 (**112**), and ZK-IV-07 (**113**), which was also designed and synthesized (Figure 19)] and would exert increased motor side effects. Ligands **111**, **112** and **113** might show sedation.

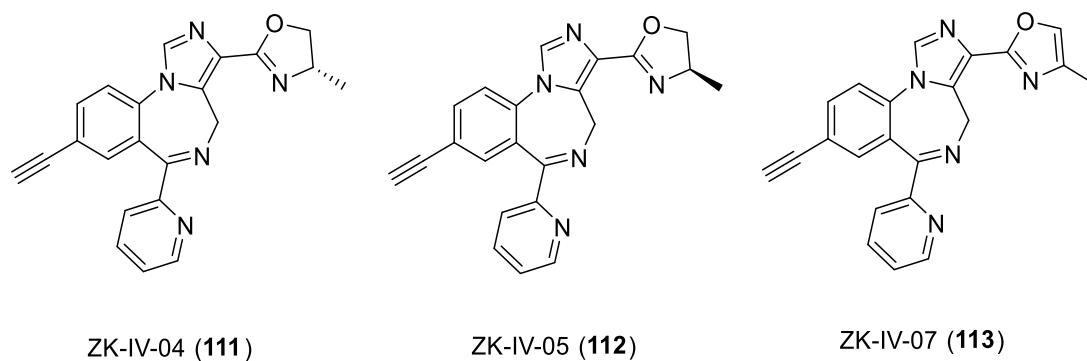


**Figure 19.** Structures of ZK-IV-04 (**111**), ZK-IV-5 (**112**) and ZK-IV-7 (**113**).

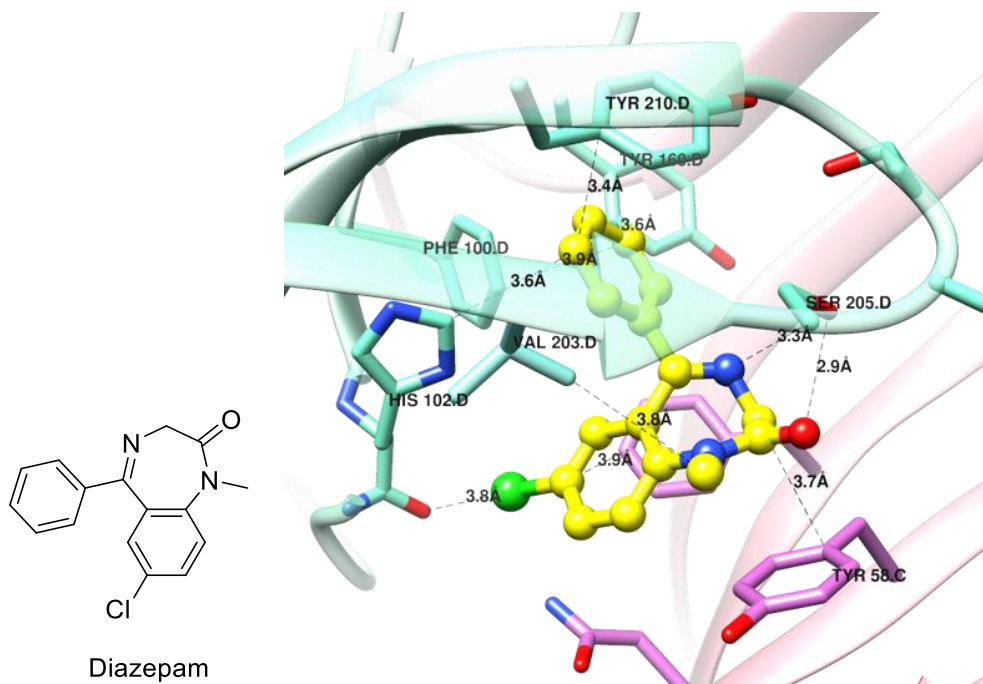
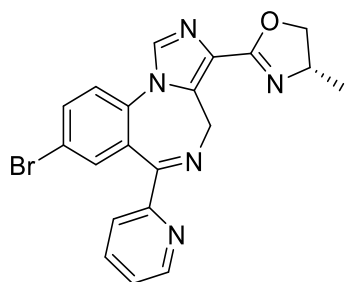
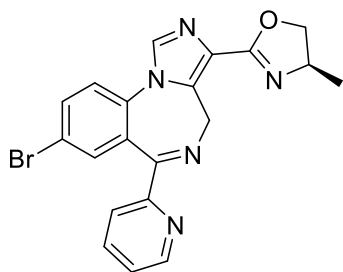
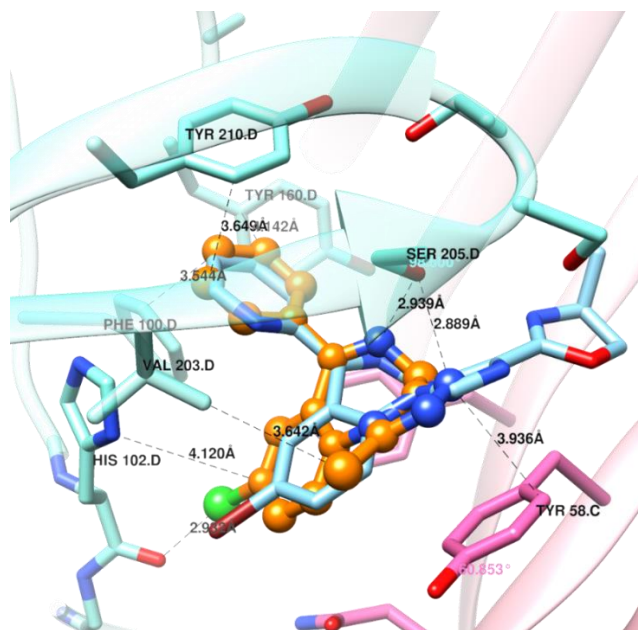


**Figure 20.** Enlarged cryoEM structure of the human full-length  $\alpha 1\beta 3\gamma 2L$  GABAA receptor ion complex with Diazepam using AutoDock Vina.



ZK-III-51 (**108**)



ZK-III-56 (**109**)

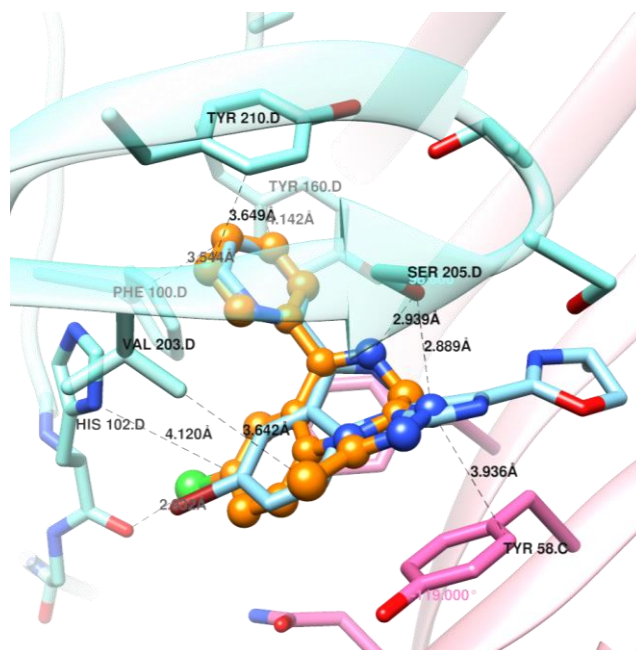
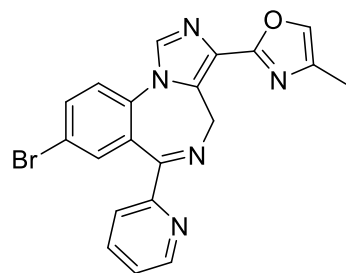
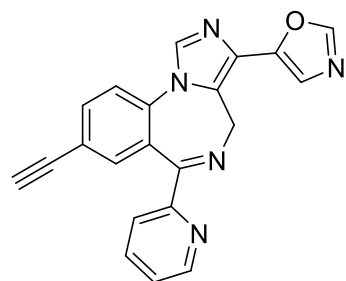
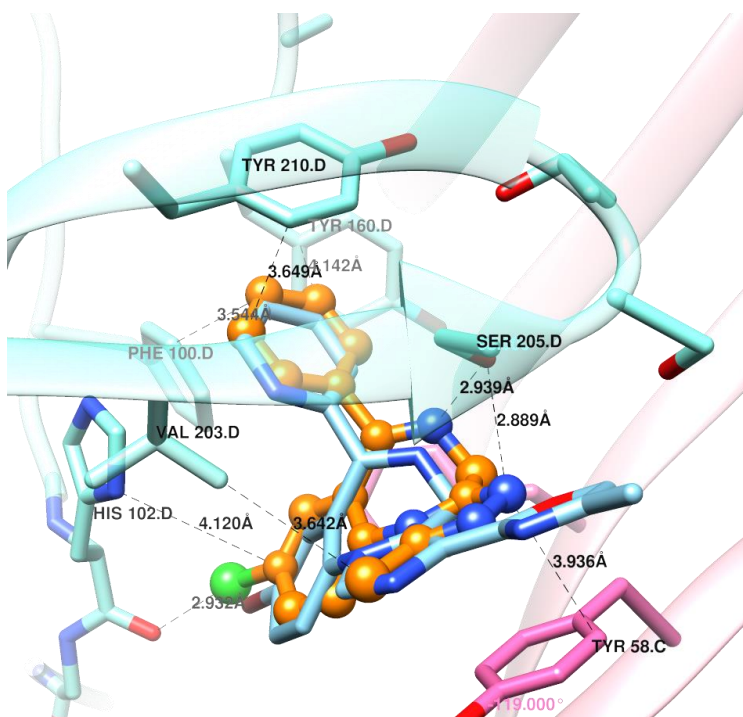


**Figure 21.** CryoEM structure of the human full-length  $\alpha 1\beta 3\gamma 2L$  GABAA receptor ion complex with ligands **108** and **109** using AutoDock Vina.



ZK-III-58 (**110**)



KRM-II-81 (**107**)

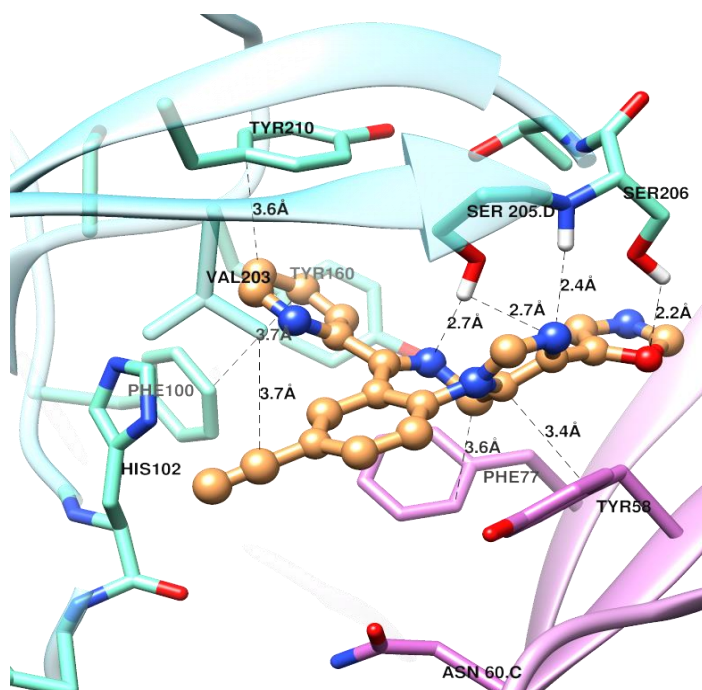


**Figure 22.** CryoEM structure of the human full-length  $\alpha 1\beta 3\gamma 2L$  GABAA receptor ion complex with ligands **110** and **107** using AutoDock Vina.

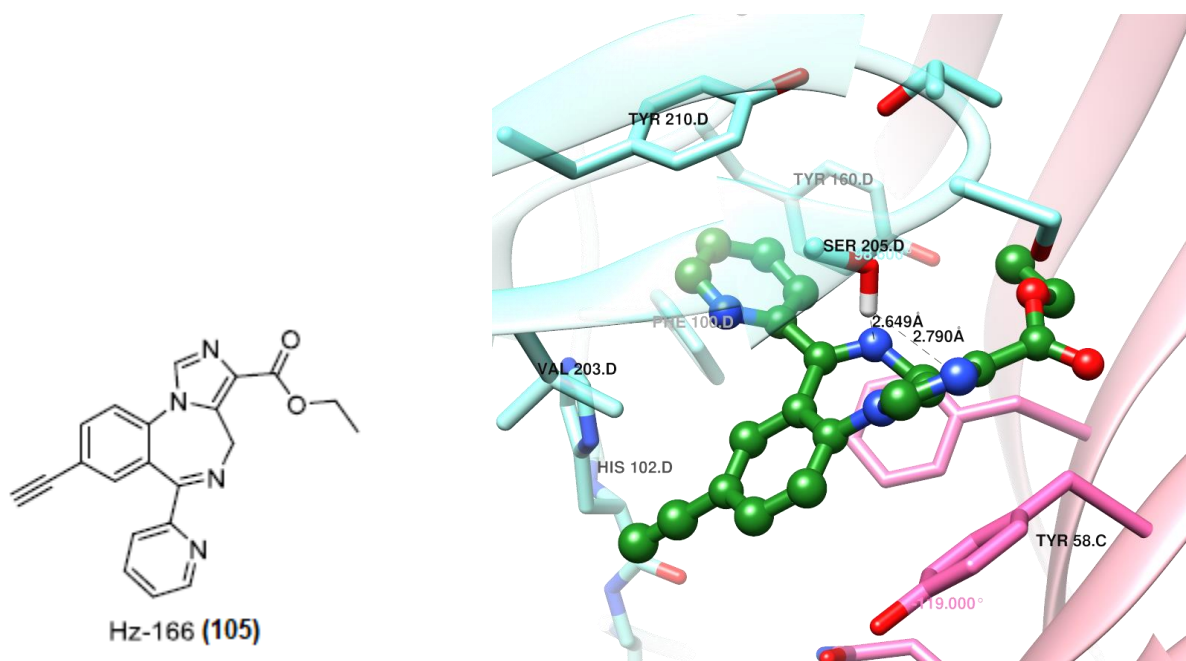


**Figure 23.** CryoEM structure of the human full-length  $\alpha 1\beta 3\gamma 2L$  GABAA receptor ion complex with ligand HZ-166 (**105**) using AutoDock Vina

Unfortunately energy minimized structure of ZK-IV-04 (**111**), ZK-IV-05 (**112**), and ZK-IV-07 (**113**) could not be docked in Auto Dock Vina as these structures would not fit into the human full-length  $\alpha 1\beta 3\gamma 2L$  GABAA receptor ion complex. This is an indication that, these ligands should not show any sedative effect which is related to the  $\alpha 1$  subtype of GABA<sub>A</sub>Rs. On the other hand they may not bind to BzR, hence the biology is important.

## 2.5 Biological Studies on KRM-II-81 (**107**)

### 2.5.1 Pharmacology of KRM-II-81

The amplification of GABA signaling by KRM-II-81(**107**) through allosteric modulation has been studied in different electrophysiological systems. During these studies, the neurotransmitter GABA was introduced into the recombinant receptors containing  $\alpha\beta\gamma_2$  receptors and in the presence of **107** the augmented current induced by GABA was measured. From this experiment, it has been found that **107** is a selective potentiator of  $\alpha_2$  and  $\alpha_3$  containing GABA<sub>A</sub>Rs with little effect on  $\alpha_1$ -containing or  $\alpha_5$  containing GABA<sub>A</sub>Rs. In fact, it shows very low efficacy at  $\alpha_5$  containing GABA<sub>A</sub>Rs as mentioned and when studied for activity against a host of other neurotransmitter receptors at PDSP it did not show any off-target liabilities. It was found from the radioligand binding studies that, the IC<sub>50</sub> value is less than 10 $\mu$ M for NMDA, AMPA, kainite, h5HT receptors (1a-f, 2a-c, and 5-HT7), hACHE, hADRa (1a, 1b, 1d, 2a, 2b, 2c), hADRB (1 and 2), hADORA3, hD1, hD2S, hDAT, hH1, hM2, hM3, hERG.<sup>163</sup> In addition to this KRM-II-81 was devoid of CYP 3A4, CYP2D6, and CYP2C9 inhibition.<sup>163</sup>

## 2.5.2 Pharmacokinetics

In a liver microsomal assay KRM-II-81 (**107**) showed high stability and the LD<sub>50</sub> value was found to be greater than 100µM in cytotoxicity assay in an HEK293T cell line.<sup>163</sup> The bioavailability of this ligand was also very good compared to the lead compound HZ-166 after intraperitoneal administration ( i.p. ) and oral administration in rats. For example, the plasma concentration of **107** was found to be 3910 nM after introducing the 10mg/Kg dose whereas the HG-166 could not achieve the concentration greater than 12.2 nM.<sup>163</sup> Experiments show that both oral and intraperitoneal dosing in rats produced detectable unbound plasma levels of KRM-II-81 from 0.25-12h post dosing with oral exposure being greatest at 1h (600 nM unbound drug levels).<sup>187</sup> These data indicate that pharmacokinetically **107** shows much better results than HZ-166.

## 2.5.3 Antiepileptic activity

Epilepsy is a chronic, life-threatening neurological disease which can occur at any age and to date it affects almost 2.3 million people in the US and over 50 million worldwide.<sup>188</sup> The common symptoms of epilepsy are convulsion, muscle spasms, disturbances of movement, strange sensations and loss of consciousness from a mild to a severe level over an extended period.<sup>123</sup> Among different kinds, the most common type is termed as idiopathic epilepsy the cause of which is unknown and it difficult to treat with present drugs. Whereas the cause of secondary epilepsy is thought to be due to prenatal brain damage, a stroke, a brain tumor, a head injury, or

infection, etc. General medications for the treatment of epilepsy include the use of benzodiazepines (BZDs), carbamazepine, phenytoin, valproate, felbamate, gabapentin, lamotrigine, levetiracetam along with treatment of status epilepticus and surgical approaches. But with these kinds of medication some epileptic symptoms can be controlled at a certain level.<sup>189</sup> But to fully control the symptoms with minimized side effects there is an urgent need of improved antiepileptic drugs. As we know the BZD ligands that target  $\alpha 2$  or  $\alpha 2/3$  subtypes are the ideal candidates for the treatment of epilepsy due to their anticonvulsant activity with minimal side effects from lack of  $\alpha 1$  efficacy, and the lack of possible tolerance from the coupling of  $\alpha 1$  and  $\alpha 5$  subtypes.<sup>189, 190</sup> KRM-II-81 which is metabolically much more stable than of HZ-166 which shows anticonvulsant activity, without the development of tolerance to this anticonvulsant effect (US patent Cook *et al.*), is a strong drug candidate for the treatment of epilepsy as shown by examination of several different anticonvulsant models.

### 2.5.3.1 Acute seizure models

From the earlier studies on HZ-166 by Rivas *et al.*<sup>173</sup> it was shown that, potentiation of  $\alpha 2/3$ -containing GABAARs was sufficient for anticonvulsant effects. Therefore, KRM-II-81 (**107**) has been also tested for anticonvulsant effects and it demonstrated significant anticonvulsant activity with no sedation nor ataxia even up to 300mg/kg in rats. It also suppressed the hyper-excitation in rat cortical neurons without altering spontaneous neuronal activity in TBI. The frequency of spiking and the frequency of bursting initiated by the removal of magnesium from the tissue bath

was significantly depressed by **107**. This ligand also significantly dampened the enhancement of the frequency of spiking and neuronal bursts in human epileptic tissue induced by the voltage-gated K<sup>+</sup>-channel blocker, 4-aminopyridine.<sup>191</sup> In vivo studies shows that ligand **107** significantly suppressed convulsions induced by a range of chemical stimuli impacting GABAARs (pentylentetrazol, picrotoxin), dopamine receptors (cocaine), potassium channels (4-aminopyridine), muscarinic receptors (pilocarpine), NMDA receptors (NMDA), glycine receptors (strychnine). Lethality induced by higher concentrations of chemoconvulsants were also significantly dampened by **107** along with clonic seizures and tonic seizures. It was much more efficacious than diazepam as it raises the seizure threshold for induction of convulsions.<sup>192</sup> In addition to that ligand **107** also demonstrated anticonvulsant activity against electrically-induced seizures in both maximal electroshock models and 6Hz electrical stimulation. This mouse model is usually used to predict novel antiepileptic treatments<sup>193</sup> and potential agents for pharmacoresistant epilepsies.<sup>194</sup>

### 2.5.3.2 Seizure sensitization models.

Seizure sensitization or seizure kindling is an effect where an occurrence of a seizure increases the future probability of seizure occurrence. In pharmacoresistant epilepsy models, seizure sensitization models and on human epileptic tissue KRM-II-81 (**107**) also showed good anticonvulsant activities.<sup>195</sup> Fully kindled seizures induced by electrical corneal stimulation, electrical stimulation of the basolateral amygdala, and by the chemoconvulsants, pentylentetrazol and cocaine was blocked by ligand **107**.<sup>192</sup> It was also active in a corneal

kindling model as compared to the standard topiramate. In an amygdala kindling model ligand **107** altered seizure severity, after-discharge duration, and after-discharge threshold.<sup>191</sup> In pentylenetetrazol induced fully kindled mice, ligand **107** completely suppressed the convulsions as did diazepam. Daily treatment of fully kindled mice with (**107** + pentylenetetrazol) also prevented the further development of seizure kindling and mice tested on day 10 with pentylenetetrazol in the absence of KRM-II-81 shows significant reduction in seizure prevalence compared to the mice given vehicle + pentylenetetrazol prior to the test session. This dose dependent effect is considerably less for diazepam than **107**.<sup>192</sup> Cocaine induced kindling is another example where KRM-II-81 shows much more effective anticonvulsant activity as compared to diazepam.<sup>192</sup> With cocaine kindling in mice (60 mg/kg for 5 consecutive days), cocaine produced convulsion in 92% of the mice on day 6. Ligand **107** suppressed the seizure prevalence in fully-kindled mice (42% seizures), as well as blocked the expression development of cocaine seizure kindling.<sup>192</sup>

### 2.5.3.3 Pharmacoresistant models

In 2014, it was reported by Franco *et al.* that epilepsy can become resistant to antiepileptic drug therapy.<sup>196</sup> KRM-II-81 was an effective anticonvulsant in a mesial temporal lobe epilepsy model in mice under a certain condition where the standard antiepileptics such as lamotrigine and valproic acid did not work. The characteristic temporal lobe epilepsy in patients can be mimicked through mice which developed enduring epileptic events.<sup>197</sup> Mice with kainate-induced mesial temporal lobe seizures shows spontaneous recurrent hippocampal paroxysmal discharges which occurred 30-60 times per hour and lasted for about 15-20 sec. In the presence of ligand **107**, a significant reduction of spontaneous discharge was observed ( $5.5 \pm 1.4$  discharges) as compared to the baseline level spontaneous discharge ( $16.8 \pm 2.5$  discharges).<sup>192</sup> In lamotrigine-insensitive model, where rats are electrically kindled by amygdala stimulation in presence of lamotrigine in such a way that, lamotrigine and some other anticonvulsants did not show anticonvulsion effects.<sup>198</sup> Under such conditions ligand **107** showed anticonvulsant activity with an ED<sub>50</sub> of 19 mg/kg. It also reduced the severe electrically-driven seizures using a minimum dose of 5 mg/kg.<sup>199</sup> In another model which enables the the monitoring of spontaneous recurrent seizures and clinically-relevant measures of epilepsy for antiepileptic drug differentiation,<sup>200</sup> ligand **107** at a dose of 20mg/kg, reduced the seizure burden and increased the percent of seizure free rats.<sup>199</sup> When given daily in the kainate-induced chronic epilepsy model, ligand **107** did not show a reduction of anticonvulsant efficacy.<sup>199</sup>

#### 2.5.3.4 Post-traumatic epilepsy

In post traumatic brain injury (TBI) and its negative biological sequelae such as post-traumatic epilepsy this is associated with affective, neurocognitive, and psychosocial disruption of life and can have a long term negative effect on health<sup>201</sup>. Ping *et al.*<sup>202</sup> described a post TBI assay using a mouse model where an early quiescence phase of neuronal activity is followed by sustained hyperactivity of cortical neurons at the time when the mice are at increased risk to develop posttraumatic epilepsy<sup>203</sup>. Experiments based on this study with KRM-II-81 (**107**), suggests that it positively reduces the probability of post-traumatic epilepsy.<sup>199</sup>

#### 2.5.3.5 Antinociceptive activity

Pain disorder is a physical phenomena where someone can experience pain in one or several parts or areas of the body and usually can originate in several different types. This can be chronic pain, complex regional pain syndrome, back pain, cancer pain, neuropathic pain, inflammatory pain, bladder pain, etc. Standard treatments for pain involve stress management, psychotherapy, behavioral therapy, acupuncture, and medication.<sup>123</sup> The medication usually used for the treatment of pain are addictive opioids, NSAIDs, acetaminophen, COX-2 inhibitors, tricyclic antidepressants, anti-epileptics SSRI's etc. Based on the fact that the pain pathways depend for the most part on GABA<sub>A</sub>R-driven inhibitory neurotransmission, the use of  $\alpha 2/\alpha 3$  PAMs, shows promise to treat pain disorders.<sup>204-208</sup> But the common problem related to these medications involves addiction, tolerance, constipation, risk of kidney damage, liver failure,

severe stomach pains, bleeding, increased risk of heart attack, high blood pressure and stroke etc. A large amount of growing evidence suggests that subtype selective ligands targeting  $\alpha 2$ -containing GABAAR can be used in the treatment of pain disorders.<sup>123</sup> Since the  $\alpha 2/3$  GABAAR PAM, the 1,3 oxazole KRM-II-81 (**107**) showed significant activity in animal models of pain due to its potency at these two subtypes, it is a lead compound to treat pain disorders. The classical BZD diazepam shows no antinociceptive activity in the early phase of the formalin assay in rats which indicates that it produces motor impairment. In contrast to that ligand **107** suppressed the pain and did not suppress the locomotor activity of rats up to a dose of 300mg/kg. KRM-II-81 was also studied in both mice and rats in acute and chronic pain models.<sup>184</sup> From these models it can be seen that ligand **107** significantly increased these pain thresholds much above baseline levels with potency and efficacy greater at particular time periods than gabapentin, the standard-of-care agent.<sup>187</sup> It was also found that ligand **107** can show antinociceptive effects in a model of chronic neuropathic pain induced by the chemotherapeutic agent paclitaxel. This ligand along with ligand **106** (MP-III-080) also fully reversed the chemotherapy-induced allodynia when dosed from day 18 to day 40 with no tolerance developed during this time frame.<sup>209</sup> The key is antinociceptive activity with no tolerance nor sedation.

For the patients with severe pain, dose escalation is sometimes necessary due to the tolerance to antinociceptive effects of pain medications.<sup>210</sup> But dose escalation can result in unwanted side effects and increase the risk of medication dependence and lethality.<sup>211</sup> In a study of CFA-induced inflammatory pain, it was found that, daily dosing with ligand **107** showed no tolerance after 3, 7, or 11 days of subchronic dosing.<sup>184</sup> It also showed similar effects for up to a

22 day period of subchronic dosing in the case of a neuropathic pain with chronic constrictive nerve injury.<sup>184</sup>

### 2.5.3.6 Anxiolytic activity

In drug discovery, anxiolytic activity with reduced sedative effects has been a long term goal. BDZs has been used for decades for the acute treatment of anxiety. For example, the drug alprazolam is widely prescribed for the treatment of anxiety. But it comes with a burden sedation, motor-impairment, as well as abuse and dependence potential.<sup>212, 213</sup> It can also suppress respiration and led to emergency room visits and deaths.<sup>187</sup> KRM-II-81 (**107**) showed anxiolytic effects in rodents without producing sedation or motor-impairment. In a marble-burying assay in mice that detects GABAergic anxiolytics as well as the antidepressant/anxiolytic's, **107** decreases the marble-burying by rodents significantly. In a rat Vogel assay, ligand **107** increased the drinking of water by the rats which had been suppressed by punishment.<sup>163</sup> These results are indicative of very good anxiolytic activity for KRM-II-81.

### 2.5.3.7 Antidepressant activity

BZDs are generally not detected as antidepressants in preclinical screens.<sup>214</sup> But in some studies with alprazolam at some doses, it has been shown that alprazolam has some antidepressant like activity.<sup>215, 216</sup> Encouraged by this result, KRM-II-81 (**107**) was also evaluated for its potential antidepressant-like effects in mice. In the forced-swim assay it showed

antidepressant like effects in mice at a dose of 30mg/kg with decreased immobility times.<sup>216</sup> In contrast to ligand **107** diazepam did not show activity in the forced swim test.<sup>217</sup> But in the presence of antagonist  $\beta$ -CCT diazepam did show some antidepressant activity. Interestingly the data with  $\beta$ -CCT suggest that elimination of the sedative effects related to  $\alpha$ 1 mediated activity decreasing depression. The related analog KRM-II-82; however did not show an antidepressant effect, but it does exert more PAM effect than KRM-II-81.

### 2.5.3.8 Study of side effects

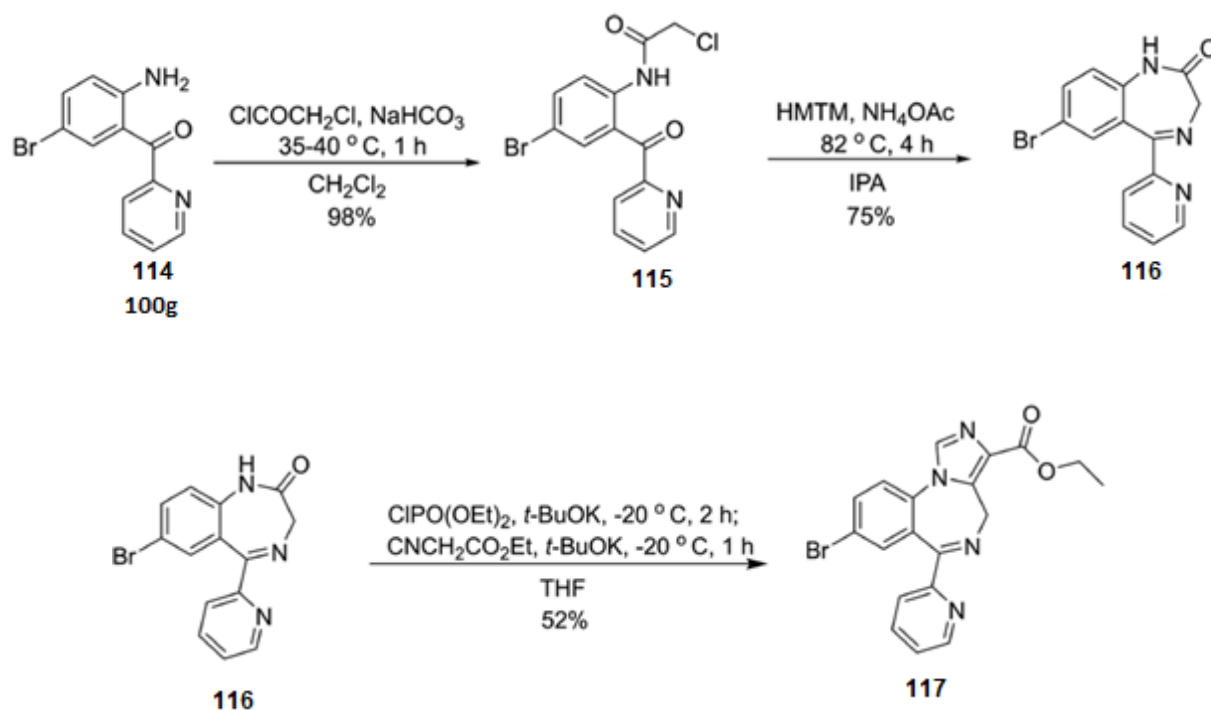
It is important to consider the side effects of drugs when one tries to determine the relationship of these drugs to their therapeutic or efficacious doses or levels. As a potential drug candidate some tests have been done to determine the side effects of KRM-II-81(**107**), as compared to the classical BZD diazepam. In the inverted screen tests in rats, an assay to detect motor impairment has shown that diazepam is more potent than **107**, consequently it causes sedation.<sup>217</sup> Comparison can be done based on the therapeutic index. In rodent seizure models, when one compared the doses that impair motor performance to the doses that produce efficacy ligand **107** expressed a much better protective index than diazepam across a host of assays.<sup>191</sup> It also showed no sedation at a dose of 300 mg/kg p.o., when given to rats at ETSP/NINDS. At 0.25, 0.5, 1, 2, 4, or 6 hr post drug administration, it showed no sign of sedation, ataxia or loss of righting reflex.<sup>199</sup> In contrast, the diazepam after 1h post dosing produced a considerable amount of sedation and ataxia at a dose of 30mg/kg p.o.<sup>199</sup> As shown before from

the structural docking studies of KRM-II-81 (Figure 22) and alprazolam (Figure 18) the pendent ring of both compounds bound similarly. But the chlorine atom at the C8 position of alprazolam formed a halogen bond with the carbonyl oxygen of the  $\alpha$ 1His102, whereas the acetyleno group (ethinyl) at the C8 position of KRM-II-81 did not interact with  $\alpha$ 1His102. The binding affinity of both alprazolam and ligand **107** were -10.8 kcal/mol and -9.4 kcal/mol, respectively. Which indicates alprazolam binds more strongly to  $\alpha$ 1 $\beta$ 3 $\gamma$ 2L GABA<sub>A</sub> receptor compared to ligand **107**. From the study of respiratory-depressant effects it was found that ligand **107** is either inactive or less potent than alprazolam.<sup>187</sup> In acid the induced pain treated rats ligand **107** did not facilitate intracranial self-stimulation (ICSS) behaviour, suggests that it has less abuse liability than diazepam since diazepam has predictive validity for abuse liability in the same model.<sup>218</sup> In fact KRM-II-81 (**107**) showed no dependence in this model. To date, ligand **107** has no demonstrated side effects, hence the interest in this thesis to employ structure based drug design and medicinal chemistry to prepare better bioisosteres of KRM-II-81 as back up compounds.

## 2.5.4 Chemistry and Results

### 2.5.4.1 Synthesis of $\alpha 2/\alpha 3$ Subtype Selective Ligands

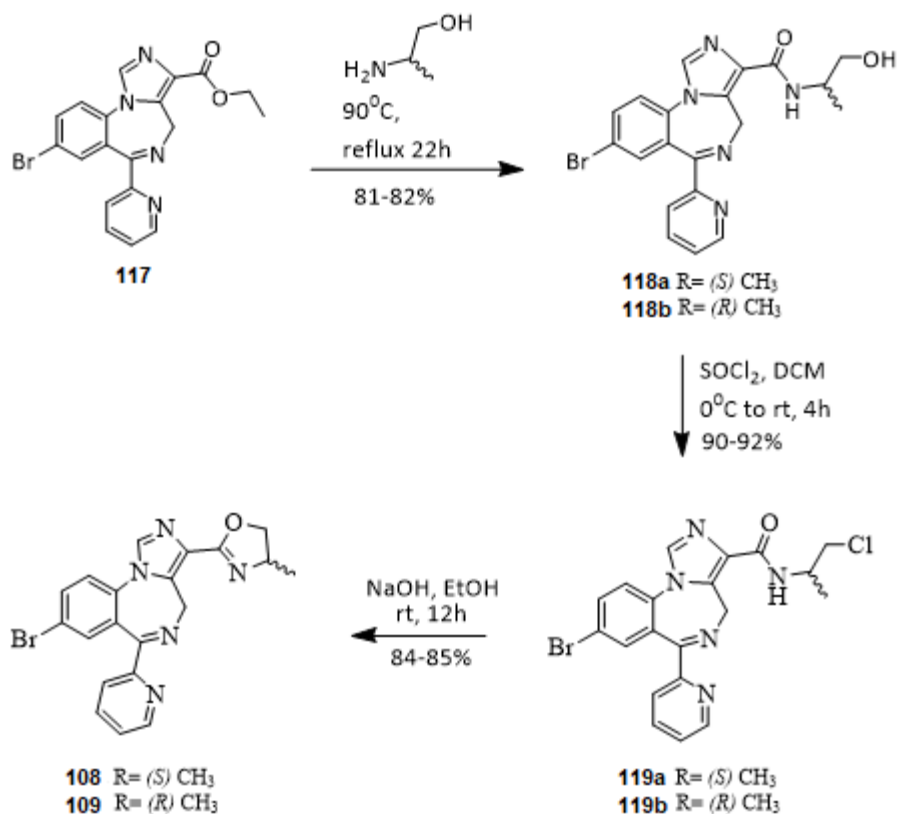
To synthesize the target ligands, first the common intermediate, ethyl ester (**13**), was synthesized on large scale following the procedure by Knutson *et al.*



**Scheme 25.** Synthesis of imidazodiazepine **117**

Starting from the commercially available amine, 2-amino-5-bromo-benzyl-2'-pyridyl ketone **114**, the acylated product **115** was synthesized in 98% overall yield using chloroacetyl chloride in the presence of sodium bicarbonate. The intermediate **115** was then treated directly with HMTM (Hexamethylenetetramine), ammonium acetate in IPA at 82 °C to provide the diazepine core **116** with 75% yield. This amide **116** was purified by recrystallization in methanol and dichloromethane to avoid column chromatography. The imidazole ring was introduced by treating the amide **116** with potassium t-butoxide and diethyl chlorophosphate at -20 °C for 2 hours using a dry ice and IPA bath to control the temperature and this was followed by addition of ethyl isocynoacetate and potassium t-butoxide. at -20 °C. The reaction was then allowed to stir for 12 hours at room temperature. The resulting imidazodiazepine **117** was purified by a TBME (t-butyl methyl ether) and cold ethanol wash followed by crystallization in dichloromethane to obtain **117** in a total yield of 52% (Scheme 25).

The ester **117** was then heated to 90 °C with substituted ethanolamines (individually) in a reflux apparatus for 22 hours to afford  $\alpha$ -hydroxy amides **118a** and **118b**, respectively. The products were purified by water wash and chromatography in 81-82% yield. The  $\alpha$ -hydroxy products **118a** and **118b** were then reacted with thionyl chloride in dichloromethane (individually) to provide  $\alpha$ -halo amides **119a** and **119b**, respectively, which were purified by crystallization, in 90-92% yield.

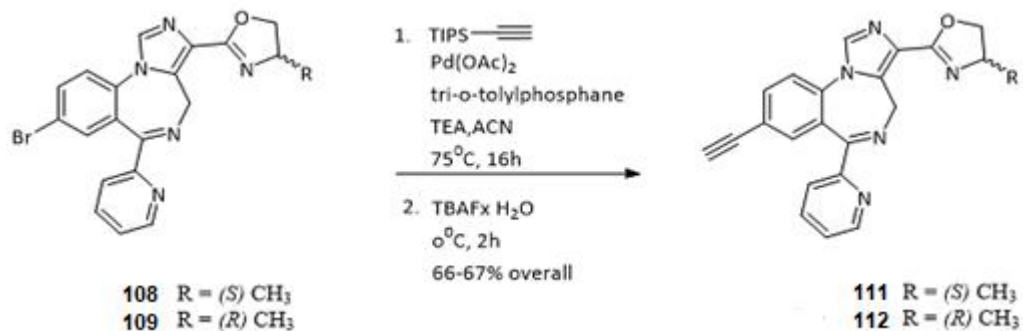


**Scheme 26.** Synthesis of 8-Bromo imidazodiazepines **108** and **109**

To afford the five membered heterocyclic oxazolines (ZK-III-51) **108** and (ZK-III-56) **109**, the  $\alpha$ -halo amides **119a** and **119b** were allowed to react (individually) with sodium hydroxide in ethanol at room temperature for 12 hours. The products which resulted were purified by crystallization in hexane and dichloromethane to afford 84-85% yield. (Scheme 26).

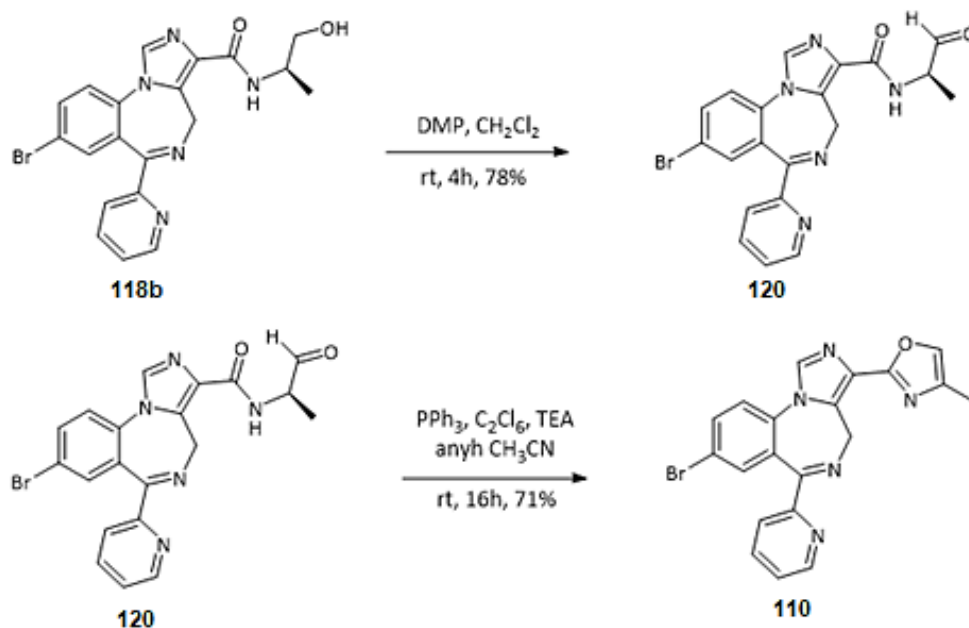
To synthesize the 8-ethynyl imidazodiazepines **111** and **112**, the bromo imidazodiazepines **108** and **109** were then subjected to a copper-free Sonogashira coupling (individually) to afford the triisopropylsilyl (TIPS) protected acetylenes (not shown). Finally, deprotection of the TIPS

group with fluoride anion provided the 8-ethynyl imidazodiazepines **111** and **112** in 66-67% overall yield (Scheme 27), respectively.



**Scheme 27.** Synthesis of 8-ethynyl imidazodiazepines (ZK-IV-4) **111** and (ZK-IV-5) **112**

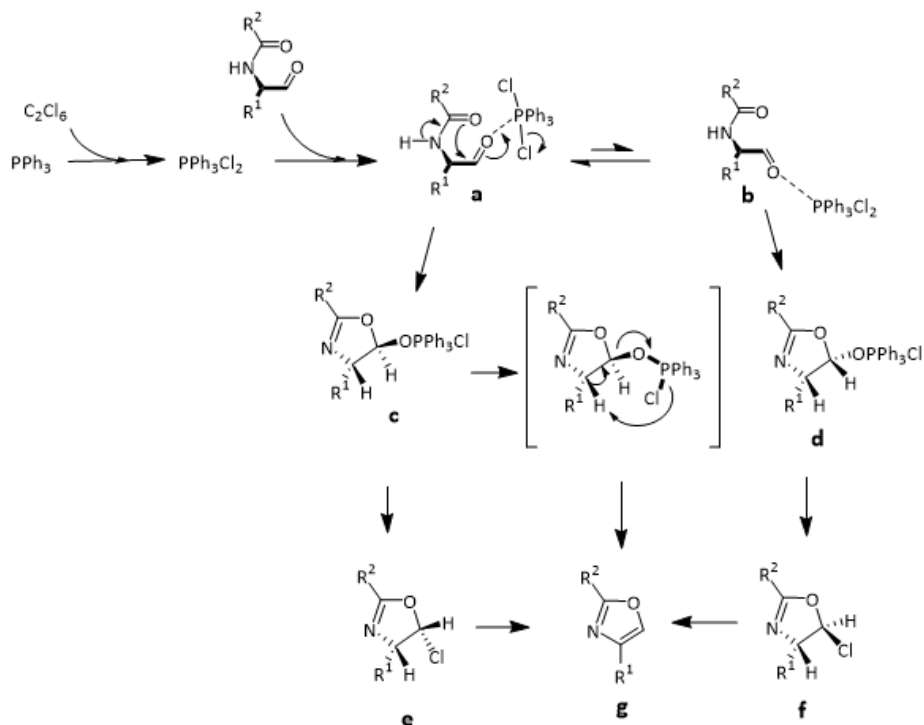
To afford the oxazoles **110** and **113**, the  $\alpha$ -hydroxy amide **118b** was oxidized by treatment with the Dess-Martin reagent to provide the corresponding  $\alpha$ -acylaminoaldehyde **120**, which was purified by crystallization in 78% yield. The oxazole (ZK-III-58) **110** was synthesized from the  $\alpha$ -acylaminoaldehyde **120**, by employing a cyclodehydration reaction (Robinson–Gabriel synthesis, Scheme 28) in 71% yield.



**Scheme 28.** Synthesis of the oxazole (ZK-III-58) **110**

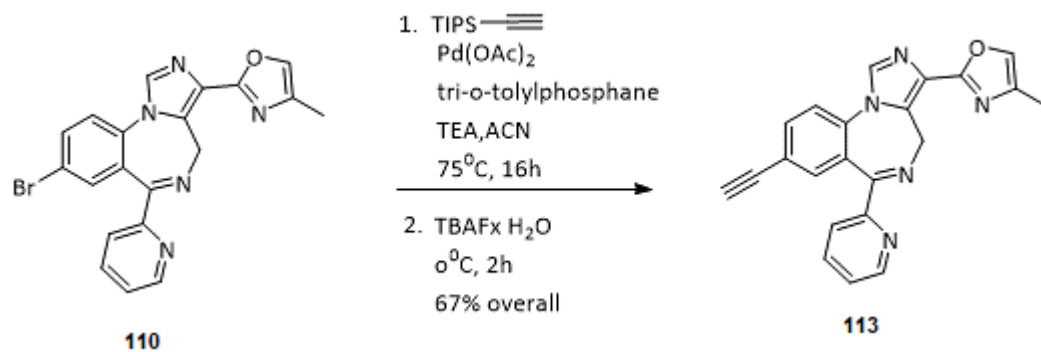
Mechanistically this oxazole formation proceeds through various pathways (Scheme 29). At first the triphenylphosphine reacts with hexachloroethane to form the triphenylphosphine chloride salt. Activation of the aldehyde by the phosphine reagent initiates an allowed intramolecular 5-exo-trig cyclization. Stereoinduction by  $R^1$  may favor conformation **a**, leading to **c**, which may progress directly to the oxazole via syn elimination, through a cyclic six-membered transition state. Alternatively, this intermediate can undergo decomposition of the oxyphosphorane with inversion providing the transient minor chloro-oxazoline adduct **e**, which is readily converted to oxazole **g** in the presence of base by anti elimination (E2). The cyclization from the alternate conformation **b** provides intermediate **d**, which does not have the option of

syn elimination through the cyclic transition state. Decomposition with inversion of **d** to the halide produces the major, long-lived adduct, **f**. This intermediate proceeds through the syn elimination of HCl to the final product **g**.



**Scheme 29.** Mechanism of the formation of oxazole **110**

To afford the oxazole **113** (ZK-IV-07), the imidazodiazepine **110** was subjected to a copper-free Sonogashira coupling to provide the triisopropylsilyl (TIPS) protected acetylenes (not shown). Then the deprotection of the TIPS group with fluoride anion provided the 8-ethynyl imidazodiazepines, target **113** in 67% overall yield (Scheme 30).



**Scheme 30.** Synthesis of oxazole (ZK-IV-07) **113**

## 2.5.4.2 Some Biological studies

### 2.5.4.2.1 Rotarod Motor Impairment Study with Nick Zahn and Coworkers

A locomotor coordination study is one of the ways to access the possibility of undesired  $\alpha 1$  mediated CNS side effects. To date, this study was conducted for some of the analogs by placing mice on a rotating rod for a maximum of 3 minutes after oral administration by gavage at a dose of 40 mg/kg (Figure 24). The mice were also observed for loss of righting reflex as well, an indication of undesired CNS effects. Most of the mice treated with the compounds exhibited no sedation or ataxia, nor loss of righting reflection as compared to the control diazepam.

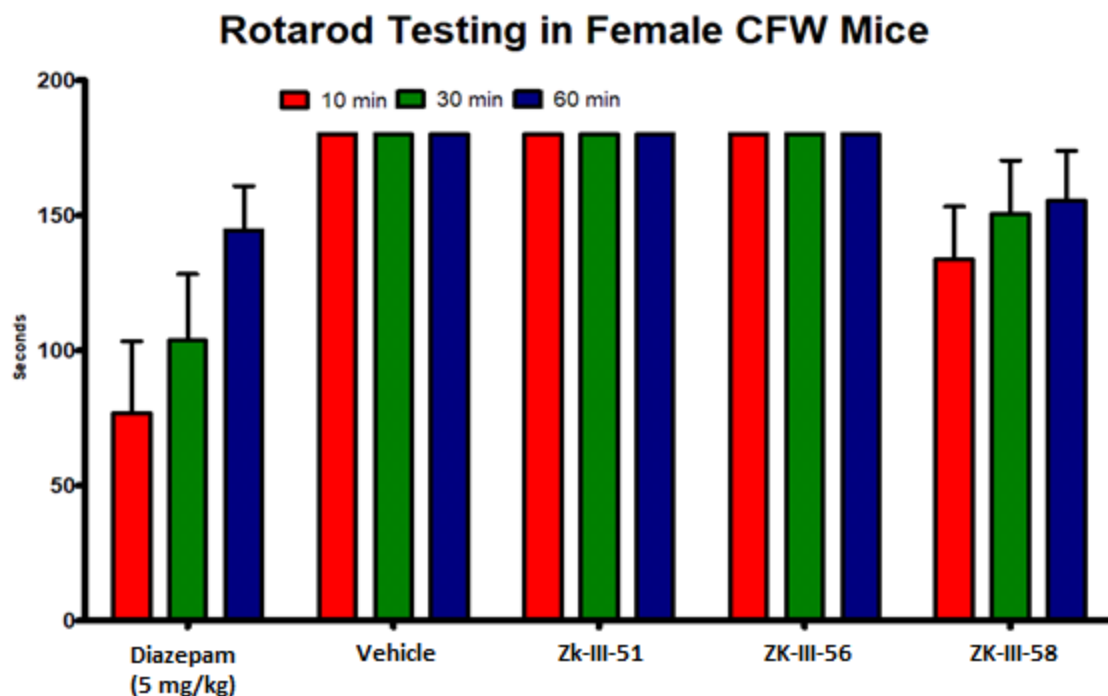


**Figure 24.** Effect of ligands ZK-III-51, ZK-III-56 and ZK-III-58 on sensorimotor coordination. Mice were placed on the rotarod at three separate time points of 10, 30, and 60 minutes after each oral gavage drug administration at 40 mg/kg. Their performance on the rotarod for 3 minutes was recorded and analyzed. After a second fall, it would be considered a failure, and that time point would be recorded. ZK-III-58 shows sedation.

Most of the compounds exhibited sensorimotor steadiness at all three time-points, which indicated no sedative/ataxic effects. However, among these compounds ZK-III-58 exhibits some sensorimotor deficits. This result suggests that ZK-III-58 produced some sedation /ataxia because of its efficacy especially at the  $\alpha$ 1-GABAAR subtype or perhaps the  $\alpha$ 5 subtype (Savic *et al.*).

### 2.5.4.2.1 clogP data

Lipophilicity plays an important role in solubility, absorption, membrane penetration, plasma protein binding, distribution, in vitro or in vivo assessment of ADME (Absorption, Distribution, Metabolism and Excretion) and PK properties during the selection or optimization of potential lead compound, CNS penetration as well and partitioning into other tissues or organs such as the liver and kidney and has an impact on the routes of clearance. The calculated LogP (cLogP) value provides a good estimation of these properties. It is known that LogP is the logarithm of the partition coefficient of a compound between n-octanol and water. According to Lipinski's rule of 5 if a compound has a cLogP value less than 5, such compound has a good absorption and permeation capability. From the calculated clogP value of the newly developed ligands **4,5,6,7,8** and **9**, it can be seen that all these compounds exhibit lower clogP value than 5, which indicates these should be good for the CNS penetration and partitioning into other tissues or organs such as brain.

**Table 14.** cLogP values of the selected ligands <sup>a</sup>

Ligands	cLogP values
ZK-III-51	2.92
ZK-III-56	2.92
ZK-III-58	2.44
ZK-IV-04	2.32
ZK-IV-05	2.32
ZK-IV-07	1.85

<sup>a</sup> cLogP values calculated using ChemBioDraw<sup>®</sup> Ultra (ver.13.0.0.3015).

#### 2.5.4.2.2 PDSP Compound-induced Radioligand Displacement Assays for 31 Receptors with Dr. Bryan Roth

The compound induced receptive primary inhibition studies have been done for ZK-III-51 (Table 15) and ZK-III-56 (Table 16) so far by the National Institute of Mental Health's Psychoactive Drug Screening Program, Contract # HHSN-271-2013-00017-C(NIMH PDSP). The NIMH PDSP is directed by Bryan L. Roth MD, PhD at the University of North Carolina at Chapel Hill and Project Officer Jamie Driscoll at NIMH, Bethesda MD, USA. From the provided data it can be seen that both the analogs displaced the radiolabeled probe [3H]flunitrazepam from the benzodiazepine (BZP) rat brain site of GABA<sub>A</sub>Rs. The BZP rat brain site is a homogenized mixture of rat brain cells and membranes consisting of all GABA<sub>A</sub>R subtypes ( $\alpha$ 1- $\alpha$ 6) where the binding affinity reflects affinity at the  $\alpha$ + $\gamma$ - site (Knutson *et al.*). It can also be seen that there is no affinity of these analogs observed for the other selected receptors except 5-HT<sub>1A</sub> receptor binding for ZK-III-51 and KOR receptor binding for both the ligands. Most of these individual interactions resulted in about 50% inhibition of binding of the respective ligand at a 10  $\mu$ M drug concentration, suggesting an

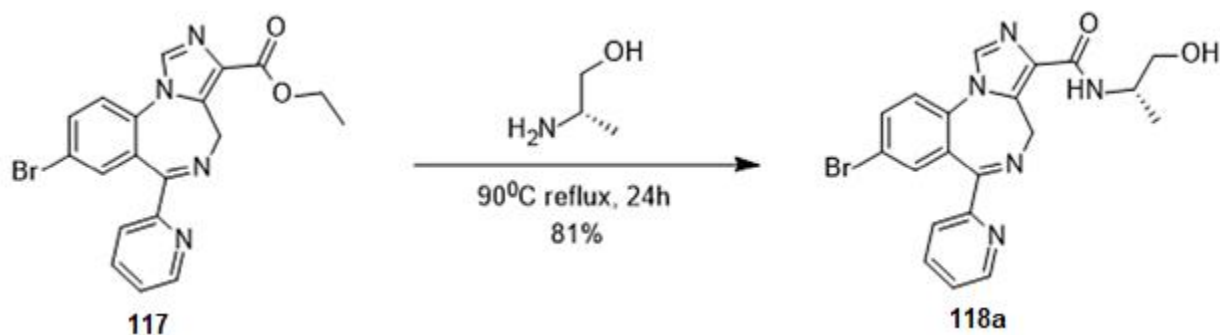
IC<sub>50</sub> of about 10 μM, which confirmed these ligands do not bind to off target receptors. Secondary binding studies (Table 6) were then conducted to determine the binding affinities for any ligand that displaced >50% radioligand in the primary (PDSP) assay, which demonstrated that off-target binding for most ligands was 1,000 times less potent compared to the primary target.

## 2.6 Conclusion

Because of the strong resemblance to potential anticonvulsant and antinociceptive drug candidate KRM-II-81 and from some biological data collected, to date, it can be said that the newly developed ligands may be future backup compounds. Although it depends largely on getting more biological data on other potential ligands **110**, **111**, **112** and **113** as well which are currently ongoing in MIDD. Previously studied C8 bromo analogs showed significant sedative effects. But from the collected rotarod data it can be seen that the C8 bromo compounds **108**, **109** and **110** showed little or no sedative effects in mice. Consequently, it can be said that along with the C8 ethynyl ligands **111**, **112** and **113**, the C8 bromo ligands **108**, **109** and **110** should be studied further to determination of sedation. These new ligands have potential to be a backup drugs of KRM-II-81 and hence are of interest. However, all of the biology, which is being waited on will be the key.

## 2.7 Experimental

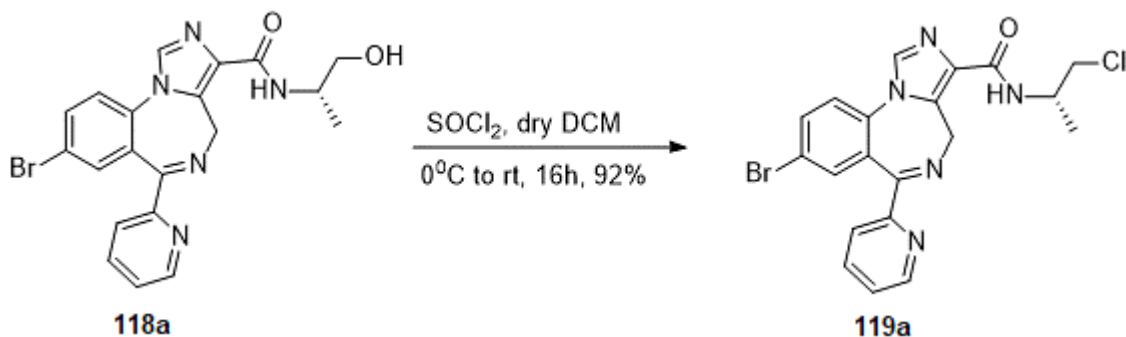
### 2.7.1 (*S*)-8-Bromo-N-(1-hydroxypropan-2-yl)-6-(pyridin-2-yl)-4H-benzo[f]imidazo[1,5-a][1,4]diazepine-3-carboxamide (**118a**)



Ethyl 8-Bromo-6-(pyridin-2-yl)-4H-benzo[f]imidazo[1,5-a][1,4]diazepine-3-carboxylate **117** (5.0g, 12.2 mmol) was mixed with excess (*S*)-2-aminopropan-1-ol (15mL, 192 mmol) and allowed to stir for 24h at 90°C using a reflux condenser. After allowing the mixture to cool to rt, the reaction progress was monitored by TLC (silica gel, EtOAc/hexane/methanol 2:1:0.5 and a few drops of 14% aq NH<sub>4</sub>OH) and it indicated the disappearance of **117**. The appearance of a new spot at ( $R_f = 0.3$ ) in TLC was observed which is polar compared to **117**. After that, 25 mL of distilled water was added to the reaction mixture and it was allowed to stir it at rt at a low setting for 5 min. The excess unreacted (*S*)-2-aminopropan-1-ol was dissolved in water while the product **118a** remained as a solid. Amide **118a** was filtered carefully using a Buchner funnel, washed with distilled water (2 x 25 mL) and kept on the Buchner funnel overnight to dry. The amide **118a** was collected from the Buchner funnel and placed in a round bottom flask and dried under high

vacuum for 12h. The final amide appeared as an off-white colored powder [4.33 g (81%)]: **m.p.** 259-260 °C;  $[\alpha]_D^{25} = -7.2$  (c 1.0, CHCl<sub>3</sub>). **<sup>1</sup>H NMR** (300 MHz, CDCl<sub>3</sub>):  $\delta_H$  8.55 (d, J 4.7 Hz, 1H), 8.14 (d, J 7.9 Hz, 1H), 7.90 – 7.81 (m, 1H), 7.77 (dd, J 8.6, 2.7 Hz, 2H), 7.59 (d, J 2.3 Hz, 1H), 7.50 – 7.39 (m, 1H), 7.39 – 7.32 (m, 1H), 7.24 (d, J 7.2 Hz, 1H), 6.24 (d, J 10.8 Hz, 1H), 4.22 (qd, J 6.7, 3.2 Hz, 1H), 4.12 (s, 1H), 3.75 (d, J 9.3 Hz, 1H), 3.64 (dd, J 11.0, 6.4 Hz, 1H), 1.98 (s, 1H), 1.28 (d, J 6.8 Hz, 3H). **<sup>13</sup>C NMR** (75 MHz, CDCl<sub>3</sub>):  $\delta_C$  166.8 (s), 163.4 (s), 156.3 (s), 148.5 (s), 136.9 (s), 135.9 (s), 135.4 (s), 134.9 (s), 134.6 (s), 133.2 (s), 131.2 (s), 128.6 (s), 124.8 (s), 124.2 (s), 124.0 (s), 120.4 (s), 67.6 (s), 48.0 (s), 44.8 (s), 17.1(s). **HRMS** (ESI/IT-TOF) m/z: [M + H]<sup>+</sup> Calculated for C<sub>20</sub>H<sub>18</sub>BrN<sub>5</sub>O<sub>2</sub> 440.0722; found 440.0694.

### 2.7.2 (S)-8-Bromo-N-(1-chloropropan-2-yl)-6-(pyridin-2-yl)-4H benzo[f]imidazo[1,5-a][1,4]diazepine-3-carboxamide (119a)

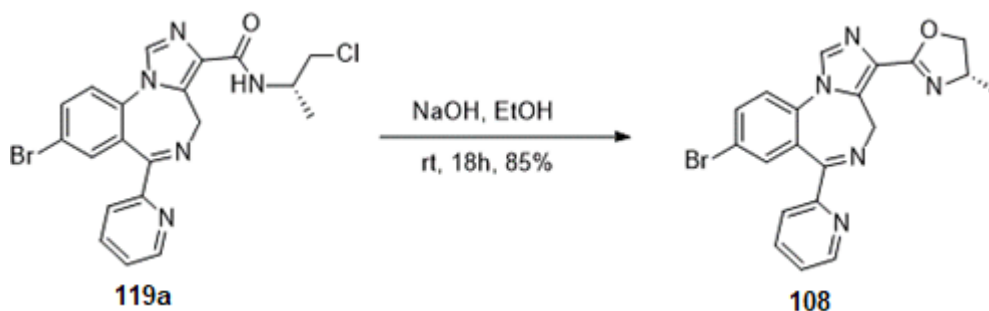


The carboxamide **118a** (3.0 g, 6.8 mmol,) was dissolved in CH<sub>2</sub>Cl<sub>2</sub> (200 mL) and the solution was cooled to 0 °C. Thionyl chloride (2.96 mL, 40.8 mmol) was added to the solution dropwise

and then the reaction mixture was allowed to stir at rt for 16 h. After completion of the process (followed by TLC: silica gel, EtOAc/hexane/methanol 2:1:0.5 and a few drops of 14% aq NH<sub>4</sub>OH) the reaction mixture was cooled to 0 °C using an ice bath and a sat. aq solution of NaHCO<sub>3</sub> (100 mL) was added dropwise using a dropping funnel. The solution was allowed to stir for 30 min at 0 °C. The organic layer was separated and the aq layer was extracted with CH<sub>2</sub>Cl<sub>2</sub> (3 × 150 mL). The combined organic layer was dried (Na<sub>2</sub>SO<sub>4</sub>). The solvent was evaporated under reduced pressure and the product which resulted, was subjected to crystallization using 25% CH<sub>2</sub>Cl<sub>2</sub> and 75% hexane. The collected crystals of chloride **119a** was off white in color and the final yield of the reaction after crystallization was 2.84g (91%): **m.p.** 190- 191<sup>0</sup>C; **[α]<sub>D</sub><sup>25</sup>** = -18.6 (c 1.07, CHCl<sub>3</sub>).

**<sup>1</sup>H NMR** (300 MHz, CDCl<sub>3</sub>): δ<sub>H</sub> 8.56 (d, J 4.5 Hz, 1H), 8.15 (d, J 7.9 Hz, 1H), 7.83 (dd, J 7.7, 1.7 Hz, 1H), 7.81 (s, 1H), 7.78 (dd, J 8.5, 2.2 Hz, 1H), 7.60 (d, J 2.2 Hz, 1H), 7.44 (d, J 8.6 Hz, 1H), 7.37 (dd, J 7.6, 4.9 Hz, 1H), 7.27 (d, J 10.2 Hz, 1H), 6.27 (d, J 12.4 Hz, 1H), 4.56 – 4.48 (m, 1H), 4.15 (d, J 12.5 Hz, 1H), 3.68 (dd, J 10.8, 3.9 Hz, 2H), 1.37 (d, J 6.7 Hz, 3H). **<sup>13</sup>C NMR** (75 MHz, CDCl<sub>3</sub>): δ<sub>C</sub> 166.8 (s), 162.1 (s), 156.3 (s), 148.6 (s), 136.9 (s), 136.0 (s), 135.4 (s), 134.9 (s), 134.6 (s), 133.2 (s), 131.3 (s), 128.6 (s), 124.8 (s), 124.2 (s), 124.0 (s), 120.4 (s), 49.2 (s), 45.1 (s), 44.8 (s), 18.1 (s). **HRMS** (ESI/IT-TOF) m/z: [M + H]<sup>+</sup> Calculated for C<sub>20</sub>H<sub>17</sub>BrClN<sub>5</sub>O 458.0383; found 458.0363.

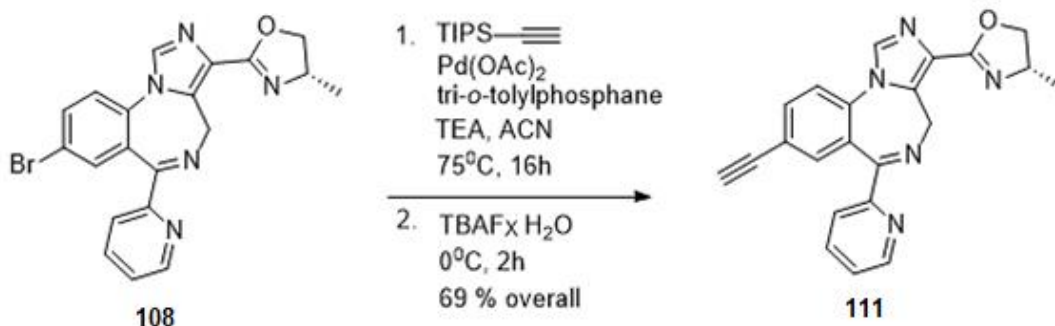
2.7.3 (S)-2-(8-Bromo-6-(pyridin-2-yl)-4H-benzo[f]imidazo[1,5-a][1,4]diazepin-3-yl)-4-methyl-4,5-dihydrooxazole (108)



The carboxamide **119a** (2.0g, 4.36 mmol) was added to ethanol (100 mL) and NaOH pellets (1.05g, 26.2 mmol) were added at rt. The solution which was obtained was allowed to stir at rt for 18h. The reaction progress was monitored by TLC (silica gel, EtOAc/hexane/methanol 2:1:0.5 and a few drops of 14% aq NH<sub>4</sub>OH) until the complete disappearance of **119a** was observed. The dihydrooxazole spot was polar on TLC (silica gel, EtOAc/hexane/methanol 2:1:0.5 and a few drops of 14% aq NH<sub>4</sub>OH) compared to **119a** (R<sub>f</sub> = 0.2). The ethanol was removed under reduced pressure to afford a solid residue. The residue was dissolved in CH<sub>2</sub>Cl<sub>2</sub> (150 mL) and washed with a saturated aq solution of NaHCO<sub>3</sub> (150 mL). The organic layer was separated and the remaining aq layer was extracted with CH<sub>2</sub>Cl<sub>2</sub> (3 × 150 mL). The combined organic layer was dried (Na<sub>2</sub>SO<sub>4</sub>). The organic solvent was removed under reduced pressure and the solid residue, which was obtained, was purified by crystallization (5% MeOH in EtOAc) to afford dihydrooxazole **108** as

white colored needle shaped crystals (1.56g, 85%) : **m.p.** 199-200 °C (crystallized from 5% MeOH in EtOAc).  $[\alpha]_D^{25} = -40$  (c 1.0, CHCl<sub>3</sub>). **<sup>1</sup>H NMR** (300 MHz, CDCl<sub>3</sub>)  $\delta_H$  8.58 (d, J 4.9 Hz, 1H), 8.08 (d, J 7.9 Hz, 1H), 7.91 (d, J 1.0 Hz, 1H), 7.83 (d, J 7.6 Hz, 1H), 7.78 (ddd, J 8.5, 2.3, 1.0 Hz, 1H), 7.57 (dd, J 2.2, 1.0 Hz, 1H), 7.51 – 7.44 (m, 1H), 7.41 – 7.33 (m, 1H), 6.05 (d, J 12.6 Hz, 1H), 4.53 (s, 1H), 4.40 (h, J 6.9 Hz, 1H), 4.18 (d, J 12.7 Hz, 1H), 3.97 (t, J 7.7 Hz, 1H), 1.38 (d, J 6.5 Hz, 3H). **<sup>13</sup>C NMR** (75 MHz, CDCl<sub>3</sub>):  $\delta_C$  167.1 (s), 159.0 (s), 156.4 (s), 148.8 (s), 136.9 (s), 135.3 (s), 135.2 (s), 135.0 (s), 134.9 (s), 134.6 (s), 128.5 (s), 127.4 (s), 124.8 (s), 124.2 (s), 124.0 (s), 120.3 (s), 73.9 (s), 61.9 (s), 45.1 (s), 21.5 (s). **HRMS** (ESI/IT-TOF) m/z: [M + H]<sup>+</sup> Calculated for C<sub>20</sub>H<sub>16</sub>BrN<sub>5</sub>O 422.0616; found 422.0608.

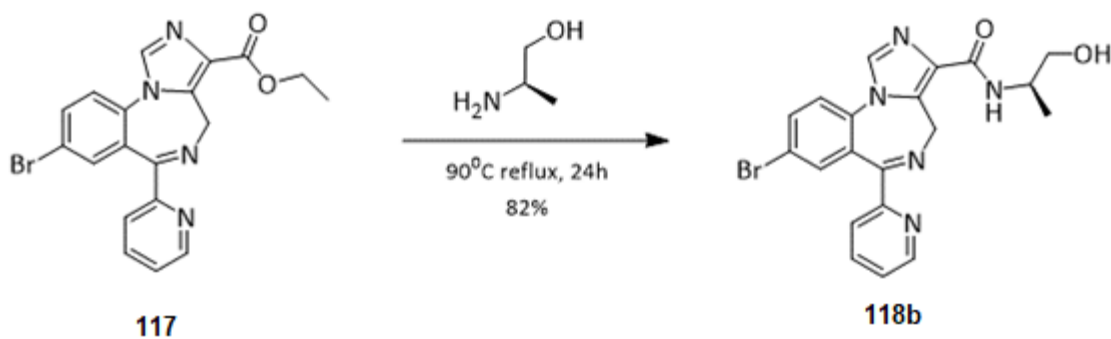
#### 2.7.4 (S)-2-(8-Ethynyl-6-(pyridin-2-yl)-4H-benzo[f]imidazo[1,5-a][1,4]diazepin-3-yl)-4-methyl-4,5-dihydrooxazole (111)



A mixture of palladium (II) acetate (13.3 mg, 0.06 mmol), tri-*o*-tolylphosphine (36 mg, 0.12 mmol) and anhydrous acetonitrile (15 mL) was allowed to stir at rt for 15 min. The bromide **108** (500 mg, 1.18 mmol), triisopropylsilylacetylene (259.1 mg, 1.42 mmol), triethylamine (358 mg, 3.54 mmol), and acetonitrile (10 mL) were added to the mixture. The reaction mixture was allowed to reflux at 75°C and monitored by TLC (silica gel, EtOAc/hexane/methanol 2:1:0.5 and a few drops of triethylamine). To complete the reaction, excess triisopropylsilylacetylene (107.6 mg, 0.59 mmol) was added in the reaction mixture. After 16h the solvent was removed under reduced pressure and the residue was dissolved in CH<sub>2</sub>Cl<sub>2</sub> (25 mL) and filtered through a bed of celite. The filtrate was washed with brine (25 mL) and dried (Na<sub>2</sub>SO<sub>4</sub>). The solvent was removed under reduced pressure and the residue was passed through a short pad of silica gel (silica gel, EtOAc/hexanes 3:1 with 3% triethylamine) to afford a light yellow colored solid (573 mg, 92%), which was used for the next step without further purification. To the mixture of this solid (573 mg, 1.1 mmol), THF (20 mL) and water (0.1 mL), TBAF xH<sub>2</sub>O (0.35 g, 1.3 mmol, 1M in THF) was added dropwise at 0 °C and the mixture was allowed to stir at rt for 1 h. Analysis by TLC (Silica gel, EtOAc/hexane/MeOH 2:1:0.5 and a few drops of 14% aq. NH<sub>4</sub>OH) indicated the disappearance of starting material. The reaction mixture was then quenched with water and diluted with EtOAc (30 mL). The organic layer was separated and washed with brine (20mL) and dried (Na<sub>2</sub>SO<sub>4</sub>). The solvents were removed under reduced pressure and the residue was purified using flash column chromatography (silica gel, EtOAc/hexane 2:1 and 3% triethylamine) to yield a light yellow colored solid, **111** (301.5 mg, 75%) : **m.p.** 226-230°C (crystallized from 5% MeOH in EtOAc). **[α]<sub>D</sub><sup>25</sup>** -9.8 (c 0.51, CHCl<sub>3</sub>). **<sup>1</sup>H NMR** (500 MHz, CDCl<sub>3</sub>) δ<sub>H</sub> 10.37 (s, 10H), 8.47 (t, J = 4.0 Hz, 12H), 8.19 (d, J = 7.9 Hz, 12H), 7.80 (d, J = 2.3 Hz, 12H), 7.74 (td, J = 8.2, 1.6 Hz, 13H), 7.71 – 7.67

(m, 12H), 7.54 – 7.50 (m, 11H), 7.49 (d, J = 1.7 Hz, 13H), 7.28 (dt, J = 4.8, 3.5 Hz, 13H), 7.05 (d, J = 7.9 Hz, 3H), 6.74 (d, J = 7.9 Hz, 3H), 5.68 (d, J = 1.0 Hz, 12H), 4.59 – 4.48 (m, 12H), 4.44 – 4.32 (m, 13H), 3.98 (dt, J = 16.6, 8.1 Hz, 13H), 3.09 (s, 11H), 1.32 (dd, J = 11.0, 6.6 Hz, 37H). <sup>13</sup>C NMR (126 MHz, CDCl<sub>3</sub>) δ 160.53 (s), 155.87 (s), 148.66 (s), 138.72 (s), 136.95 (s), 135.88 (s), 135.42 (s), 134.50 (s), 127.39 (s), 124.82 (s), 124.35 (s), 122.65 (s), 121.54 (s), 81.65 (s), 80.41 (s), 79.64 (s), 77.28 (s), 77.03 (s), 76.77 (s), 74.79 (s), 61.05 (s), 21.20 (s).

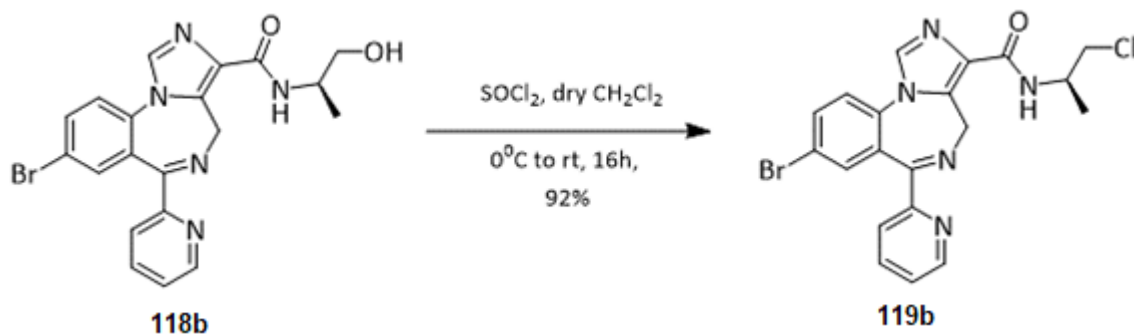
### 2.7.5 (R)-8-Bromo-N-(1-hydroxypropan-2-yl)-6-(pyridin-2-yl)-4H-benzo[f]imidazo[1,5-a][1,4]diazepine-3-carboxamide (118b)



Ethyl 8-Bromo-6-(pyridin-2-yl)-4H-benzo[f]imidazo[1,5-a][1,4]diazepine-3-carboxylate **117** (5.0g, 12.2 mmol) was mixed with excess (*R*)-2-aminopropan-1-ol (15mL, 192 mmol) and allowed to stir for 24h at 90°C using a reflux condenser. After allowing the mixture to cool to rt, the reaction progress was monitored by TLC (silica gel, EtOAc/hexane/methanol 2:1:0.5 and a few drops of 14% aq NH<sub>4</sub>OH) and it indicated the disappearance of **117**. The appearance of a new

spot at ( $R_f = 0.3$ ) in TLC was observed which is polar compared to **117**. After that, 25 mL of distilled water was added to the reaction mixture and it was allowed to stir it at rt at a low setting for 5 min. The excess unreacted (S)-2-aminopropan-1-ol was dissolved in water while the product **118b** remained as a solid. Amide **118b** was filtered carefully using a Buchner funnel, washed with distilled water (2 x 25 mL) and kept on the Buchner funnel overnight to dry. The amide **118b** was collected from the Buchner funnel and placed in a round bottom flask and dried under high vacuum for 12h. The final amide **118b** appeared as an off-white colored powder [4.38 g (82%)]: m.p. 261-262 °C (20% MeOH in EtOAc).  $^1\text{H NMR}$  (300 MHz,  $\text{CDCl}_3$ ):  $\delta_{\text{H}}$  8.56 (d, J 4.4 Hz, 1H), 8.15 (d, J 7.9 Hz, 1H), 7.83 (dd, J 7.7, 1.8 Hz, 1H), 7.77 (dd, J 8.5, 2.3 Hz, 2H), 7.59 (d, J 2.2 Hz, 1H), 7.43 (d, J 8.6 Hz, 1H), 7.39 – 7.32 (m, 1H), 7.23 (d, J 7.2 Hz, 1H), 6.26 (d, J 12.6 Hz, 1H), 4.22 (qd, J 6.9, 3.4 Hz, 1H), 4.13 (d, J 13.2 Hz, 1H), 3.75 (d, J 10.9 Hz, 1H), 3.64 (dd, J 11.1, 6.5 Hz, 1H), 1.87 (s, 1H), 1.28 (d, J 6.6 Hz, 3H).  $^{13}\text{C NMR}$  (75 MHz,  $\text{CDCl}_3$ ):  $\delta_{\text{C}}$  166.8 (s), 163.5 (s), 156.3 (s), 148.5 (s), 136.9 (s), 136.0 (s), 135.4 (s), 134.9 (s), 134.6 (s), 133.2 (s), 131.2 (s), 128.6 (s), 124.8 (s), 124.2 (s), 124.0 (s), 120.5 (s), 67.7 (s), 48.1 (s), 44.8 (s), 17.1 (s). HRMS (ESI/IT-TOF) m/z:  $[\text{M} + \text{H}]^+$  Calcd for  $\text{C}_{20}\text{H}_{18}\text{BrN}_5\text{O}_2$  440.0722; found 440.0699.

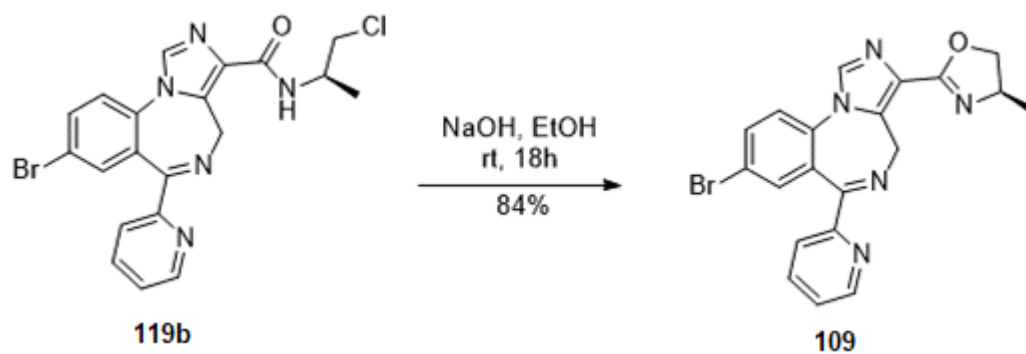
2.7.6 (R)-8-Bromo-N-(1-chloropropan-2-yl)-6-(pyridin-2-yl)-4H-benzo[f]imidazo[1,5-a][1,4]diazepine-3-carboxamide (**119b**)



The carboxamide **118b** (3.0 g, 6.8 mmol,) was dissolved in  $\text{CH}_2\text{Cl}_2$  (200 mL) and the solution was cooled to  $0^\circ\text{C}$ . Thionyl chloride (2.96 mL, 40.8 mmol) was added to the solution dropwise and then the reaction mixture was allowed to stir at rt for 16 h. After completion of the process (followed by TLC: silica gel, EtOAc/hexane/methanol 2:1:0.5 and a few drops of 14% aq  $\text{NH}_4\text{OH}$ ) the reaction mixture was cooled to  $0^\circ\text{C}$  using an ice bath and a sat. aq solution of  $\text{NaHCO}_3$  (100 mL) was added dropwise using a dropping funnel. The solution was allowed to stir for 30 min at  $0^\circ\text{C}$ . The organic layer was separated and the aq layer was extracted with  $\text{CH}_2\text{Cl}_2$  (3  $\times$  150 mL). The combined organic layer was dried ( $\text{Na}_2\text{SO}_4$ ). The solvent was evaporated under reduced pressure and the product which resulted, was subjected to crystallization using 25%  $\text{CH}_2\text{Cl}_2$  and 75% hexane. The collected crystals of chloride **119b** was off white in color and the final yield of the reaction after crystallization was 2.84g (91%): **m.p.**  $191\text{-}192^\circ\text{C}$  ;  **$^1\text{H NMR}$**  (300 MHz,  $\text{CDCl}_3$ ):  $\delta_{\text{H}}$  8.56 (d, J 4.5 Hz, 1H), 8.15 (d, J 7.9 Hz, 1H), 7.83 (dd, J 7.7, 1.7 Hz, 1H), 7.81 (s, 1H), 7.76 (dd, J

8.5, 2.2 Hz, 1H), 7.60 (d, J 2.2 Hz, 1H), 7.44 (d, J 8.5 Hz, 1H), 7.37 (ddd, J 7.7, 4.8, 1.2 Hz, 1H), 7.27 (d, J 10.2 Hz, 1H), 6.28 (d, J 12.4 Hz, 1H), 4.52 (s, 1H), 4.15 (d, J 13.0 Hz, 1H), 3.68 (dd, J 10.8, 3.9 Hz, 2H), 1.37 (d, J 6.6 Hz, 3H). <sup>13</sup>C NMR (75 MHz, CDCl<sub>3</sub>): δ<sub>c</sub> 166.8 (s), 162.1 (s), 156.3 (s), 148.6 (s), 136.9 (s), 136.0 (s), 135.4 (s), 134.9 (s), 134.6 (s), 133.2 (s), 131.3 (s), 128.6 (s), 124.8 (s), 124.2 (s), 124.0 (s), 120.5 (s), 49.2 (s), 45.1 (s), 44.8 (s), 18.0 (s). HRMS (ESI/IT-TOF) m/z: [M + H]<sup>+</sup> Calcd for C<sub>20</sub>H<sub>17</sub>BrClN<sub>5</sub>O 458.0383; found 458.0367.

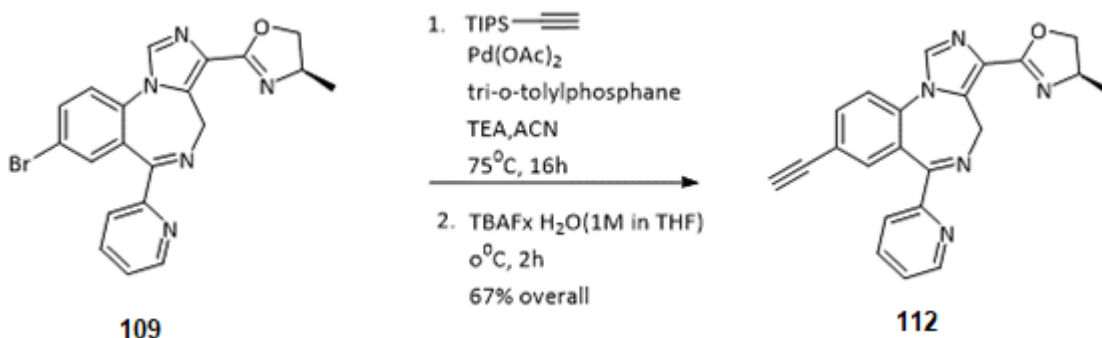
### 2.7.7 (R)-2-(8-Bromo-6-(pyridin-2-yl)-4H-benzo[f]imidazo[1,5-a][1,4]diazepin-3-yl)-4-methyl-4,5-dihydrooxazole (109)



The carboxamide **119b** (2.0g, 4.36 mmol) was added to ethanol (100 mL) and NaOH pellets (1.05g, 26.2 mmol) were added at rt. The solution which was obtained was allowed to stir at rt for 18 h. The reaction progress was monitored by TLC (silica gel, EtOAc/hexane/methanol 2:1:0.5 and a few drops of 14% aq NH<sub>4</sub>OH) until the complete disappearance of **119b** was observed. The

dihydrooxazole spot was polar on TLC (silica gel, EtOAc/hexane/methanol 2:1:0.5 and a few drops of 14% aq NH<sub>4</sub>OH) compared to **119b** (R<sub>f</sub> = 0.2). The ethanol was removed under reduced pressure to afford a solid residue. The residue was dissolved in CH<sub>2</sub>Cl<sub>2</sub> (150 mL) and washed with a saturated aq solution of NaHCO<sub>3</sub> (150 mL). The organic layer was separated and the remaining aq layer was extracted with CH<sub>2</sub>Cl<sub>2</sub> (3 × 150 mL). The combined organic layer was dried (Na<sub>2</sub>SO<sub>4</sub>). The organic solvent was removed under reduced pressure and the solid residue, which was obtained, was purified by crystallization (5% MeOH in EtOAc) to afford dihydrooxazole **109** as white colored needle shaped crystals (1.55g, 84%) : **m.p.** 201-202 °C (crystallized from 5% MeOH in EtOAc). **[α]<sub>D</sub><sup>25</sup>** = +44 (c 1.0, CHCl<sub>3</sub>). **<sup>1</sup>H NMR** (500 MHz, CDCl<sub>3</sub>): δ<sub>H</sub> 8.58 (d, J 4.0 Hz, 1H), 8.07 (d, J 7.9 Hz, 1H), 7.91 (s, 1H), 7.81 (td, J 7.8, 1.8 Hz, 1H), 7.77 (dd, J 8.6, 2.2 Hz, 1H), 7.56 (d, J 2.3 Hz, 1H), 7.47 (d, J 8.6 Hz, 1H), 7.37 (ddd, J 7.6, 4.8, 1.2 Hz, 1H), 6.05 (d, J 11.1 Hz, 1H), 4.53 (dd, J 7.2, 2.1 Hz, 1H), 4.45 – 4.35 (m, 1H), 4.17 (d, J 12.7 Hz, 1H), 4.00 – 3.91 (m, 1H), 1.37 (d, J 6.6 Hz, 3H). **<sup>13</sup>C NMR** (126 MHz, CDCl<sub>3</sub>): δ<sub>C</sub> 167.1 (s), 159.0 (s), 156.4 (s), 148.8 (s), 136.9 (s), 135.3 (s), 135.2 (s), 135.0 (s), 134.9 (s), 134.7 (s), 128.5 (s), 127.4 (s), 124.8 (s), 124.3 (s), 124.0 (s), 120.3 (s), 73.9 (s), 61.9 (s), 45.1 (s), 21.5 (s). **HRMS** (ESI/IT-TOF) m/z: [M + H]<sup>+</sup> Calcd for C<sub>20</sub>H<sub>16</sub>BrN<sub>5</sub>O 422.0616; found 422.0594.

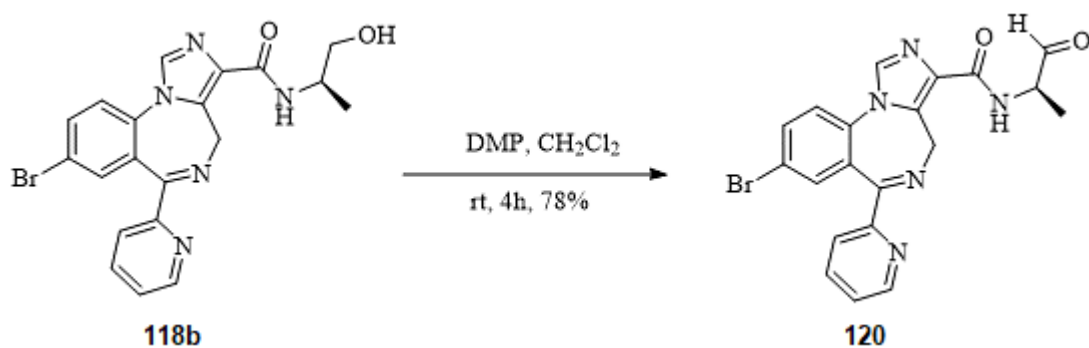
## 2.7.8 (R)-2-(8-Ethynyl-6-(pyridin-2-yl)-4H-benzo[f]imidazo[1,5-a][1,4]diazepin-3-yl)-4-methyl-4,5-dihydrooxazole (112)



A mixture of palladium (II) acetate (13.3 mg, 0.06 mmol), tri-*o*-tolylphosphine (36 mg, 0.12 mmol) and anhydrous acetonitrile (15 mL) was allowed to stir at rt for 15 min. The bromide **109** (500 mg, 1.18 mmol), triisopropylsilylacetylene (259.1 mg, 1.42 mmol), triethylamine (358 mg, 3.54 mmol), and acetonitrile (10 mL) were added to the mixture. The reaction mixture was allowed to reflux at 75°C and monitored by TLC (silica gel, EtOAc/hexane/methanol 2:1:0.5 and a few drops of triethylamine). To complete the reaction, excess triisopropylsilylacetylene (107.6 mg, 0.59 mmol) was added in the reaction mixture. After 18 h the solvent was removed under reduced pressure and the residue was dissolved in CH<sub>2</sub>Cl<sub>2</sub> (25 mL) and filtered through a bed of celite. The filtrate was washed with brine (25 mL) and dried (Na<sub>2</sub>SO<sub>4</sub>). The solvent was removed under reduced pressure and the residue was passed through a short pad of silica gel (silica gel, EtOAc/hexanes 3:1 with 3% triethylamine) to afford a light yellow colored solid (559 mg, 90%),

which was used for the next step without further purification. To the mixture of this solid (559 mg, 1.06 mmol), THF (20 mL) and water (0.1 mL), TBAF  $\cdot$   $\text{H}_2\text{O}$  (0.35 g, 1.3 mmol, 1M in THF) was added dropwise at 0 °C and the mixture was allowed to stir at rt for 1 h. Analysis by TLC (Silica gel, EtOAc/hexane/MeOH 2:1:0.5 and a few drops of 14% aq.  $\text{NH}_4\text{OH}$ ) indicated the disappearance of starting material. The reaction mixture was then quenched with water and diluted with EtOAc (30 mL). The organic layer was separated and washed with brine (20mL) and dried ( $\text{Na}_2\text{SO}_4$ ). The solvents were removed under reduced pressure and the residue was purified using flash column chromatography (silica gel, EtOAc/hexane 2:1 and 3% triethylamine) to yield a light yellow colored solid, **112** (301.5 mg, 77%) : **m.p.** 220-223 °C (crystallized from 5% MeOH in EtOAc).  $[\alpha]_D^{25} = +10.2$  (c 1.02,  $\text{CHCl}_3$ ).  **$^1\text{H NMR}$**  (300 MHz,  $\text{CDCl}_3$ )  $\delta$  8.58 (d, J 4.9 Hz, 1H), 8.08 (d, J 7.9 Hz, 1H), 7.91 (d, J 1.0 Hz, 1H), 7.83 (d, J 7.6 Hz, 1H), 7.78 (ddd, J 8.5, 2.3, 1.0 Hz, 1H), 7.57 (dd, J 2.2, 1.0 Hz, 1H), 7.51 – 7.44 (m, 1H), 7.41 – 7.33 (m, 1H), 6.05 (d, J 12.6 Hz, 1H), 4.53 (s, 1H), 4.40 (h, J 6.9 Hz, 1H), 4.18 (d, J 12.7 Hz, 1H), 3.97 (t, J 7.7 Hz, 1H), 3.10 (s, 1H), 1.38 (d, J 6.5 Hz, 3H).  **$^{13}\text{C NMR}$**  (126 MHz,  $\text{CDCl}_3$ )  $\delta_C$  160.53 (s), 155.87 (s), 148.66 (s), 138.72 (s), 136.95 (s), 135.88 (s), 135.42 (s), 134.50 (s), 127.39 (s), 124.82 (s), 124.35 (s), 122.65 (s), 121.54 (s), 81.65 (s), 80.41 (s), 79.64 (s), 77.28 (s), 77.03 (s), 76.77 (s), 74.79 (s), 61.05 (s), 21.20 (s).

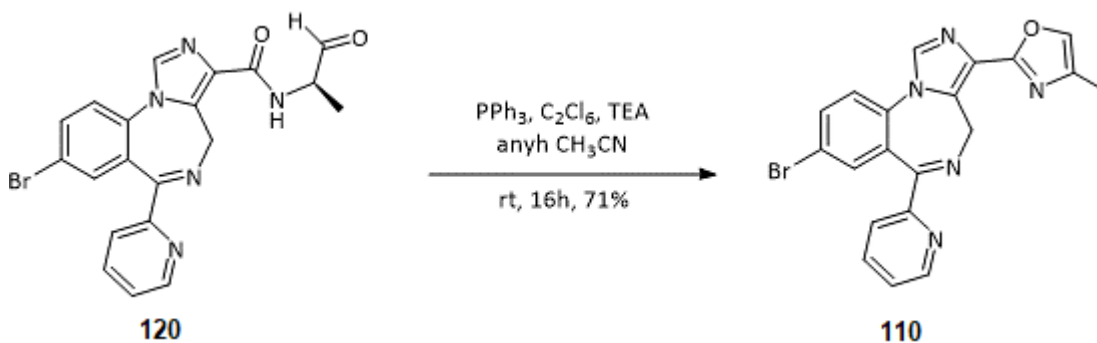
2.7.9 (R)-8-bromo-N-(1-oxopropan-2-yl)-6-(pyridin-2-yl)-4H-benzo[f]imidazo[1,5-a][1,4]diazepine-3-carboxamide (**120**)



To a solution of (R)-8-Bromo-N-(1-hydroxypropan-2-yl)-6-(pyridin-2-yl)-4H-benzo[f]imidazo[1,5-a][1,4]diazepine-3-carboxamide **118b** (3 g, 6.8 mmol) in CH<sub>2</sub>Cl<sub>2</sub> (70 mL), the Dess-Martin periodinane (5.78 g, 13.6 mmol) was added in one portion and the mixture was stirred at rt for 4 h. The reaction mixture was analyzed by TLC (silica gel, EtOAc/hexane/MeOH 2:1:0.5). After the completion of the reaction by TLC, the mixture was diluted with CH<sub>2</sub>Cl<sub>2</sub> (100 mL) and quenched by addition of a sat. aq NaHCO<sub>3</sub> solution (80 mL) and a sat. solution of aq Na<sub>2</sub>S<sub>2</sub>O<sub>3</sub> (80 mL). The mixture was stirred for 20 min and the layers were separated. The aq layer was extracted with CH<sub>2</sub>Cl<sub>2</sub>(100 mL x 2) and the combined organic layer was washed with brine (100 mL) and dried (Na<sub>2</sub>SO<sub>4</sub>). The solvent was removed under reduced pressure and the residue was purified by flash chromatography (silica gel, 100% EtOAc) to provide amide **120** as a light-yellow powder (2.4 g, 81%). **m.p.** 246-249 °C,  $[\alpha]_D^{25} = +32.7$  (c 1.02, CHCl<sub>3</sub>) <sup>1</sup>H NMR (500 MHz, CDCl<sub>3</sub>):  $\delta_H$  9.67 (s, 1H), 8.57 (ddd, *J* 4.8, 1.8, 0.9 Hz, 1H), 8.15 (dt, *J* 7.9, 1.1 Hz, 1H), 7.87 – 7.80

(m, 2H), 7.78 (dd, *J* 8.6, 2.2 Hz, 1H), 7.61 (t, *J* 4.5 Hz, 2H), 7.45 (d, *J* 8.5 Hz, 1H), 7.37 (ddd, *J* 7.6, 4.8, 1.2 Hz, 1H), 6.25 (d, *J* 12.5 Hz, 1H), 4.63 (m, 1H), 4.14 (d, *J* 12.7 Hz, 1H), 1.46 (d, *J* 7.4 Hz, 3H). <sup>13</sup>C NMR (75 MHz, CDCl<sub>3</sub>): δ<sub>c</sub> 199.5 (s), 166.8 (s), 162.7 (s), 156.3 (s), 148.6 (s), 136.9 (s), 136.1 (s), 135.4 (s), 134.9 (s), 134.6 (s), 133.3 (s), 130.7 (s), 128.6 (s), 124.8 (s), 124.2 (s), 124.0 (s), 120.5 (s), 54.0 (s), 44.8 (s), 14.6 (s). HRMS (ESI/IT-TOF) *m/z*: [M + H]<sup>+</sup> Calcd for C<sub>20</sub>H<sub>16</sub>BrN<sub>5</sub>O<sub>2</sub> 438.0566; found 438.0549.

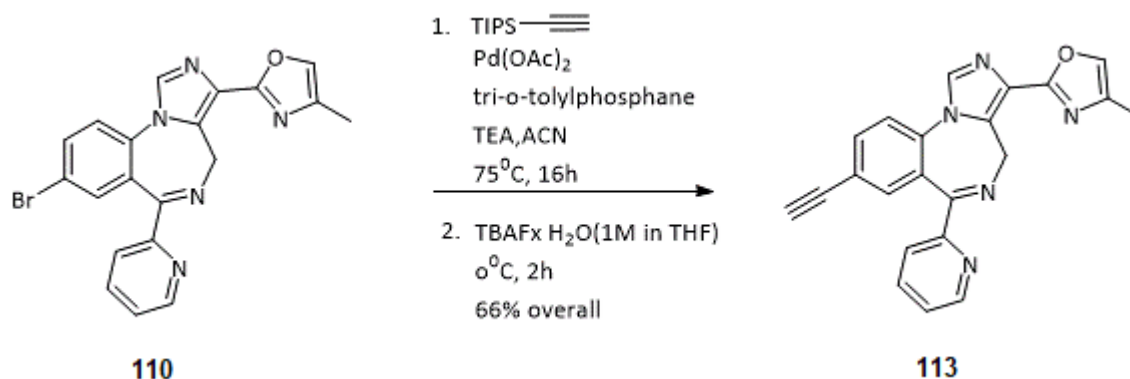
### 2.7.10 2-(8-bromo-6-(pyridin-2-yl)-4H-benzo[f]imidazo[1,5-a][1,4]diazepin-3-yl)-4-methyloxazole (110)



The hexachloroethane (2.4 g, 10.5 mmol) was dissolved in anhydrous acetonitrile (20 mL). The carboxamide **120** (1.5 g, 3.5 mmol) was dissolved in anhydrous acetonitrile (12 mL) and added to the above solution. After that, the triethylamine (2.1 g, 21.2 mmol) was added dropwise. Triphenylphosphine (2.76 g, 10.5 mmol) was then added to the above solution. The ice bath was

removed, and the reaction mixture was allowed to stir for 16 h at rt. The reaction progress was monitored by TLC (silica gel, EtOAc/hexane/ methanol 2:1:0.5 and a few drops of 14% aq. NH<sub>4</sub>OH). After completion of reaction, water (20 mL) was added. The aq layer was extracted with ethyl acetate (25 mL x 2). The combined organic layer was washed with brine (20 mL) and dried (Na<sub>2</sub>SO<sub>4</sub>). The solvents were removed under reduced pressure and the residue was purified by flash chromatography (silica gel, EtOAc/hexane 2:1, and 3% triethylamine) to afford oxazole **110** as a light yellow colored solid (1.02 g, 72%). A small amount of oxazole **110** crystallized in EtOH for a melting point (white needle shaped crystals). **m.p.** 238-240 °C. **<sup>1</sup>H NMR** (500 MHz, CDCl<sub>3</sub>) δ 8.58 (d, J = 4.5 Hz, 1H), 8.09 (d, J = 7.9 Hz, 1H), 7.95 (s, 1H), 7.80 (ddd, J = 10.8, 8.2, 1.7 Hz, 2H), 7.58 (d, J = 2.0 Hz, 1H), 7.50 (d, J = 8.6 Hz, 1H), 7.43 (s, 1H), 7.37 (dd, J = 7.0, 5.2 Hz, 1H), 6.17 (d, J = 11.4 Hz, 1H), 4.28 (d, J = 11.7 Hz, 1H), 2.26 (s, 3H). **<sup>13</sup>C NMR** (126 MHz, CDCl<sub>3</sub>) δ 167.1 (s), 156.8 (s), 156.4 (s), 148.7 (s), 137.4 (s), 136.9 (s), 135.4 (s), 134.9 (d, J = 16.5 Hz), 133.5 (s), 132.8 (s), 128.5 (s), 127.7 (s), 124.8 (s), 124.2 (s), 124.0 (s), 120.3 (s), 53.4 (s), 45.0 (s), 11.7 (s). **HRMS** (ESI/IT-TOF) m/z: [M + H]<sup>+</sup> Calcd for C<sub>20</sub>H<sub>14</sub>BrN<sub>5</sub>O 420.0454; found 420.0492.

2.7.11 2-(8-Ethynyl-6-(pyridin-2-yl)-4H-benzo[f]imidazo[1,5-a][1,4]diazepin-3-yl)-4-methyloxazole (113)



A mixture of palladium (II) acetate (7.8 mg, 0.04 mmol), tri-*o*-tolylphosphine (21.3 mg, 0.07 mmol) and anhydrous acetonitrile (10 mL) was allowed to stir at rt for 15 min. The bromide **110** (300 mg, 0.7 mmol), triisopropylsilylacetylene (153.2 mg, 0.84 mmol), triethylamine (213 mg, 2.1 mmol), and acetonitrile (10 mL) were added to the mixture. The reaction mixture was allowed to reflux at 75°C and monitored by TLC (silica gel, EtOAc/hexane/methanol 2:1:0.5 and a few drops of triethylamine). To complete the reaction, excess triisopropylsilylacetylene (63.8 mg, 0.35 mmol) was added in the reaction mixture. After 18 h the solvent was removed under reduced pressure and the residue was dissolved in CH<sub>2</sub>Cl<sub>2</sub> (25 mL) and filtered through a bed of celite. The filtrate was washed with brine (25 mL) and dried (Na<sub>2</sub>SO<sub>4</sub>). The solvent was removed under reduced pressure and the residue was passed through a short pad of silica gel (silica gel, EtOAc/hexanes 3:1 with 3% triethylamine) to afford a light yellow colored solid (320.2 mg, 86%), which was used for the next step without further purification. To the mixture of this solid (559 mg, 1.06

mmol), THF (20 mL) and water (0.1 mL), TBAF x H<sub>2</sub>O (0.25 g, 1.3 mmol, 1M in THF) was added dropwise at 0°C and the mixture was allowed to stir at rt for 1 h. Analysis by TLC (Silica gel, EtOAc/hexane/MeOH 2:1:0.5 and a few drops of 14% aq. NH<sub>4</sub>OH) indicated the disappearance of starting material. The reaction mixture was then quenched with water and diluted with EtOAc (30 mL). The organic layer was separated and washed with brine (20mL) and dried (Na<sub>2</sub>SO<sub>4</sub>). The solvents were removed under reduced pressure and the residue was purified using flash column chromatography (silica gel, EtOAc/hexane 2:1 and 3% triethylamine) to yield a light yellow colored solid, **113** (172.57 mg, 77%). **m.p.** 235-240 °C. **<sup>1</sup>H NMR** (500 MHz, CDCl<sub>3</sub>) δ<sub>H</sub> 8.59 (d, *J* = 3.5 Hz, 1H), 8.08 (d, *J* = 7.7 Hz, 1H), 7.98 (s, 1H), 7.84 – 7.74 (m, 2H), 7.59 (d, *J* = 8.2 Hz, 1H), 7.56 (s, 1H), 7.44 (s, 1H), 7.41 – 7.33 (m, 1H), 6.17 (s, 1H), 4.28 (s, 1H), 3.17 (s, 1H), 2.27 (s, 3H). **<sup>13</sup>C NMR** (126 MHz, CDCl<sub>3</sub>) δ<sub>C</sub> 167.7 (s), 156.7 (s), 148.8 (s), 137.4 (s), 136.8 (s), 136.3 (s), 135.8 (s), 135.3 (s), 134.9 (s), 133.5 (s), 132.8 (s), 127.7 – 127.6 (m), 127.1 (s), 124.7 (s), 124.0 (s), 122.8 (s), 120.9 (s), 81.8 (s), 79.3 (s), 45.0 (s), 11.7 (s).

## 2.8 Rotarod assay

The study was conducted by placing mice on a rotating rod for a maximum of 3 minutes after oral administration by gavage at a dose of 40 mg/kg including diazepam as the positive control (5 mg/kg), elicited the greatest impairment of sensorimotor steadiness at 10 minutes, followed by 30 and 60 minutes on the rotarod. The vehicle used for this test was 10 % DMSO, 50 % PBS, 40 % propylene glycol. If the compound was not soluble in vehicle, then it was subsequently

administered via oral gavage at 40 mg/kg in a vehicle of 2 % polyethylene glycol and 2.5 % hydroxypropyl methylcellulose solution.

### 3 Reference

1. Cordell, G. A.; Quinn-Beattie, M. L.; Farnsworth, N. R., The potential of alkaloids in drug discovery. *Phytother Res* **2001**, *15* (3), 183-205.
2. Mothes, K., Schütte, H. R., Luckner, M., Eds., *Alkaloids Derived from Tryptophan. In Biochemistry of Alkaloids*. VCH: Florida, 1985.
3. Taylor, W. I. M., R. H. F., Ed., The Ajmaline-Sarpagine Alkaloids. In *The Alkaloids: Chemistry and Physiology*, Academic Press: New York, 1965; Vol. VIII, pp 789-812.
4. Talapatra, S. K. C., N. A., *Sci. Cult. (Calcutta)*. **1958**, *24*, 243-245.
5. Isidro, N. M., G. D. J., *Philipp. Pharma. Assoc.* **1967**, *53*, 9-19.
6. Wright, C. W.; Allen, D.; Cai, Y.; Phillipson, J. D.; Said, I. M.; Kirby, G. C.; Warhurst, D. C., In vitro antiamoebic and antiplasmodial activities of alkaloids isolated from *Alstonia angustifolia* roots. *Phytotherapy Research* **1992**, *6* (3), 121-124.
7. Burke, D. E.; Cook, J. M.; Le Quesne, P. W., Biomimetic synthesis of the bisindole alkaloids villalstonine and alstonisidine. *Journal of the American Chemical Society* **1973**, *95* (2), 546-552.
8. Ghedira, K.; Zeches-Hanrot, M.; Richard, B.; Massiot, G.; Le Men-Olivier, L.; Sevenet, T.; Goh, S. H., Alkaloids of *Alstonia angustifolia*. *Phytochemistry* **1988**, *27* (12), 3955-3962.
9. Burke, D. E.; DeMarkey, C. A.; Le Quesne, P. W.; Cook, J. M., Biomimetic synthesis of the bis-indole alkaloid macralstonine. *Journal of the Chemical Society, Chemical Communications* **1972**, (24), 1346-1347.
10. Garnick, R. L.; Le Quesne, P. W., Biomimetic transformations among monomeric macroline-related indole alkaloids. *Journal of the American Chemical Society* **1978**, *100* (13), 4213-4219.
11. Keawpradub, N.; Eno-Amooquaye, E.; Burke, P. J.; Houghton, P. J., Cytotoxic Activity of Indole Alkaloids from *Alstonia macrophylla*. *Planta Med* **1999**, *65* (04), 311-315.

12. Keawpradub, N.; Kirby, G. C.; Steele, J. C. P.; Houghton, P. J., Antiplasmodial Activity of Extracts and Alkaloids of Three *Alstonia* Species from Thailand. *Planta Med* **1999**, *65* (08), 690-694.
13. Burkill, I. H., *A Dictionary of the Economic Products of the Malay Peninsular*. 1935; Vol. I (A-H), p 112-117.
14. Perry, L. M. M., J., *Medicinal Plants of East and Southeast Asia*. MIT Press: Cambridge, 1980.
15. Feng, Y. G., H.; Zeng, G., Comparison of the effects of spegatrine and dispegatrine on  $\alpha$ -adrenoceptors. *Yaoxue. Xuebao*. **1986**, *21*, 1-6.
16. Lin, M. Y., B.; Yu, D., Studies on the quaternary alkaloids of *Rauvolfia verticillata* (lour.) Baill var. *Hainanensis* Tsiang. *Yaoxue. Xuebao*. **1986**, *21*, 114-118.
17. Elderfield, R. C., Australian trees and high blood pressure. *American Scientist* **1960**, *48* (2), 193-208.
18. Hesse, M.; Bodmer, F.; Gemenden, C. W.; Joshi, B. S.; Taylor, W. I.; Schmid, H., Die Struktur des *Alstonia*-Alkaloides Villalstonin. *Helvetica Chimica Acta* **1966**, *49* (3), 1173-1182.
19. Hesse, M.; Huerzeler, H.; Gemenden, C. W.; Joshi, B. S.; Taylor, W. I.; Schmid, H., The structure of the *alstonia* alkaloid villalstonon. *Helv Chim Acta* **1965**, *48*, 689-704.
20. Edwankar, C. R.; Edwankar, R. V.; Rallapalli, S.; Cook, J. M., General Approach to the Total Synthesis of Macroline-Related Sarpagine and Ajmaline Alkaloids<sup>1</sup>. *Natural Product Communications* **2008**, *3* (11), 1934578X0800301114.
21. Esmond, R. W.; Le Quesne, P. W., Biomimetic synthesis of macroline. *Journal of the American Chemical Society* **1980**, *102* (23), 7116-7117.
22. Garnick, R. L. L., P. W. Studies on the Chemistry of Indole Alkaloids. Ph.D. Thesis. Northeastern University, 1977.

23. Edwankar, R. V. The first enantiospecific, stereospecific total synthesis of the C-19 methyl substituted sarpagine indole alkaloids 19(S), 20(R)-dihydroperaksine, 19(S), 20-(R)-dihydroperaksine-17-al and peraksine. University of Wisconsin Milwaukee, Milwaukee, WI, USA, 2010.
24. Hava, M., *The Vinca Alkaloids*. Marcel Dekker: New York, 1973.
25. Svoboda, G. H. B., D. A., *The Catharanthus Alkaloids*. Marcel Dekker: New York, 1974.
26. Gui, L.; Xin, L.; Xiao-zhang, F., Ervayunine: A New Indole Alkaloid from *Ervatamia yunnanensis*. *Planta Med* **1988**, *54* (06), 519-521.
27. Keawpradub, N.; Houghton, P. J., Indole alkaloids from *Alstonia macrophylla*. *Phytochemistry* **1997**, *46* (4), 757-762.
28. Leclercq, J.; De Pauw-Gillet, M.-C.; Bassleer, R.; Angenot, L., Screening of cytotoxic activities of *Strychnos* alkaloids (methods and results). *Journal of Ethnopharmacology* **1986**, *15* (3), 305-316.
29. Tan, G. T.; Miller, J. F.; Kinghorn, A. D.; Hughes, S. H.; Pezzuto, J. M., HIV-1 and HIV-2 reverse transcriptases: A comparative study of sensitivity to inhibition by selected natural products. *Biochemical and Biophysical Research Communications* **1992**, *185* (1), 370-378.
30. Verpoorte, R.; Bohlin, L.; Dwuna-Badu, D.; Rolfsen, W.; Strömbom, J., 11-Methoxy-Macusine A. A New Quaternary Alkaloid from *Strychnos angolensis*. *Journal of Natural Products* **1983**, *46* (4), 572-575.
31. Le Men, J.; Taylor, W. I., A uniform numbering system for indole alkaloids. *Experientia* **1965**, *21* (9), 508-510.
32. Lounasmaa, M. H., P.; Westersund, M., The Sarpagine Group of Indole Alkaloids. In *The Alkaloids*, Cordell, G., Ed. Academic Press: San Diego, CA, 1999; Vol. 52, pp 103-195.
33. Lounasmaa, M.; Hanhinen, P., Interpretation of the Formation of Nine "Artifact Indole Alkaloids" in the Ajmaline/Sarpagine Series. *Journal of Natural Products* **2000**, *63* (10), 1456-1460.
34. Sheludko, Y.; Gerasimenko, I.; Kolshorn, H.; Stöckigt, J., New Alkaloids of the Sarpagine Group from *Rauvolfia serpentina* Hairy Root Culture. *Journal of Natural Products* **2002**, *65* (7), 1006-1010.

35. Akinloye, B. A.; Court, W. E., Stem Bark Alkaloids of *Rauwolfia volkensii*. *Planta Med* **1979**, *37* (12), 361-366.
36. Pillay, P. P.; Rao, D. S.; Rao, S. B., Chemical investigation of *Rauwolfia micrantha* Hook f. *Journal of Scientific and Industrial Research, Section B. Physical Sciences* **1960**, 135-7.
37. Martinez, J. A.; Gomez, C.; Santana, T.; Velez, H., Alkaloids from *Rauwolfia cubana* Stem Bark. *Planta Med* **1989**, *55* (03), 283-285.
38. Itoh, A.; Kumashiro, T.; Yamaguchi, M.; Nagakura, N.; Mizushima, Y.; Nishi, T.; Tanahashi, T., Indole Alkaloids and Other Constituents of *Rauwolfia serpentina*. *Journal of Natural Products* **2005**, *68* (6), 848-852.
39. Aginiwa, J. S., S.; Kubo, A.; Hamamoto, T., Alkaloids of *Gardneria nutans* Sieb. et Zucc. *Yakugaku Zasshi* **1967**, *87*, 1484-1488.
40. Naranjo, J.; Pinar, M.; Hesse, M.; Schmid, H., Über die Indolalkaloide von *Pleiocarpa talbotii* Wernham. 145. Mitteilung über Alkaloide. *Helvetica Chimica Acta* **1972**, *55* (3), 752-771.
41. Monnerat, C. S.; Souza, J. J. d.; Mathias, L.; Braz-Filho, R.; Vieira, I. J. C., A new indole alkaloid isolated from *Tabernaemontana hystrix* steud (Apocynaceae). *Journal of the Brazilian Chemical Society* **2005**, *16*, 1331-1335.
42. Wan, A. S. C. Y., M.; Ogata, K.; Aimi, N.; Sakai, S, Structure of Pelirine and Chemical Conversion of Gardnerine to 11-Methoxy-16-epiaffinine. *Heterocycles* **1987**, *26*, 1211-1214.
43. Cava, M. P. T., S. K.; Weisbach, J. A.; Douglas, B.; Raffauf, R. F.;; Ribeiro, O., *Chem. Ind. (London)* **1964**, *26*, 1193-1194.
44. Kogure, N.; Nishiya, C.; Kitajima, M.; Takayama, H., Six new indole alkaloids from *Gelsemium sempervirens* Ait. f. *Tetrahedron Letters* **2005**, *46* (35), 5857-5861.
45. Rahman, M. T. Shorter and improved access to the key tetracyclic core of C-19 methyl substituted bioactive sarpagine-macroline-ajmaline indole alkaloids via a new ambidextrous asymmetric Pictet-

Spengler reaction beginning from either D-(+)- or L(-)-tryptophan. University of Wisconsin Milwaukee, Milwaukee, WI, 2018.

46. Zhan, G.; Miao, R.; Zhang, F.; Hao, X.; Zheng, X.; Zhang, H.; Zhang, X.; Guo, Z., Monoterpene indole alkaloids with diverse skeletons from the stems of *Rauvolfia vomitoria* and their acetylcholinesterase inhibitory activities. *Phytochemistry* **2020**, *177*, 112450.
47. Forgacs, P.; Jehanno, A.; Provost, J.; Thal, C.; Guilhem, J.; Pascard, C.; Moretti, C., An indole alkaloid from *Strychnos erichsonii*. *Phytochemistry* **1986**, *25* (4), 969-971.
48. Bert, M. B., G.; Tillequin, F.; Koch, M., Pagicerine — A New Indole Alkaloid from *Pagantha derifera* (Pancher et Sébert) Markgraf (Apocynaceae). *Heterocycles* **1985**, *23*, 2505-2508.
49. Hu, X.-J.; He, H.-P.; Zhou, H.; Di, Y.-T.; Yang, X.-W.; Hao, X.-J.; Kong, L.-Y., New Indole Alkaloids from *Rauvolfia yunnanensis*. *Helvetica Chimica Acta* **2006**, *89* (7), 1344-1350.
50. Bert, M. B., G.; Tillequin, F.; Koch, M., Pagisulfine — The First Sulfur-containing Indole-monoterpene Alkaloid. *Heterocycles* **1986**, *24*, 1567-1570.
51. Hamaker, L. K. C., J. M., *Alkaloids: Chemical and Biological Perspectives*. Elsevier Science: New York, 1995; Vol. 9.
52. Rahman, M. T.; Tiruveedhula, V. V. N. P. B.; Cook, J. M., Synthesis of Bisindole Alkaloids from the Apocynaceae Which Contain a Macroline or Sarpagine Unit: A Review. *Molecules* **2016**, *21* (11), 1525.
53. Namjoshi, O. A. C., J. M., In *The Alkaloids: Chemistry and Biology*, Kn€olker, H.-J., Ed. Academic Press: San Diego, CA, 2016; Vol. 76, p 63.
54. Edwankar, C. R.; Edwankar, R. V.; Namjoshi, O. A.; Rallapalli, S. K.; Yang, J.; Cook, J. M., Recent progress in the total synthesis of indole alkaloids. *Curr Opin Drug Discov Devel* **2009**, *12* (6), 752-771.
55. Fonseca, G. O.; Cook, J. M., Modern Methods for Total Synthesis of Important Oxindole Alkaloids. *Organic Chemistry Insights* **2016**, (6), 1-55.

56. Hobson, J. D.; Raines, J.; Whiteoak, R. J., 656. Synthetical approaches to alkaloids of the sarpagine and ajmaline groups. Part I. The preparation of some tetracyclic intermediates. *Journal of the Chemical Society (Resumed)* **1963**, (0), 3495-3503.
57. Yoneda, N., Synthesis of 12-Methyl-1, 2, 3, 4, 6, 7, 12, 12b-octahydro-2, 6-methanoindolo[2, 3-a]quinolizine. *Chem. Pharm. Bull.* **1965**, *13* (5), 622-625.
58. Cloudsdale, I. S.; Kluge, A. F.; McClure, N. L., Synthetic studies in the ajmaline series. *The Journal of Organic Chemistry* **1982**, *47* (6), 919-928.
59. Mashimo, K.; Sato, Y., On the synthesis of ajmaline. *Tetrahedron Letters* **1969**, *10* (11), 905-906.
60. Soerens, D.; Sandrin, J.; Ungemach, F.; Mokry, P.; Wu, G. S.; Yamanaka, E.; Hutchins, L.; DiPierro, M.; Cook, J. M., Study of the Pictet-Spengler reaction in aprotic media: synthesis of the .beta.-galactosidase inhibitor, pyridindolol. *The Journal of Organic Chemistry* **1979**, *44* (4), 535-545.
61. Shimizu, M.; Ishikawa, M.; Komoda, Y.; Nakajima, T.; Yamaguchi, K.; Sakai, S., Asymmetric Synthesis and Absolute Configuration of (-)-Trypargine. *Chemical and Pharmaceutical Bulletin* **1984**, *32* (4), 1313-1325.
62. Zhang, L.-h. C., J. M., Pictet-Spengler reactions in aprotic media. N<sub>b</sub>-benzyl promoted retention of optical activity in the synthesis of an indole substituted azabicyclo[3.3.1]nonane, a key template for the synthesis of macroline alkaloids. *Heterocycles* **1988**, *27*, 2795-2802.
63. Bailey, P. D.; Hollinshead, S. P.; McLay, N. R.; Morgan, K.; Palmer, S. J.; Prince, S. N.; Reynolds, C. D.; Wood, S. D., Diastereo- and enantio-selectivity in the Pictet-Spengler reaction. *Journal of the Chemical Society, Perkin Transactions 1* **1993**, (4), 431-439.
64. Sandrin, J.; Hollinshead, S. P.; Cook, J. M., Pictet-Spengler reactions in aprotic media. Stereospecificity in the Pictet-Spengler reaction. *The Journal of Organic Chemistry* **1989**, *54* (23), 5636-5640.

65. Ungemach, F.; DiPierro, M.; Weber, R.; Cook, J. M., Stereospecific synthesis of trans-1,3-disubstituted-1,2,3,4-tetrahydro- $\beta$ -carbolines. *The Journal of Organic Chemistry* **1981**, *46* (1), 164-168.
66. Rahman, M. T.; Namjoshi, O. A.; Cook, J. M., The stereospecific and enantiospecific synthesis of indole alkaloids which culminated in the ambidextrous Pictet–Spengler reaction for the C-19 methyl-substituted sarpagine family. In *Progress in Heterocyclic Chemistry*, Gribble, G. W.; Joule, J. A., Eds. Elsevier: 2021; Vol. 32, pp 1-26.
67. Li, J. Enantiospecific total synthesis of (+)-ajmaline and alkaloid G as well as studies directed toward the synthesis of 19-Hydroxy-N<sub>6</sub>-methylraumacline via the asymmetric Pictet-Spengler reaction. University of Wisconsin-Milwaukee, Milwaukee, WI, 1999.
68. Rakhimov, D. A.; Sharipov, M. R.; Aripov, K. N.; Malikov, V. M.; Shakirov, T. T.; Yunusov, S. Y., The polybuffer separation of the alkaloids of *Vinca erecta*. *Chemistry of Natural Compounds* **1970**, *6* (6), 724-727.
69. Rallapalli, S. K.; Namjoshi, O. A.; Tiruveedhula, V. V. N. P. B.; Deschamps, J. R.; Cook, J. M., Stereospecific Total Synthesis of the Indole Alkaloid Ervincidine. Establishment of the C-6 Hydroxyl Stereochemistry. *The Journal of Organic Chemistry* **2014**, *79* (9), 3776-3780.
70. Fonseca, G. O.; Wang, Z.-J.; Namjoshi, O. A.; Deschamps, J. R.; Cook, J. M., First stereospecific total synthesis of (-)-affinisine oxindole as well as facile entry into the C(7)-diastereomeric chitosenine stereochemistry. *Tetrahedron Letters* **2015**, *56* (23), 3052-3056.
71. Stephen, M. R.; Rahman, M. T.; Tiruveedhula, V.; Fonseca, G. O.; Deschamps, J. R.; Cook, J. M., Concise Total Synthesis of (-)-Affinisine Oxindole, (+)-Isoalstonisine, (+)-Alstofoline, (-)-Macrogentine, (+)-N(a)-Demethylalstonisine, (-)-Alstonoxine A, and (+)-Alstonisine. *Chemistry* **2017**, *23* (62), 15805-15819.

72. Rahman, M. T.; Deschamps, J. R.; Imler, G. H.; Schwabacher, A. W.; Cook, J. M., Total Synthesis of Macroparpines D and E via an Enolate-Driven Copper-Mediated Cross-Coupling Process: Replacement of Catalytic Palladium with Copper Iodide. *Organic Letters* **2016**, *18* (17), 4174-4177.
73. Rahman, M. T.; Cook, J. M., Unprecedented Stereocontrol in the Synthesis of 1,2,3-Trisubstituted Tetrahydro- $\beta$ -carbolines through an Asymmetric Pictet–Spengler Reaction towards Sarpagine-Type Indole Alkaloids. *European Journal of Organic Chemistry* **2018**, *2018* (24), 3224-3229.
74. Verpoorte, R., In *Alkaloids: Biochemistry, Ecology and Medicinal Applications*, Roberts, M. F. W., M., Ed. Plenum Press: New York, 1998.
75. Vieira, I. J.; Medeiros, W. L.; Monnerat, C. S.; Souza, J. J.; Mathias, L.; Braz-Filho, R.; Pinto, A. C.; Sousa, P. M.; Rezende, C. M.; Epifanio Rde, A., Two fast screening methods (GC-MS and TLC-ChEI assay) for rapid evaluation of potential anticholinesterasic indole alkaloids in complex mixtures. *An Acad Bras Cienc* **2008**, *80* (3), 419-26.
76. Giacobini, E., Cholinesterase inhibitors: new roles and therapeutic alternatives. *Pharmacological Research* **2004**, *50* (4), 433-440.
77. Struwe, L.; Albert, V. A.; Bremer, B., Cladistics and Family Level Classification of the Gentianales. *Cladistics* **1994**, *10* (2), 175-206.
78. Ornduff, R., The systematics and breeding system of Gelsemium (Loganiaceae). *Journal of the Arnold Arboretum* **1970**, *51* (1), 1-17.
79. Wyatt, R.; Broyles, S. B.; Hamrick, J. L.; Stoneburner, A., Systematic Relationships Within Gelsemium (Loganiaceae): Evidence from Isozymes and Cladistics. *Systematic Botany* **1993**, *18* (2), 345-355.
80. Wu, Z. R., P. H.; Garden, M. B., *Flora of China*. Beijing and Missouri botanical garden press: 1996; Vol. 15.

81. administration, E. c. o. Z. B. n. t. C. h., Shanghai science and technology publishing house: Shanghai, 1999.
82. Jin, G.-L.; Su, Y.-P.; Liu, M.; Xu, Y.; Yang, J.; Liao, K.-J.; Yu, C.-X., Medicinal plants of the genus *Gelsemium* (Gelsemiaceae, Gentianales)—A review of their phytochemistry, pharmacology, toxicology and traditional use. *Journal of Ethnopharmacology* **2014**, *152* (1), 33-52.
83. Yu, P.; Wang, T.; Li, J.; Cook, J. M., Enantiospecific Total Synthesis of the Sarpagine Related Indole Alkaloids Talpinine and Talcarpine as Well as the Improved Total Synthesis of Alstonerine and Anhydromacrosalpine-methine via the Asymmetric Pictet–Spengler Reaction. *The Journal of Organic Chemistry* **2000**, *65* (10), 3173-3191.
84. Lorenz, M.; L. Van Linn, M.; M. Cook, J., The Asymmetric Pictet-Spengler Reaction. *Current Organic Synthesis* **2010**, *7* (3), 189-223.
85. Van Linn, M. L.; Cook, J. M., Mechanistic Studies on the Cis to Trans Epimerization of Trisubstituted 1,2,3,4-Tetrahydro- $\beta$ -carbolines. *The Journal of Organic Chemistry* **2010**, *75* (11), 3587-3599.
86. Cox, E. D.; Cook, J. M., The Pictet-Spengler condensation: a new direction for an old reaction. *Chemical Reviews* **1995**, *95* (6), 1797-1842.
87. Czerwinski, K. C., J. M., Stereochemical control of the Pictet-Spengler reaction in the synthesis of natural products. JAI Press: Greenwich, 1996; Vol. 3.
88. Han, D.; Försterling, F. H.; Deschamps, J. R.; Parrish, D.; Liu, X.; Yin, W.; Huang, S.; Cook, J. M., Conformational Analysis of the cis- and trans-Adducts of the Pictet–Spengler Reaction. Evidence for the Structural Basis for the C(1)–N(2) Scission Process in the cis- to trans-Isomerization. *Journal of Natural Products* **2007**, *70* (1), 75-82.
89. Kumpaty, H. J.; Van Linn, M. L.; Kabir, M. S.; Försterling, F. H.; Deschamps, J. R.; Cook, J. M., Study of the Cis to Trans Isomerization of 1-Phenyl-2,3-disubstituted Tetrahydro- $\beta$ -carbolines at C(1).

Evidence for the Carbocation-Mediated Mechanism. *The Journal of Organic Chemistry* **2009**, *74* (7), 2771-2779.

90. Yang, J.; Rallapalli, S. K.; Cook, J. M., The first enantiospecific total synthesis of the 3-oxygenated sarpagine indole alkaloids affinine and 16-epiaffinine, as well as vobasinediol and 16-epivobasinediol. *Tetrahedron Letters* **2010**, *51* (5), 815-817.

91. Wang, T.; Cook, J. M., General Approach for the Synthesis of Sarpagine/Ajmaline Indole Alkaloids. Stereospecific Total Synthesis of the Sarpagine Alkaloid (+)-Velloimine. *Organic Letters* **2000**, *2* (14), 2057-2059.

92. Zhao, S.; Liao, X.; Wang, T.; Flippen-Anderson, J.; Cook, J. M., The Enantiospecific, Stereospecific Total Synthesis of the Ring-A Oxygenated Sarpagine Indole Alkaloids (+)-Majvinine, (+)-10-Methoxyaffinisine, and (+)-Na-Methylsarpagine, as Well as the Total Synthesis of the Alstonia Bisindole Alkaloid Macralstonidine. *The Journal of Organic Chemistry* **2003**, *68* (16), 6279-6295.

93. Krafft, M. E.; Cran, J. W., A Convenient Protocol for the  $\alpha$ -Iodination of  $\alpha,\beta$ -Unsaturated Carbonyl Compounds with I<sub>2</sub> in an Aqueous Medium. *Synlett* **2005**, *2005* (08), 1263-1266.

94. Cook, J. M.; Le Quesne, P. W.; Elderfield, R. C., Alstonerine, a new indole alkaloid from *Alstonia muelleriana*. *Journal of the Chemical Society D: Chemical Communications* **1969**, (22), 1306-1307.

95. Schill, G.; Priester, C. U.; Windhovel, U. F.; Fritz, H., Eine neue synthese von vinblastin-derivaten v. konzept und untersuchungen zur synthese von 20'-desethyl-20'-desoxy- c'-homovinblastin—octahydro-3H-azecino[5,4-b]indol-derivate. *Tetrahedron* **1990**, *46* (4), 1211-1220.

96. Bonjoch, J.; Fernàndez, J.-C.; Valls, N., Total Syntheses of ( $\pm$ )-Deethylbophyllidine Using a Crisscross Annulation: Ring Cleavage of Octahydroindolo[2,3-a]quinolizines Followed by Tandem Cyclizations of Octahydroazecino[5,4-b]indoles. *The Journal of Organic Chemistry* **1998**, *63* (21), 7338-7347.

97. Ohkuma, T.; Kitamura, M.; Noyori, R., Enantioselective synthesis of 4-substituted  $\gamma$ -lactones. *Tetrahedron Letters* **1990**, *31* (38), 5509-5512.
98. Ensley, H. E.; Buescher, R. R.; Lee, K., Reaction of organotin hydrides with acetylenic alcohols. *The Journal of Organic Chemistry* **1982**, *47* (3), 404-408.
99. Kuehne, M. E.; Wang, T.; Seraphin, D., Syntheses of Strychnos and Aspidospermatan-Type Alkaloids. 8. Selective Total Syntheses of Mossambine and 14-epi-Mossambine by a Radical Cyclization Reaction1. *The Journal of Organic Chemistry* **1996**, *61* (22), 7873-7881.
100. Pfitzner, A.; Stöckigt, J., Characterization of Polyneuridine Aldehyde Esterase, a Key Enzyme in the Biosynthesis of Sarpagine/Ajmaline Type Alkaloids. *Planta Med* **1983**, *48* (08), 221-227.
101. Siegel GJ, A. B., Albers RW, et al., *Basic Neurochemistry: Molecular, Cellular and Medical Aspects*. 6th ed.; Philadelphia, 1999.
102. Sparling, B. A.; DiMauro, E. F., Progress in the discovery of small molecule modulators of the Cys-loop superfamily receptors. *Bioorg Med Chem Lett* **2017**, *27* (15), 3207-3218.
103. Lorenz-Guertin, J. M.; Jacob, T. C., GABA type a receptor trafficking and the architecture of synaptic inhibition. *Developmental Neurobiology* **2018**, *78* (3), 238-270.
104. Hyland, N. P.; Cryan, J. F., A Gut Feeling about GABA: Focus on GABA(B) Receptors. *Front Pharmacol* **2010**, *1*, 124.
105. Kaila, K.; Price, T. J.; Payne, J. A.; Puskarjov, M.; Voipio, J., Cation-chloride cotransporters in neuronal development, plasticity and disease. *Nat Rev Neurosci* **2014**, *15* (10), 637-54.
106. Alexander, S. P. K., E.; Marrion, N. V.; Peters, J. A.; Faccenda, E.; Harding, S. D.; Pawson, A. J.; Sharman, J. L.; Southan, C.; Buneman, O. P.; Cidlowski, J. A.; Christopoulos, A.; Davenport, A. P.; Fabbro, D.; Spedding, M.; Striessnig, J.; Davies, J. A., The concise guide to pharmacology, 2017/18: Overview. *Br J Pharmacol* **2017**, *174 Suppl 1* (Suppl Suppl 1), S1-s16.

107. Chen, Z. W.; Olsen, R. W., GABAA receptor associated proteins: a key factor regulating GABAA receptor function. *J Neurochem* **2007**, *100* (2), 279-94.
108. Watanabe, M.; Maemura, K.; Kanbara, K.; Tamayama, T.; Hayasaki, H., GABA and GABA receptors in the central nervous system and other organs. *Int Rev Cytol* **2002**, *213*, 1-47.
109. Sieghart, W.; Sperk, G., Subunit composition, distribution and function of GABA(A) receptor subtypes. *Curr Top Med Chem* **2002**, *2* (8), 795-816.
110. Sieghart, W.; Ernst, M., Heterogeneity of GABAA Receptors: Revived Interest in the Development of Subtype-selective Drugs. *Current Medicinal Chemistry - Central Nervous System Agents* **2005**, *5* (3), 217-242.
111. Clayton, T.; Chen, J. L.; Ernst, M.; Richter, L.; Cromer, B. A.; Morton, C. J.; Ng, H.; Kaczorowski, C. C.; Helmstetter, F. J.; Furtmüller, R.; Ecker, G.; Parker, M. W.; Sieghart, W.; Cook, J. M., An updated unified pharmacophore model of the benzodiazepine binding site on gamma-aminobutyric acid(a) receptors: correlation with comparative models. *Curr Med Chem* **2007**, *14* (26), 2755-75.
112. Chiou, L.-C.; Tzeng, H.-R.; Fan, P.-C.; Sieghart, W.; Ernst, M.; Knutson, D. E.; Cook, J., A Novel Drug Target for Migraine: The GABAA Receptor  $\alpha 6$  Subtype in Trigeminal Ganglia. *The FASEB Journal* **2019**, *33* (S1), lb78-lb78.
113. Knutson, D. E.; Kodali, R.; Divović, B.; Treven, M.; Stephen, M. R.; Zahn, N. M.; Dobričić, V.; Huber, A. T.; Meirelles, M. A.; Verma, R. S.; Wimmer, L.; Witzigmann, C.; Arnold, L. A.; Chiou, L. C.; Ernst, M.; Mihovilovic, M. D.; Savić, M. M.; Sieghart, W.; Cook, J. M., Design and Synthesis of Novel Deuterated Ligands Functionally Selective for the  $\gamma$ -Aminobutyric Acid Type A Receptor (GABA(A)R)  $\alpha 6$  Subtype with Improved Metabolic Stability and Enhanced Bioavailability. *J Med Chem* **2018**, *61* (6), 2422-2446.

114. Maramai, S.; Benchekroun, M.; Ward, S. E.; Atack, J. R., Subtype Selective  $\gamma$ -Aminobutyric Acid Type A Receptor (GABA(A)R) Modulators Acting at the Benzodiazepine Binding Site: An Update. *J Med Chem* **2020**, *63* (7), 3425-3446.
115. Zhu, S.; Noviello, C. M.; Teng, J.; Walsh, R. M., Jr.; Kim, J. J.; Hibbs, R. E., Structure of a human synaptic GABA(A) receptor. *Nature* **2018**, *559* (7712), 67-72.
116. Sieghart, W., Structure and pharmacology of gamma-aminobutyric acidA receptor subtypes. *Pharmacol Rev* **1995**, *47* (2), 181-234.
117. Nutt, D., GABAA receptors: subtypes, regional distribution, and function. *J Clin Sleep Med* **2006**, *2* (2), S7-11.
118. Olsen, R. W.; Hancher, H. J.; Meera, P.; Wallner, M., GABAA receptor subtypes: the "one glass of wine" receptors. *Alcohol* **2007**, *41* (3), 201-9.
119. Sawyer, E. K.; Moran, C.; Sirbu, M. H.; Szafir, M.; Van Linn, M.; Namjoshi, O.; Phani Babu Tiruveedhula, V. V.; Cook, J. M.; Platt, D. M., Little evidence of a role for the  $\alpha$ 1GABAA subunit-containing receptor in a rhesus monkey model of alcohol drinking. *Alcohol Clin Exp Res* **2014**, *38* (4), 1108-17.
120. Barnard, E. A.; Skolnick, P.; Olsen, R. W.; Mohler, H.; Sieghart, W.; Biggio, G.; Braestrup, C.; Bateson, A. N.; Langer, S. Z., International Union of Pharmacology. XV. Subtypes of gamma-aminobutyric acidA receptors: classification on the basis of subunit structure and receptor function. *Pharmacol Rev* **1998**, *50* (2), 291-313.
121. Engin, E.; Benham, R. S.; Rudolph, U., An Emerging Circuit Pharmacology of GABA(A) Receptors. *Trends Pharmacol Sci* **2018**, *39* (8), 710-732.
122. Fritschy, J. M.; Mohler, H., GABAA-receptor heterogeneity in the adult rat brain: differential regional and cellular distribution of seven major subunits. *J Comp Neurol* **1995**, *359* (1), 154-94.

123. Li, G. Design and synthesis of achiral and chiral imidazodiazepine (IMDZ) GABA(A)R subtype selective ligands for the treatment of CNS disorders as well as asthma. University of Wisconsin Milwaukee, 2019.
124. Pirker, S.; Schwarzer, C.; Wieselthaler, A.; Sieghart, W.; Sperk, G., GABA(A) receptors: immunocytochemical distribution of 13 subunits in the adult rat brain. *Neuroscience* **2000**, *101* (4), 815-50.
125. Lavery, D.; Desai, R.; Uchański, T.; Masiulis, S.; Stec, W. J.; Malinauskas, T.; Zivanov, J.; Pardon, E.; Steyaert, J.; Miller, K. W.; Aricescu, A. R., Cryo-EM structure of the human  $\alpha 1\beta 3\gamma 2$  GABA(A) receptor in a lipid bilayer. *Nature* **2019**, *565* (7740), 516-520.
126. Masiulis, S.; Desai, R.; Uchański, T.; Serna Martin, I.; Lavery, D.; Karia, D.; Malinauskas, T.; Zivanov, J.; Pardon, E.; Kotecha, A.; Steyaert, J.; Miller, K. W.; Aricescu, A. R., GABA(A) receptor signalling mechanisms revealed by structural pharmacology. *Nature* **2019**, *565* (7740), 454-459.
127. Hillestad, L.; Hansen, T.; Melsom, H.; Drivenes, A., Diazepam metabolism in normal man. I. Serum concentrations and clinical effects after intravenous, intramuscular, and oral administration. *Clin Pharmacol Ther* **1974**, *16* (3), 479-84.
128. Haefely, W., The biological basis of benzodiazepine actions. *J Psychoactive Drugs* **1983**, *15* (1-2), 19-39.
129. Stevenson, I. H.; Browning, M.; Crooks, J.; O'Malley, K., Changes in human drug metabolism after long-term exposure to hypnotics. *Br Med J* **1972**, *4* (5836), 322-4.
130. Garattini, S. M., E.; Marucci, F.; Guaitani, A., Metabolic studies on benzodiazepines in various animal species. In *The Benzodiazepines*, Eds. Raven Press: New York, 1973; pp pp 75-97.
131. Haefely, W.; Facklam, M.; Schoch, P.; Martin, J. R.; Bonetti, E. P.; Moreau, J. L.; Jenck, F.; Richards, J. G., Partial agonists of benzodiazepine receptors for the treatment of epilepsy, sleep, and anxiety disorders. *Adv Biochem Psychopharmacol* **1992**, *47*, 379-394.

132. Sternbach, L. H., The benzodiazepine story. *Journal of Medicinal Chemistry* **1979**, *22* (1), 1-7.
133. Study, R. E.; Barker, J. L., Diazepam and (–)-pentobarbital: fluctuation analysis reveals different mechanisms for potentiation of gamma-aminobutyric acid responses in cultured central neurons. *Proc Natl Acad Sci U S A* **1981**, *78* (11), 7180-4.
134. MacDonald, R. L., Benzodiazepine mechanisms of action. In *Antiepileptic Drugs*, Levy, R. H. M., R. H.; Meldrum, B. S.; Perucca, E., Ed. Lippincott Williams and Wilkins: Philadelphia, 2002; pp 179-186.
135. Killam, E. K. S., A., Benzodiazepines. In *Antiepileptic Drugs: Mechanisms of Action*, Glaser, G. H. P., J. K.; Woodbury, D. M., Ed. Raven Press: New York, 1980; pp 597-615.
136. Rogawski, M. A., Principles of antiepileptic drug action. In *Antiepileptic Drugs*, 5th ed.; Levy, R. H. M., R. H.; Meldrum, B. S.; Perucca, E., Ed. Lippincott Williams and Wilkins: Philadelphia, 2002; pp 3-22.
137. Rudolph, U.; Crestani, F.; Benke, D.; Brünig, I.; Benson, J. A.; Fritschy, J. M.; Martin, J. R.; Bluethmann, H.; Möhler, H., Benzodiazepine actions mediated by specific gamma-aminobutyric acid(A) receptor subtypes. *Nature* **1999**, *401* (6755), 796-800.
138. Collinson, N.; Kuenzi, F. M.; Jarolimek, W.; Maubach, K. A.; Cothliff, R.; Sur, C.; Smith, A.; Otu, F. M.; Howell, O.; Atack, J. R.; McKernan, R. M.; Seabrook, G. R.; Dawson, G. R.; Whiting, P. J.; Rosahl, T. W., Enhanced learning and memory and altered GABAergic synaptic transmission in mice lacking the alpha 5 subunit of the GABAA receptor. *J Neurosci* **2002**, *22* (13), 5572-80.
139. Paul, J.; Yévenes, G. E.; Benke, D.; Lio, A. D.; Ralvenius, W. T.; Witschi, R.; Scheurer, L.; Cook, J. M.; Rudolph, U.; Fritschy, J.-M.; Zeilhofer, H. U., Antihyperalgesia by  $\alpha 2$ -GABAA Receptors Occurs Via a Genuine Spinal Action and Does Not Involve Supraspinal Sites. *Neuropsychopharmacology* **2014**, *39* (2), 477-487.
140. McKernan, R. M.; Rosahl, T. W.; Reynolds, D. S.; Sur, C.; Wafford, K. A.; Atack, J. R.; Farrar, S.; Myers, J.; Cook, G.; Ferris, P.; Garrett, L.; Bristow, L.; Marshall, G.; Macaulay, A.; Brown, N.; Howell, O.; Moore, K. W.; Carling, R. W.; Street, L. J.; Castro, J. L.; Ragan, C. I.; Dawson, G. R.; Whiting, P. J.,

Sedative but not anxiolytic properties of benzodiazepines are mediated by the GABA(A) receptor alpha1 subtype. *Nat Neurosci* **2000**, 3 (6), 587-92.

141. Morris, H. V.; Dawson, G. R.; Reynolds, D. S.; Atack, J. R.; Stephens, D. N., Both alpha2 and alpha3 GABAA receptor subtypes mediate the anxiolytic properties of benzodiazepine site ligands in the conditioned emotional response paradigm. *Eur J Neurosci* **2006**, 23 (9), 2495-504.

142. Dias, R.; Sheppard, W. F.; Fradley, R. L.; Garrett, E. M.; Stanley, J. L.; Tye, S. J.; Goodacre, S.; Lincoln, R. J.; Cook, S. M.; Conley, R.; Hallett, D.; Humphries, A. C.; Thompson, S. A.; Wafford, K. A.; Street, L. J.; Castro, J. L.; Whiting, P. J.; Rosahl, T. W.; Atack, J. R.; McKernan, R. M.; Dawson, G. R.; Reynolds, D. S., Evidence for a significant role of alpha 3-containing GABAA receptors in mediating the anxiolytic effects of benzodiazepines. *J Neurosci* **2005**, 25 (46), 10682-8.

143. Yee, B. K.; Keist, R.; von Boehmer, L.; Studer, R.; Benke, D.; Hagenbuch, N.; Dong, Y.; Malenka, R. C.; Fritschy, J.-M.; Bluethmann, H.; Feldon, J.; Möhler, H.; Rudolph, U., A schizophrenia-related sensorimotor deficit links  $\alpha$ 3-containing GABA<sub>A</sub> receptors to a dopamine hyperfunction. *Proceedings of the National Academy of Sciences of the United States of America* **2005**, 102 (47), 17154-17159.

144. Crestani, F.; Keist, R.; Fritschy, J.-M.; Benke, D.; Vogt, K.; Prut, L.; Blüthmann, H.; Möhler, H.; Rudolph, U., Trace fear conditioning involves hippocampal  $\alpha$ <sub>5</sub> GABA<sub>A</sub> receptors. *Proceedings of the National Academy of Sciences* **2002**, 99 (13), 8980-8985.

145. Ralvenius, W. T.; Benke, D.; Acuña, M. A.; Rudolph, U.; Zeilhofer, H. U., Analgesia and unwanted benzodiazepine effects in point-mutated mice expressing only one benzodiazepine-sensitive GABAA receptor subtype. *Nature Communications* **2015**, 6 (1), 6803.

146. Mizuta, K.; Xu, D.; Pan, Y.; Comas, G.; Sonett, J. R.; Zhang, Y.; Panettieri, R. A., Jr.; Yang, J.; Emala, C. W., Sr., GABAA receptors are expressed and facilitate relaxation in airway smooth muscle. *Am J Physiol Lung Cell Mol Physiol* **2008**, 294 (6), L1206-16.

147. Gallos, G.; Yim, P.; Chang, S.; Zhang, Y.; Xu, D.; Cook, J. M.; Gerthoffer, W. T.; Emala, C. W., Sr., Targeting the restricted  $\alpha$ -subunit repertoire of airway smooth muscle GABAA receptors augments airway smooth muscle relaxation. *Am J Physiol Lung Cell Mol Physiol* **2012**, *302* (2), L248-56.
148. Gallos, G.; Yocum, G. T.; Siviski, M. E.; Yim, P. D.; Fu, X. W.; Poe, M. M.; Cook, J. M.; Harrison, N.; Perez-Zoghbi, J.; Emala, C. W., Sr., Selective targeting of the  $\alpha$ 5-subunit of GABAA receptors relaxes airway smooth muscle and inhibits cellular calcium handling. *Am J Physiol Lung Cell Mol Physiol* **2015**, *308* (9), L931-42.
149. Cook, J. M. E., R.; Poe, M. M.; Tiruveedhula, V. V. N. P. B.; Witzigmann, C., Synthesis of natural products and related heterocyclic compounds. Search for agents to treat neuropathic pain, epilepsy and anxiety disorders as well as simple molecules to treat TB and MRSA infections. In *Mona Symposium on Natural Products and Medicinal Chemistry*, Kingston, Jamaica, 2014.
150. Löw, K.; Crestani, F.; Keist, R.; Benke, D.; Brünig, I.; Benson, J. A.; Fritschy, J. M.; Rüllicke, T.; Bluethmann, H.; Möhler, H.; Rudolph, U., Molecular and neuronal substrate for the selective attenuation of anxiety. *Science* **2000**, *290* (5489), 131-4.
151. Yang, W.; Drewe, J. A.; Lan, N. C., Cloning and characterization of the human GABAA receptor alpha 4 subunit: identification of a unique diazepam-insensitive binding site. *Eur J Pharmacol* **1995**, *291* (3), 319-25.
152. Korpi, E. R.; Seeburg, P. H., Natural mutation of GABAA receptor  $\alpha$ 6 subunit alters benzodiazepine affinity but not allosteric GABA effects. *European Journal of Pharmacology: Molecular Pharmacology* **1993**, *247* (1), 23-27.
153. Vasović, D.; Divović, B.; Treven, M.; Knutson, D. E.; Steudle, F.; Scholze, P.; Obradović, A.; Fabjan, J.; Brković, B.; Sieghart, W.; Ernst, M.; Cook, J. M.; Savić, M. M., Trigeminal neuropathic pain development and maintenance in rats are suppressed by a positive modulator of  $\alpha$ 6 GABAA receptors. *European Journal of Pain* **2019**, *23* (5), 973-984.

154. Davies, M.; Bateson, A. N.; Dunn, S. M., Structural requirements for ligand interactions at the benzodiazepine recognition site of the GABA(A) receptor. *J Neurochem* **1998**, *70* (5), 2188-94.
155. Dunn, S. M. J.; Davies, M.; Muntoni, A. L.; Lambert, J. J., Mutagenesis of the Rat  $\alpha 1$  Subunit of the  $\gamma$ -Aminobutyric Acid<sub>A</sub> Receptor Reveals the Importance of Residue 101 in Determining the Allosteric Effects of Benzodiazepine Site Ligands. *Molecular Pharmacology* **1999**, *56* (4), 768-774.
156. Sigel, E.; Schaerer, M. T.; Buhr, A.; Baur, R., The Benzodiazepine Binding Pocket of Recombinant  $\alpha 1\beta 2\gamma 2$   $\gamma$ -Aminobutyric Acid<sub>A</sub> Receptors: Relative Orientation of Ligands and Amino Acid Side Chains. *Molecular Pharmacology* **1998**, *54* (6), 1097-1105.
157. Rudolph, U.; Möhler, H., GABA-based therapeutic approaches: GABAA receptor subtype functions. *Curr Opin Pharmacol* **2006**, *6* (1), 18-23.
158. Mendelson, W. B.; Owen, C.; Skolnick, P.; Paul, S. M.; Martin, J. V.; Ko, G.; Wagner, R., Nifedipine blocks sleep induction by flurazepam in the rat. *Sleep* **1984**, *7* (1), 64-8.
159. Ninan, P. T.; Insel, T. M.; Cohen, R. M.; Cook, J. M.; Skolnick, P.; Paul, S. M., Benzodiazepine receptor-mediated experimental "anxiety" in primates. *Science* **1982**, *218* (4579), 1332-4.
160. Cook, J. M. Z., H.; Huang, S.; Sarma, P. V. V. S.; Zhang, C. Stereospecific anxiolytic and anticonvulsant agents with reduced muscle-relaxant, sedative-hypnotic and ataxic effects. US 7618958 B2, Nov 17, 2009.
161. Cook, J. M. H., Q.; He, X.; Li, X.; Yu, J.; Han, D.; Lelas, S.; McElroy, J. F. Anxiolytic agents with reduced sedative and ataxic effects. Patent: US7119196 B2, Oct 10, 2006.
162. Fischer, B. D.; Licata, S. C.; Edwankar, R. V.; Wang, Z. J.; Huang, S.; He, X.; Yu, J.; Zhou, H.; Johnson, E. M., Jr.; Cook, J. M.; Furtmüller, R.; Ramerstorfer, J.; Sieghart, W.; Roth, B. L.; Majumder, S.; Rowlett, J. K., Anxiolytic-like effects of 8-acetylene imidazobenzodiazepines in a rhesus monkey conflict procedure. *Neuropharmacology* **2010**, *59* (7-8), 612-8.

163. Poe, M. M.; Methuku, K. R.; Li, G.; Verma, A. R.; Teske, K. A.; Stafford, D. C.; Arnold, L. A.; Cramer, J. W.; Jones, T. M.; Cerne, R.; Krambis, M. J.; Witkin, J. M.; Jambrina, E.; Rehman, S.; Ernst, M.; Cook, J. M.; Schkeryantz, J. M., Synthesis and Characterization of a Novel  $\gamma$ -Aminobutyric Acid Type A (GABA(A)) Receptor Ligand That Combines Outstanding Metabolic Stability, Pharmacokinetics, and Anxiolytic Efficacy. *J Med Chem* **2016**, *59* (23), 10800-10806.
164. Witkin, J. M.; Cerne, R.; Wakulchik, M.; S, J.; Gleason, S. D.; Jones, T. M.; Li, G.; Arnold, L. A.; Li, J. X.; Schkeryantz, J. M.; Methuku, K. R.; Cook, J. M.; Poe, M. M., Further evaluation of the potential anxiolytic activity of imidazo[1,5-a][1,4]diazepin agents selective for  $\alpha$ 2/3-containing GABA(A) receptors. *Pharmacol Biochem Behav* **2017**, *157*, 35-40.
165. Atack, J. R.; Hallett, D. J.; Tye, S.; Wafford, K. A.; Ryan, C.; Sanabria-Bohórquez, S. M.; Eng, W. S.; Gibson, R. E.; Burns, H. D.; Dawson, G. R.; Carling, R. W.; Street, L. J.; Pike, A.; De Lepeleire, I.; Van Laere, K.; Bormans, G.; de Hoon, J. N.; Van Hecken, A.; McKernan, R. M.; Murphy, M. G.; Hargreaves, R. J., Preclinical and clinical pharmacology of TPA023B, a GABAA receptor  $\alpha$ 2/ $\alpha$ 3 subtype-selective partial agonist. *J Psychopharmacol* **2011**, *25* (3), 329-44.
166. Vinkers, C. H.; Korte-Bouws, G. A. H.; Sastre Toraño, J.; Mirza, N. R.; Nielsen, E. Ø.; Ahring, P. K.; de Jong, G. J.; Olivier, B., The rapid hydrolysis of chlordiazepoxide to demoxepam may affect the outcome of chronic osmotic minipump studies. *Psychopharmacology* **2010**, *208* (4), 555-562.
167. Fischer, B. D.; Schlitt, R. J.; Hamade, B. Z.; Rehman, S.; Ernst, M.; Poe, M. M.; Li, G.; Kodali, R.; Arnold, L. A.; Cook, J. M., Pharmacological and antihyperalgesic properties of the novel  $\alpha$ 2/3 preferring GABA(A) receptor ligand MP-III-024. *Brain Res Bull* **2017**, *131*, 62-69.
168. Clayton, T.; Poe, M. M.; Rallapalli, S.; Biawat, P.; Savić, M. M.; Rowlett, J. K.; Gallos, G.; Emala, C. W.; Kaczorowski, C. C.; Stafford, D. C.; Arnold, L. A.; Cook, J. M., A Review of the Updated Pharmacophore for the Alpha 5 GABA(A) Benzodiazepine Receptor Model. *International Journal of Medicinal Chemistry* **2015**, *2015*, 430248.

169. Dostalova, Z.; Zhou, X.; Liu, A.; Zhang, X.; Zhang, Y.; Desai, R.; Forman, S. A.; Miller, K. W., Human  $\alpha 1\beta 3\gamma 2$ L gamma-aminobutyric acid type A receptors: High-level production and purification in a functional state. *Protein Sci* **2014**, *23* (2), 157-66.
170. Tan, K. R.; Rudolph, U.; Lüscher, C., Hooked on benzodiazepines: GABAA receptor subtypes and addiction. *Trends Neurosci* **2011**, *34* (4), 188-97.
171. Wieland, H. A.; Lüddens, H.; Seeburg, P. H., A single histidine in GABAA receptors is essential for benzodiazepine agonist binding. *J Biol Chem* **1992**, *267* (3), 1426-9.
172. Rudolph, U.; Knoflach, F., Beyond classical benzodiazepines: novel therapeutic potential of GABAA receptor subtypes. *Nat Rev Drug Discov* **2011**, *10* (9), 685-97.
173. Rivas, F. M.; Stables, J. P.; Murphree, L.; Edwankar, R. V.; Edwankar, C. R.; Huang, S.; Jain, H. D.; Zhou, H.; Majumder, S.; Sankar, S.; Roth, B. L.; Ramerstorfer, J.; Furtmüller, R.; Sieghart, W.; Cook, J. M., Antiseizure Activity of Novel  $\gamma$ -Aminobutyric Acid (A) Receptor Subtype-Selective Benzodiazepine Analogues in Mice and Rat Models. *Journal of Medicinal Chemistry* **2009**, *52* (7), 1795-1798.
174. Di Lio, A.; Benke, D.; Besson, M.; Desmeules, J.; Daali, Y.; Wang, Z. J.; Edwankar, R.; Cook, J. M.; Zeilhofer, H. U., HZ166, a novel GABAA receptor subtype-selective benzodiazepine site ligand, is antihyperalgesic in mouse models of inflammatory and neuropathic pain. *Neuropharmacology* **2011**, *60* (4), 626-32.
175. Namjoshi, O. A.; Wang, Z. J.; Rallapalli, S. K.; Johnson, E. M., Jr.; Johnson, Y. T.; Ng, H.; Ramerstorfer, J.; Varagic, Z.; Sieghart, W.; Majumder, S.; Roth, B. L.; Rowlett, J. K.; Cook, J. M., Search for  $\alpha 3\beta 2/\gamma 2$  subtype selective ligands that are stable on human liver microsomes. *Bioorg Med Chem* **2013**, *21* (1), 93-101.
176. Boström, J.; Hogner, A.; Llinàs, A.; Wellner, E.; Plowright, A. T., Oxadiazoles in Medicinal Chemistry. *Journal of Medicinal Chemistry* **2012**, *55* (5), 1817-1830.
177. Burger, A., Isosterism and bioisosterism in drug design. *Prog Drug Res* **1991**, *37*, 287-371.

178. Langmuir, I., Isomorphism, isosterism and covalence. *Journal of the American Chemical Society* **1919**, *41* (10), 1543-1559.
179. Patani, G. A.; LaVoie, E. J., Bioisosterism: A Rational Approach in Drug Design. *Chemical Reviews* **1996**, *96* (8), 3147-3176.
180. Cook, J. H., S.; Edwankar, R.; Namjoshi, O. A.; Wang, Z. J. Selective agents for pain suppression. US 8835424 B2, Sep. 16, 2014.
181. Cook, J. M. Z., H.; Huang, S.; Sarma, P. V. V. S.; Zhang, C. Stereospecific anxiolytic and anticonvulsant agents with reduced muscle-relaxant, sedative-hypnotic and ataxic effects. US 7618958 B2, Nov. 17, 2009.
182. Cook, J. P., M. M. J.; Methuku, K. R.; Li, G. GABAergic ligands and their uses. WO2016154031 A1, Sep 29, 2016.
183. Shimazaki, T.; Iijima, M.; Chaki, S., Anxiolytic-like activity of MGS0039, a potent group II metabotropic glutamate receptor antagonist, in a marble-burying behavior test. *Eur J Pharmacol* **2004**, *501* (1-3), 121-5.
184. Lewter, L. A.; Fisher, J. L.; Siemian, J. N.; Methuku, K. R.; Poe, M. M.; Cook, J. M.; Li, J.-X., Antinociceptive Effects of a Novel  $\alpha 2/\alpha 3$ -Subtype Selective GABAA Receptor Positive Allosteric Modulator. *ACS Chemical Neuroscience* **2017**, *8* (6), 1305-1312.
185. Trott, O.; Olson, A. J., AutoDock Vina: Improving the speed and accuracy of docking with a new scoring function, efficient optimization, and multithreading. *Journal of Computational Chemistry* **2010**, *31* (2), 455-461.
186. Koebel, M. R.; Schmadeke, G.; Posner, R. G.; Sirimulla, S., AutoDock VinaXB: implementation of XBSF, new empirical halogen bond scoring function, into AutoDock Vina. *Journal of Cheminformatics* **2016**, *8* (1), 27.

187. Witkin, J. M.; Cerne, R.; Davis, P. G.; Freeman, K. B.; do Carmo, J. M.; Rowlett, J. K.; Methuku, K. R.; Okun, A.; Gleason, S. D.; Li, X.; Krambis, M. J.; Poe, M.; Li, G.; Schkeryantz, J. M.; Jahan, R.; Yang, L.; Guo, W.; Golani, L. K.; Anderson, W. H.; Catlow, J. T.; Jones, T. M.; Porreca, F.; Smith, J. L.; Knopp, K. L.; Cook, J. M., The  $\alpha$ 2,3-selective potentiator of GABA(A) receptors, KRM-II-81, reduces nociceptive-associated behaviors induced by formalin and spinal nerve ligation in rats. *Pharmacol Biochem Behav* **2019**, *180*, 22-31.
188. Krisberg, K., New research: More Americans have epilepsy than ever before. *The Nation's Health* **2017**, *47* (8), 10-10.
189. Zaccara, G.; Schmidt, D., Antiepileptic Drugs in Clinical Development: Differentiate or Die? *Curr Pharm Des* **2017**, *23* (37), 5593-5605.
190. van Rijnsoever, C.; Täuber, M.; Choulli, M. K.; Keist, R.; Rudolph, U.; Mohler, H.; Fritschy, J. M.; Crestani, F., Requirement of  $\alpha$ <sub>5</sub>-GABA<sub>A</sub> Receptors for the Development of Tolerance to the Sedative Action of Diazepam in Mice. *The Journal of Neuroscience* **2004**, *24* (30), 6785-6790.
191. Witkin, J. M.; Smith, J. L.; Ping, X.; Gleason, S. D.; Poe, M. M.; Li, G.; Jin, X.; Hobbs, J.; Schkeryantz, J. M.; McDermott, J. S.; Alatorre, A. I.; Siemian, J. N.; Cramer, J. W.; Airey, D. C.; Methuku, K. R.; Tiruveedhula, V.; Jones, T. M.; Crawford, J.; Krambis, M. J.; Fisher, J. L.; Cook, J. M.; Cerne, R., Bioisosteres of ethyl 8-ethynyl-6-(pyridin-2-yl)-4H-benzo[f]imidazo [1,5-a][1,4]diazepine-3-carboxylate (HZ-166) as novel alpha 2,3 selective potentiators of GABA(A) receptors: Improved bioavailability enhances anticonvulsant efficacy. *Neuropharmacology* **2018**, *137*, 332-343.
192. Knutson, D. E.; Smith, J. L.; Ping, X.; Jin, X.; Golani, L. K.; Li, G.; Tiruveedhula, V. V. N. P. B.; Rashid, F.; Mian, M. Y.; Jahan, R.; Sharmin, D.; Cerne, R.; Cook, J. M.; Witkin, J. M., Imidazodiazepine Anticonvulsant, KRM-II-81, Produces Novel, Non-diazepam-like Antiseizure Effects. *ACS Chemical Neuroscience* **2020**, *11* (17), 2624-2637.

193. Barton, M. E.; Klein, B. D.; Wolf, H. H.; White, H. S., Pharmacological characterization of the 6 Hz psychomotor seizure model of partial epilepsy. *Epilepsy Res* **2001**, *47* (3), 217-27.
194. Wilcox, K. S.; Dixon-Salazar, T.; Sills, G. J.; Ben-Menachem, E.; White, H. S.; Porter, R. J.; Dichter, M. A.; Moshé, S. L.; Noebels, J. L.; Privitera, M. D.; Rogawski, M. A., Issues related to development of new antiseizure treatments. *Epilepsia* **2013**, *54 Suppl 4* (0 4), 24-34.
195. Goddard, G. V.; McIntyre, D. C.; Leech, C. K., A permanent change in brain function resulting from daily electrical stimulation. *Exp Neurol* **1969**, *25* (3), 295-330.
196. Franco, V.; Canevini, M. P.; Capovilla, G.; De Sarro, G.; Galimberti, C. A.; Gatti, G.; Guerrini, R.; La Neve, A.; Rosati, E.; Specchio, L. M.; Striano, S.; Tinuper, P.; Perucca, E., Off-label prescribing of antiepileptic drugs in pharmaco-resistant epilepsy: a cross-sectional drug utilization study of tertiary care centers in Italy. *CNS Drugs* **2014**, *28* (10), 939-49.
197. Bouilleret, V.; Ridoux, V.; Depaulis, A.; Marescaux, C.; Nehlig, A.; Le Gal La Salle, G., Recurrent seizures and hippocampal sclerosis following intrahippocampal kainate injection in adult mice: electroencephalography, histopathology and synaptic reorganization similar to mesial temporal lobe epilepsy. *Neuroscience* **1999**, *89* (3), 717-729.
198. Srivastava, A. K.; Alex, A. B.; Wilcox, K. S.; White, H. S., Rapid loss of efficacy to the antiseizure drugs lamotrigine and carbamazepine: a novel experimental model of pharmaco-resistant epilepsy. *Epilepsia* **2013**, *54* (7), 1186-94.
199. Witkin, J. M.; Li, G.; Golani, L. K.; Xiong, W.; Smith, J. L.; Ping, X.; Rashid, F.; Jahan, R.; Cerne, R.; Cook, J. M.; Jin, X., The Positive Allosteric Modulator of  $\alpha 2/3$ -Containing GABA(A) Receptors, KRM-II-81, Is Active in Pharmaco-Resistant Models of Epilepsy and Reduces Hyperexcitability after Traumatic Brain Injury. *J Pharmacol Exp Ther* **2020**, *372* (1), 83-94.

200. West, P. J.; Saunders, G. W.; Billingsley, P.; Smith, M. D.; White, H. S.; Metcalf, C. S.; Wilcox, K. S., Recurrent epileptiform discharges in the medial entorhinal cortex of kainate-treated rats are differentially sensitive to antiseizure drugs. *Epilepsia* **2018**, *59* (11), 2035-2048.
201. Semple, B. D.; Zamani, A.; Rayner, G.; Shultz, S. R.; Jones, N. C., Affective, neurocognitive and psychosocial disorders associated with traumatic brain injury and post-traumatic epilepsy. *Neurobiol Dis* **2019**, *123*, 27-41.
202. Ping, X.; Jin, X., Transition from Initial Hypoactivity to Hyperactivity in Cortical Layer V Pyramidal Neurons after Traumatic Brain Injury In Vivo. *J Neurotrauma* **2016**, *33* (4), 354-61.
203. Bolkvadze, T.; Pitkänen, A., Development of post-traumatic epilepsy after controlled cortical impact and lateral fluid-percussion-induced brain injury in the mouse. *J Neurotrauma* **2012**, *29* (5), 789-812.
204. Hammond, D. L.; Drower, E. J., Effects of intrathecally administered THIP, baclofen and muscimol on nociceptive threshold. *Eur J Pharmacol* **1984**, *103* (1-2), 121-5.
205. Dirig, D. M.; Yaksh, T. L., Intrathecal baclofen and muscimol, but not midazolam, are antinociceptive using the rat-formalin model. *J Pharmacol Exp Ther* **1995**, *275* (1), 219-27.
206. Enna, S. J.; McCarron, K. E., The role of GABA in the mediation and perception of pain. *Adv Pharmacol* **2006**, *54*, 1-27.
207. Etlin, A.; Bráz, J. M.; Kuhn, J. A.; Wang, X.; Hamel, K. A.; Llewellyn-Smith, I. J.; Basbaum, A. I., Functional Synaptic Integration of Forebrain GABAergic Precursors into the Adult Spinal Cord. *The Journal of Neuroscience* **2016**, *36* (46), 11634-11645.
208. Zeilhofer, H. U.; Ralvenius, W. T.; Acuña, M. A., Restoring the spinal pain gate: GABA(A) receptors as targets for novel analgesics. *Adv Pharmacol* **2015**, *73*, 71-96.
209. Biggerstaff, A.; Kivell, B.; Smith, J. L.; Mian, M. Y.; Golani, L. K.; Rashid, F.; Sharmin, D.; Knutson, D. E.; Cerne, R.; Cook, J. M.; Witkin, J. M., The  $\alpha$ 2,3-selective potentiators of GABA(A) receptors, KRM-II-

81 and MP-III-80, produce anxiolytic-like effects and block chemotherapy-induced hyperalgesia in mice without tolerance development. *Pharmacol Biochem Behav* **2020**, *196*, 172996.

210. Kalant, H.; LeBlanc, A. E.; Gibbins, R. J., Tolerance to, and dependence on, some non-opiate psychotropic drugs. *Pharmacol Rev* **1971**, *23* (3), 135-91.

211. Hwang, J. K.; Kim, D. S., From Resection to Disconnection for Seizure Control in Pediatric Epilepsy Children. *J Korean Neurosurg Soc* **2019**, *62* (3), 336-343.

212. Reissig, C. J.; Harrison, J. A.; Carter, L. P.; Griffiths, R. R., Inhaled vs. oral alprazolam: subjective, behavioral and cognitive effects, and modestly increased abuse potential. *Psychopharmacology (Berl)* **2015**, *232* (5), 871-83.

213. Onyett, S. R., The benzodiazepine withdrawal syndrome and its management. *J R Coll Gen Pract* **1989**, *39* (321), 160-3.

214. Kostowski, W.; Malatyńska, E.; Płaźnik, A.; Dyr, W.; Danysz, W., Comparative studies on antidepressant action of alprazolam in different animal models. *Pol J Pharmacol Pharm* **1986**, *38* (5-6), 471-81.

215. Flugy, A.; Gagliano, M.; Cannizzaro, C.; Novara, V.; Cannizzaro, G., Antidepressant and anxiolytic effects of alprazolam versus the conventional antidepressant desipramine and the anxiolytic diazepam in the forced swim test in rats. *Eur J Pharmacol* **1992**, *214* (2-3), 233-8.

216. El Zahaf, N. A.; Elhwuegi, A. S., The effect of GABA mimetics on the duration of immobility in the forced swim test in albino mice. *Libyan J Med* **2014**, *9* (1), 23480.

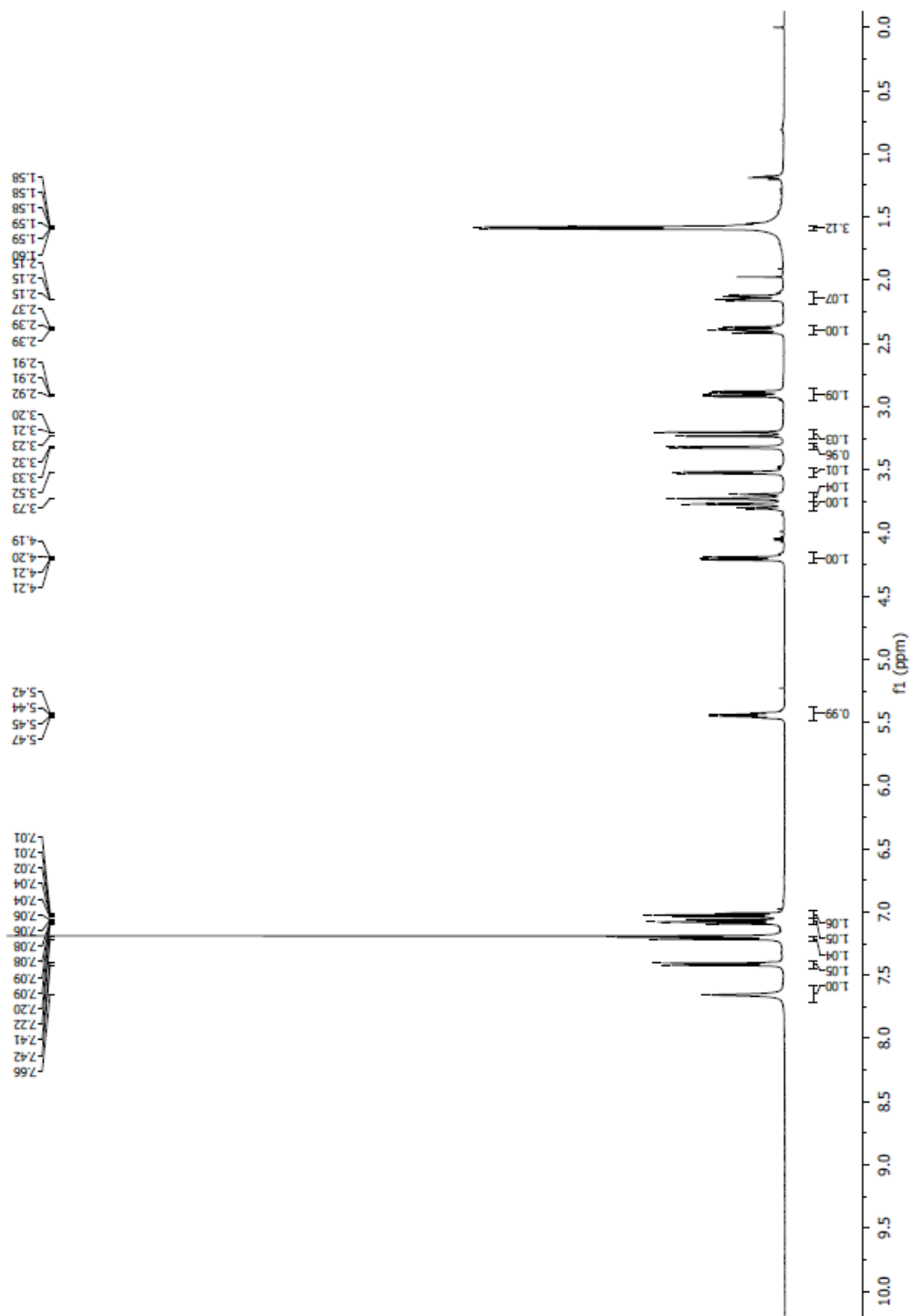
217. Witkin, J. M.; Knutson, D. E.; Rodriguez, G. J.; Shi, S., Rapid-Acting Antidepressants. *Curr Pharm Des* **2018**, *24* (22), 2556-2563.

218. Moerke, M. J.; Li, G.; Golani, L. K.; Cook, J.; Negus, S. S., Effects of the  $\alpha 2/\alpha 3$ -subtype-selective GABA<sub>A</sub> receptor positive allosteric modulator KRM-II-81 on pain-depressed behavior in rats: comparison with ketorolac and diazepam. *Behav Pharmacol* **2019**, *30* (5), 452-461.

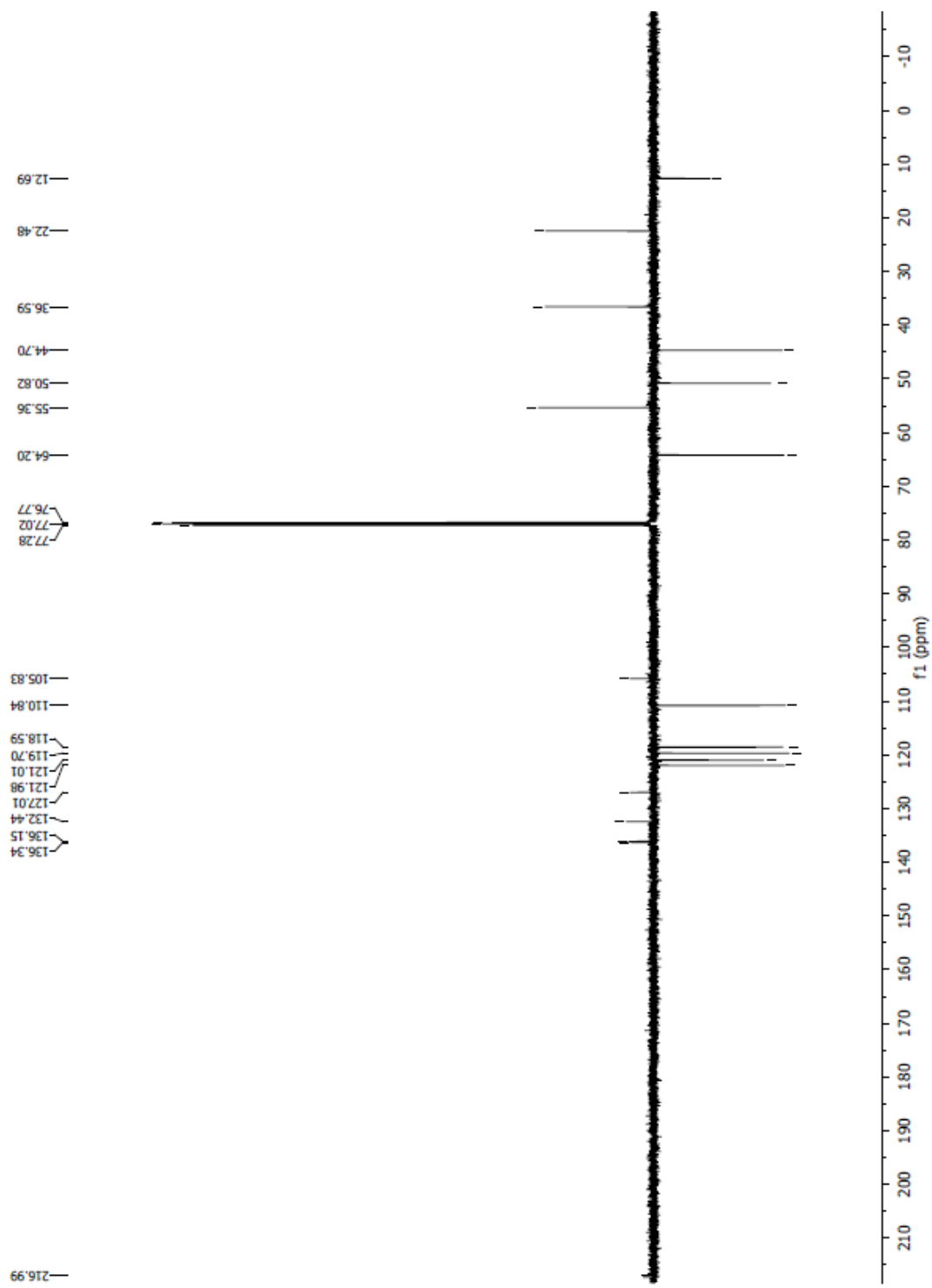


## Appendix Part 1

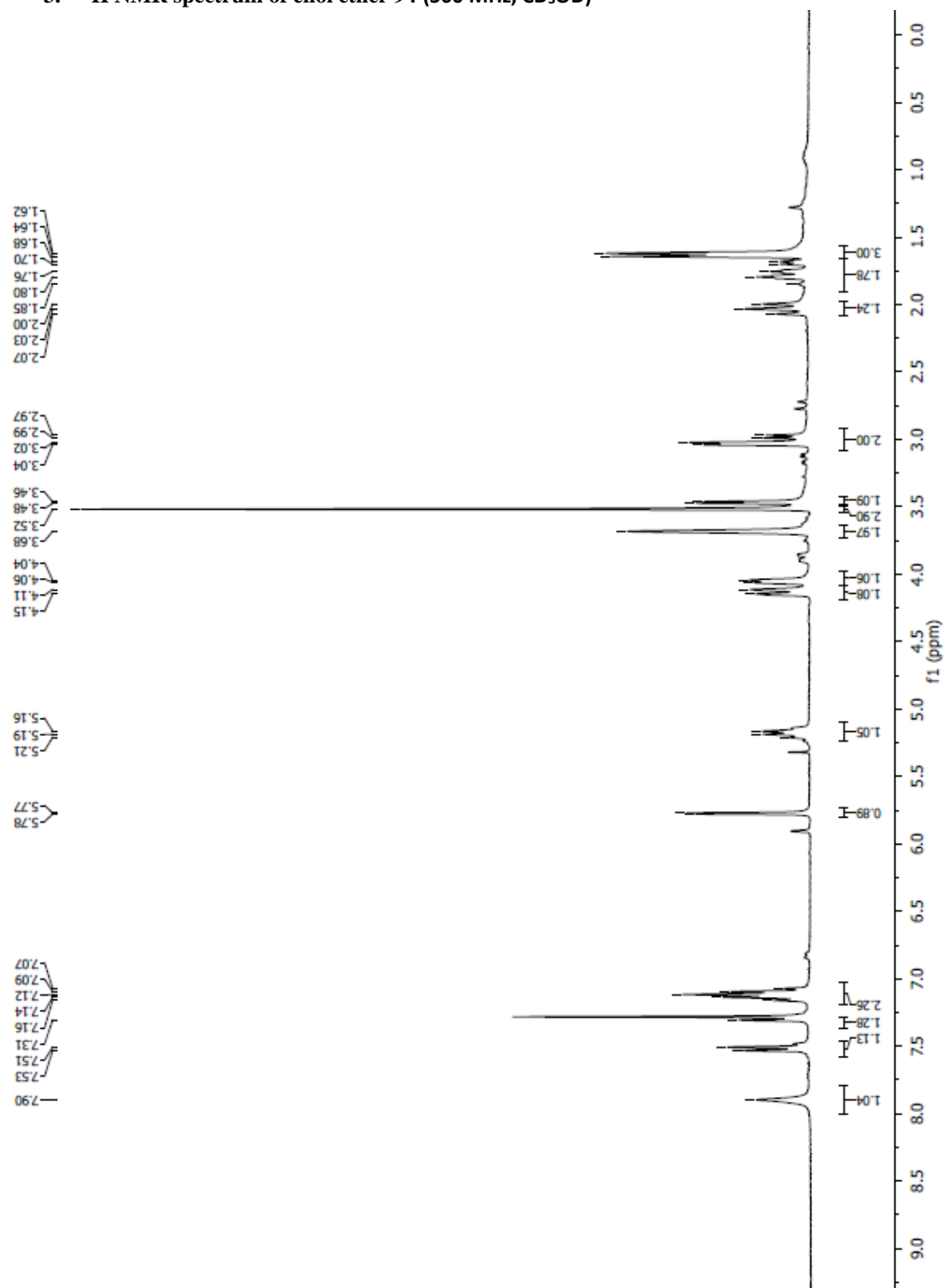
### 1. $^1\text{H}$ NMR spectrum of pentacyclic ketone 29 (500 MHz, $\text{CD}_3\text{OD}$ )



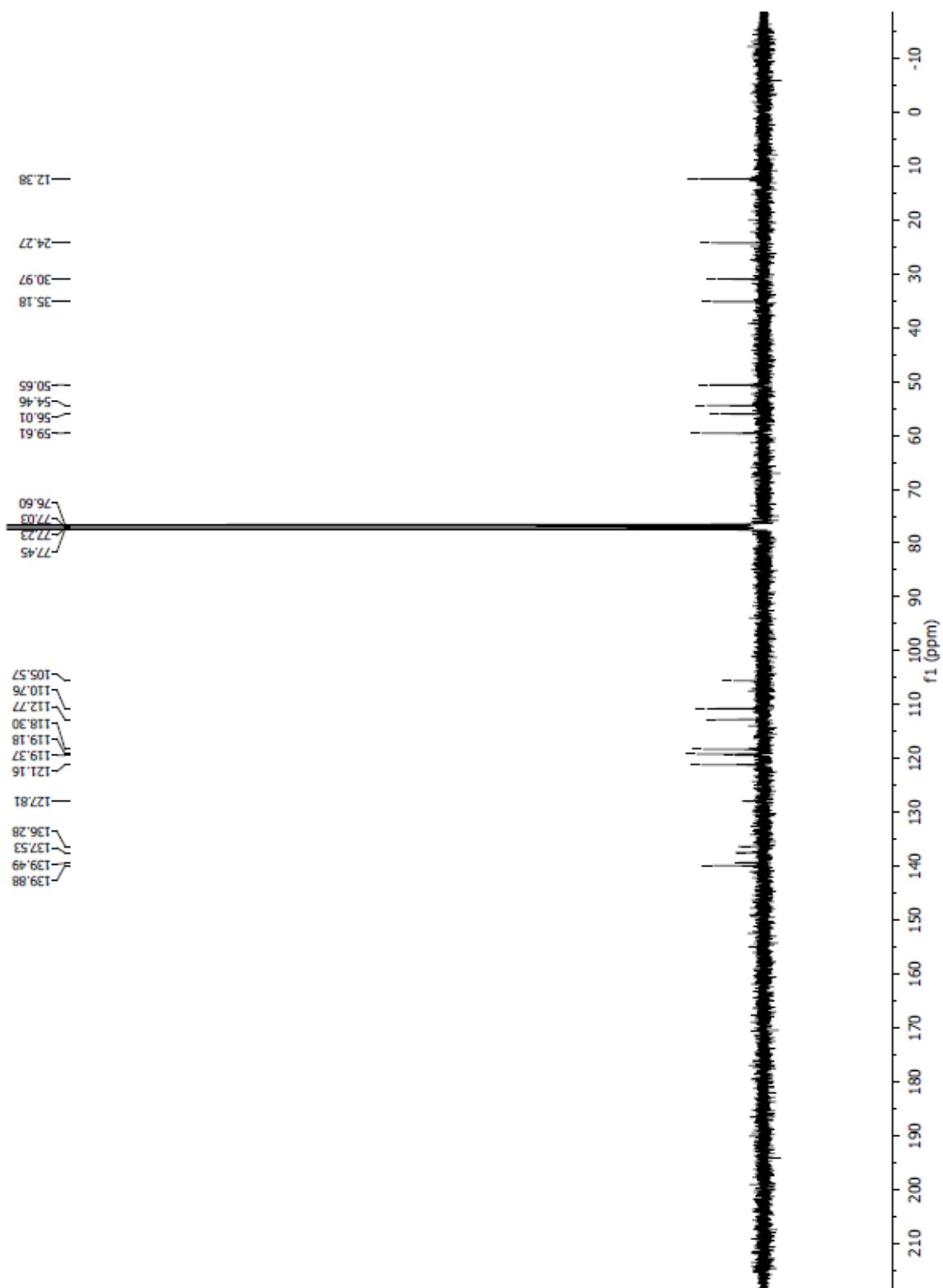
2.  $^{13}\text{C}$  APT NMR spectrum of pentacyclic ketone **29** (500 MHz,  $\text{CD}_3\text{OD}$ )



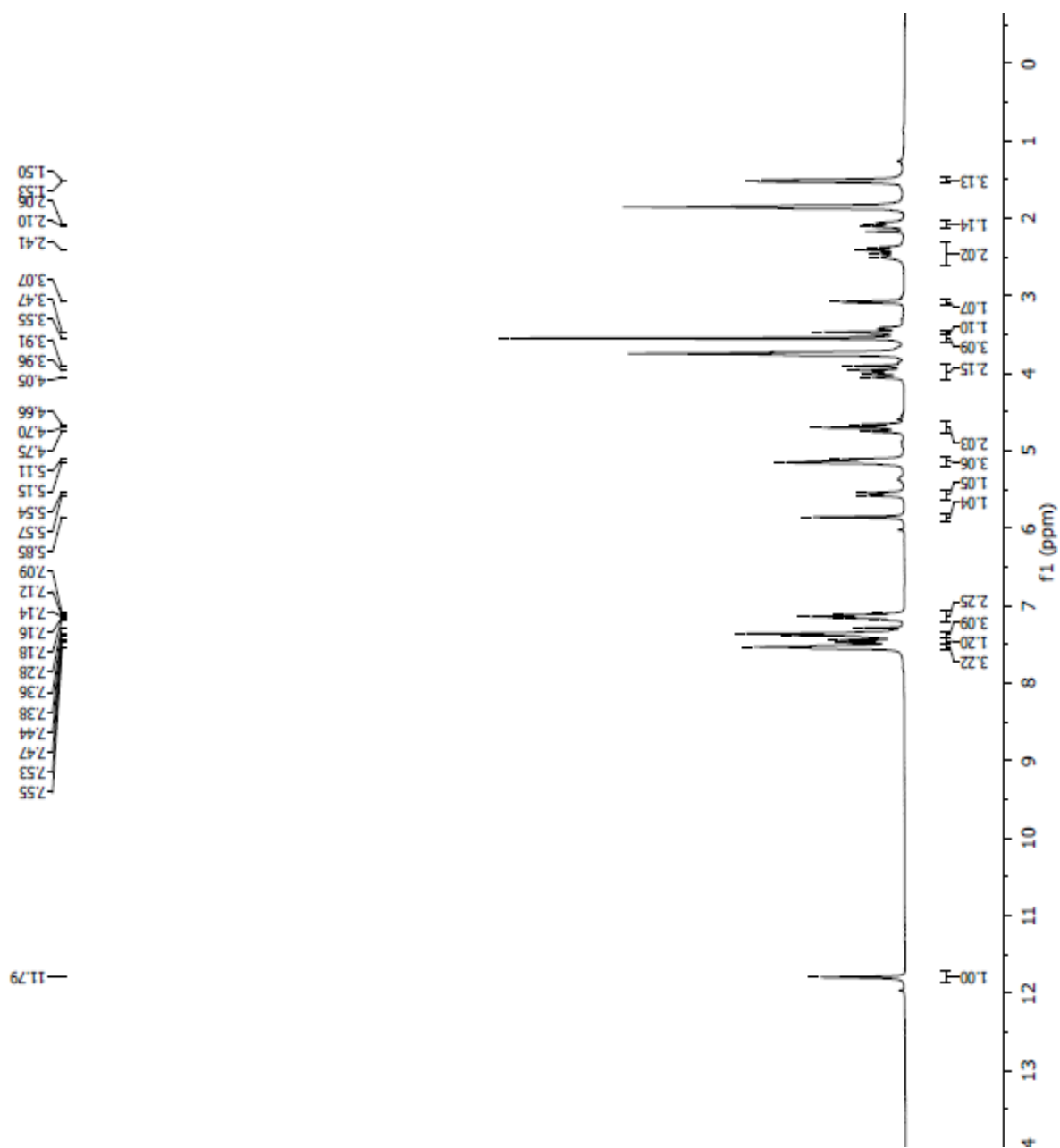
3.  $^1\text{H}$  NMR spectrum of enol ether 94 (500 MHz,  $\text{CD}_3\text{OD}$ )



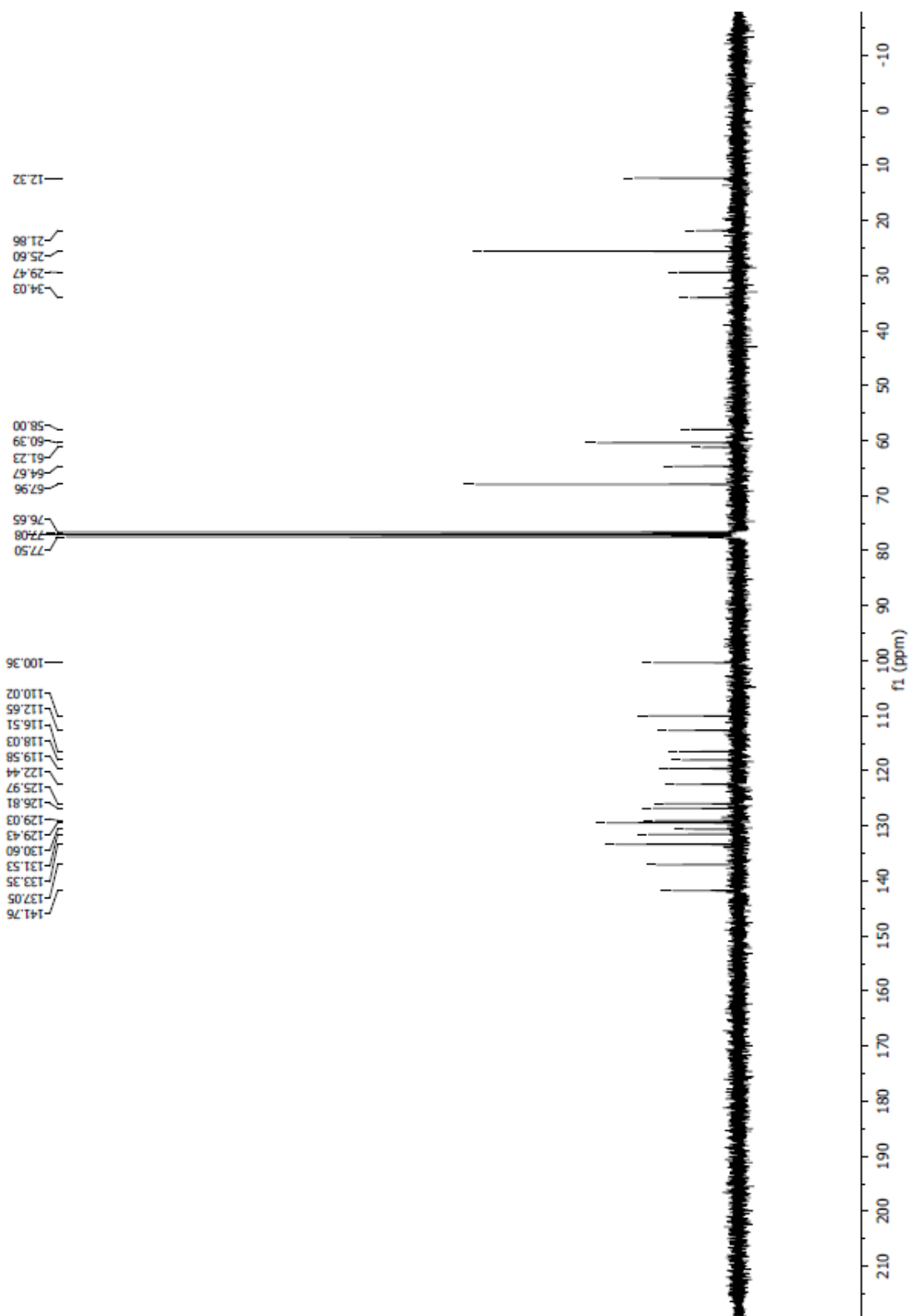
4.  $^{13}\text{C}$  NMR spectrum of enol ether 94 (500 MHz,  $\text{CD}_3\text{OD}$ )



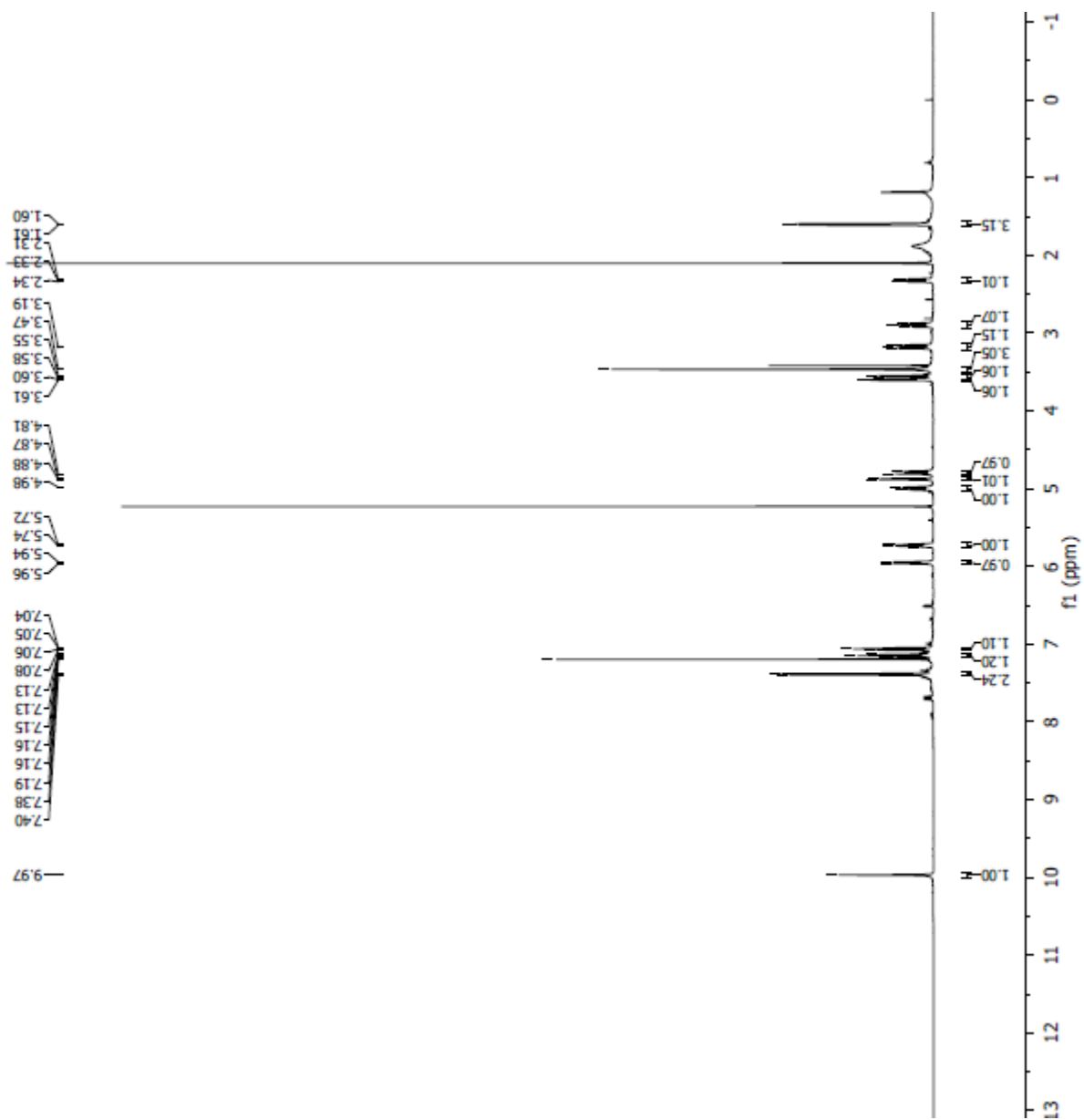
5.  $^1\text{H}$  NMR spectrum of 94b (500 MHz,  $\text{CD}_3\text{OD}$ )



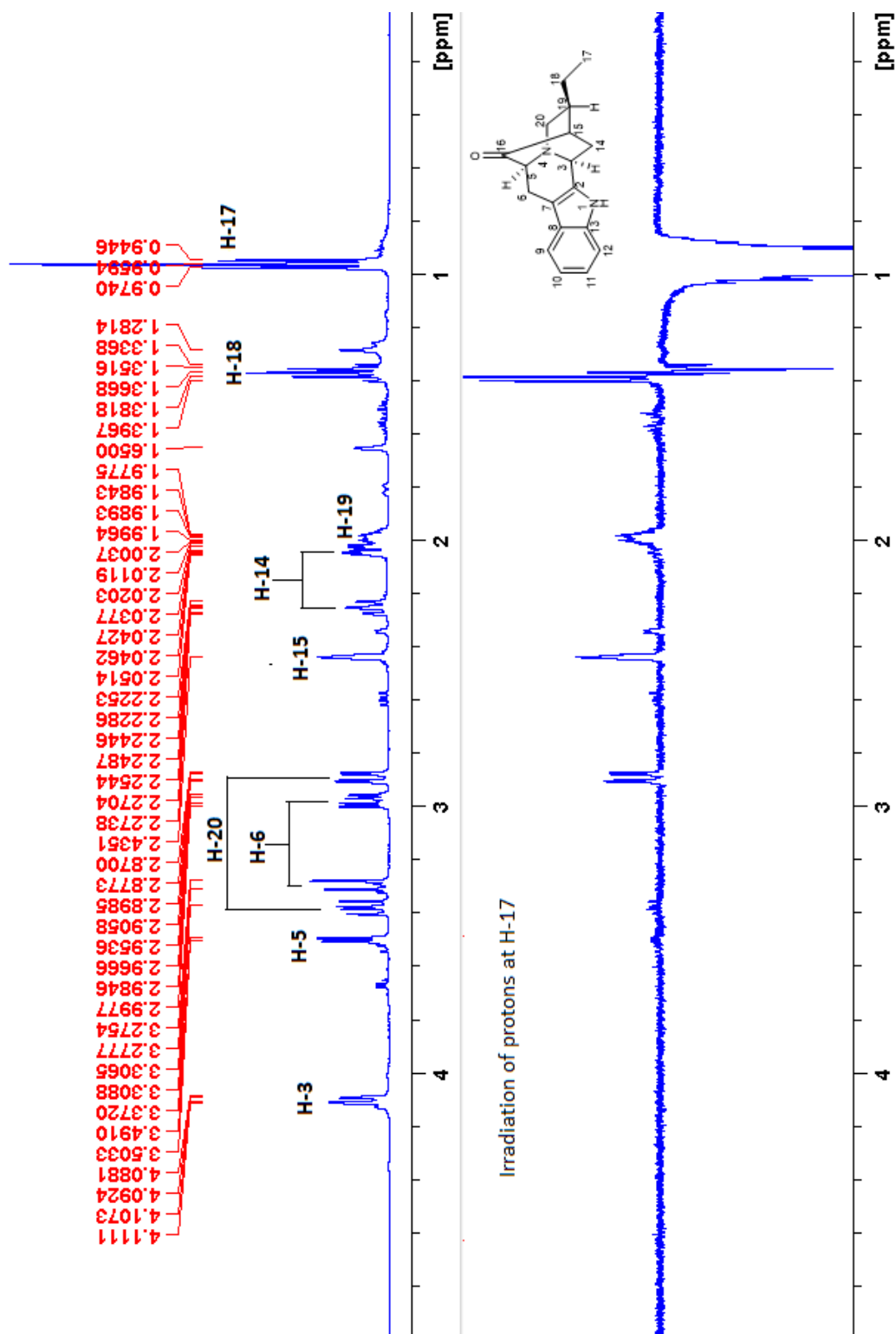
6.  $^{13}\text{C}$  NMR spectrum of 94b (500 MHz,  $\text{CD}_3\text{OD}$ )



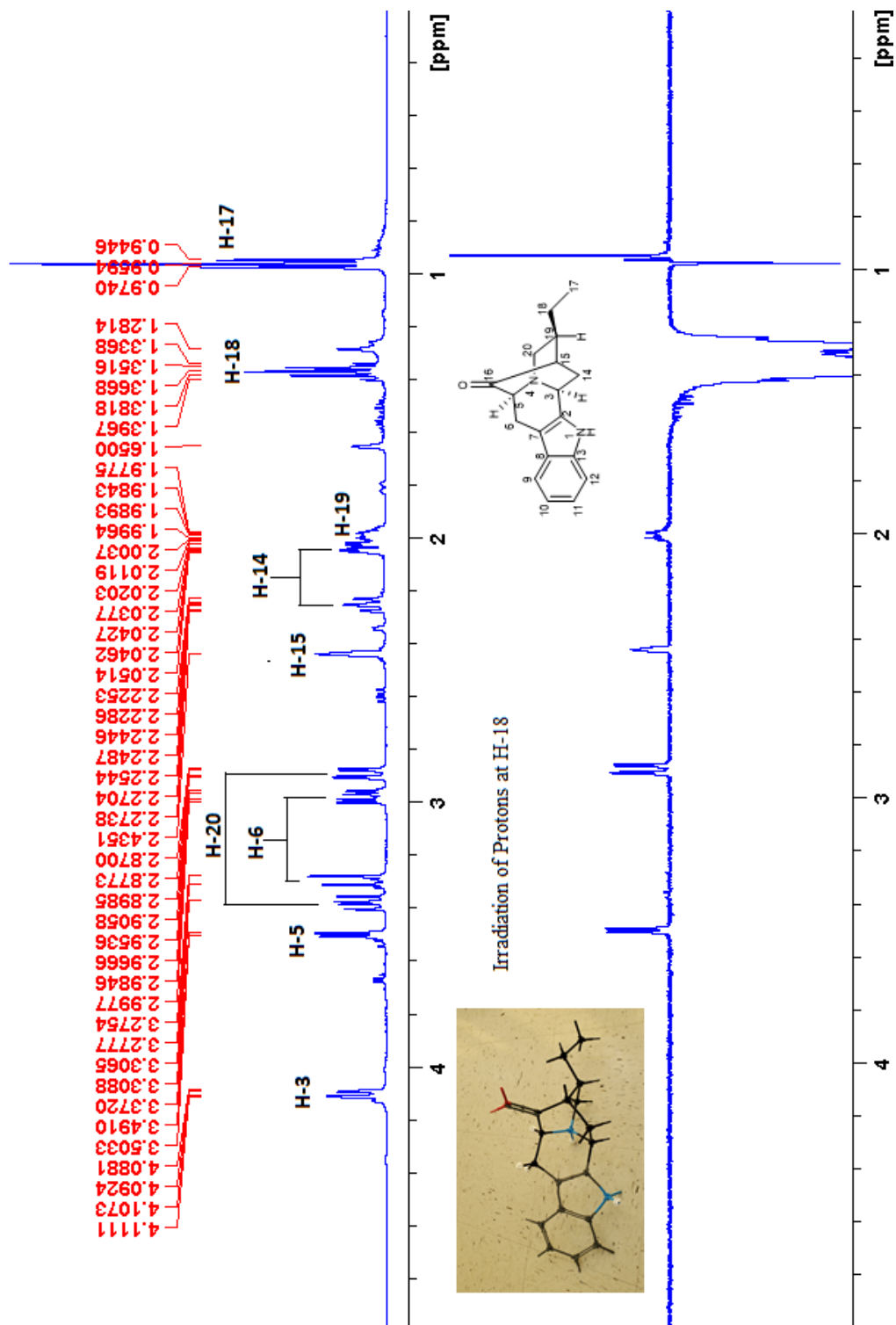
7.  $^1\text{H}$  NMR spectrum of 93 (500 MHz,  $\text{CD}_3\text{OD}$ )



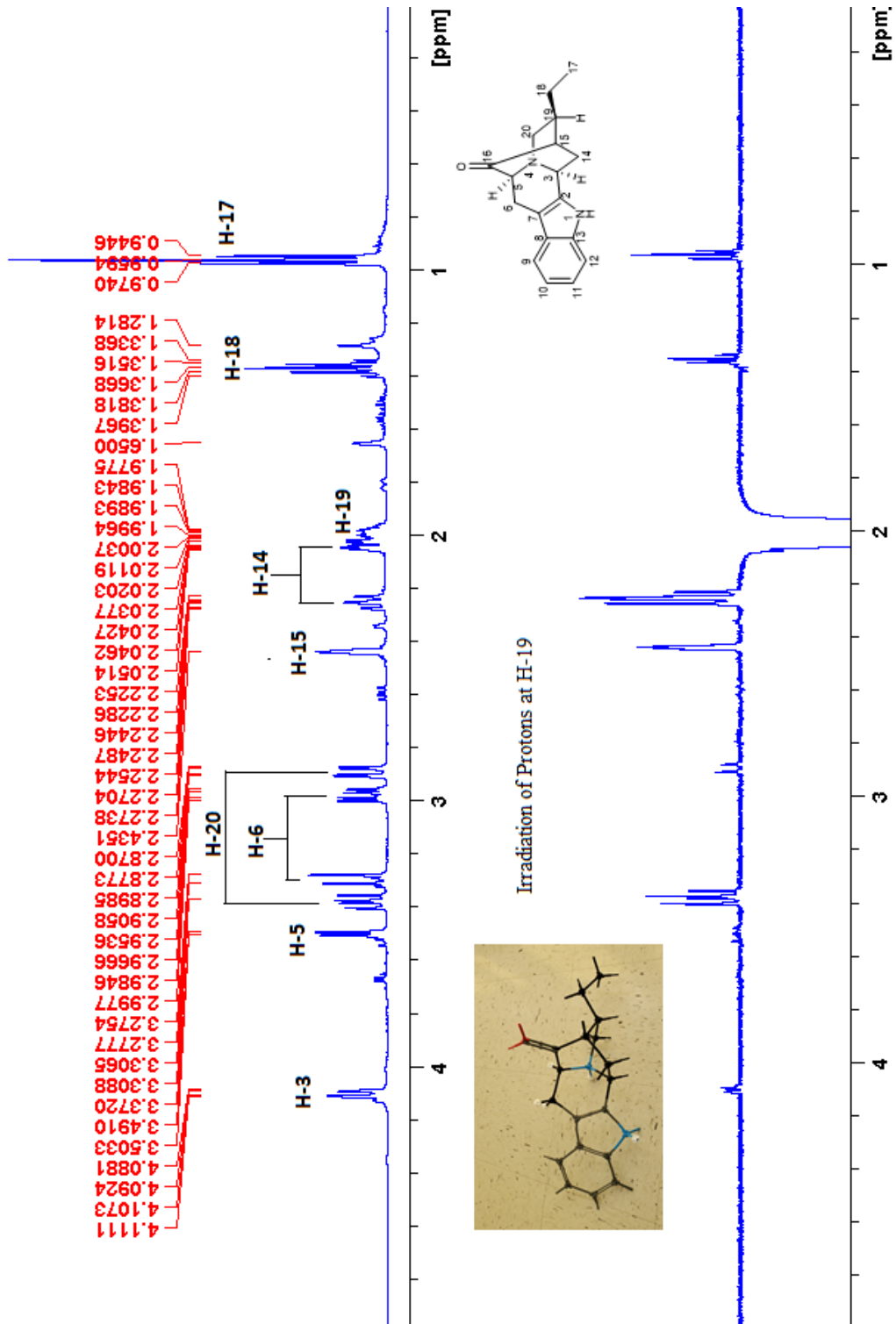
8. 1D NOEs Observed after Irradiation of Protons at H-17 of 103 (500 MHz, CD<sub>3</sub>OD)



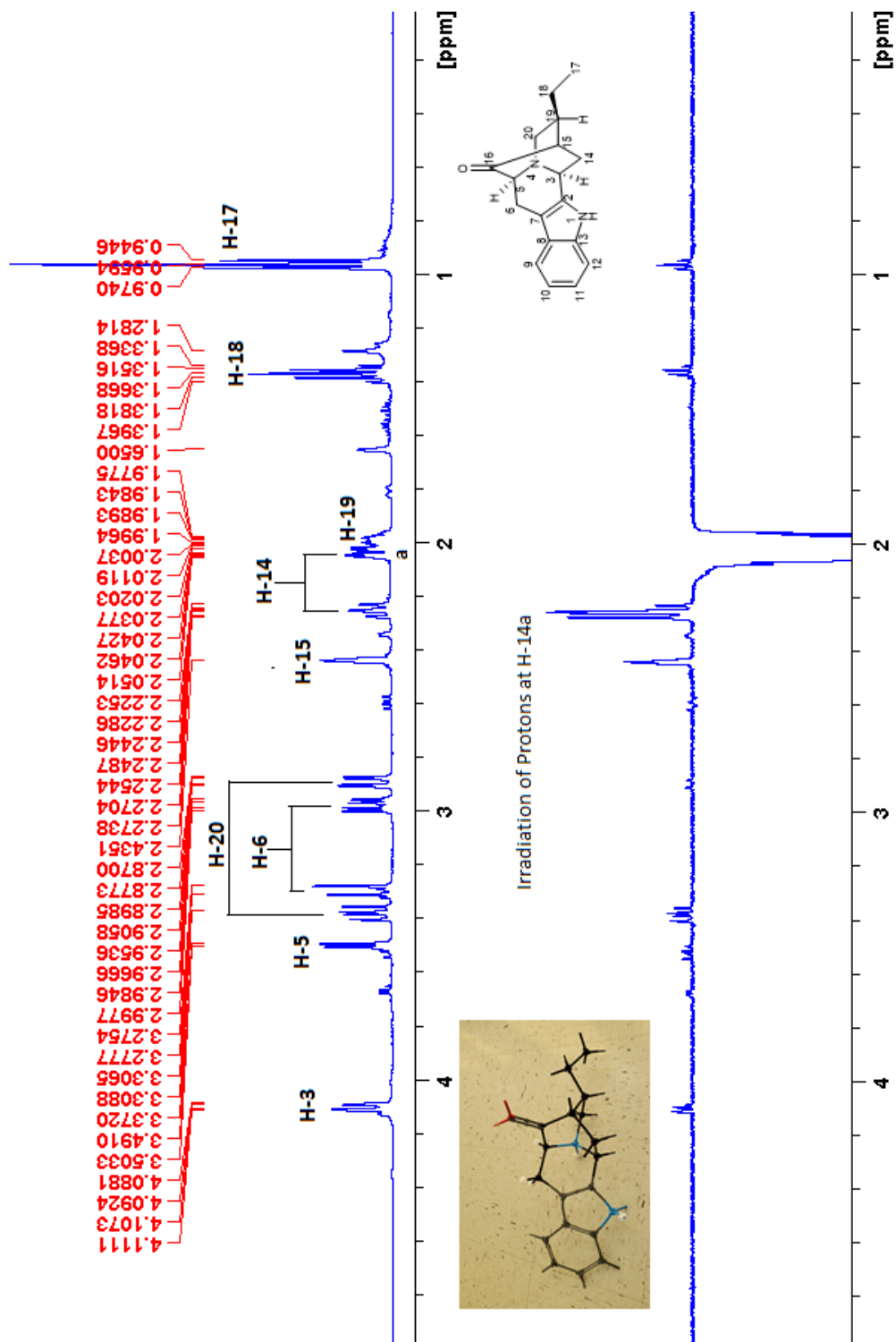
9. 1D NOEs Observed after Irradiation of Protons at H-18 of 103 (500 MHz, CD<sub>3</sub>OD)



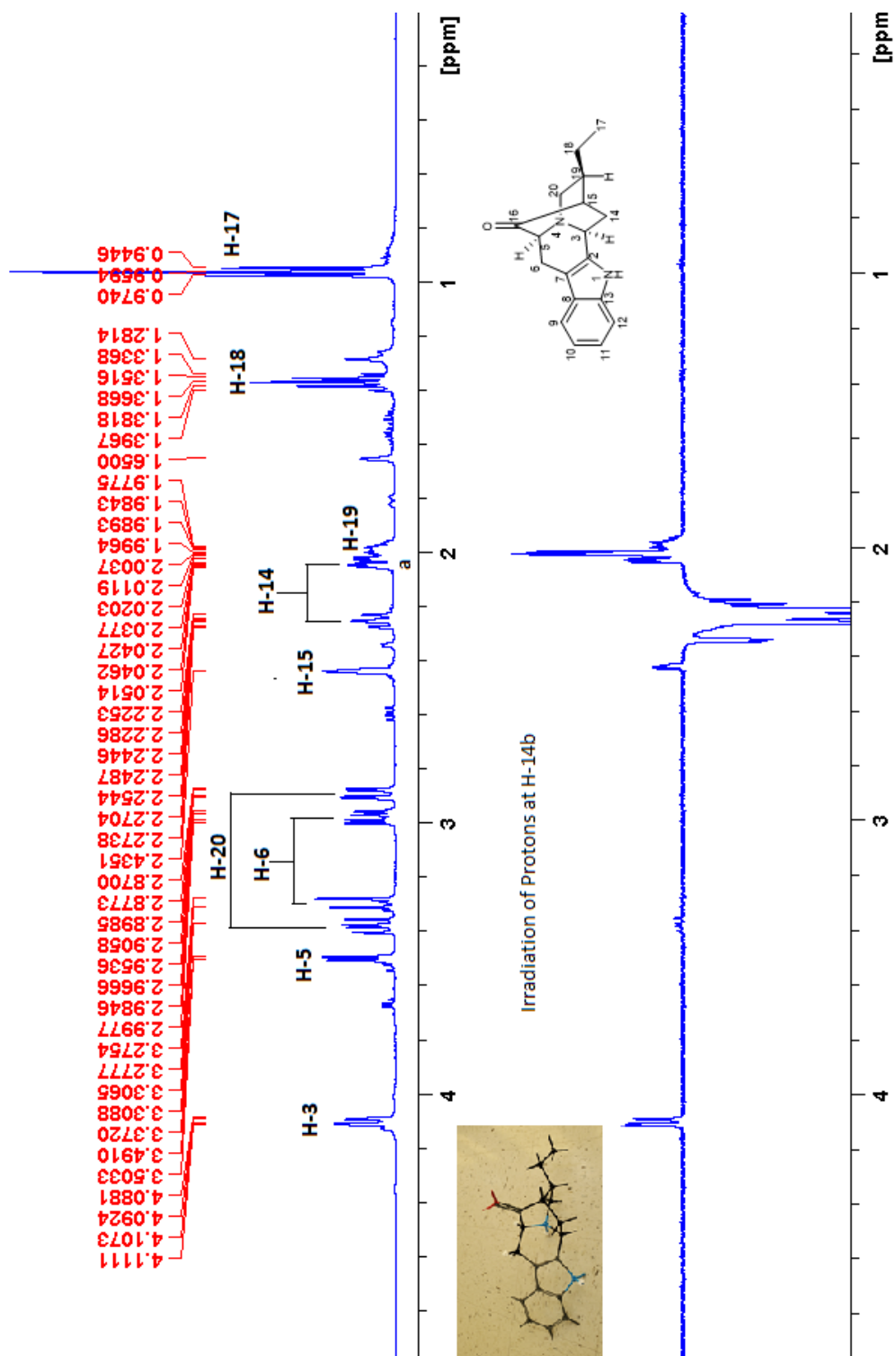
10. 1D NOEs Observed after Irradiation of Protons at H-19 of 103 (500 MHz, CD<sub>3</sub>OD)



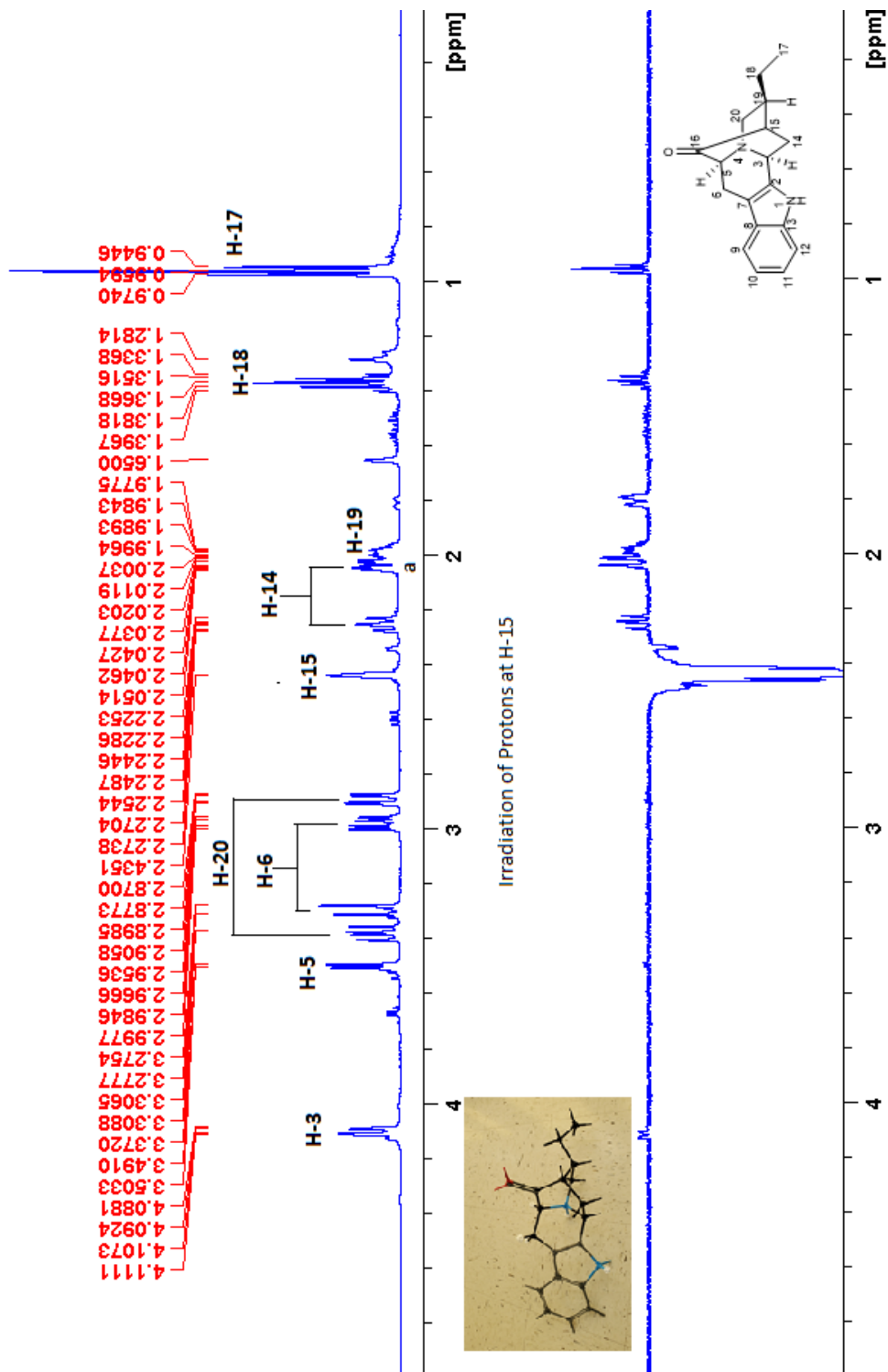
11. 1D NOEs Observed after Irradiation of Protons at H-14a of 103 (500 MHz, CD<sub>3</sub>OD)



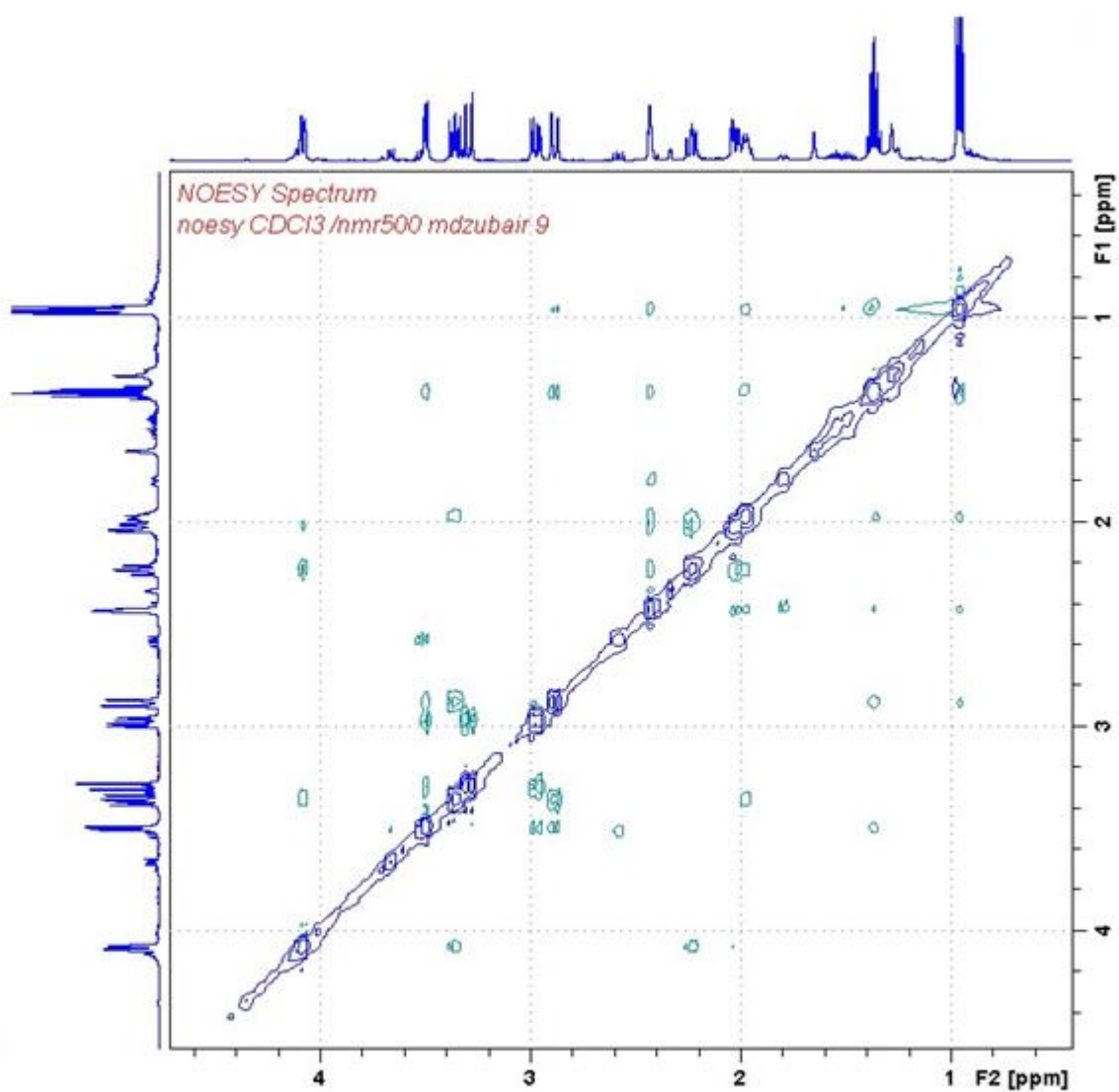
12. 1D NOEs Observed after Irradiation of Protons at H-14b of 103 (500 MHz, CD<sub>3</sub>OD)



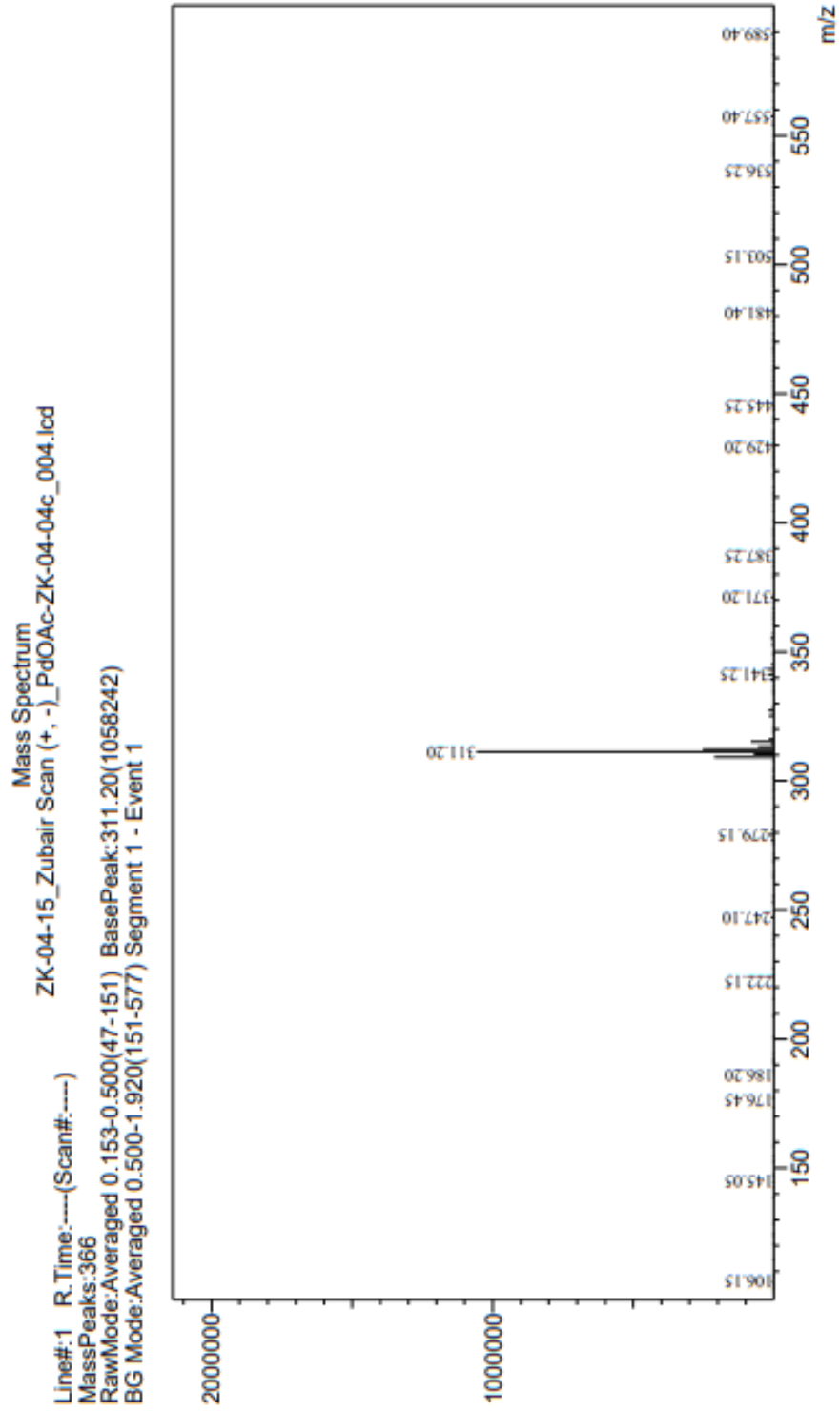
13. 1D NOEs Observed after Irradiation of Protons at H-15 of 103 (500 MHz, CD<sub>3</sub>OD)



14. 2D NOESY spectrum of 103 (500 MHz, CD<sub>3</sub>OD)

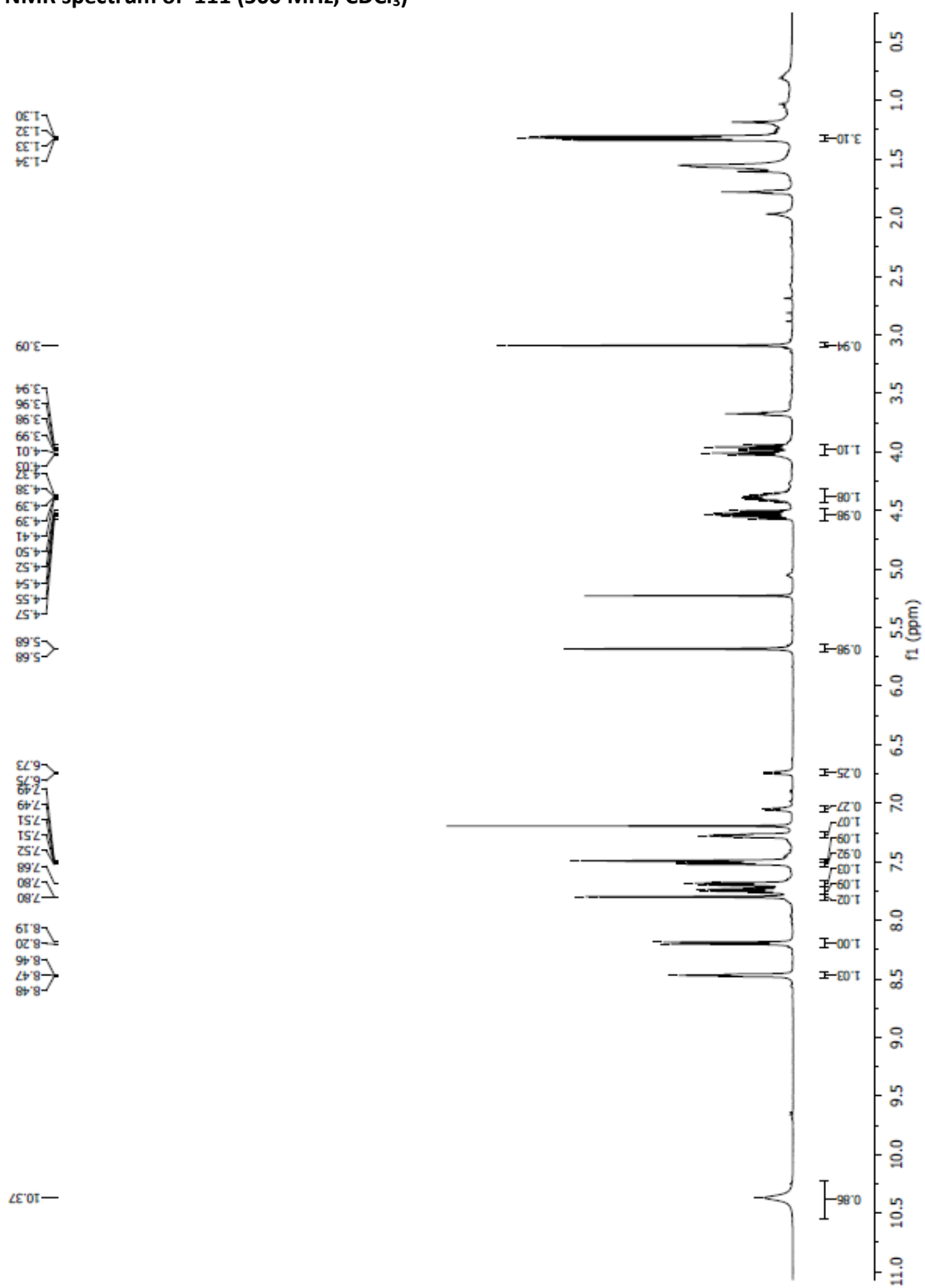


15. Mass spectrum of 99

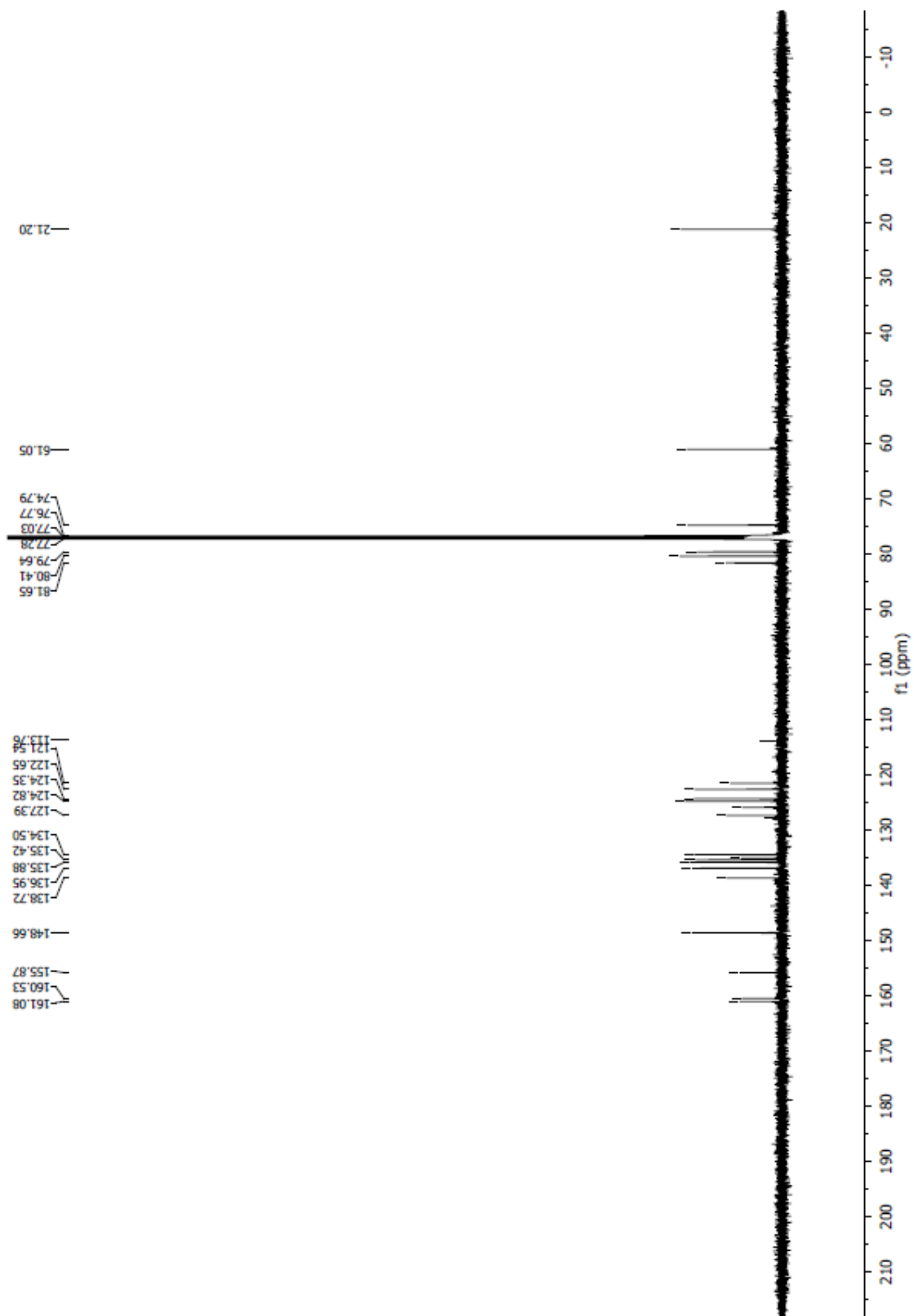


## Appendix Part 2

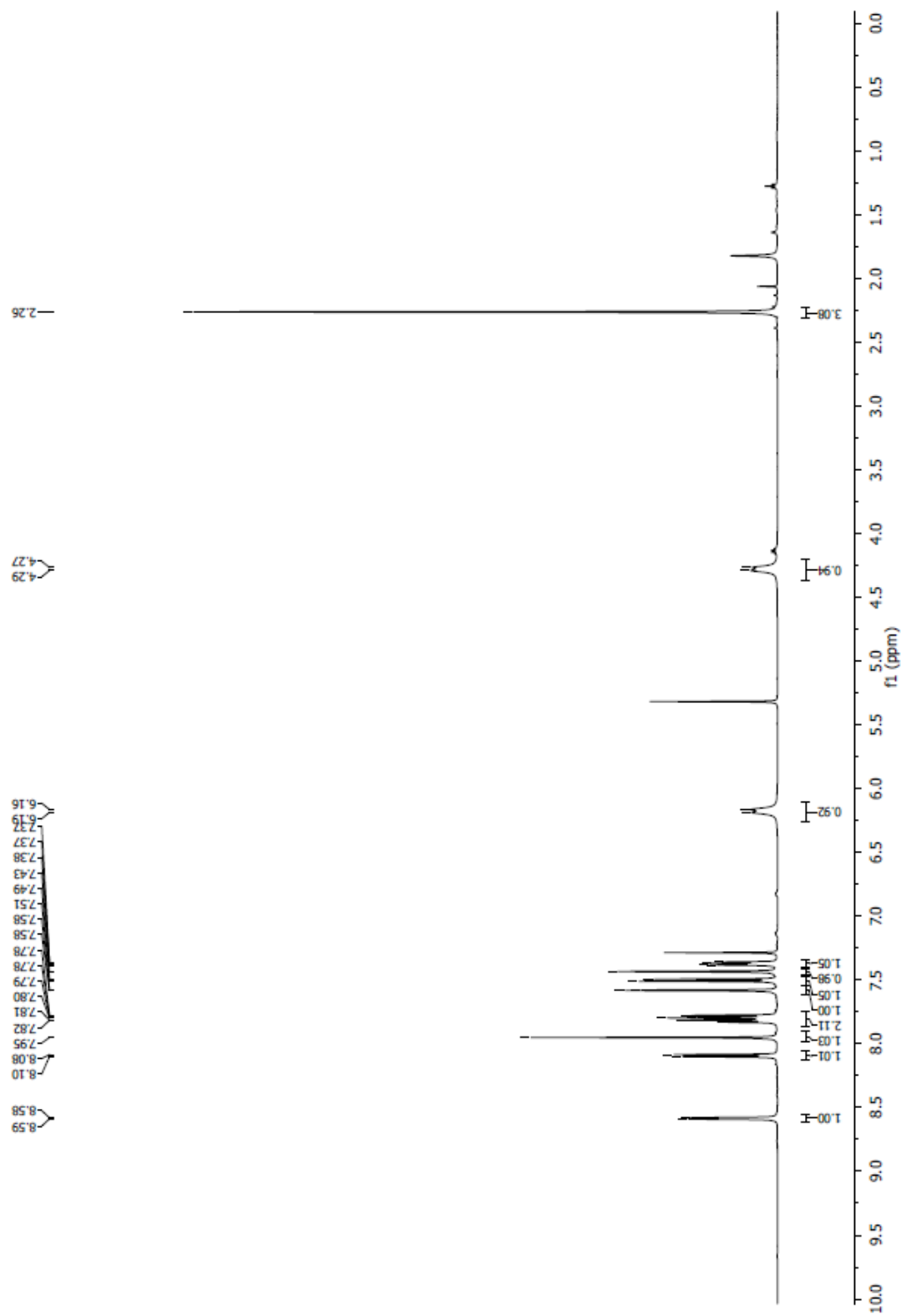
### 1. $^1\text{H}$ NMR spectrum of 111 (500 MHz, $\text{CDCl}_3$ )



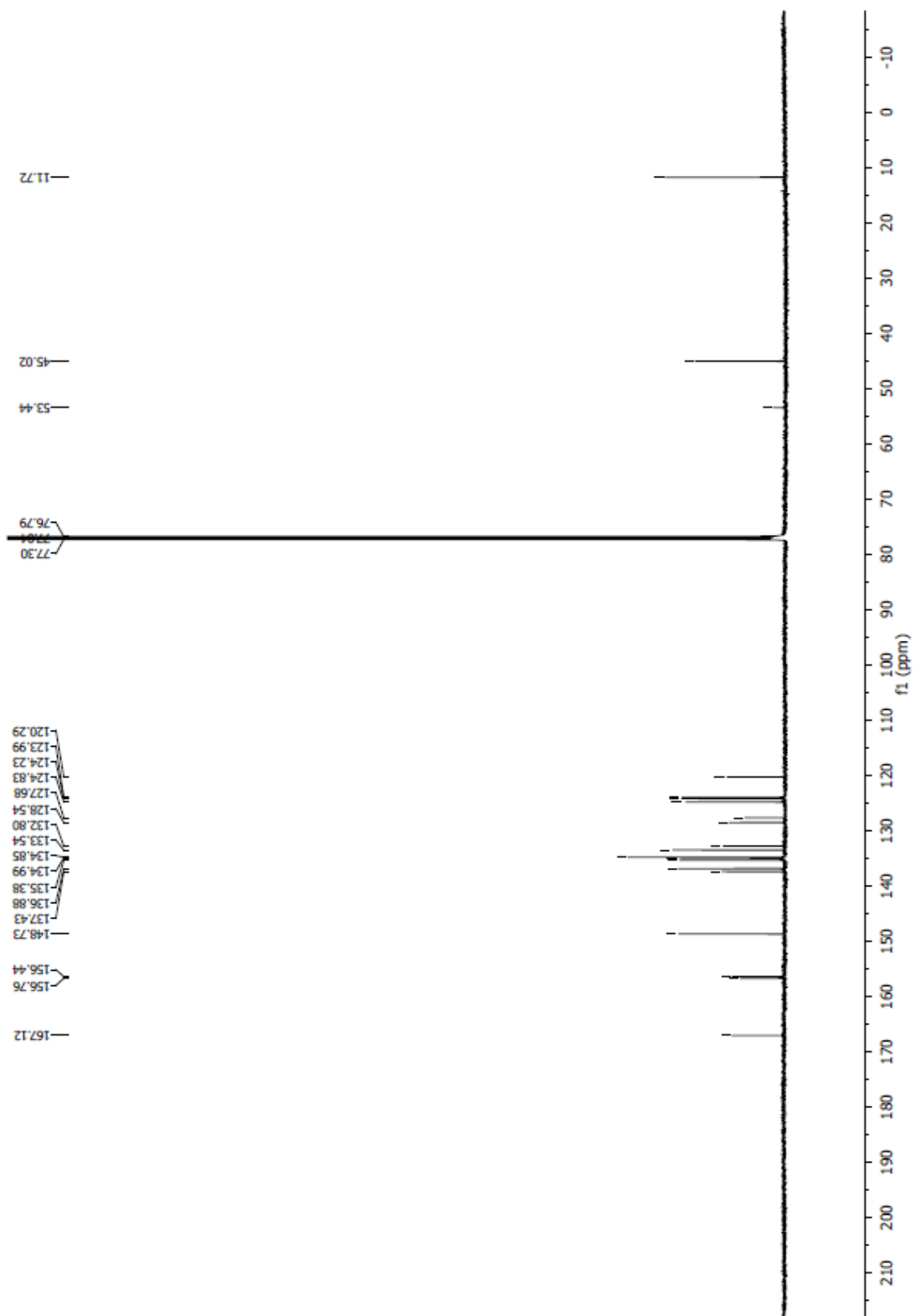
2.  $^{13}\text{C}$  NMR spectrum of 111 (500 MHz,  $\text{CDCl}_3$ )



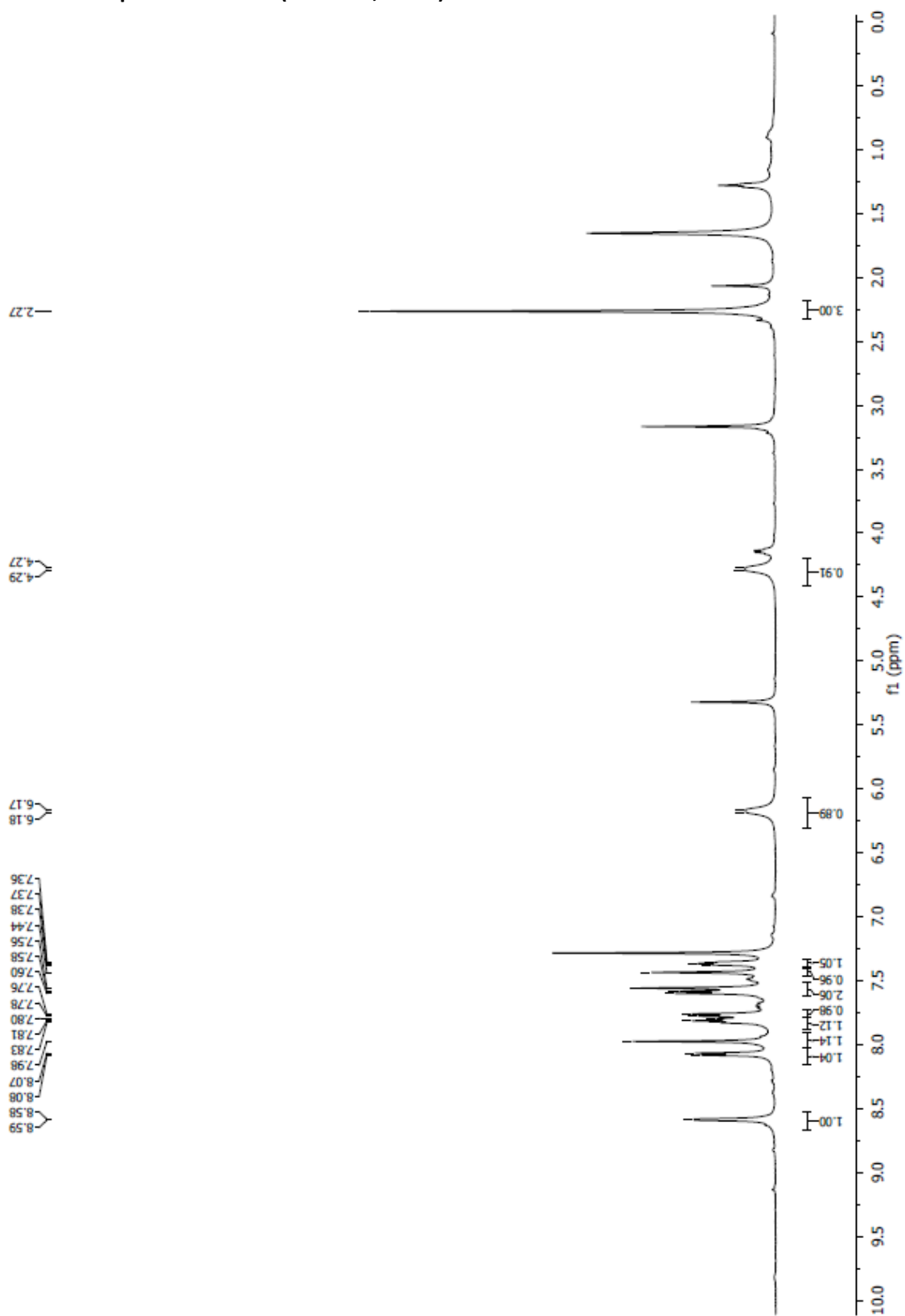
3.  $^1\text{H}$  NMR spectrum of 110 (500 MHz,  $\text{CDCl}_3$ )



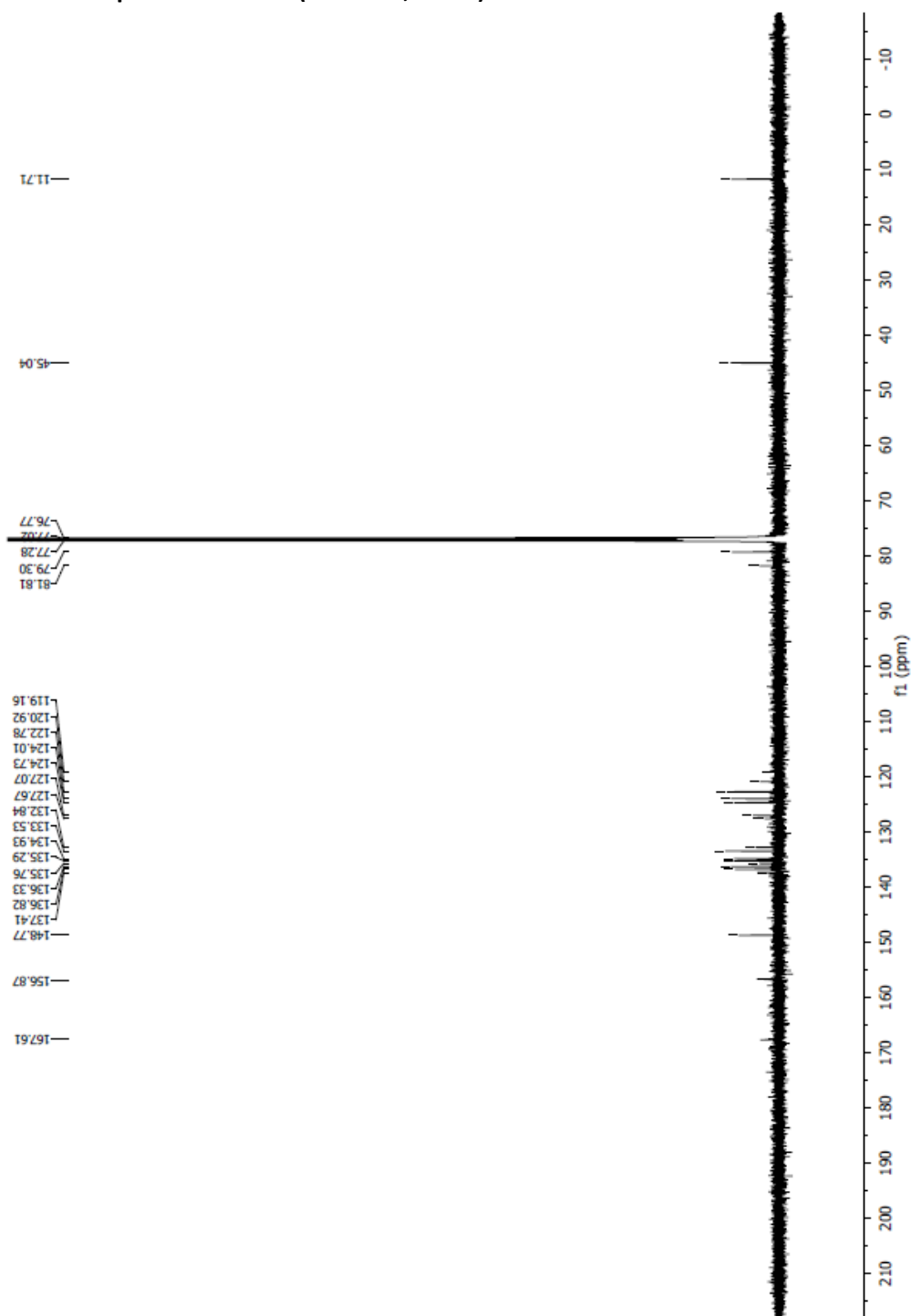
4.  $^{13}\text{C}$  NMR spectrum of 110 (500 MHz,  $\text{CDCl}_3$ )



5.  $^1\text{H}$  NMR spectrum of 113 (500 MHz,  $\text{CDCl}_3$ )



6.  $^{13}\text{C}$  NMR spectrum of 113 (500 MHz,  $\text{CDCl}_3$ )



**Note:** Additional  $^1\text{H}$  and  $^{13}\text{C}$  NMR can be found in the research article (Design, synthesis and characterization of novel gamma aminobutyric acid type A receptor ligands (Arkivoc, 2020 (Part (vii)), 242-256))

**Table A:** Primary Radioligand Binding Assays for ZK-III-51. Compound-induced radioligand displacement assays for 31 receptors, transporters and channels conducted by the National Institute of Medical Health Psychoactive Drugs Screening Program (B. Roth et al., UNC, available at <http://pdsp.med.unc.edu>).<sup>a</sup>

Receptor	Inhibition 1	Inhibition 2	Inhibition 3	Inhibition 4	Mean %
5-HT1A	54.12	49.93	49.93	53.61	51.9
5-HT1B	-8.87	17.4	-12.53	-4.18	-2.05
5-HT1D	-13.06	-7.26	-23.85	-10.99	-13.79
5-HT1E	9.39	3.17	4.15	7.32	6.01
5-HT2A	12.87	21.79	49.15	10.41	23.56
5-HT2B	37.06	7.23	-8.22	7.95	11.01
5-HT2C	17.74	-13.08	-12.45	-0.29	-2.02
5-HT3	22.31	4.05	-0.71	4.05	7.43
5-HT4	7.26	13.99	24.92	-4.52	10.41
5-HT5A	6.18	-22.02	-7.82	3.42	-5.06
5-HT6	7.21	-3.82	-0.88	4.26	1.69
5-HT7A	10.71	-12.74	-7.82	-17.66	-6.88
Alpha1A	5.49	5.27	4.42	1.03	4.05
Alpha1B	10.51	10.3	7.36	12.69	10.22
Alpha1D	22.07	11.87	9.31	24.88	17.03
Alpha2A	12.89	0.25	-14.07	-7.58	-2.13
Alpha2B	16.17	9.31	5.72	21.19	13.1
Alpha2C	0.38	-20.67	-28.48	-13.7	-15.62
Beta3	48.46	12.71	21.93	9.03	23.03
BZP Rat Brain Site	86.73	87.92	87.81	87.49	87.49
D1	17.2	14.85	8.4	11.68	13.03
D2	-0.71	-9.97	2.12	6.53	-0.51
D3	7.57	2.79	39.73	11.5	15.4
D4	3.72	-20.59	-19.65	-0.91	-9.36
D5	12.93	30.58	5.34	21.54	17.6
DAT	2.97	-10.55	-27.92	-4.3	-9.95
DOR	16.67	-21.03	0.69	-5.27	-2.24
GABAA	24.42	-2.87	-6.43	12.95	7.02
H1	-6.83	-33.46	28.79	-12.54	-6.01
H2	3.34	27.9	40.05	29.55	25.21
H3	3.79	-15.86	-1.54	-6.24	-4.96
H4	25.69	18.9	30.67	39.5	28.69
KOR	74.8	68.2	64.84	60.92	67.19

Receptor	Inhibition 1	Inhibition 2	Inhibition 3	Inhibition 4	Mean %
M1	-3.17	15.07	21.03	22.29	13.81
M2	-9.24	-2.71	0.84	11.3	0.05
M3	6.4	-6.53	18.92	20.92	9.93
M4	19.55	4.4	4.81	-0.51	7.06
M5	0.84	-7.81	-11.6	0.64	-4.48
MOR	3.54	4.02	7.23	12.28	6.77
NET	-6.58	-7.38	-11.45	-17.04	-10.61
PBR	49.84	42.67	32.06	60.73	46.33
SERT	11.52	-4.18	1.05	1.56	2.49
Sigma 1	10.57	11.74	2.57	13.59	9.62
Sigma 2	18.55	32.12	36.09	16.23	25.75
NMDA	52.88	41.62	36.64	48.55	44.92
NR2B	19.99	17.55	26.59	17.77	20.48
Ca channel v1.2 human	50.95	26.53	8.21	21.95	26.91
Alpha2Beta2	14.03	1.9	7.81	0.23	5.99
Alpha2Beta4	10.26	5.9	7.03	11.95	8.79
Alpha3Beta2	2.58	7.34	-2.98	11.31	4.56
Alpha3Beta4	0.51	0	9.1	6.07	3.92
Alpha4Beta2	11.8	6.16	1.59	11.44	7.75
Alpha4Beta2 (Rat Brain)	0.86	-2.76	-1.88	-0.2	-1
Alpha4Beta4	6.55	-2.04	-3.58	5.89	1.71
Alpha7	-1.01	1.16	12.62	-2.71	2.52

<sup>a</sup> Data are the percent inhibition induced by 10  $\mu$ M of each respective compound on the specific binding at the screened target. The higher the number the more the radioligand was displaced.

**Table B:** Primary Radioligand Binding Assays for **ZK-III-56** Compound-induced radioligand displacement assays for 31 receptors, transporters and channels conducted by the National Institute of Medical Health Psychoactive Drugs Screening Program (B. Roth et al., UNC, available at <http://pdsp.med.unc.edu>).<sup>a</sup>

Receptor	Inhibition 1	Inhibition 2	Inhibition 3	Inhibition 4	Mean %
5-HT1A	18.25	23.78	9.87	5.51	14.35
5-HT1B	1.39	-4.52	-17.92	28.36	1.83
5-HT1D	19.28	-12.65	-57.85	-22.6	-18.46
5-HT1E	11.22	11.95	0	6.59	7.44
5-HT2A	1.65	15.49	4.57	21.33	10.76
5-HT2B	34.91	6.51	-12.89	-16.13	3.1
5-HT2C	-3.85	7.26	-22.72	19.84	0.13
5-HT3	1.98	-0.56	5.66	-0.17	1.73
5-HT4	19.03	7.26	20.72	7.26	13.57
5-HT5A	7.24	1.09	-37.5	-0.82	-7.5
5-HT6	9.85	-0.44	-3.09	-6.32	0
5-HT7A	-2.03	-1.16	-5.79	-10.71	-4.92
Alpha1A	-1.52	-11.27	4	-9.37	-4.54
Alpha1B	17.48	0.39	12.36	12.47	10.68
Alpha1D	1.15	17.99	24.37	17.99	15.38
Alpha2A	12.78	-3.44	65.25	3.27	19.47
Alpha2B	9.71	4.75	5.32	10.4	7.55
Alpha2C	-1.64	-21.44	-18.16	-16	-14.31
Beta3	18.98	12.71	25.98	35.19	23.22
BZP Rat Brain Site	87.92	85.43	87.7	89.65	87.68
D1	16.26	12.39	18.85	33.05	20.14
D2	5.85	4.72	-2.18	9.24	4.41
D3	2.51	2.93	13.75	11.22	7.6
D4	17.73	-16.49	-1.54	-3.65	-0.99
D5	7.82	2.43	10.59	15.12	8.99
DAT	1.3	-16.14	-14.76	-18.69	-12.07
DOR	-6.12	-4.85	-16.13	4.95	-5.54
GABAA	22.44	-11.96	-4.05	-19.87	-3.36
H1	-9.6	-8.73	-4.41	1.47	-5.32
H2	1.69	22.24	22.24	24.39	17.64
H3	-3.79	-13.82	2.76	2.15	-3.18
H4	26.83	44.93	44.48	25.69	35.48
KOR	72.11	60.58	75.47	65.06	68.31

Receptor	Inhibition 1	Inhibition 2	Inhibition 3	Inhibition 4	Mean %
M1	-6.84	14.04	3.37	11.97	5.64
M2	8.68	-7.28	0.84	4.2	1.61
M3	-7.63	5.16	-5.21	24.59	4.23
M4	26.51	-0.72	-2.15	14.02	9.42
M5	16.38	23.96	1.42	15.02	14.2
MOR	4.66	-2.56	4.02	6.11	3.06
NET	2.21	-8.42	-36.77	-2.99	-11.49
PBR	33.97	23.18	29.96	29.87	29.25
SERT	5.2	-3.09	0.11	-3.6	-0.35
Sigma 1	-5.23	-18.98	-8.45	-6.5	-9.79
Sigma 2	3.49	6.05	-11.74	-17.78	-5
NMDA	26.24	29.27	26.24	32.3	28.51
NR2B	20.16	20.54	24.48	5.52	17.68
Ca channel v1.2 human	24.14	-4.98	36.4	22.61	19.54
Alpha2Beta2	9.48	4.78	25.26	12.67	13.05
Alpha2Beta4	0.7	-0.98	1.55	15.04	4.08
Alpha3Beta2	15.14	2.58	5.75	-0.99	5.62
Alpha3Beta4	-1.52	1.85	13.99	-0.67	3.41
Alpha4Beta2	8.8	9.16	4.83	4.71	6.88
Alpha4Beta2 (Rat Brain)	5.55	-2.32	3.96	4.31	2.88
Alpha4Beta4	7.21	-0.28	0.61	6.55	3.52
Alpha7	12.77	2.4	22.68	22.52	15.09

<sup>a</sup> Data are the percent inhibition induced by 10  $\mu$ M of each respective compound on the specific binding at the screened target. The higher the number the more the radioligand was displaced.

**Table C:** Secondary Radioligand Binding Assays. Binding affinity ( $K_i$ , nM) values obtained from non-linear regression of radioligand competition binding isotherms. Testing conducted by the National Institute of Medical Health Psychoactive Drugs Screening Program (B. Roth et al., UNC, available at <http://pdsp.med.unc.edu>).<sup>a</sup>

Compounds	5-HT1A	KOR
ZK-III-51	4669.89	2015.82
ZK-III-56	NA	2438.05

<sup>a</sup>  $K_i$  values are calculated from best fit  $IC_{50}$  values using the Cheng-Prusoff equation. Values are an average of  $n = 2$ . NA are for compounds/receptors not testing for Secondary Screening results.

## CURRICULUM VITAE

Md Zubair Ahmed Khan

Place of Birth: Dhaka, Bangladesh

### Education:

- Ph.D., University of Wisconsin-Milwaukee, May-2021  
Major: Organic Chemistry  
Title: Part 1: Approach toward the total synthesis of some sarpagine related indole alkaloids: hystrixnine, gelsempervine A, gelsempervine B, O-methylmacusine B, 19,20- dihydro - O - methylmacusine B.  
Part 2: Design, Synthesis and biological study of some novel gamma-aminobutyric acid type A receptor ligands.
- M.Sc., University of Dhaka, June-2011  
Major: Organic Chemistry
- B.Sc., University of Dhaka, June-2010  
Major: Chemistry

### Awards:

- 2018-2019 Best Teaching Assistant Award (Laboratory), Organic Chemistry, UWM
- 2014-2015 Student Success Award, UWM

### Publications:

- Design, synthesis and characterization of novel gamma aminobutyric acid type A receptor ligands (Arkivoc, 2020 (Part (vii)), 242-256).
- Protracted positive vs. negative allosteric modulation of  $\alpha 5$  GABAA receptors in 5xFAD mice: Sex-dependent behavioral and  $\alpha 5$  subunit expression consequences
- Symptomatic and Disease-Modifying Effects of GABAA Receptor Positive Allosteric Modulation in a Mouse Model of Chronic Stress

### Teaching & research experience:

- Teaching assistant on CHEM 102, 103, 221, 342, 344, 582
- Research experience as a graduate student in Dr. Cook lab